Linear poly(ethylene imine)-poly(ethylene glycol) copolymers for nucleic acid delivery

Synthesis and characterization

Dissertation zur Erlangung des Doktorgrades der Naturwissenschaften (Dr. rer. nat.)

der Fakultät Chemie und Pharmazie der Universität Regensburg

Vorgelegt von

Sonja Bauhuber

aus Bayerbach

im November 2012

Diese Arbeit entstand im Zeitraum von Dezember 2007 bis Oktober 2012 am Lehrstuhl für Pharmazeutische Technologie an der Universität Regensburg.

Die Arbeit wurde von Prof. Dr. Achim Göpferich angeleitet.

Promotionsgesuch eingereicht am: 05. November 2012

Mündliche Prüfung am: 30. November 2012

Prüfungsausschuss: Prof. Dr. Sigurd Elz   (Vorsitzender)

    Prof. Dr. Achim Göpferich   (Erstgutachter)

    Prof. Dr. Torsten Blunk   (Zweitgutachter)

    Prof. Dr. Joachim Wegener   (Drittprüfer)

Meinen Eltern

in Liebe und Dankbarkeit gewidmet

„In der Wissenschaft gibt es nie ein Erreichen des Ziels. In der Wissenschaft gibt es immer nur Etappenziele.“

Henning M. Beier

Table of contents

Chapter 1

Delivery of nucleic acids via disulfide-based carrier systems

Abstract

Nucleic acids are not only expected to assume a pivotal position as 'drugs' in the treatment of genetic and acquired diseases, but could also act as molecular cues to control the microenvironment during tissue regeneration. Despite this promise the efficient delivery of nucleic acids to their side of action is still the major hurdle. One among many prerequisites for a successful carrier system for nucleic acids is a high stability in the extracellular environment, accompanied by an efficient release of the cargo in the intracellular compartment. A promising strategy to create such an interactive delivery system that adapts its properties to the conditions of the microenvironment, is to exploit the redox gradient between the extra- and intracellular compartment. In this review, emphasis is placed on the biological rationale for the synthesis of redox sensitive, disulfide-based carrier systems for nucleic acids as well as the extra- and intracellular processing of macromolecules containing disulfide bonds. Moreover, the basic synthesis approaches for introducing disulfide bonds into carrier molecules together with examples which demonstrate the benefit of disulfides at the individual stages of nucleic acid delivery will be presented.

Delivery of nucleic acids via disulfide-based carrier systems

1. Introduction

The delivery of nucleic acids is a promising strategy for the modulation of gene expression inside cells. On the one hand, it offers the opportunity to insert therapeutic genes via DNA, on the other hand the expression of non-functional or harmful proteins can be inhibited by the application of therapeutic RNA. Both approaches can be used for the therapy of inherited or acquired diseases as well as for the regeneration of defective tissue. For tissue regeneration the delivery of nucleic acids could be very beneficial, because a controlled environment which promotes cell proliferation and regeneration is needed.[1-3] Here, the right cues, e.g. for the synthesis of growth factors, must be present at the right time point and for the appropriate time period. While many signalling proteins have a very short half-life, genes are expressed over a longer period and, thus, provide longer effects.

Despite this promise, the effective delivery of nucleic acids remains a major problem and the carrier has to overcome many natural barriers in order to transport its cargo to the side of action.[4] The carrier, which should be non-toxic, non-immunogenic, and preferably biodegradable, must compact the nucleic acid into small particles to prevent degradation. Beyond this, the carrier must prevent non-specific interactions with the biological environment and allow cellular uptake in a target specific-manner. After successful cellular uptake, the next hurdle that a delivery system must clear is endosomolysis. During this stage, the system should release the nucleic acid into the cytosol of the cell.[5-10] Subsequently, to induce gene expression, the DNA must enter the nucleus.[11-13] In contrast, therapeutic RNAs need only to be present within the cytoplasm for activity. Lipids and polymers (lipids form lipoplexes and polymers polyplexes, respectively, with nucleic acids) are of special interest as delivery vehicles, as they can easily be modified with functional domains to fulfil these demands. Several polymer-based materials such as poly(L-lysine) (pLL) [14-18] or poly(ethylene imine) (PEI) [19-23], natural polymers [24-35] and lipids [24, 36-38] have been shown to overcome some of the inherent challenges

discussed herein. However, each is associated with its own concerns, and a comprehensive building plan for an ideal delivery system remains elusive. To this end, the most important issue to address involves determining how to assemble a carrier system such that presentation of the appropriate functional domain for each specific task occurs at the correct spatiotemporal point, both inside and outside the cell. Presenting the appropriate signals at the appropriate time point is a major challenge, e.g. for regenerative medicine the concomitant action of multiple factors is indispensable for tissue regeneration. Carrier systems with multifunctional domains which are triggerable based on conditions prevailing in the physiological environment, such as pH, redox gradients, the osmotic pressure or the presence of enzymes could be highly convenient for this purpose.

In this context, disulfide bonds play an exceedingly important role because they can exploit the redox potential gradient between the extra- and intracellular space. Consequently, outside of cells they provide for a temporarily high stability of the delivery system, but are rapidly cleaved inside cells facilitating the release of therapeutic nucleic acids. Especially for tissue engineering (TE) a long-term stability of the delivery system in the extracellular compartment followed by an efficient release of cargo in the target cell is an important concern, since the tissue regeneration may last for weeks or even months. Although, the delivery of nucleic acids in the field of TE is quite auspicious, this approach still remains in its experimental phases [39-54], and only a very limited number of studies have been conducted that apply carriers that rely on the described redox potential gradient.[55, 56]

This review will focus on the redox-potential trigger between the extra- and intracellular environment. Furthermore, the basic synthesis approaches for introducing disulfide bonds into molecules will be described. Additionally, the review will provide examples that demonstrate the significance of disulfide bonds for the different aspects of delivery.

2. Redoxsensitive carriers

Countless redoxsensitive carrier systems for non-viral nucleic acid delivery have been previously described in literature. Although oxidation-sensitive block copolymers based on poly(propylene sufide) (PPS) have been tried for the use of nucleic acid delivery, the field is dominated by disulfides (symbolized as –SS- in this review).[57, 58] The fact that disulfide containing carriers can take advantage of the large intra-/extracellular redoxgradient makes them very attractive for the design of gene delivery systems. Once inside the cell their cargo is very quickly released. In contrast, the cleavage of widely used acid-labile linkages like esters or hydrazones is a rate dependent phenomenon, i.e. the hydrolysis is proportional to the pH. For these linkages, a decrease of one pH unit a 10-fold difference in the hydrolysis rate can be expected.[59] Therefore, premature (extracellular) release of cargo in an acidic environment found in the vicinity of tumors or inflamed tissue is possible. This is a significant concern in cancer therapy as well as in tissue engineering applications as they are often associated with inflammation.[60] Hence, acid-labile linkages must compromise between a fast hydrolysis rate in the intracellular compartment and a slower hydrolysis in the extracellular space.[59, 61]

3. Biological rationale

3.1. Cellular uptake

This section gives a short overview of the cellular uptake of non-viral gene carriers. The first barrier a gene delivery vehicle has to overcome on its way into the cell is the plasma membrane. Cationic polymers and lipids primarily enter cells via endocytosis and are, therefore, directed to the endolysosomal compartment **(Figure 1)**.[62, 63] In general, many different endocytotic pathways are known: 1) unspecific (adsorptive, **Figure 1, (2)**) und specific (receptor mediated, **Figure 1, (3)**) clathrin dependent, 2) lipid-raft mediated (caveoline dependent and independent, **Figure 1, (1)**) endocytosis, 3) phagocytosis and 4) macropinocytosis. For carriers without

receptor ligands the main entrance to the cell is suggested to be the non-specific, adsorptive, clathrin dependent endocytosis. In this case an electrostatic interaction between the positively charged cationic carrier and the negatively charged syndecans on the cell membrane is assumed.[64] In case of ligand containing carriers, besides this unspecific uptake the receptor-mediated endocytosis plays a role. The receptors can then be recycled back to the plasma membrane in early endosomes, while their ligands (including the carrier) are trafficked to later stages of the pathway.[65] A distinct separation, however, cannot be made as the extent of participation of the different pathways seems to be dependent on cell type, carrier composition and carrier size.[66, 67] For instance, PEI/DNA polyplexes are believed to be taken up by caveolae and clathrin-coated pits, while lipoplexes made from N-(1-(2,3-dioleoyloxy)propyl)-N,N,N-trimethylammonium chloride (DOTAP)/DNA proceed solely by clathrin dependent endocytosis.[62] In a recent study the transport of PEI/DNA polyplexes could be followed by live-cell imaging, beginning from binding to the cell surface until the active transport inside of endosomes along microtubules.[64] It would certainly be of great benefit to perform similar experiments with disulfide containing gene carriers in order to gain more insight into their degradation and trafficking.

Once inside the endolysosomal system, nucleic acids must escape into the cytoplasm in order to reach their target and to circumvent lysosomal degradation by nucleases. The precise escape mechanism is dependent on the type of carrier, but for carriers with buffering capacity like PEI, the most common explanation, among others, is the proton sponge mechanism. Polymers like poly-L-lysine (pLL) lack this ability to avoid lysosomal trafficking.[62, 68] For cationic lipid based vectors, an interaction between the liposomes and anionic lipids in the endosomal membrane has been proposed.[62]

clathrin mediated endocytosis

adsorptive

receptor mediated

caveoline
mediated endocytosis

① ② ③

recycling
endosomes ④ sorting
endosomes

cytosol ⑧

nucleus

ECV ⑤ ⑦

late
endosomes

⑥ lysosomes
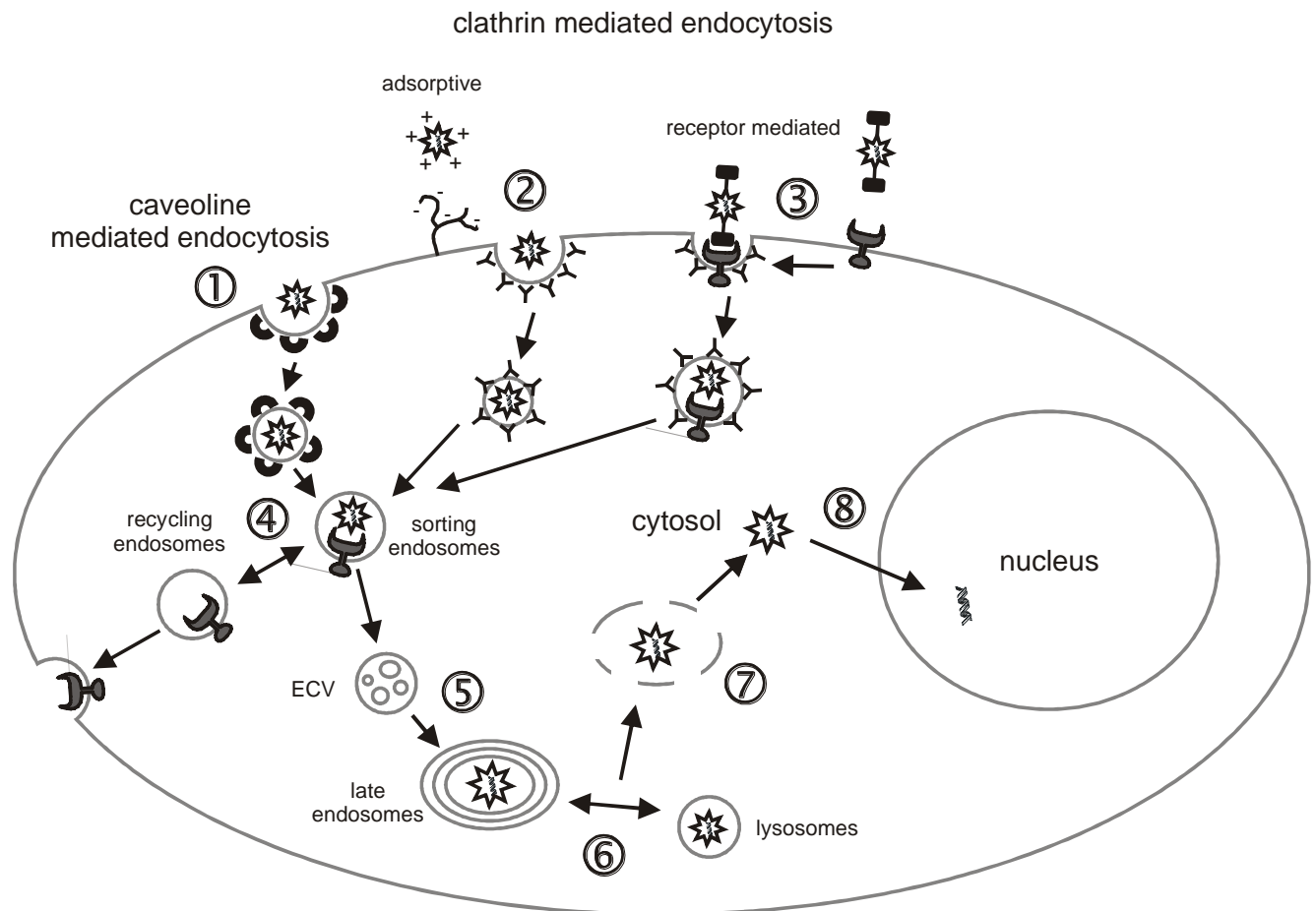
Figure 1. *Into the cell – simplified scheme of the cellular trafficking of non-viral gene delivery systems: The two most common non-viral gene delivery systems, polyplexes and lipoplexes (□), are taken up mainly by endocytosis. Several different mechanisms are known: Calveoli formation (1), adsorptive (2) or receptor mediated (3) endocytosis. The last two mechanisms can also be clathrin independent. After rapid uncoating the newly formed vesicle fuses with early endosomes (sorting endosomes and recycling endosomes (4)). The processing of ligand-receptor complexes also takes place here: Sorting endosomes are slightly acidic which leads to a dissociation of ligands from their receptors. These receptors can then be recycled back to the plasma membrane whereas their ligands are trafficked differently. After further acidification the endosome carrier vehicle (ECV) transfers material from early endosomes to late endosomes (5). These are the main site for proteolysis and stay in dynamic equilibrium with lysosomes (6). In*

order to avoid lysosomal degradation and to reach their targets (8) in the cytosol (most RNA therapeutics) or nucleus (pDNA) the nucleic acids must escape endosomal entrapment (7). The stage at which the nucleic acid dissociates from its carrier depends on the carrier system.

The versatility of disulfide carriers has been shown in many different approaches, but the underlying biological rationale is poorly understood thus far. Where and how internalized disulfides are processed is still a disputable matter. Some evidence discussed here suggests that disulfide cleavage occurs along the endolysosomal pathway.[69-71] However, there are other indications that this is not the case.[72, 73] It seems that the process of disulfide reduction, like the uptake of the carrier, depends on numerous variables. It must also be remembered that the cellular redox environment is not static, as it varies throughout the different stages of the cell cycle.[74] Furthermore, many studies which our knowledge of cellular disulfide reduction is based on were not performed with cationic polymers, and as such, the relevance of these studies for non-viral gene carriers is unknown.[72, 75]

3.2.   Cellular redox environment

The existence of a redox gradient between intra- and extracellular space was shown some time ago. While the extracellular space is oxidizing, most cellular compartments are reducing.[76] Nature has exploited this fact for the "delivery" of toxins (like diphtheria or cholera toxin) and viruses that have served as templates for artificial therapeutic disulfide conjugates like Gemtuzumab ozogamicin (Mylotarg®).[70] In recent years, more non-viral vectors employing disulfides to promote nucleic acid delivery have emerged.

In order to pinpoint the location of disulfide cleavage, detailed knowledge about the cellular redox environment is essential. The term "redox environment" was defined by Schafer *et al.*: "The redox environment of a linked set of redox couples […] is the summation of the products of the reduction potential and reducing capacity of the linked redox couples present.".[74]

Cellular disulfide reduction and isomerization is mediated by small redox molecules, either alone or in conjunction with redox proteins. These redox active proteins typically need the presence of cofactors or enzymes to regenerate their activity.[70, 76] In the eukaryotic cytosol, two main redox systems are responsible for maintaining protein thiols in their reduced state: the thioredoxin (Trx) and the glutaredoxin (Grx) system.[70, 77] Trx is regenerated by the enzyme thioredoxin reductase and Grx is non-enzymatically reduced by another important redox factor: glutathione (GSH). In principle, both Trx and Grx can catalyze redox reactions in both directions. However, due to the high cytosolic abundance of GSH and thioredoxin reductase, they are primarily reducing.[70]

3.2.1. Compartmentation of GSH

The high level of GSH, which can reach millimolar concentrations ($c_{intracell.}$(GSH)=1-11 mM, $c_{extracell.}$(GSH)=10 μM [74, 76]) is maintained by glutathione reductase (GR). This enzyme regenerates GSH from glutathione disulfide (GSSG).[74, 77] GSH by far outnumbers any other cellular redox system (c(Trx)~1/100-1/1000 c(GSH)) so the GSH/GSSG system therefore is, regarded as the major cellular redox buffer. It serves as a representative redox couple to measure the redox environment.[74] In literature, the cellular redox state is mostly described by the GSH:GSSG ratio (cytosol: GSH:GSSG=30:1 to 100:1 [74]), but according to Nernst's equation the reduction potential depends on $[GSH]^2/[GSSG]$. Thus, absolute GSH concentration must be known.[74]

A large GSH-pool with similar or even higher GSH-levels than in the cytosol is found in the nucleus.[76] In terms of gene delivery, it is important to know that nuclear GSH is required for DNA synthesis and repair, and it keeps a number of transcription factors in reduced state. For polyplexes, it was concluded that reduction primarily takes place in the cytosol or the nucleus.[76] This finding, however, does not necessarily apply to all types of gene carriers. In a recent report

the roles of nuclear and cytosolic GSH on the relative transfection activities of reducible pLL (rpLL: -(Cys-Lys$_{10}$-Cys)$_n$-) and non-reducible pLL polyplexes (including DOTAP to enhance endosomal escape) were investigated. The polyplexes were formed with two nuclearly (pDNA, asODN) and two cytosolically (mRNA, siRNA) active nucleic acids. The authors used Bcl-2 protein (B-cell lymphoma 2) overexpressing cells that have an increased intracellular GSH level (compared to non-Bcl-2 overexpressing cells: 1.5- to 2-fold) and a partial GSH redistribution to the nucleus (60-67 % of total cellular glutathione). Polyplexes composed of mRNA showed a much higher increase in relative transfection activity (control: 5 and Bcl-2: 79) when compared with polyplexes of pDNA (control: 3 and Bcl-2: 5.7). Hence, an increased GSH-level was more benefical for mRNA- than for pDNA-delivery. The authors concluded that the difference in behavior must be due to differences in subcellular trafficking and disassembly of the carriers. While it appeared that, there is an efficient nuclear unpacking mechanism for pDNA-polyplexes there was no evidence for a similar mechanism that processes cytoplasmic mRNA-polyplexes. An increased GSH-level consequently has a higher influence on mRNA-polyplexes. The influence of the GSH concentration on the enhancement of relative activity of asODN and siRNA complexes was less pronounced. The disulfide reduction is likely to have a smaller effect on low molecular weight nucleic acids due to a smaller influence of the polycation size on the unpacking rates.[78]

The endoplasmic reticulum (ER), which is topologically connected to the extracellular space, is about one hundred times more oxidizing than the cytosol or nucleus (GSH:GSSG ranging from 1:1 to 3:1 [74]).[70] The ER is responsible for the synthesis and processing of secretory and membrane proteins to which protein disulfide bonds are mainly restricted to. An environment favoring the formation of disulfides is, therefore, pivotal for correct protein folding and processing.[70, 79] One enzyme of the thioredoxin family, disulfide isomerase (PDI), plays an important role in these activities. Its relevance for processing internalized disulfides will be discussed in the next section.

3.2.2. Cellular disulfide processing

3.2.2.1.   Surface reduction

Despite the oxidizing extracellular space, thiol containing redox enzymes are found on the plasma membrane, suggesting a cellular microenvironment that supports redox reactions, e.g. reductions.[70, 76] One of those redox enzymes is the highly abundant PDI.

It is found throughout the endocytotic pathway. On the cell surface PDI is only a reductant while in the ER it acts both as oxidant and disulfide isomerase. Cell surface associated PDI was shown to cleave disulfides in the gp120 HIV-protein, thus triggering the membrane fusion process eventually resulting in HIV entry.[80] PDI is also supposed to play a role in processing macromolecular drugs. In order to investigate the involvement of PDI in disulfide reduction, inhibitors including monoclonal anti-PDI antibodies and membrane impermeant reagents like DTNB (5,5'-dithio-bis(2-nitrobenzoic acid)) or the antibiotic bacitracin were developed.[80]

Feener *et al.* linked [^{125}I]iodotyramine through a disulfide spacer to poly(D-lysine), which resists degradation by lysosomal proteases.[73] They demonstrated that the linker's reductive cleavage consists of two phases. The first phase began immediately after internalization and was sensitive against DTNB and, as shown later, against an anti-PDI antibody. Even so, after a lag-time of thirty minutes, the reduction process continued. This not only implies a reduction along the endolysosomal pathway, but also suggests participation of PDI in the first phase. Similar results with diphtheria toxin show that disulfide bond reduction of macromolecules might begin at the cell surface and progress into early endosomes due to co-internalized surface enzymes.[70] The significance of this surface related reduction remains unclear, but several facts indicate that this mode of cleavage, especially as mediated by PDI, is irrelevant. First, efficient PDI function requires an efficient regenerating system outside of cells.[70, 80] While such an intracellular system has already been found, its extracellular counterpart has not yet been identified. Second, after

internalization, endosomes are quickly acidified, and proteins of the thioredoxin family have an activity optimum at neutral pH. Therefore, high PDI activity would be restricted to only the initial endocytotic compartments.[70] The relevance of this reduction mode has further been brought into question by several more recent studies that used different disulfide containing constructs.

Shen *et al.* linked methotrexate (MTX), an antimetabolitic drug, to the polycationic carrier poly(D-lysine).[69] This conjugate inhibits cell growth of wild type and of MTX transport-defective CHO mutants. If surface cleavage was a major factor, the MTX transport-defective cells would be less affected by MTX-SS-poly(D-lysine), as the extracellularly released free MTX alone would not be taken up. However this was not the case. Similar conclusions were drawn by Saito *et al.*[81] They developed an enhanced disulfide containing cytosolic gene delivery system by using the pore forming, cytotoxic agent lysteriolysin O (LLO) coupled with protamine (PN). In its uncleaved form, the LLO-SS-PN construct was not cytotoxic. The ratio of free LLO to LLO-SS-PN strongly suggested that linker reduction was more dominant after internalization. Moreover, LLO-SS-PN was only cytotoxic at high concentrations, presumably indicating infrequent reduction events on the cell surface. Austin *et al.* used rhodamine red (RR) linked to the anti-HER2 antibody trastuzumab (trastuzumab-SPP-RR).[72] Rhodamine red showed self-quenching at higher labeling ratios, allowing it to be used in a dequenching assay as an indicator for the SPP linker cleavage **(Figure 2)**. Their observations also revealed that surface cleavage must be very ineffective. The same results using another cell-line were obtained in the work of Yang *et al.*, where a disulfide reduction sensitive FRET probe was coupled to folate.[75] In a another current work, a bioresponsive non-viral gene carrier composed of poly(aspartamide) (P[Asp(DET)]) shielded with polyethylene glycol (PEG) was investigated.[71] The outer PEG layer reduced the electrostatic interaction between cell membrane and polyplex thus preventing unspecific endocytosis. The authors hypothesized that if surface reduction took place, a larger amount of PEG-SS-P[Asp(DET)] would be taken up in comparison to non-reducible PEG-P[Asp(DET)], as

the removal of the PEG shielding would restore the membrane-polyplex interaction, but this was not the case.

3.2.2.2.   *Endolysosomal compartment*

These studies above all leave the question unanswered where, if not at the cell surface or in the earliest endocytotic compartment, disulfides are cleaved. The redox properties of endosomes and lysosomes are not as well characterized as those of the cytosol or the ER. A case can be made both for and against the possibility of reduction in the endolysosomal pathway. Feener *et al.* assessed the second phase of intracellular reduction by using percoll gradient subcellular fractionation and excluded the participation of endosomes, lysosomes or the endoplasmic reticulum, leaving only the Golgi apparatus as a possible location for reduction.[73] Unfortunately, the techniques used were not suitable to provide a high resolution picture of disulfide processing. It is possible that organelles might have been ruptured during work up cross contaminating compartments of different redox properties.[75] The group around Yang *et al.* was unable to verify the involvement of the Golgi apparatus in the reduction process.[75]

Several studies on specialized cells of the immune system, the professional antigen presenting cells (APCs) like macrophages or activated B-cells, could shed a new light on these subjects as they imply a reducing capacity in endolysosomal organelles. APCs present fragments of endocytosed proteins (antigens) on their surface.[82] Prior to this presentation these proteins are digested by cathepsines and proteases in endosomes and lysosomes.[82, 83] Disulfide reduction was shown to be a prerequisite for efficient antigen processing.[84] It is believed that this enhancement of substrate proteolysis might be a general effect which is not limited to antigen processing.[65] In this context, Collins *et al.* proposed the following model: after endocytosis, antigens pass through early and late endosomes (LEs) where they are only partially proteolytically degraded as proteolysis is restricted to those regions that are easily accessible to endosomal enzymes. Disulfides usually remain intact, thus limiting further antigen unfolding.[82]
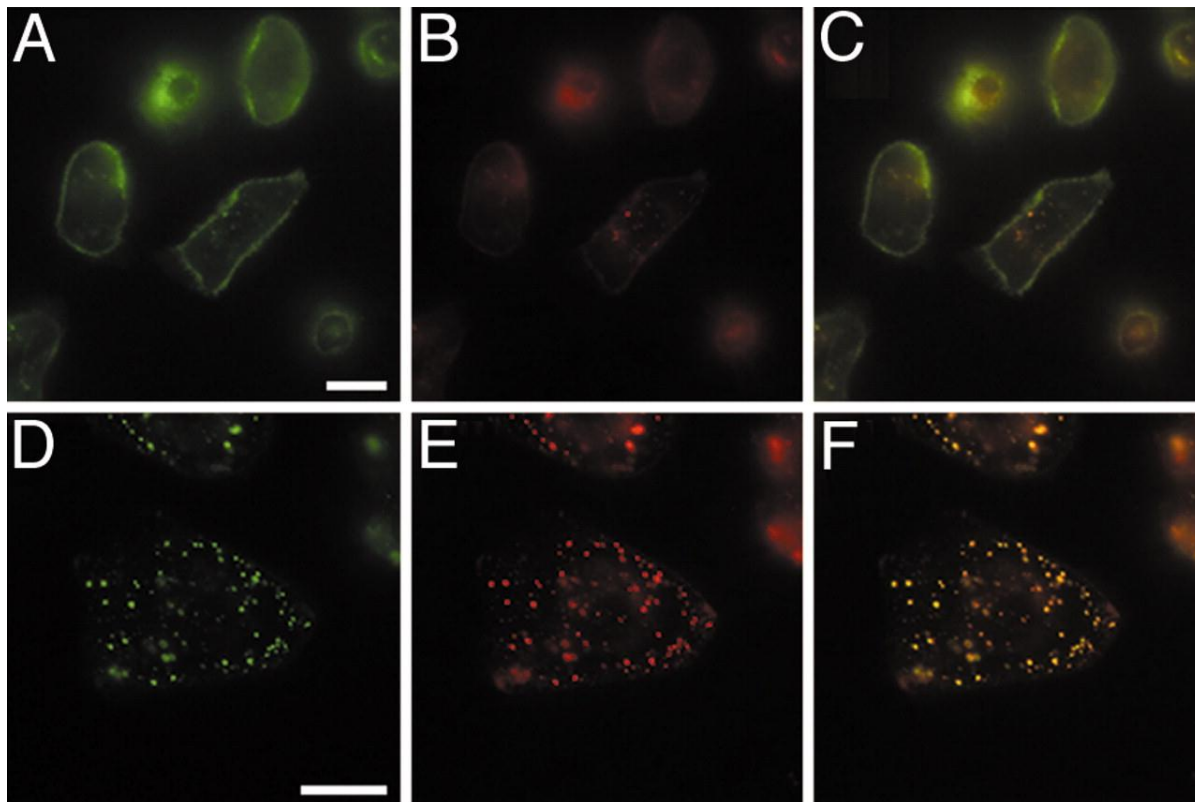
Figure 2. *Rhodamine Red (RR) fluorescence dequenching of a dual-labeled ^{488}trastuzumab-SPP-RR$^{4.5}$ conjugate upon geldanamycin-induced routing to the lysosomal pathway: Alexa-488 (green) was conjugated to trastuzumab-SPP-RR$^{4.5}$ to serve as a reference. SKBr3 cells with surface-bound conjugate were incubated with (D–F) or without (A–C) geldanamycin. Red fluorescence dequenching upon lysosomal routing can be recognized as a red shift in the merged dual color image (compare C with F). The dequenching is not a result of disulfide cleavage but lysosomal degradation of the antibody. (Scale bars: 20 μm)* [72]

After transfer to lysosomes, the disulfide bonds are reduced due to a high cysteine (Cys) concentration there. Previously inaccessible regions are now exposed to lysosomal enzymes The validity of this model was underpinned in a later study where the cysteine transport pathways of macrophage hybridoma and B cell lymphoma were investigated.[84] It was

suggested that organelles with Cys-transport activity, in this case endosomes and/or lysosomes depending on the cell type, could be the locations where antigens are processed. Such Cys and Cys_2-specific transporters that produce a net influx of Cys and efflux of Cys_2 in endolysosomes are required to achieve a high Cys/Cys_2-ratio. Although the exact parameters are unknown a ratio of 500-600:1 would be necessary according to the Nernst equation to have an environment as reducing as the cytosol (-221 mV to -236 mV). The reason for this is the unfavored thiol deprotonation (-SH → -S$^-$ + H$^+$) at the acidic conditions in the endolysosomal system. Such nucleophilic thiolate anions (S$^-$) are required for disulfide exchange reactions in biological systems.[65, 75]

Endolysosomal reduction mediated only by Cys would have a low specificity and efficiency, and it therefore requires for enzymatic support. One of such an enzyme, the Gamma-interferon-inducible lysosomal thiol reductase (GILT), was observed in antigen presenting and other cells.[85] GILT is a 30 kDa thiol reductase that is constitutively expressed in APCs. It is distantly related to the members of the thioredoxin family. Precursor-GILT (35 kDa), which is also catalytically active can be found in the EE, ER and Golgi apparatus. It is proteolytically processed to mature GILT along the endocytotic pathway.[85] Mature GILT exclusively colocalizes in MHC class II containing compartments, so it was suggested that precursor-GILT reduces internalized antigens in early endosomes, while mature GILT is responsible for disulfide cleavage in subsequent endolysosomal compartments.[70] A number of characteristics distinguish GILT from members of the thioredoxin family. To begin with, thioredoxins typically have exhibit optimal activity in a pH range from 6 to 7. Contrastingly, GILT is much more efficient at pH ranging from 4 to 5, as is found in late endocytotic compartments.[85] Another difference is the choice of co-reductands as, unlike PDI, GILT is activated only by cysteine, not by glutathione.[83] It is not yet clear if similar redox proteins are present in endosomes or lysosomes of other cells, but some evidences suggest that this might indeed be the case.[70] For the

construction of bioresponsive carriers it would also be interesting to know if these oxireductases recognize all synthetic disulfide linkers.[72]

Additionally, some recent workings indicate the participation of other enzymes which are usually not associated with thiol reduction of internalized disulfides. Our current models might be overly simplistic: Yang *et al.* not only excluded PDI as a major reducing factor in KB cells but also showed that the cellular reduction machinery is active all along the endocytotic folate receptor pathway.[75] This machinery was neither associated with any particular trafficking organelle, nor relied on fusion with lysosomes or an interaction with the Golgi network **(Figure 3)**. So far, no GILT expression has been observed in this cell line; nonetheless, the results signaled the presence of an endosomal redox function. They speculated that this function might be associated with the transferrin receptor (TfR) pathway, as the folate receptor (FR) is rapidly colocalized with TfR after uptake. The disulfide cleavage could be mediated by an endosomal ferrireductase that normally converts Fe^{3+} to Fe^{2+} in the TfR cycle. This and a later study of this group also have interesting implications for the trafficking of receptor ligand-based targeted gene delivery vehicles.[86] Multivalent folate conjugates, as they would be used in cationic polymeric carriers, rapidly traffic to LEs or lysosomes, whereas trafficking of monovalent conjugates does not involve acidic compartments. Hence, in case of gene delivery with targeting receptor ligands, it would be advantageous to use acid labile linkers instead of disulfide linkers. The experiments done with the selfquenching trastuzumab-SPP-rhodamine red construct (Austin *et al.* [72]) further emphasize our still limited knowledge on cellular disulfide cleavage. In spite of extensive trafficking through the endocytotic recycling pathway, their construct unexpectedly resulted in little dequenching, i.e. linker reduction. They also diverted their probe to lysosomes using geldanamycin, where dequenching was observed. They showed that this was not attributed to disulfide reduction but to proteolytic degradation of the antibody. Lysosomal reduction appeared to be rather ineffective. These findings were confirmed with fusion proteins of redox sensitive roGFP1 (reduction-oxidation-sensitive green fluorescent protein) with different endocytotic
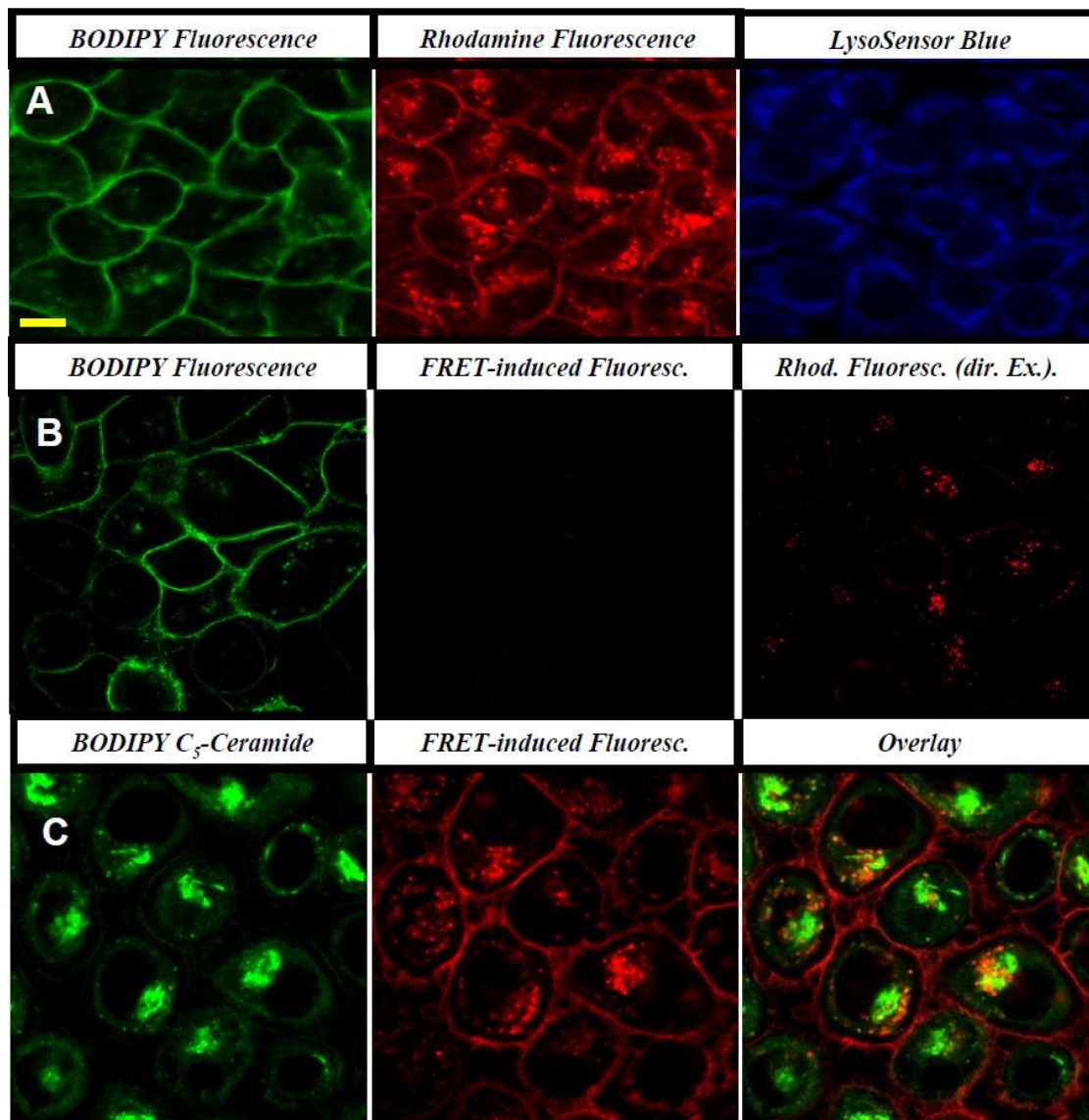
Figure 3. Lysosomes or Golgi/trans-Golgi network (TGN) system are involved in disulfide bond reduction of a folate-FRET reporter: The FRET probe consisted of rhodamine linked via a disulfide bond to BODIPY-folate. The intact conjugate shows red fluorescence. (A) Lysosomes are no significant site of disulfide reduction. Neither the folate-FRET reporter nor its reduced fragments localize in lysosomes. (B) The collapse of the Golgi network induced by brefeldin A (BFA) does not interrupt disulfide reduction of the folate-FRET conjugate. (C) The Folate-FRET conjugate is not trafficked to the Golgi/TGN system. (Ceramide is a Golgi/TGN-marker). [75]

markers. Surprisingly, endosomes and lysosomes were found to be oxidizing. Minor subsets of reducing lysosomes, however, could not be detected with this method because the average fluorescence of the whole endocytotic compartment was measured. Besides, the lysosomal proteins used were membrane bound such that subregions (middle of the lumen) of reducing potential within any one endolysosome could not be excluded.[72] The comparability to other studies is also unclear. For example, Trastuzumab-SS-RR might have been directed to another pathway with other redox characteristics than the folate-probe from Yang *et al.*, or redox active enzymes could not recognize this linker.[86]

If we assume that the endolysosomal compartment is indeed oxidizing then why do so many studies indicate a reducing environment? The proteolysis of antigens in APCs might already be so efficient that there is no need for an additional disulfide reduction step. Also, GILT-like enzymes could act reducing despite oxidizing conditions.[72] In case of disulfide bearing drugs, the experimental setup might explain their *in vitro* and *in vivo* potency. The disulfide cleavage might indeed be very slow and ineffective but given that *in vitro* cytotoxicity studies typically require several days (and even longer in *in vivo* studies) before proliferation effects can be observed still a sufficient amount of drug should be released.[72]

The multitude of (sometimes contradicting) results and the uncertainty in whether or not those results can be transferred directly to cationic gene delivery devices leave many unanswered questions. Among many other factors, cellular disulfide reduction seems to depend on the expression level and location of redox enzymes (PDI, GILT, etc.). Vesicular trafficking properties vary with carrier type, composition and the type of delivered nucleic acid.[66, 67, 87] It is also likely that the linker has an influence, but this factor has not examined in detail yet.

It must also be kept in mind that the cell lines used in most *in vitro* studies are not directly comparable to primary cells, as they tend to have adapted to the *in vitro* culture environment.[1] In a study related to this three different cell lines and primary cultures of fibroblast and BMM

(bone marrow-derived macrophages) were transfected with LLO-SS-PN/luciferase.[81] Expression levels were tested in the presence of the membrane-impermeant thiol blocker DTNB. DTNB treatment resulted in higher luciferase levels in BMM exclusively indicating that the situation in primary cells may be much different.[1]

4. Synthesis of disulfides

Although contradictory results are obtained in some studies, there is no doubt that disulfides are an advantageous functional group. However, disulfides are not as commonly used as, for example, amine groups and, but many different ways for the conversion of other groups as well as the use of linkers are known.

4.1. Use of inherently present thiol groups

The easiest way to form disulfide bonds is by oxidizing thiol groups that are inherently present in the chosen molecule. Oxidation of the thiol to disulfide can be accomplished with oxygen or with a mild oxidizing reagent like dimethyl sulfoxide (DMSO).[88] A great advantage of DMSO is that the disulfide formation is very controllable, resulting in products with well-defined molecular weights.[89] This was shown for linear PEI that was synthesized by connecting low molecular weight PEI molecules with terminal thiol groups.[90]

### 4.2. Conversion of other functional groups

If no thiol group is present in the molecule of interest, other functional groups can be used for its formation. One possibility is to convert a hydroxyl group through the addition of a thioacetate which is subsequently cleaved to the thiol group **(Table 1)**.[90-93]
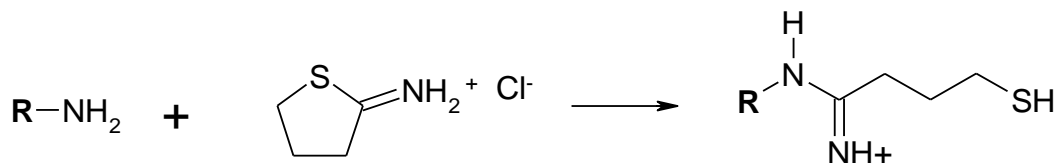
4.2.1. Conversion of amino groups

The most common way of introducing thiol groups starting from amino groups is by using 2-iminothiolane, commonly known as Traut´s reagent **(Table 1)**. This compound reacts easily with primary amines at pH 7-10 [94-96] in both molecules with low molecular weight and macromolecules such as chitosan.[97] This is advantageous in that the positive charge inherent in primary amine groups at physiologic pH is maintained after the reaction.[98] Moreover, a number of derivatives of Traut´s reagent have been synthesized allowing the creation of a more stable disulfide bond.[99, 100] An alternative way to accomplish the same thing involves the ring-opening addition of N-acetylhomocysteine thiolactone [101, 102] or methyl thiirane [103] to primary amino groups. The introduction of a protected thiol group is possible if S-acetylmercaptosuccinic anhydride (SAMSA) is applied **(Table 1)**. The anhydride ring can be opened, thereby creating a free carboxylate group that exhibits a negative charge, in contrast to the positively charged amino group present in the molecule initially.[104] Insertion of protected thiol groups is especially convenient because this allows for long-term storage and the formation of a mixed molecule consisting of two different thiol-containing substances. Protected thiols can also be inserted if N-succinimidyl S-acetylthioacetate (SATA) or succinimdyl acetylthiopropionat (SATP) are used. These two differ only in chain length, and both of them form stable amide bonds. The protection of the thiol group ensures the formation of a single product as seen for SAMSA.[94, 95, 105]

Table 1. Conversion of different functional groups into thiol groups

Conversion of hydroxyl groups
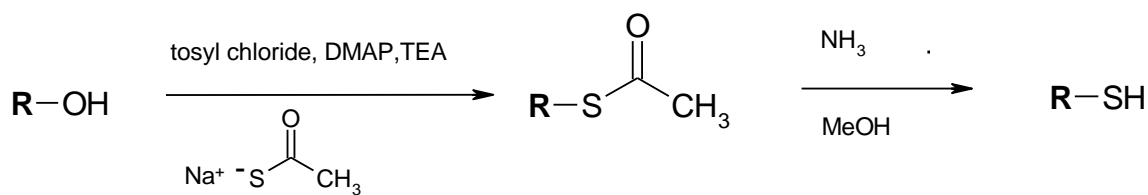
Conversion of amino groups using Traut´s reagent

Conversion of amino groups using SAMSA
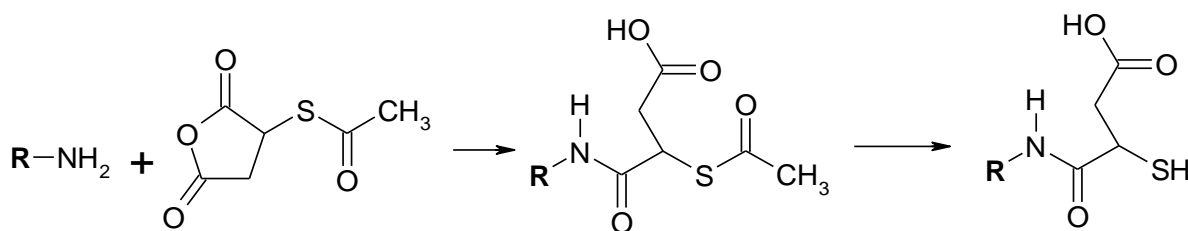
Conversion of carbonyl groups using AMBH
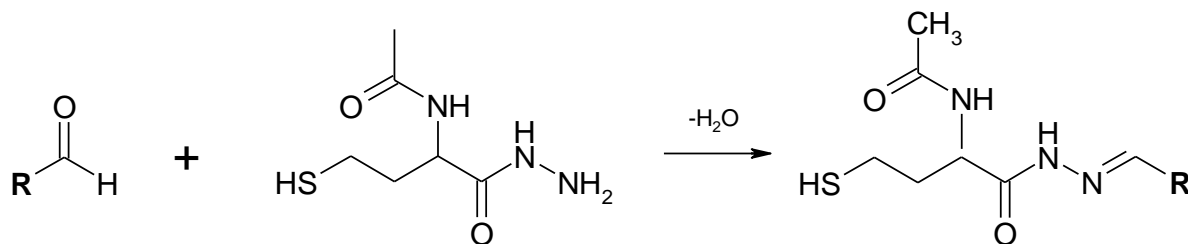
Conversion of carboxyl groups using cystamine
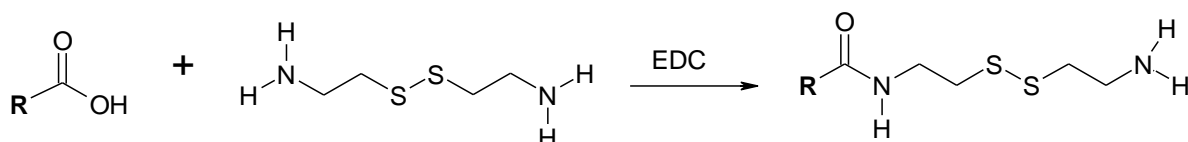
4.2.2. Conversion of carbonyl groups

2-acetamido-4-mercaptobutyric acid hydrazide (AMBH) contains a thiol group and is reactive

with aldehydes and ketones. These carbonyl compounds can be easily created from

carbohydrates by oxidation with sodium periodate under mild conditions. When ketones and aldehydes react with the hydrazide group of AMBH, they form hydrazone linkages **(Table 1)**.[95] Cystamine can also be used for this purpose. In this case, the amine group of cystamine reacts with the carbonyl group, creating a thiol group at the end of the conjugate after reductive cleavage of the disulfide bond.[106]

4.2.3. Conversion of carboxyl groups

Cystamine can not only be conjugated with carbonyl groups, but it is also beneficial for conjugation with activated carboxyl groups, leading to the formation of a stable amide bond. Further conjugation steps can be carried out with the second amino group of cystamine **(Table 1)**.[106-110]

4.3.   Use of linkers

In many cases, the use of linkers may be preferable to the conversion of functional groups, as linkers usually require fewer reaction steps and therefore provide higher yields. There are two main classes of linkers, homo- and heterobifunctional ones. Homobifunctional linkers possess the same terminal functional groups, so they are ideally suited for the connection of similar molecules forming dimers. In contrast, heterobifunctional linkers are generally utilized if two different molecules need to be connected selectively.

4.3.1. Homobifunctional linkers

4.3.1.1.   Amine-reactive linkers

Among the homobifunctional linkers, amine reactive linkers are especially important because amines are ubiquitous in biological molecules. One of the most popular crosslinkers containing a central disulfide bridge is dithiobis(succinimidylpropionate) (DSP), also known as Lomant´s reagent **(Table 2)**. Here, the two NHS-ester moieties rapidly react with primary and secondary

aliphatic amino groups to yield stable amide bonds. For conjugation reactions in aqueous phases, the hydrophobic linker molecule must be dissolved in polar organic solvents before being added to the reaction solution, which would ideally be a buffer at pH of 7-9.[95] In order to create a water-soluble linker dithiobis(sulfosuccinimidyl propionate (DTSSP), which includes two sulfonated NHS-ester groups, was synthesized.[95, 111]

Another homobifuctional amine-reactive linker is dimethyl 3,3`-dithiobispropionimidate (DTBP), commonly called Wang and Richard´s reagent **(Table 2)**. The water-soluble molecule reacts with amines in a pH range of 7-10. The special feature of this linker is that it preserves the positive charges of the amino groups due to the linker molecule`s intrinsic positive charge.[95, 109, 112] Cystamine bisacrylamide (CBA) is also able to crosslink amino groups by Michael addition, yielding reductively cleavable products.[113, 114]

4.3.1.2.   *Thiol-reactive linkers*

One example in which linkers react with thiol groups involves 1,4-di[3`-(2`-pyridyldithio)propionamido]butane (DPDPB) **(Table 2)**. Both ends of this 14-atom linker are dithiopyridyl groups that are able to undergo disulfide exchanges with free thiols resulting in a product containing two disulfide bridges.[95, 115]

4.3.1.3.   *Photo-reactive linkers*

While the linkers mentioned herein react specifically with one particular functional group, unspecific reactions with many different functional groups can be obtained with bis-[β-(4-acidosalicylamido)ethyl]disulfide (BASED), a symmetrical photoreactive linker with a disulfide bridge in its center **(Table 2).** The aryl azide groups at the linker's ends are substituted with a hydroxyl group, which activates it for nucleophilic attacks and allows for radioiodination with ^{125}I prior to conjugation. After crosslinking, the central disulfide bond can be cleaved while the radioiodide label is still available on each of the formerly crosslinked molecules.[95]

Table 2. Homobifunctional linkers

Amine reactive linkers

DSP
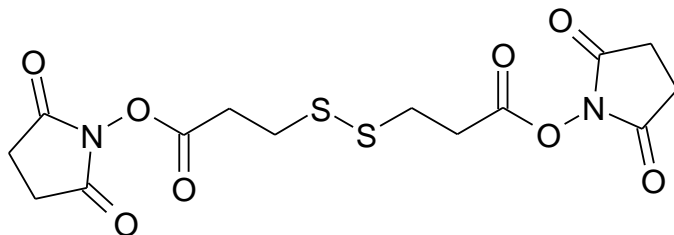
DTBP
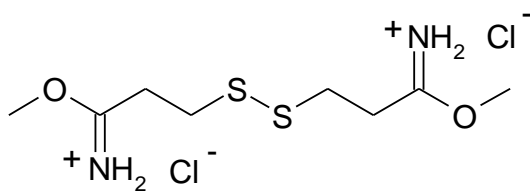
Sulfhydryl reactive linker

DPDPB
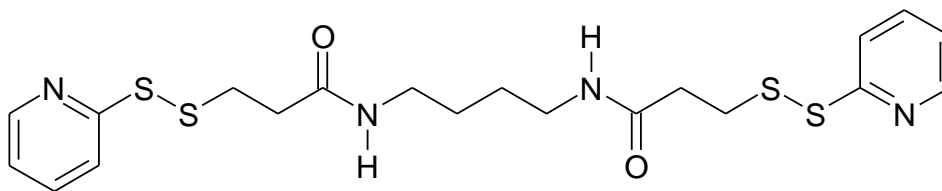
Photoreactive linker

BASED
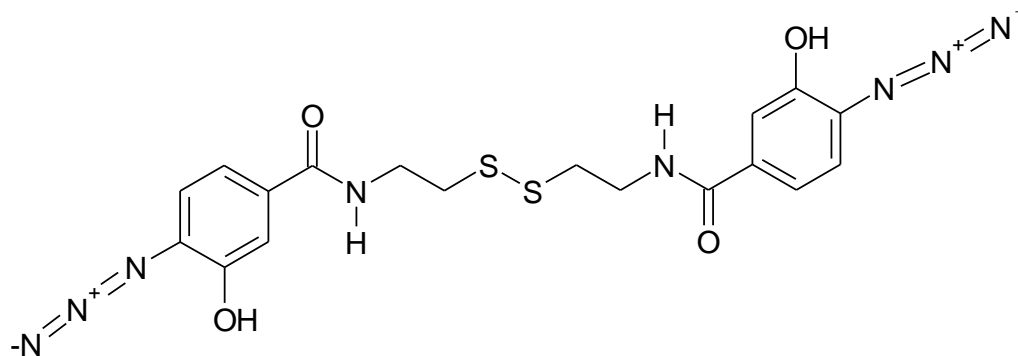
4.3.2.   Heterobifunctional linkers

Although crosslinkages between two equal groups can be easily performed with homobifunctional linkers, this approach lacks selectivity. If a conjugate of two different molecules is desired, the use of heterobifunctional linkers must be considered. If a disulfide bond should be present in the conjugate, amine-and thiolreactive linkers are especially advantageous, as would be linkers that are photosensitive and amine- or thiolreactive.

4.3.2.1.   Amine-and thiol-reactive linkers

One of the most common heterobifunctional crosslinkers is N-succinimidyl 3-(2-pyridyldithio)propionate (SPDP) **(Table 3)**. One end of this molecule contains an NHS-ester moiety that reacts selectively with amines at pH 7-9 and allows for the differentiation between ε- and α-amino groups through variation of the pH. The product can be stored since the 2-dipyridyl disulfide acts as a protecting group. In the presence of thiol groups, disulfide exchange takes place.[116] Analogous linkers include LC-SPDP (the long chain version of SPDP) [95], sulfo-LC-SPDP (water-soluble long-chain derivate) [95] and SPP (N-succinimidyl 4-(2-pyridyldithio)pentanoate) (a branched, longer chain derivative).[72]

S-4-succinimidyloxycarbonyl benzyl thiosulfate (SBT) is another linker that is able to connect amines with thiol groups via an NHS-ester moiety and a thiosulfate group **(Table 3).** Here, the attachment of the thiol group is quite labor-intensive as there are many reaction steps involved.[117] The same applies to the sterically more demanding and, thus, more stable structure analogue, S-4-succinimidyloxycarbonyl-αmethyl-benzyl thiosulfate (SMBT).[118]

Similar in structure, but easier to work with due to fewer reaction steps, are 4-succinimidyloxycarbonyl-α-methyl-α(2-pyridyldithio)toluene (SMPT) and the water-soluble analog sulfosuccinimidyl-6-[α-methyl-α-(2-pyridyldithio)toluamido] hexanoate (Sulfo-LC-SMPT). Both form disulfide bridges by simple disulfide exchanges.[118] Another possibility for crosslinking

amines is the reaction with thioimidate groups, as in the case of 3-(4-carboxyamidophenyldithio)-propionthioimidate (CDPT) and ethyl S-acetyl-propionimidate (AMPT) **(Table 3)**. Both linkers can be used for controlled reactions because of their protected thiol moiety.[119, 120] Disulfide bridges with sulfosuccinimidyl N-[3-(acetylthio)-3-methylbytyryl-β-alaninate (sNHS-ATMBA) are very stable due to a sterically hindered α-carbon atom.[121]

4.3.2.2.   *Thiol- and carbonyl-reactive linkers*

Due to its pyridyl disulfide end, 3-(2-pyridyldithio)propionyl hydrazide (PDPH) undergoes disulfide exchanges **(Table 3)**. The hydrazide reacts with carbonyl compounds and, thus, the molecule is extremely useful if glycoproteins or antibodies are coupled, because the carbohydrate moieties usually are far away from the active centers. As a result, their activity is not impaired.[95, 122]

4.3.2.3.   *Amine- and photo-reactive linkers*

The great advantage of photoreactive linkers is the fact that they can be made reactive "on demand" by simple exposure to light. Most linkers contain aryl azide moieties that are activated by irradiation with light in the long UV region. The optimal excitation wavelength depends on the substituents at the aryl azide. If a nitro group is present, the molecule can be photolysed with light of a wavelength of about 350 nm, due to the electron withdrawing effect of the substituent. In contrast, if the aryl azide is substituted with a hydroxyl group, the linker can undergo electrophilic substitutions. Hence, radioiodide labelling prior to use of the linker is possible. Though these linkers exhibit many advantages due to their flexibility, they lack specificity for particular functional groups and yields are generally not high: in many cases only around 10 % of the linker react.[95, 115]

Two examples of photoreactive linkers containing disulfides are the water-insoluble N-succinimidyl(4-azidophenyl)-1,3`-dithiopropionate (SADP) **(Table 3)** and its water-soluble analog

N-sulfo- succinimidyl(4-azidophenyl)-1,3`-dithiopropionate (Sulfo-SADP). They can be activated by irradiation in the range of 265-275 nm [95], while sulfosuccinimidyl-2-(m-azido-o-nitrobenzamido)-ethyl-1,3`-dithiopropionate (SAND), substituted at the benzyl ring with an nitro group, can be activated with light of a slightly lower wavelength **(Table 3)**.[95] Sulfosuccinimidyl-2-(p-acidosalicylamido)ethyl-1,3`-dithiopropionate (SASD) **(Table 3)** is a linker that is suitable for radioiodination.[95, 123] Further developments in linker design have led to the synthesis of sulfosuccinimidyl-2(7-azido-4-methyl  coumarin-3-acetamide)ethyl-1,3`-dithiopropionate (SAED) **(Table 3).** This reagent becomes fluorecescent after initiation of the photolysis, indicating the amount of molecules modified by the intensity of fluorescence detectable.[95]

Table 3. Heterobifunctional linkers

<u>Amine- and thiol-reactive linkers</u>

SPDP

SBT
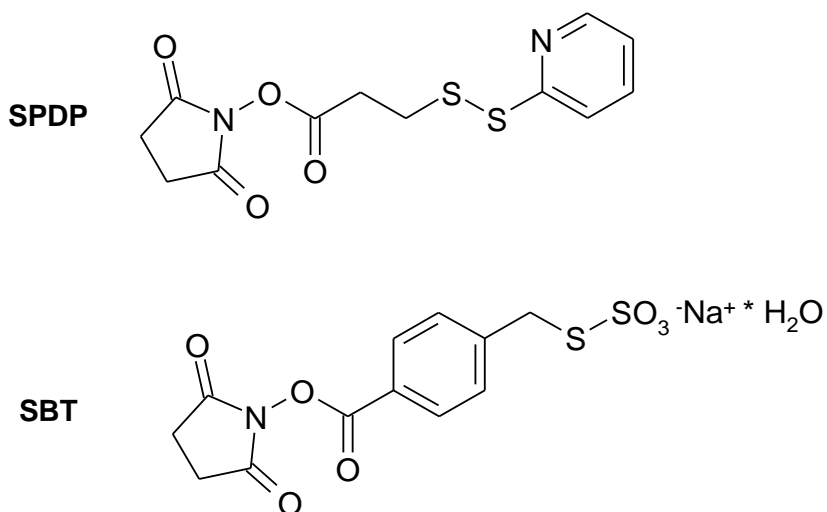
CDPT
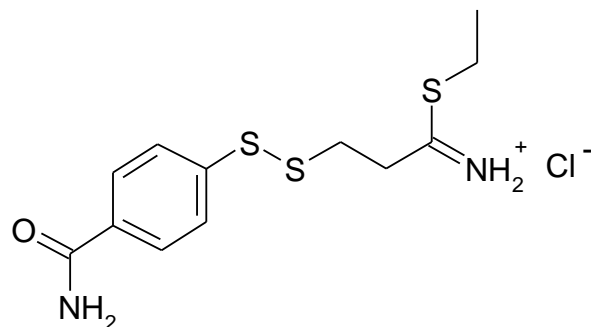
AMPT
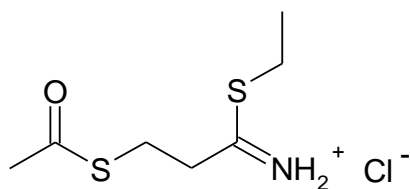
Thiol- and carbonyl-reactive linker

PDPH
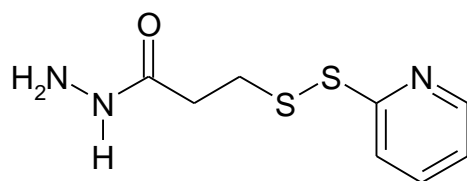
Amine- and photo-reactive linkers

SADP
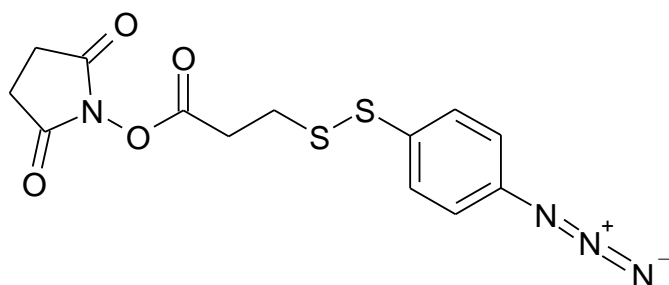
SAND
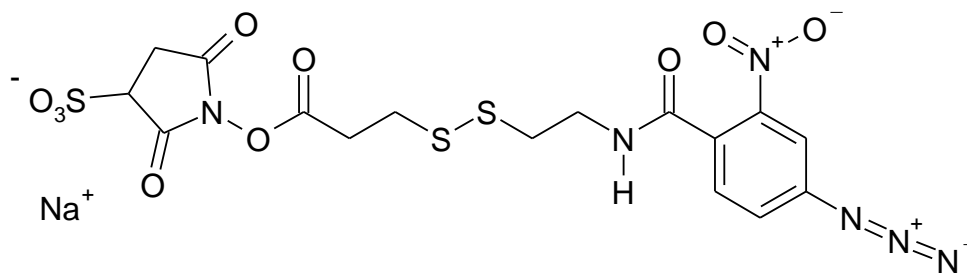
SASD
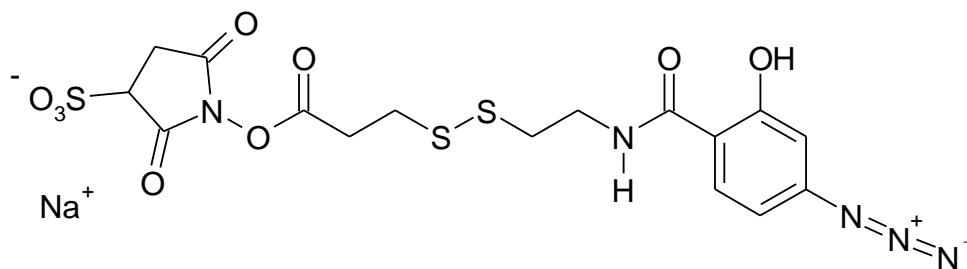
SAED
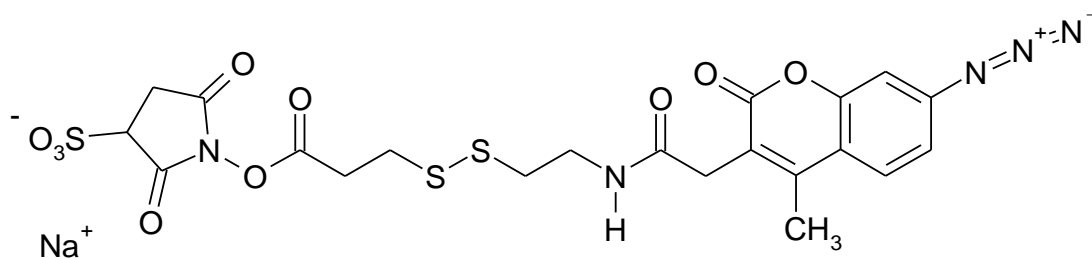
Thiol- and photo-reactive linker

ADPD
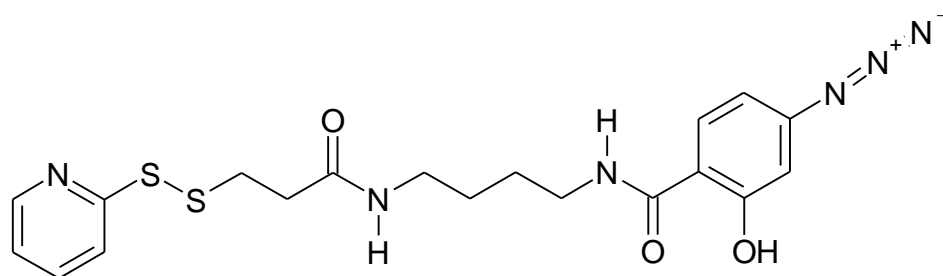
4.3.2.4.   Thiol- and photo-reactive linkers

Though amine reactive photolinkers are predominant, a thiol reactive linker exists, namely the radioiodinatable   N-[4-(p-azidosalicylamido)butyl]-3`-(2`-pyridyldithio)propionamide   (ADPD), which undergoes disulfide exchanges **(Table 3)**.[123, 124]

5. Examples for the use of disulfides

5.1.   Disulfides for the stabilization of the carrier

A prerequisite for every systemic nucleic acid delivery system is stability in the blood stream prior to reaching its target cell. Therefore, the carrier must prevent the premature release of its load. As already discussed, especially in tissue engineering applications, long-term stability, which is adjusted to tissue formation, is a major requirement as well. In order to enhance the stability of the delivery system either the surface of the carriers was crosslinked, or the low molecular weight materials were sulfhydryl polymerized.[125-129]

The principle of stabilization via disulfide bonds has been demonstrated for many liposome-based carriers, e.g. for $C_{12}CCP$. This cationic detergent was synthesized by amide bond formation between dodecanoic acid, cysteinyl-cysteine and diaminopropane. Due to intermolecular disulfide bond formation, stable liposomes with pDNA were obtained. These lipoplexes were indifferent towards anion exchange, but when treated with 1,4-dithiothreitol (DTT), their load was released immediately as shown by gel retardation. However, the disulfides could not be destabilized by glutathione, the natural reducing cofactor present within cells.[130]

Guanidinocysteine N-decylamide (C_{10}-C^{G+}), a cationic amphiphile, was also used to form disulfide stabilized particles with individual pDNA molecules. These complexes were "frozen" on the template DNA when the cysteine detergent was dimerized by oxidation, and the resulting spherical polyplexes remained unchanged at physiological salt concentrations for several days

(Figure 4).[131] Another kind of template polymerization was investigated with bis(2-aminoethyl)-1,3-propandiamine (AEDP). It was polymerized by crosslinking with disulfide containing linkers such as DTBP. The formation of polyplexes was only possible if pDNA was present during the polymerization reaction. After treatment with DTT the disulfides were reduced, thereby releasing pDNA, which led to significantly increased transfection efficiency.[132] The same "caging effect" could be observed when pLL was crosslinked with DTBP in presence of pDNA.[133]
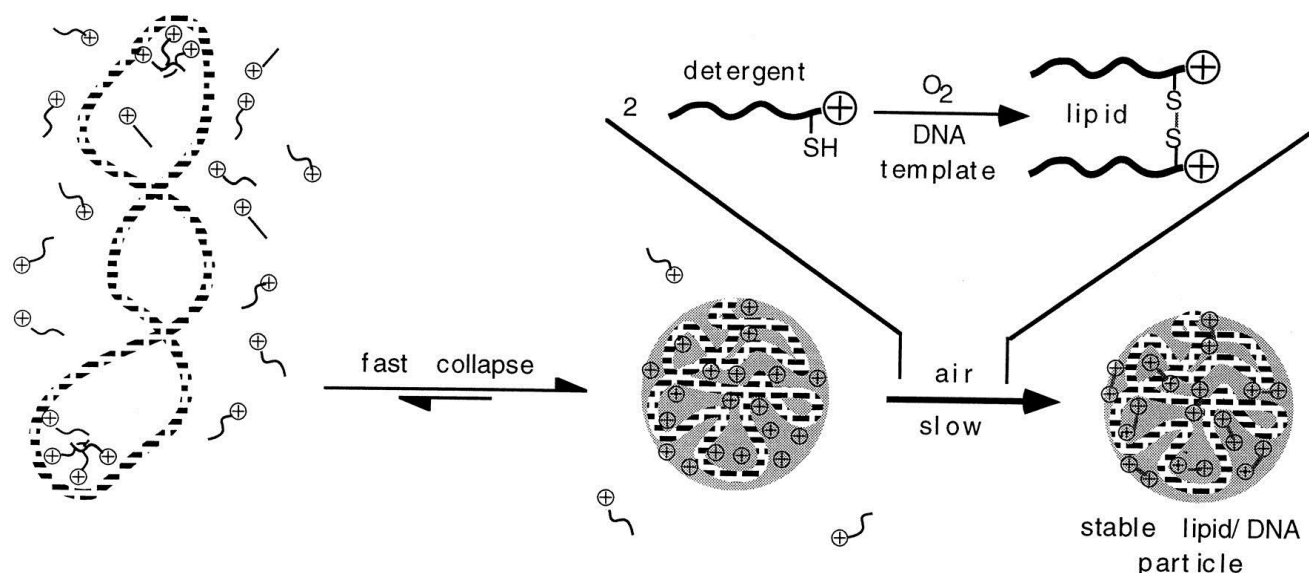
Figure 4. *Schematic representation of a disulfide-stabilized liposome. First, the detergent molecules are collapsing in presence of a template such as DNA, thereby forming detergent/DNA-particles. Thereafter, the oxygen of the air slowly oxidizes the detergent molecules forming stable, disulfide-crosslinked lipid/DNA particles.*[131]

Another liposome that benefited from disulfide bonds in terms of enhanced stability was formed from 1,2-dioleoyl-sn-glycero-3-succinyl-2-hydroxyethyl disulfide ornithine conjugate (DOGSDSO) and L-dioleoyl phosphatidyl ethanolamine (DOPE). The disulfide bond was cleaved in reducing media *in vitro*, thus destabilizing the liposome/DNA complex and increasing the pDNA release. This led to enhanced transfection activity in different neural animal cell lines. Compared to its

non-disulfide analogue, up to a 50-fold higher transgene production was obtained.[134, 135] However, using this delivery vehicle did not significantly diminish cytotoxicity. It is speculated that the linker was probably too strong to be degraded on the required time scale. To overcome this problem, another cationic lipid, cholesteryl hemidithioglycolyl tris(aminoethyl)amine (CHDTAEA), was synthesized. Herein, dithioglycolic acid was used as a trigger for the reductive environment. The incorporated disulfide bond was weaker compared to the one in DOGSDSO, and therefore, it was easily cleaved in presence of 10 mM GSH, releasing more than 50 % of the DNA. The overall transfection efficiency was higher than that of its non-disulfide analogue, and the cytotoxicity decreased significantly. [136]

Other carriers such as chitosan (deacetylated chitin [26]) were also stabilized via disulfide bonds. For this purpose, the primary amino groups of low molecular weight chitosan were thiolated with 2-iminothiolane. These modified polymers, i.e. chitosan-thiobutylamidines, were mixed with pDNA to form coacervates in the nanometer range. After disulfide crosslinkage, they were stable at acidic pH and exhibited increased resistance against salt-induced ion-exchange, which was ascribed to the tighter binding of pDNA to the thiolated matrix.[128] In another approach thiols were introduced into 33 kDa chitosan with thioglycolic acid and crosslinked afterwards. These chitosans exhibited improved physical stability and increased mucoadhesiveness due to better cell adhesion as mediated by the disulfides. Moreover, crosslinking resulted in enhanced cellular uptake and, thus, reporter gene expression and the subsequent duration were increased significantly in *in vivo* experiments.[137]

α,β-poly(N-2-hydroxyethyl)-D,L-aspartatamide (PHEA) is another gene carrier that benefits from disulfides. This carrier can be functionalized with ethylene diamine to obtain primary amino groups that can be further modified to provide a disulfide bond and a positive charge. When utilized, this non-viral vector condensed DNA into particles stable towards polyanion exchange. The stability of these "thioplexes" was so high that they were capable of circulating in the blood

stream without release of the entrapped DNA. Furthermore, the complexes dissociated in presence of glutathione, thus liberating their load and providing high transfection levels and low toxicity in *in vitro* experiments with murine B16F10 melanoma cells and murine N2A neuroblastoma cells.[125]

Peptides containing many lysines and histidines were used for the complexation of nucleic acids, while cysteines were introduced to obtain stable and reductively degradable carriers. A series of different vehicles was built from sequences of many lysines, tryptophan and a variable number of cysteines. All obtained peptides were able to condense DNA into particles and exhibited increased stability after disulfide formation. The disulfide crosslinked carriers conveyed 5 to 60 fold higher gene expression as compared to their non-crosslinked analogues. The degree of gene expression was dependent on the number of incorporated cysteines, with a maximum for terminally inserted cysteines.[138] Since these peptides were quite promising, they were further modified with PEG and triantennary peptide for successful liver targeting.[139] A shorter peptide sequence, cysteine-histidine-lysine$_6$-histidine-cysteine, was able to condense DNA effectively as well.[140] Another approach to condensing pDNA into particles involved a system containing cysteine-rich peptides that were coupled to either PEG or the triantennary peptide, a moiety that is capable of targeting hepatocytes. Shielding and targeting moieties were coupled to the N-terminal cysteine, while the internal cysteines were transiently acetamidomethyl-protected. Thereafter, the PEG-peptides as well as the glycopeptides were mixed with pDNA and the resulting particles were polymerized by disulfide formation of the internal cysteines, thus creating stable gene vectors.[141, 141]

Two similar lysine-rich and cysteine-terminated petides were also used to deliver DNA. They were 21 amino acids long and possessed either a transglutaminase substrate site or a NLS. These peptides condensed DNA efficiently and could be covalently immobilized into a fibrin matrix with the help of the transglutaminase sequence. When the fibrin-matrix was degraded,

DNA was released and the cells seeded in the matrix were transfected.[142] Such a system was also employed for the *in vivo* delivery of an oxygen-insensitive hypoxia-inducible factor-1α variant which induces vascular endothelial growth factor (VEGF) expression. Here, the carriers embedded in the fibrin matrix were applied to dermal wounds in mice. As a consequence, one week after treatment 4 times more mature blood vessels were detected compared to the application of VEGF-A$_{165}$ protein.[56]

Plasmid DNA encoding VEGF was also delivered with a reducible disulfide poly(amido ethylenediamine (SS-PAED). In this study hypoxia-inducible VEGF expression in a rabbit myocardial infarct model was up to 4 times higher than the control showing the usefulness of disulfide stabilised carrier systems for the in vivo delivery of growth factors [55] which are usually degraded within minutes.[143]

A very prominent example to enhance the stability of the carrier was shown by Chen *et al.* They used melittin, the main component of bee venom, which is known for its endosomolytic activity. It was modified with some additional lysine residues and a terminal cysteine at each end. Since a single melittin molecule does not exhibit enough positive charges to bind to DNA, it was polymerized via disulfide bonds. The obtained molecule condensed DNA efficiently and possessed reduced hemolytic activity when bound to DNA. Cell transfection experiments revealed up to ten-fold better results for this system when compared to the control-peptide, cysteine-tryptophan-lysine$_{17}$-cysteine. Although the hemolytic activity was reduced by this modification, it seemed to still be enough for endosomal release and carrier disassembly in the reductive environment of the cytosol.[127]

The modification of the ε-amino groups of pLL with 3-(2-aminoethyldithio)propionyl residues [144] or their crosslinking with DTBP comprises another approach utilizing reductively degradable gene carriers.[145] These molecules were able to complex nucleotides into particles that were stable under physiological conditions but disintegrated upon treatment with GSH.

PEI 25 kDa was also stabilized via disulfide containing linkers, namely, DSP and DTBP. If the crosslinking reaction was conducted at low molar ratios (≥ 10:1   linker : PEI 25 kDa), the PEI/DNA polyplexes were stable against polyion disruption, while the crosslinking could be reversed using 20 mM dithioerythritol.[146] In *in vivo* experiments, disulfide crosslinked polyplexes showed increased blood concentrations and longer circulation times, both of which depended on the crosslinking degree.[147]

Lee *et al.* used thiolated hyaluronic acid for the encapsulation of oligonucleotides as well. Nanogels were formed by crosslinking via disulfide bond formation in presence of siRNA. The release of the load from the nanogels was proportional to the amount of glutathione in the buffer making this very controllable, while the disulfides were stable in a non-reducing environment. The gels were readily taken up by hyaluronic acid receptor positive cells, and the gene encoding for green fluorescent protein (GFP) was efficiently silenced, indicating triggered erosion/biodegradation in a reductive environment.[148] Thiol groups were also inserted into polyacrylic acid. Here, the carboxy groups of the acid reacted with L-cysteine. Thereafter, the polymer was gelated by adjusting the ion concentration and crosslinked via disulfides. Due to these bonds, particles stable under acidic conditions and with longer residence time in the gastrointestinal tract were obtained, seeming to be suitable to deliver therapeutic proteins, genes or antigens orally as well as transdermally.[149]

Zelikin *et al.* demonstrated that the stability of Layer-by-Layer (LbL) films can be controlled via disulfides. Polymethacrylic acid was functionalized with cysteamine, and this polymer was applied for the fabrication of capsules with polyvinylpyrrolidon (PVP). They were assembled by an LbL-technique to form hydrogen-bonded polymer multilayers that were crosslinked by disulfide bonds. These deposits were stable at physiological pH, but were amenable to degradation in the presence of reducing agents such as DTT.[150] The same degradation phenomenon was observed for an LbL-film that consisted of CBA-crosslinked N-tert-

butoxycarbonyl-1,4-diaminobutane and DNA.[151] The LbL-technique was used to coat a stainless-steel mesh. Here, the layers consisted of DNA and reducible hyperbranched poly(amidoamine). *In vitro* these films showed higher levels of transgene expression compared to films built of DNA and bPEI 25kDa. Furthermore, the duration of transfection was significantly longer in NIH-3T3 cells. The authors speculated that this was due to the mild reducing microenvironment of the plasma membrane of the growing cells which reduced the disulfide bonds. The authors concluded that the very high levels of alkaline phosphatase that were induced by the coated meshes in *in vivo* experiments were due to the sustained gene expression from the LbL-film rather than the persistence in the plasma.[152]

5.2.   Disulfides for the attachment of a shielding moiety

Polyplexes and lipoplexes do not only interact with target cells, but can also adhere nonspecifically to other cells and extracellular components such as serum proteins. Especially for cationic polyplexes, interaction with components of the immune system is a major problem. This issue can be alleviated by modifying the surface of the particles with hydrophilic or uncharged "protein repulsive" molecules, such as polyethylene glycol (PEG) [153] or poly[N-(2-Hydroxypropyl)methacrylamide] (PHPMA). [154] Such a shielding additionally provides reduced toxicity, prevents aggregation and prolongs the half-life of polyplexes. [155]

One approach to enhance the stability of so-called polyion micelles (PIC micelles), which are micellar structures formed from ionic block copolymers and nucleic acids via disulfides, entails mixing thiolated poly(ethylene glycol)-block-poly(L-lysine) (PEG-thiopLL) and oligodesoxynucleotides (ODNs). These molecules were seen to spontaneously associate and form a crosslinked core. The disulfide provided appreciably increased stability for these micelles and allowed the liberation of ODNs and dissociation in the presence of GSH at intracellular concentrations.[156]

Stable gene vehicles were also attained when a terminally thiol-functionalized branched six-arm PEG was used to solubilize DNA. Disulfides crosslinked the DNA/PEG nanocomplexes, resulting in DNA/PEG nanogels that were stable in aqueous solutions but able to release DNA in reducing environments, as shown by gel retardation assays before and after DTT treatment.[157]

DOPE and N-[2-ϖ-methoxypoly(ethylene glycol)-α-aminocarbonylethyl-dithiopropionate] formed a liposome that was covalently coupled to distearoylphosphatidylethanolamine (mPEG-S-S-DSPE). The incorporation of the mPEG-S-S-DSPE stabilized these liposomes at low pH, but the stabilizing effect was reversed as soon as the carrier was incubated with either DTT or cell-free extracts. Under these conditions, the disulfides were reduced, and thus the protecting PEG chains were cleaved, and the vehicle became degradable at low pH, releasing its load.[158, 159]

Disulfides were used for the formation of copolymers consisting of bPEI 25 kDa and PEG of 20 kDa or 30 kDa. The connection of PEG via DSP led to a 125 % increase in blood levels and decreased hemolysis compared to bPEI 25 kDa.[160] Carlisle *et al.* showed the stabilization of PEI polyplexes with DNA. To this end, thiol groups were inserted at the chain ends of branched PEI (bPEI). Next, disulfide bonds were formed with thiol-reactive derivatives of PHPMA, creating stable surface-coated nanoparticles that were able to condense pDNA. The disulfides provided stability against a 250-fold excess of the counterion poly(aspartic acid) (pAA). After treatment with DTT, the disulfides were reduced, leading to complete release of the pDNA. In comparison to the thioether analogues, the reducible nanoparticles exhibited 40-100-fold higher transfection efficiency. [161]

Generally, the kind of linker affects the degradation of the disulfide bond and hence the liberation of the load. This was nicely demonstrated for a copolymer of PEG and L-lysine, which was coupled to the peptide Tat9K(bio)-Cys via a disulfide bond. Either an unsubstituted disulfide or a sterically hindered disulfide was used. Both formulations were stable in an oxidative environment, but exhibited marked differences when exposed to a reductive milieu. In this case,

the polymer with the unhindered disulfide bond exhibited a fairly short half-life of release, whereas the sterically hindered disulfide bond released its load about 100 times more slowly.[107] The influence of the kind of crosslinkage was also shown for another polyethylene glycol-poly-L-lysine (PEG-pLL) system. Here, thiol groups were introduced into the block copolymers, either with the crosslinker SPDP or with Traut´s reagent. In case of Traut´s reagent, the positive charges of pLL´s amino groups were preserved after derivatisation, while for SPDP, the positive charges were neutralized due to formation of an amide bond. Both thiolated PEG-pLLs efficiently complexed pDNA into disulfide crosslinked polyplexes thatwere more stable than the unmodified ones. Moreover, the crosslinking prevented them from dissociation through counterion exchange. However, in contrast to the polyplexes treated with Traut´s reagent, the polyplexes thiolated with SPDP were able to release pDNA in response to a reductive environment. These carriers also showed 50 times higher transfection efficiencies compared to the polyplexes with conserved charge and thus, the overall strength of binding was higher.[162] Generally, the complexation ability of gene carriers is strongly dependent on the type of linker [163] or the resulting charge density, but the degree of thiolation also plays a role. In this context, it was shown that a thiolation degree of 28 % balanced the demands of stability and efficient release of pDNA in reductive environment in an optimal manner.[162] The stability of these micelles was also tested when the model drug pAA was incorporated. These disulfide crosslinked micelles again showed enhanced stability.[164] In another study on the crosslinked PEG-pLL system, a thiolation degree of more than 13 % of the lysine residues was needed to freeze-dry the vector without the use of any lyoprotectants to make it stable for long-term storage.[165]

5.3. Disulfides for the attachment of a targeting moiety

For a successful accumulation of the nucleic acid in the target cell, the delivery system requires the attachment of a specific "recognition element".[166, 167] However, since many targeting

moieties are rather large, they hamper effective unpacking of the gene vector. Thus, inside cells, it is very important to remove them to facilitate the disassembly of the load. Here, disulfides can be quite useful, as they can be cleaved at the cell surface during cellular entry or in the cytosol. Muratovska *et al.* successfully demonstrated the attachment of such targeting moieties via disulfide bonds. They coupled the membrane permeant peptides (MPP) penetratin and transportan to siRNA that was thiol-modified at the 5` ends. In contrast to untargeted siRNAs, the MPP-siRNA was able to allow for the cellular uptake of siRNA into many different cells. A long-lasting decrease in luciferase activity compared to cells that were treated with siRNAs transfected by lipofectamine 2000 was observed. Similar results were obtained when siRNA against GFP was used **(Figure 5)**.[168]

For active targeting, asODNs can also be combined with asialoglycoprotein (ASGP). To this end, a thiol-modified oligonucleotide was connected with the glycoprotein via sulfo-LC-SPDP, a disulfide containing linker with a long spacer arm providing sufficient conformational stability for receptor binding. These conjugated asODNs were directed towards one of the most important signal transduction proteins in inflammation. They were more efficient than "naked" antisense oligonucleotides in a cell culture model, but they were not able to achieve complete inhibition of the protein production. Nevertheless, this approach showed that the number of targeting ligands could be controlled by the amount of linker. At the same time, the biological activity of the ligands was maintained as shown by transfection experiments.[169] Another targeting ligand is mannose-6-phosphate (M6P), which is internalized by membrane lectins, which are sugar binding receptors. For enhanced uptake, oligonucleotides were thiol-modified at their 3`end and coupled by a covalent disulfide bond to an M6P bovine serum albumine (M6P-BSA) conjugate via linkers. Additionally, this molecule was radioiodinated or fluorescently labelled at its 5´-end. Consequently, both ends of the oligonulceotide were modified, and nuclease activity was abolished. The oligonucleotide as well as the disulfide linkage between the M6P-BSA were stable in culture medium as tested by gel electrophoresis. The targeted oligonucleotides

mediated increased cellular uptake approximately 20-fold in comparison to free oligonucleotides. Within acidic vesicles (endosomes and/or lysosomes), their concentration was increased, and
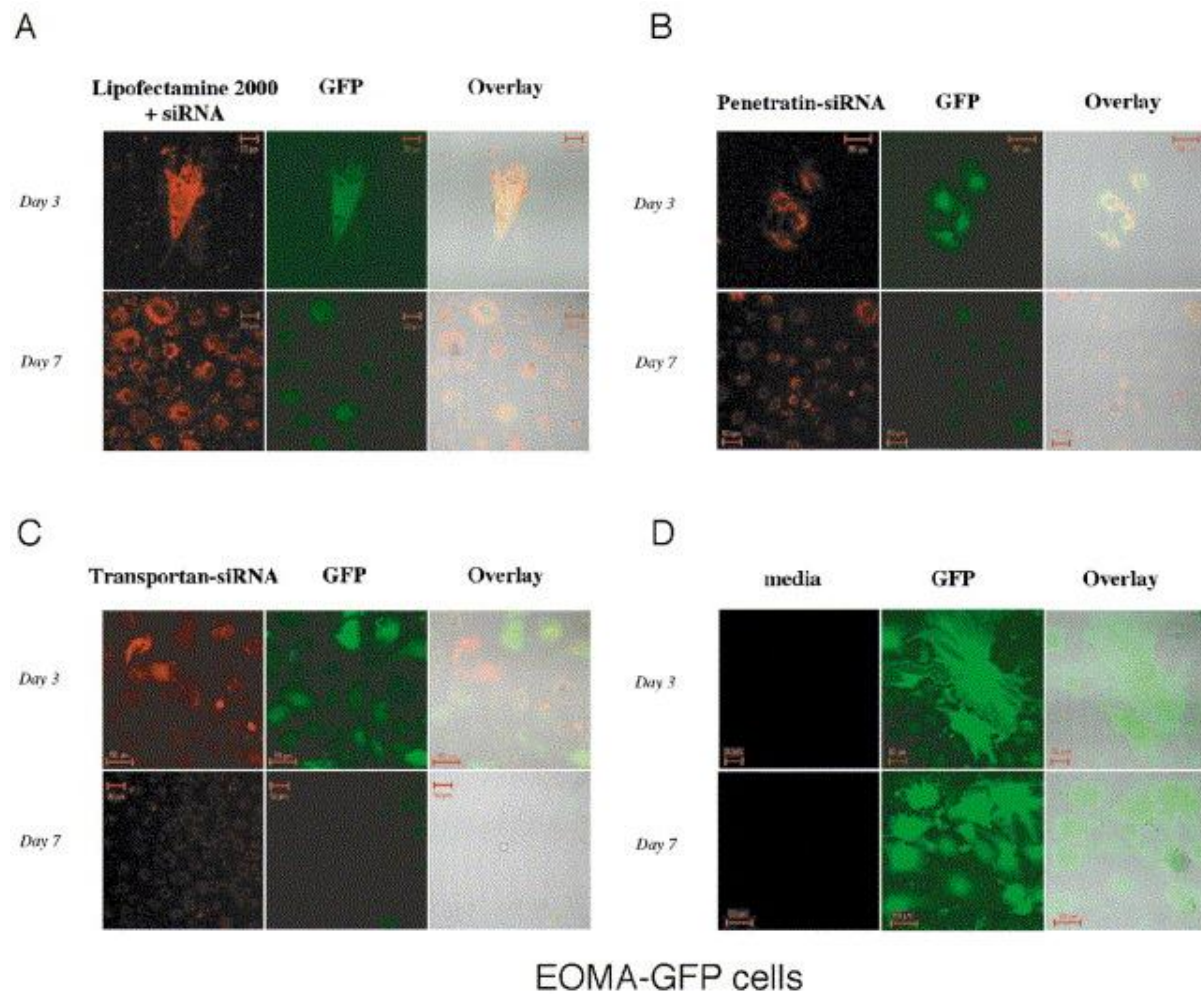
EOMA-GFP cells

Figure 5. *Silencing of GFP in mouse fibroblast cell lines stably expressing GFP: C166-GFP and EOMA-GFP cell lines were treated with 25 nM GFP siRNAs delivered by liposomes or MPP. A–D: Double fluorescence staining of EOMA-GFP cells treated with siRNAs. The following transfectionconditions were used: (A) Lipofectamine, (B) penetratin, (C) transportan, or (D) media only as a control. The red fluorophore Cy3 was used to label siRNAs.   The green fluorescence from GFP was also visualized using confocal fluorescence microscopy after 3 and 7 days.[168]*

thus it was speculated that the amount of oligonucleotides released from the carrier by reduction also increased.[170]

Unfortunately, in all examples, only the differences between targeted and untargeted carriers were studied. Thus, the influence of the type of connection, such as triggerable disulfides, is hard to determine. Although the exact location of disulfide cleavage inside cells still remains unclear, it can be concluded that they do not remain intact within the reductive environment of the cytosol.

5.4.   Disulfides for the attachment of endosomolytic agents

After the delivery system has crossed the cell membrane – which should ideally occur by receptor-mediated endocytosis – endosomal escape is a critical barrier for access of the system to the cytoplasm or nucleus. In order to enhance endosomal escape, fusogenic peptides can be attached to the delivery system [5, 6, 171], or carriers that exhibit intrinsic endosomolytic ability can be used.[172] However, since there is no clear evidence whether endosomes or lysosomes provide a reductive environment, only few examples are known in which an endosomolytic moiety is attached to the carrier via disulfide bonds.

One approach towards the attachment of endosomolytic components via disulfide bonds is the application of LLO, a pore-forming cytolysin that contains a single cysteine residue controlling the activity of the whole peptide. As soon as this cysteine forms any disulfide linkage, LLO becomes inactive. This characteristic was exploited for the development of a gene carrier consisting of LLO and protamine, an arginine-rich cationic polypeptide. The cytolysin was covalently coupled to protamine via the thiol group of its cysteine residue. Thus, the hemolytic activity was completely annulled, but it could be restored after addition of a reductant such as DTT. For pDNA/protamine polyplexes, a degree of substitution of only 1.2 % LLO-S-S-PN was sufficient to produce luciferase reporter gene expression nearly three orders of magnitude higher

than obtained with pDNA/protamine complexes. Since these results were obtained without external addition of a reducing agent, it was concluded that upon cell association, the disulfide bonds were cleaved en route to lysosomes. Thus, LLO was separated from the carrier, and at the same time, transferred into the activated, pore-forming state, destroying the endosome membrane and allowing for the release of its cargo **(Figure 6)**.[81]
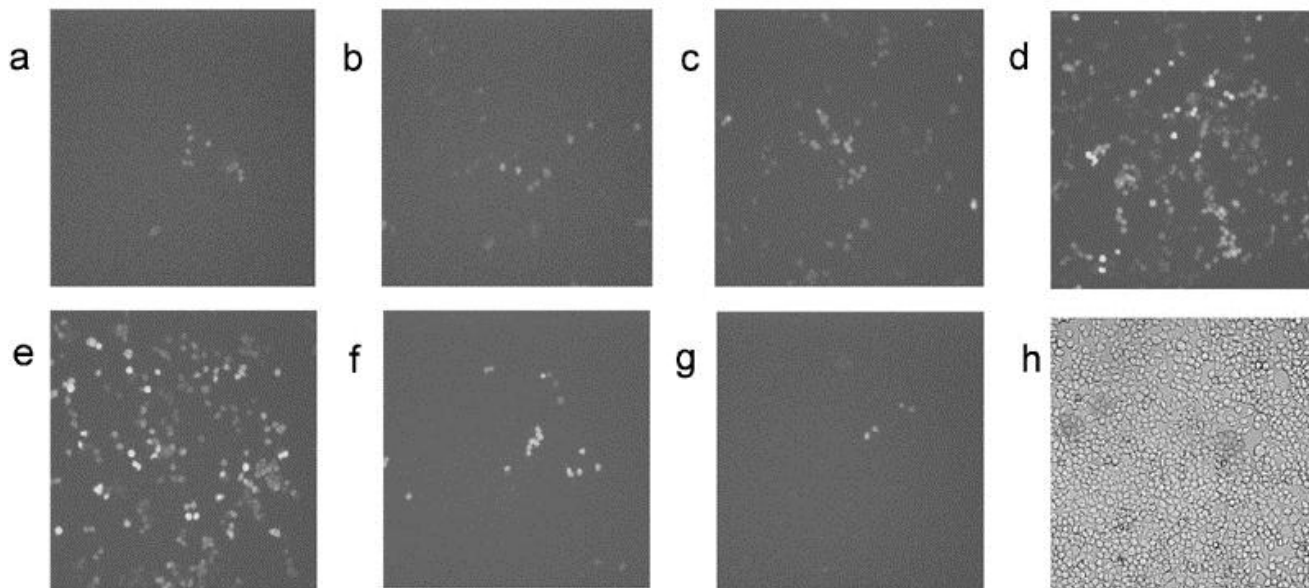
Figure 6. *GFP gene expression in HEK293 cells mediated by LLO-s-s-PN- at varying PN/pDNA weight ratios: LLO-s-s-PN-mediated GFP expression 2 days post-transfection using LLO-s-s-PN/PN/pDNA complexes incorporating fixed amounts of LLO-s-s-PN (0.06 g) and pDNA (0.5 g) and increasing amounts of PN. PN/pDNA weight ratios increased from 0.32 (a) to 2.14 (g). (h) shows a typical transmission image of cells 2 days post-transfection.[81]*

While LLO forms pores, melittin, the major component of the bee venom, destabilizes membranes by perturbation of their structure. Its lytic activity strongly depends on the number of amines available in the peptide. Therefore, amines should not be used for conjugation reactions. Instead, disulfides play an important role, since the thiol group of the cysteine on melittin can be used for coupling reactions. This approach was pursued when melittin was conjugated to a

modified PEI 25 kDa. The resulting polyplexes exhibited a strong increase in transfection activity. Additionally, gene expression started as early as 4 h after transfection, and was also high in slowly dividing cells. The early onset of reporter gene expression was thought to be due to the endosomolytic activity of melittin.[173] Unfortunately, melittin shows this high lytic activity not only at acidic, but also at neutral pH, which consequently leads to toxic side-effects before internalization into the cells. In order to circumvent this problem, a melittin derivative was synthesized in which the amino groups were masked with an acid-labile protecting group. The protected melittin was coupled to pLL via the cysteine residue and showed no cytotoxicity at neutral pH, whereas its lytic activity was regained within the acidic milieu of the endosome **(Figure 7)**.[174, 175]

Endosomolysis can not only be achieved with toxins known from nature; some synthetic vectors display this feature as well. For example bPEI is not only used for the complexation of nucleotides, it is also known to have some inherent endosomolytic ability.[172] This feature was exploited when disulfide bonds were employed for the covalent attachment of PEG to asODNs that were mixed with bPEI to form PIC micelles. These micelles showed significant antisense effect against luciferase gene expression. This was attributed to the fact that bPEI was able to mediate successful escape from the endosome.[176] Although the exact site of disulfide cleavage is still unclear, these approaches nevertheless show the usefulness of the attachment of endosomolytic agents via disulfide bonds.
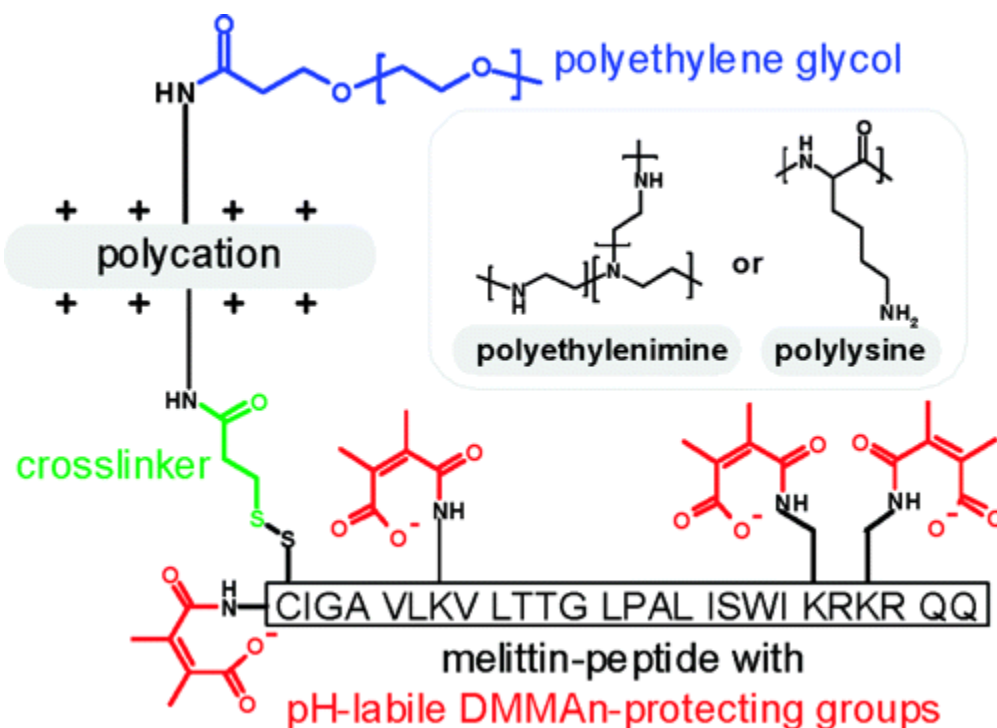
Figure 7. *Schematic structure of the pH-responsive endosomolytic polycation-PEG-DMMAn-Melittin nucleic acid carrier: the pH-drop in the endosome triggers the fast cleavage of the dimethylmaleic anhydride protecting groups thereby restoring the lytic activity of melittin.*[174]

5.5.   Disulfide bonds to decrease the cytotoxicity

A dilemma in non-viral nucleic acid delivery is exemplified by considering the polymeric transfection agent PEI, which is often referred to as the gold standard for polymer-based gene carriers due to the relatively high transfection efficacy of its polyplexes.[6, 21] Unfortunately, efficacy and adverse reactions seem to be strongly associated with the use of PEI. A popular strategy to reduce the toxicity of polyplexes is to use low MW polycations or cationic monomers that are less cytolytic and crosslink them with agents that can be cleaved or activated by the intracellular environment.[177] Numerous reports describe the synthesis of carrier systems containing disulfide bonds that allow for a compaction and protection of the nucleic acid in the

47

extracellular environment accompanied by reduced toxicity due to intracellular polymer degradation. A few selected examples will be presented in the following.

The group of Park synthesized linear PEI (lPEI) derivatives with disulfide bonds in the backbone. The linear poly(ethylene imine disulfide) (l-PEIS) with an amine density similar to PEI showed transfection efficiency nearly comparable to ExGen 500, its non-degradable counterpart with a MW of 22 kDa, and exhibited very low toxicity as evaluated in HeLa cells.[178] The kinetics of polymer degradation after incubation in 5 mM glutathione buffer were determined by multiple angle light scattering (MALS). Total degradation was measured after approximately 100 minutes. To observe polymer degradation inside cells, l-PEIS was labelled with BODYPY-FL. In fluorescence microscopy pictures, an increase of the fluorescence signal of BODIPY-FL due to dequenching indicated intracellular polymer degradation over time, and this effect was not observed for ExGen 500.

In another approach, also a lPEI derivative was used as starting material, but here, the components were crosslinked with different amounts of dithiodipropionic acid or cystine linkages.[177] In comparison to seven commercial transfection reagents, the resulting polymers exhibited outstandingly high transfection efficiencies in seven different cell lines, and at the same time, their toxicity was substantially lower **(Figure 8)**. Treatment of CHO-k1 cells with duroquinone, an agent that oxidizes NADPH/H$^+$, thereby lowering its intracellular reducing potential, reduced the number of transfected cells significantly.

Gosselin *et al.* demonstrated that the type of disulfide-based linker may have an influence on the toxicity.[179] Low MW bPEI (800 Da) was crosslinked with DSP or DTBP. Conjugates with DSP (primary amine:NHS reactive group of 2:1) displayed a higher toxicity in CHO cells, but both conjugates were less toxic as compared to bPEI 25 kDa.

A series of different poly(disulfide amines) were synthesized by Michael addition of N,N`-cystamine bisacrylamide (CBA) to different N-protected diamines (N-Boc-1,2-diaminoethane (DAE), N-Boc-1,4-diamonobutane (DBA), and N-Boc-1,6-diaminohexane (DAH)).[61] The luciferase expression using poly(CBA/DAH) as carrier depended on the side-chain spacer length. For three cell lines, the luciferase expression was similar to that observed for
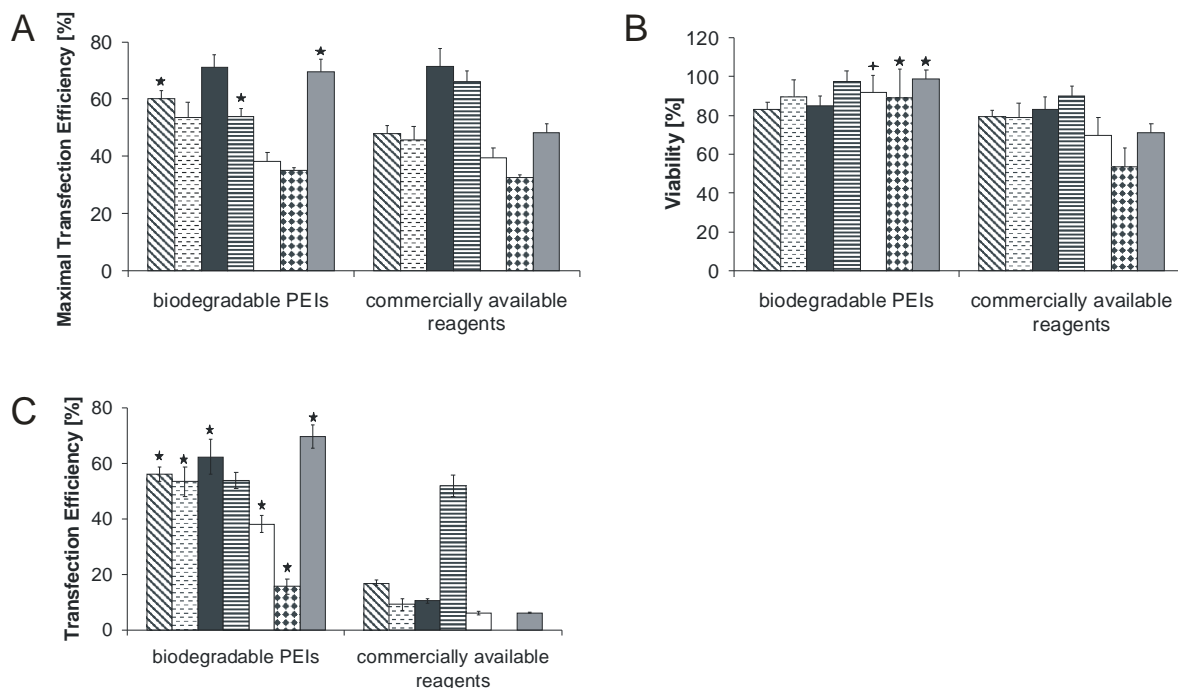
Figure 8. *Comparison of biodegradable PEIs with commercially available transfection reagents: (A and B) EGFP-positive cells expressed as maximal transfection efficiency (A) and corresponding cell viability (B) of various biodegradable PEIs and commercially available transfection reagents complexed with pEGFP-N1 in (from left to right) CHO-K1 (diagonally hatched bars), COS-7 (horizontally hatched bars), NIH/3T3 (black bars), HepG2 (horizontally striped bars), HCT116 (white bars), HeLa (diamond-hatched bars), and HEK-293 (gray bars) cells as determined by flow cytometry. (C) Transfection efficiency under conditions where cell viability is >90%. Statistically significant differences of biodegradable PEIs compared with other transfection reagents are denoted by ✦ (P < 0.05) or by ★ (P < 0.01).[177]*

bPEI 25 kDa, while in C2C12 cells at certain N/P ratios, it was slightly higher. The toxicity of the polyplexes was much lower in NIH3T3 cells as compared to PEI 25 kDa. In a similar approach, Lin *et al.* applied various oligoamines for addition to CBA, providing insight into the relationship between the structure of the side chain and buffer capacity, transfection efficiency and toxicity.[180] Secondary amines in the side chain allowed for a high buffer capacity as along with high transfection efficiency and low cytotoxicity. Increasing the alkyl spacer length by switching from ethylene to propylene between the amines abolished this effect and resulted in significantly higher cytotoxicity.

The group of Oupicky used high MW polycondensates of the TAT peptide, a protein transduction domain from the transcriptional activator protein from HIV-1, to form polyplexes with pDNA.[181] The TAT sequence was flanked by terminal cysteines which were oxidatively condensated or underwent template polymerization with DNA, thus forming polyplexes **(Figure 9).** In comparison to PEI 25 kDa, the cytotoxicity was reduced in both cases. The transfection efficiency was several orders of magnitudes lower, but after addition of chloroquine, it was comparable to bPEI 25 kDa. The incorporation of histidine residues into the molecule allowed for more effective escape from the endosomal compartment. The molecules were not toxic in cell culture testing, and the gene transfection efficiency increased manifold.[182]
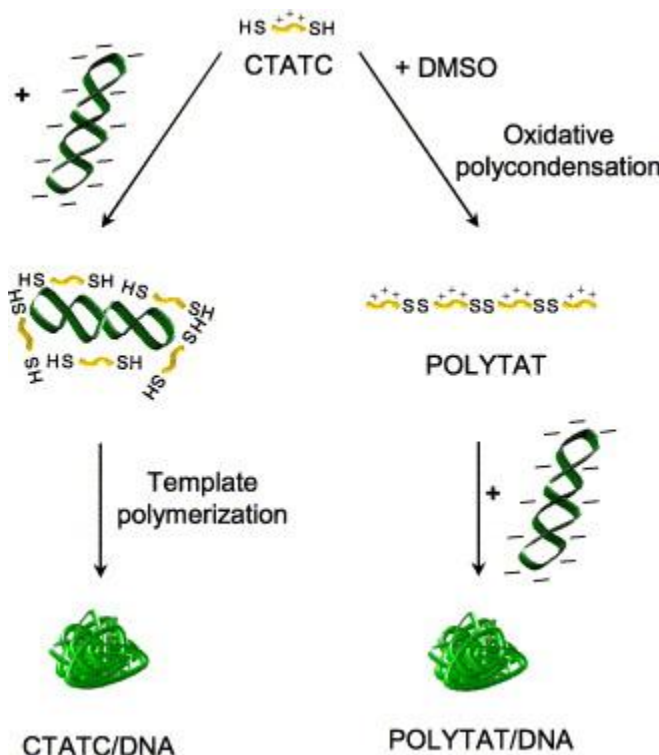
Figure 9. *Schematic representation of the two approaches leading to DNA polyplexes containing high-molecular-weight TAT polypeptides. For the template polymerisation the single molecules are polymerized through their terminal thiol-groups in presence of the template DNA-strand. In the oxidative polycondensation the peptides are oxidised in presence of DMSO forming the TAT-polypeptides. Thereafter, the polyplexes are formed from the DNA-strand and the polypeptides.[181]*

5.6.   Disulfide bonds to enhance the intracellular release of the nucleic acid

Efficient nucleic acid condensation is required for the transport of the cargo to the target cell, but once there, the delivery system must effectively disassemble in order for the nucleic acid to become biologically active. Therefore, the stability of polyplexes and lipoplexes inside cells is heavily investigated.[21, 22, 183-188] One approach to facilitate disassembly involves the use of materials that degrade inside cells. Here, disulfide bonds possess great potential, as the

degradation of the carrier not only reduces the toxicity as described previously, but also allows for efficient release of the nucleic acid as a consequence of reduced interaction with degradation products **(Figure 10.)**[189]
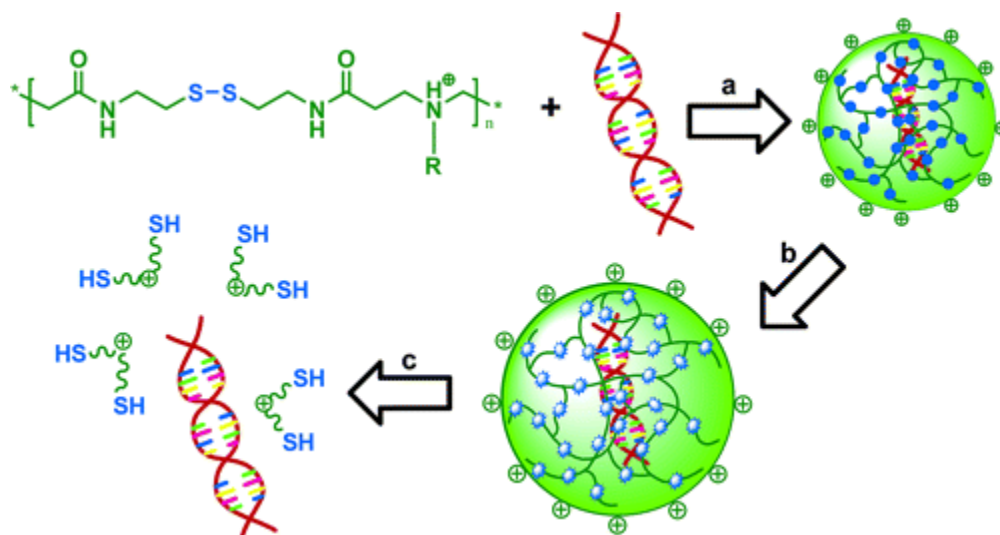
Figure 10. *This scheme illustrates the concept of DNA condensation and subsequent intracellular release: (a) Polyplexes that are built with SS-PAAs and DNA are stable in the extracellular environment. (b) The disulfide linkages in the polymer of the polyplex are reduced intracellular. (c) DNA dissociates from the degraded polymer.* [188]

To this end, confocal laser scanning microscopy (CLSM) was used to evaluate the intracellular distribution and release of fluorescently-labeled siRNA using the following PEI derivatives as carriers: lPEI, commercially available bPEI 25 kDa and a PEI derivative that was synthesized by crosslinking low MW lPEIs via disulfide bonds (ssPEI**) (Figure 11)**.[187] Discrete green spots seen within the cells were interpreted as siRNA associated with the carrier, whereas a homogeneous green cell staining indicated that siRNA was released from the polymer and distributed throughout the cell. The confocal images supported the hypothesis that degradable PEI facilitates the intracellular release of siRNA, as the nucleic acid was homogenously distributed inside cells **(Figure 11 A).** bPEI and especially lPEI seemingly were not able to liberate siRNA to

a great extent because specific spots of polyplexes were predominant, and very few cells showed a homogeneous faint green fluorescence over the cytosol **(Figure 11 B and C, respectively)**.
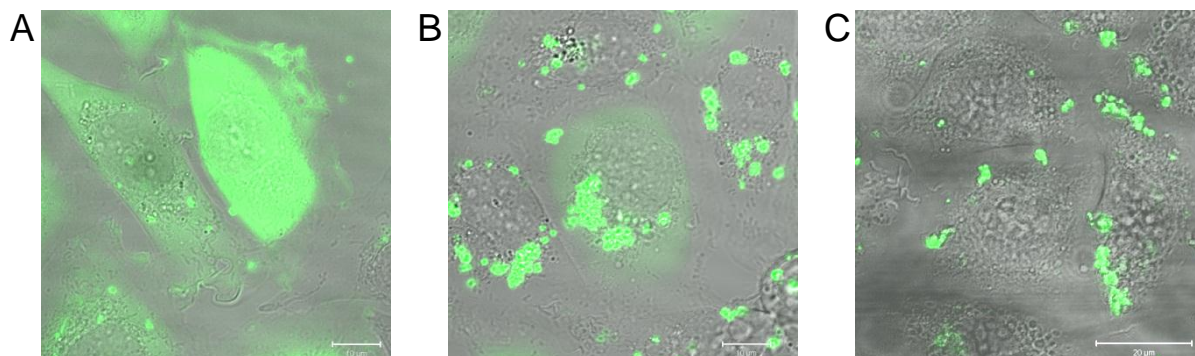
Figure 11. *Confocal laser scanning images of CHO-K1 cells after 5 hours of incubation with polyplexes which were fabricated with fluorescently-labeled siRNA (green) and (A) ssPEI, (B) bPEI and (C) lPEI at N/P 30. The picture is an overlay of transmitted light and fluorescence image (Scale bar: 10µm or 20µm).*[187]

The idea of exploiting disulfide bonds to trigger the release of siRNA in the cytoplasm has also been investigated for other polymers.[114, 190, 191] It has been demonstrated that the reducible poly(amido ethylenimine) (SS-PAEI) poly(triethylenetetramine/cystamine bisacrylamide) (poly(TETA/CBA) is more effective than lPEI 25kDa for VEGF suppression in PC-3 cells.[114] This superior gene silencing activity correlated well with the homogenous distribution of siRNA throughout the cell (cytoplasm and nucleus) after 5 hours of incubation with polyplexes. In contrast, complexes formed with lPEI 25 kDa were distributed as discrete spots within the cell as shown by CLSM. The same group applied three different SS-PAEIs that were synthesized from Michael addition reactions between CBA and three different ethylene amine monomers, i.e. ethylenediamine (EDA), diethylenetriamine (DETA) and triethylenetetramine (TETA), for pDNA delivery. The higher transfection efficiency of poly(EDA/CBA) in particular as compared to

bPEI 25 kDa was signified by the dispersed fluorescence of pDNA inside cells, indicating release after just 90 minutes as observed by CLSM.[113]

Byk *et al.* nicely showed that the release of pDNA from lipopolyamines can be modulated by the location of the linker.[192] The lipopolyamines consisted of 1) a lipid with two fatty acids, 2) a cationic entity such as a polyamine, 3) a spacer between these two molecules and 4) a targeting side-chain. **Figure 12.** shows the positions where the disulfide bridges were introduced. The expression level of luciferase was used to interpret the disulfide cleavage. If the disulfide bond was inserted between the lipid and the polyamine, transfection activity was totally lost, probably due to premature release of pDNA during or directly after cell penetration. In contrast, increased transfection efficiency was found if the disulfide bridge was inserted between one lipid chain and the rest of the molecule. This increase was attributed to disruption of the lipids caused by the reducible side-chain entity. Here, additional studies to confirm the interpretation based on transfection results are necessary.
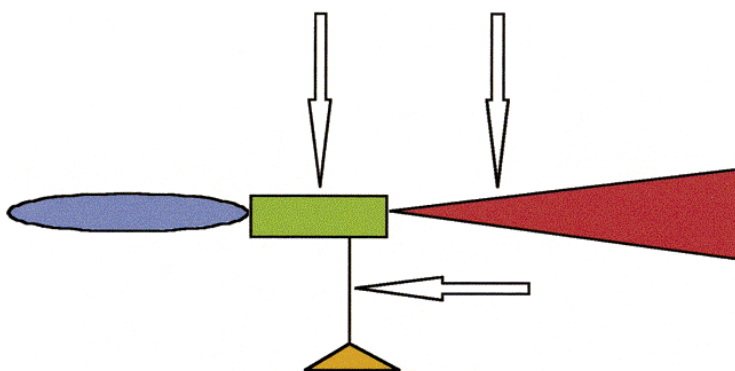
Figure 12. *Schematic representation of the design of lipopolyamines which bear disulfide bridges at different positions within lipopolyamine: blue spheres, polyamine; green boxes, linker; red triangles, fatty chains; orange triangles, side chain entity (Arrows indicate the sites where disulfide bridges can be introduced in lipopolyamines).[192]*

5.7. Gene delivery systems with multiple triggerable functionalities

Although disulfide bonds have proven to be very efficient, especially when used in the carrier backbone, it is not enough to address just one step in the process of gene delivery. Moieties that are responsive to different incentives must be combined to result in an appropriate set of diverse trigger mechanisms at different time points.[193] Such moieties might be cleaved in acidic environments, show good buffering capacity, be redoxactive or enzymatically cleavable, or be stimulated by some extragenous stimuli such as heat [194], magnetic fields [195] or irradiation.[196]

A promising example of a triggerable system was created by the synthesis of a liposomal carrier that was comprised of a membrane permeable ligand and a reductively detachable PEG-coating. The surface cover consisted of PEG coupled to DOPE via a thiolytically cleavable linker, while the ligand, an ariginine octamer, was immobilized onto cholesteryl hemisuccinate (CHEMS). These conjugates were mixed with dipalmitoylphosphatidylcholin (DPPC) and unmodified DOPE to form liposomes. The authors expected this formulation to dispose of its coating at its destination through a mild reductive trigger such as external L-cysteine. Upon activation of the trigger, the arginine octamer would be exposed, causing cellular uptake of the liposome. Once in the cytosol, the remaining disulfide bonds would be cleaved, ultimately resulting in the destabilization the whole carrier **(Figure 13.)**.[197]

Other attempts to incorporate multiple triggers in one carrier system to allow for controlled nucleic acid delivery have also been made. In one such attempt, polymers were designed to possess 1) a targeting moiety for receptor-mediated endocytosis, 2) a pH-responsive element for the disruption of endosomal membranes and 3) a disulfide bound biomolecular therapeutic agent to be delivered in free form into the cytoplasm. For this purpose, a copolymer of dimethylaminoethyl methacrylate (DMAEMA) and hydrophobic alkyl methacrylates (BMA) as well as alkylacrylates (BA) were chosen for the formation of the membrane-disruptive backbone. PEG was grafted around the polymer for stealth effects. In order to obtain pH sensitivity, acid-
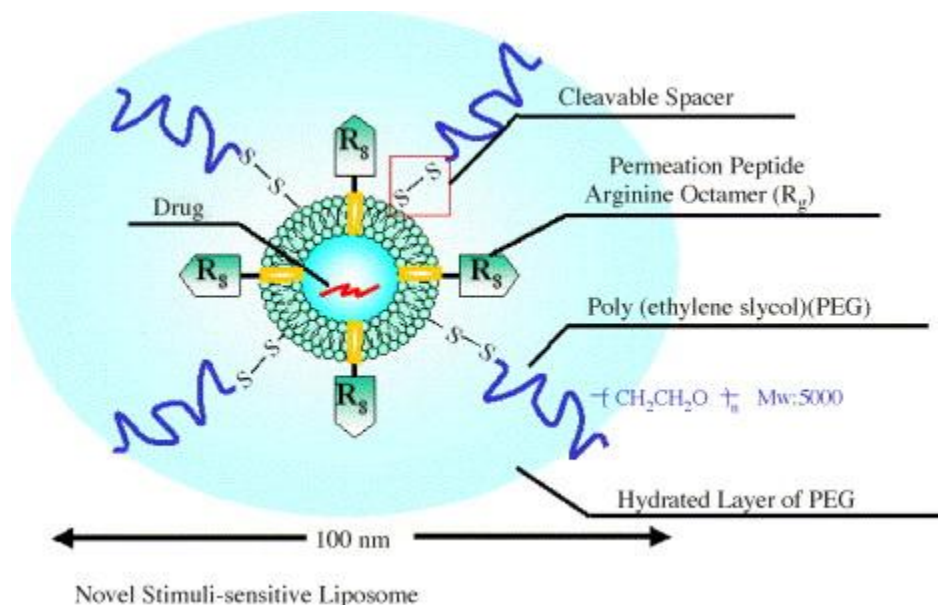
Figure 13. *Scheme of a stimuli-responsive liposome: the liposomal carrier possesses membrane-permeable ligands and a detachable coating which is intended for the intracellular delivery of drugs or genes.*[197]

degradable acetal bonds were introduced for the attachment of PEG or PEGylated drugs and targeting moieties to the backbone. The acetal linkages readily degraded in the acidic endosome and could be tracked by a change in UV absorption. This hydrolysis unmasked the membrane-disruptive backbone which led to release into the cytosol where the remaining disulfide bonds were cleaved allowing the drug to be liberated. This release was followed by fluorescence measurements of the labelled peptides **(Figure 14)**.[198]

A similar approach used DMAEMA, BMA and PEG grafted via an acid-degradable linker. The PEG chains in this formulation were further modified. One fraction of PEG was coupled with a hexalysine component for complexation of ODNs, while the rest was reacted with lactose in order to aid cellular uptake mediated by the asiaglycoprotein receptor. This gene delivery system significantly enhanced endosomal release and cytoplasmic delivery .[199] Another
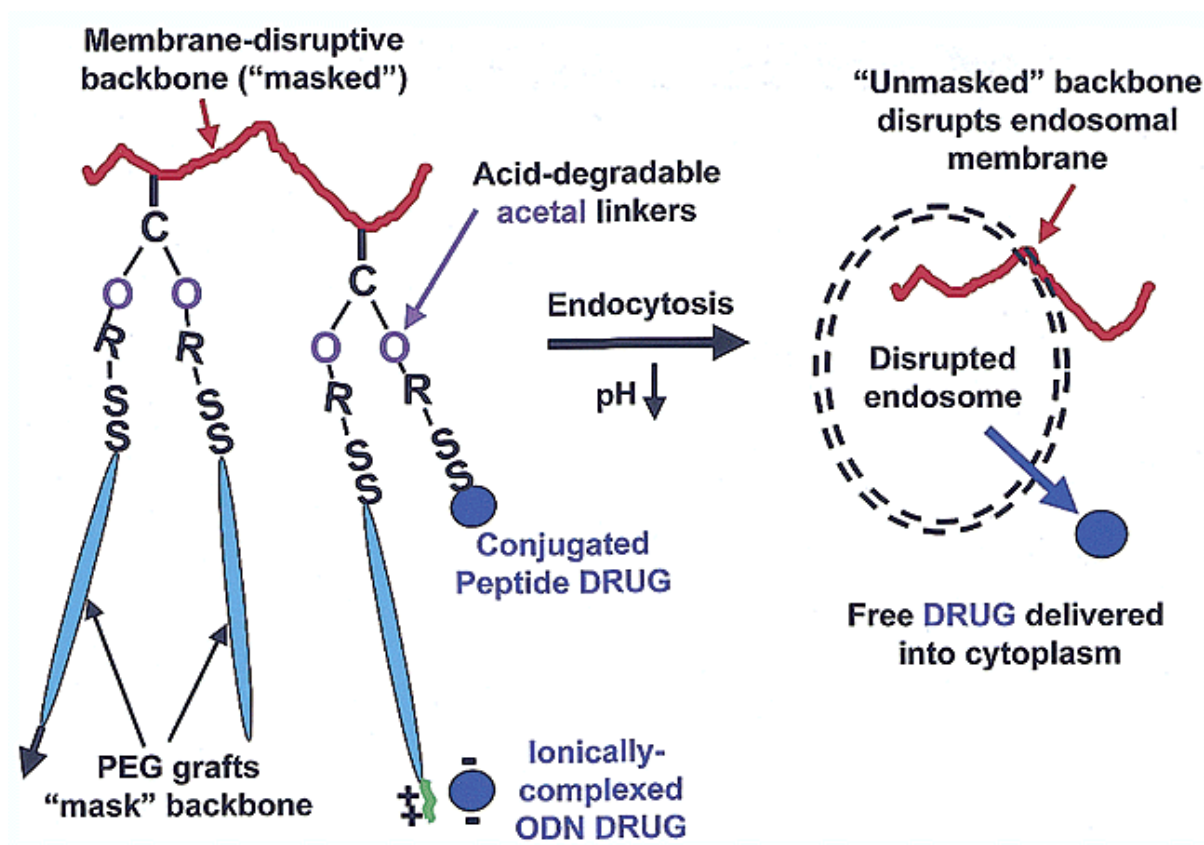
Figure 14. *Schematic representation of the encrypted polymer design: The polymers are PEGylated and are stable in serum at pH 7.4 and they are able to disrupt the endosomal membrane at the acidic pH of the endosome. The polymers contain a membrane-disruptive backbone (red line), acid-degradable linkers (purple circle), PEG grafts (aqua ellipsoid), conjugated or ionically complexed drug molecules (blue circle), hexalysine peptide (green line), and targeting ligands (black arrow). At pH 7.4 the polymers are masked" by the PEG chains. After endocytosis the acid-degradable linker is cleaved and the polymer backbone gets rid of its PEG- strands (" is unmasked") and becomes at the same time membrane-disruptive. The PEGs can be conjugated to the backbone via acid-degradable linkages as well as disulfide bonds. The latter are reduced in the cytoplasm releasing the free drug.[198]*

polymeric carrier was formed from methacrylic acid (MAAc), BA and pyridyldisulfide acrylate (PDSA). This poly(MAAc-co-BA-co-PDSA) was accessorily conjugated with peptides that allowed for the electrostatic complexation of oligonucleotides. The terpolymer mediated uptake and enhanced cytoplasmic delivery of fluorescein isothiocyanate (FITC)-labelled ODNs in THP-1 macrophage-like cells.[200]

The slightly more acidic pH of tumors compared to normal tissue was employed in another delivery system.[201] Here, a biodegradable micelle system for tumor-targeted delivery was synthesized. It consisted of poly(L-lactic acid)-b-poly(ethylene glycol) (PLLA-b-PEG) conjugated to TAT. This was wrapped in poly(L-cysteine bisamide-g-sulfadiazine)-b-PEG (PCBS-b-PEG), which is a shielding, pH-sensitive diblock copolymer. The pH responsive block could also be rapidly degraded in the presence of cysteine due to the incorporated disulfide bridges. Not only the single blocks were able to degrade; the whole micelle was deshielded at low pH. Moreover, this system was able to distinguish between a pH of 7.2 and 7.0, the latter of which is found in tumors.[202] This discrimination was demonstrated when the anticancer drug doxorubicin was incorporated into the TAT micelles. At the lower pH, cytotoxicity increased due to the larger amount of deshielded micelles. Upon partial deshielding, the TAT component was able to guide the included drug into the cell. Inside the cells, the remaining PCBS-b-PEG components could be degraded by disulfide reduction, thus, liberating the drug load **(Figure 15.)**

All of these systems combine multiple trigger mechanisms, making them very potent therapeutic agents. With slight variations, for example of the targeting moieties, multiple applications are easily possible. Therefore, gene delivery vehicles that are responsive to different changes in the environment will be very important for future therapeutic strategies.
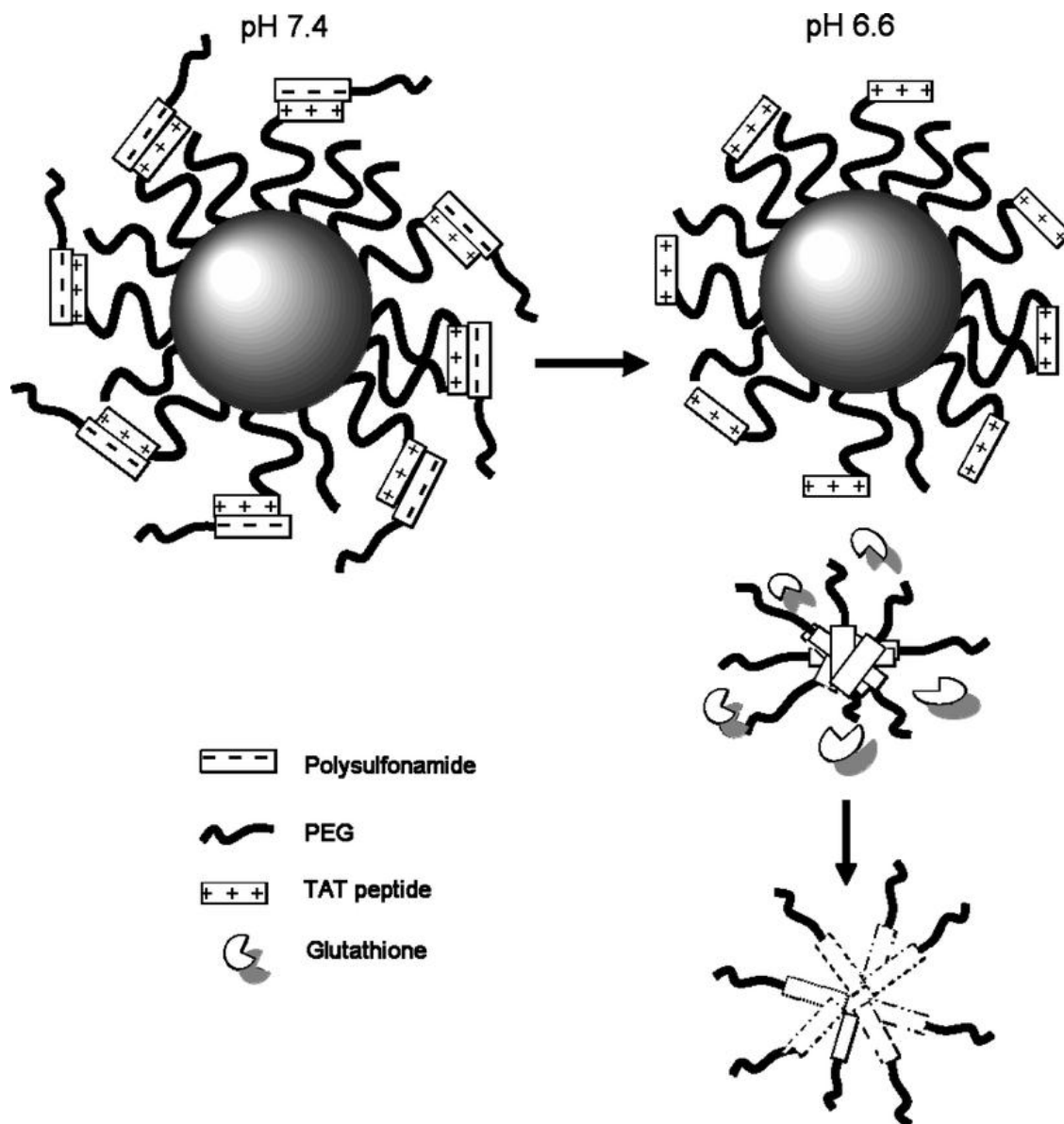
Figure 15. *Schematic model of a pH- and redox-sensitive drug delivery system: The carrier system comprises two different building blocks: 1) a PLLA-b-PEG micelle connected with TAT and 2) a pH sensitive diblock polymer PCBS-b-PEG. The sulfadiazine is negatively charged at normal blood pH (i.e. pH 7.4). After mixing with the TAT-micelle, the sulfadiazine shields the TAT electrostatically. On the surface of the carrier are only PEG chains which provide for long circulation times. As soon as there is a drop in pH (e.g. near tumor pH 6.6) the sulfonamide becomes uncharged and detaches from the micelles. Then TAT is exposed and can interact with tumor cells; while the detached PCBS polymer is degraded rapidly by the native glutathione.*[202]

59

6. Conclusion

Although nucleic acids have revolutionized biomedical research and pharmaceutical development, their role as clinically applied drugs is still modest. For future applications it will be important to effectively deliver the nucleic acid to its side of action and to adopt nucleic acid delivery systems to the disease-specific demands. In this context, disulfides within the carrier will hold a unique position. They can stabilize the vehicles for a time scale which may even be long enough for tissue repair as well as guarantee for the release of their load in the cytosol of the cell while providing for carrier decomposition at the same time - two features that sparely can be achieved with other linkages.

7. Reference List

[1] L. De Laporte, L. D. Shea, Matrices and Scaffolds for DNA delivery in tissue engineering. *Advanced Drug Delivery Reviews* (2007) *59*, 292-307.

[2] R. Langer, J. P. Vacanti, Tissue Engineering. *Science* (1993) *260*, 920-926.

[3] E. Lavik, R. Langer, Tissue engineering: current state and perspectives. *Applied Microbiology and Biotechnology* (2004) *65*, 1-8.

[4] M. D. Brown, A. G. Schaetzlein, I. F. Uchegbu, Gene delivery with synthetic (non viral) carriers. *International Journal of Pharmaceutics* (2001) *229*, 1-21.

[5] E. Wagner, J. Kloeckner, Gene Delivery Using Polymer Therapeutics. *Advances in Polymer Science* (2006) *192*, 135-173.

[6] U. Lungwitz, M. Breunig, T. Blunk, A. Goepferich, Polyethyleneimine-based non-viral gene delivery systems. *European Journal of Pharmaceutics and Biopharmaceutics* (2005) *60*, 247-266.

[7] E. Wagner, Application of membrane-active peptides for nonviral gene delivery. *Advanced Drug Delivery Reviews* (1999) *38*, 279-289.

[8] A. C. Hunter, Molecular hurdles in polyfection design and mechanistic background to polycation induced cytotoxicity. *Advanced Drug Delivery Reviews* (2006) *58*, 1523-1531.

[9] H. Lv, S. Zhang, B. Wang, S. Cui, J. Yan, Toxicity of cationic lipids and cationic polymers in gene delivery. *Journal of Controlled Release* (2006) *114*, 100-109.

[10] D. Fischer, Y. Li, B. Ahlemeyer, J. Krieglstein, T. Kissel, In vitro cytotoxicity testing of polycations: influence of polymer structure on cell viability and hemolysis. *Biomaterials* (2003) *24*, 1121-1131.

[11] M. A. E. M. van der Aa, E. Mastrobattista, R. S. Oosting, W. E. Hennink, G. A. Koning, D. J. A. Crommelin, The Nuclear Pore Complex: The Gateway to Successful Nonviral Gene Delivery. *Pharmaceutical Research* (2006) *23*, 447-459.

[12] D. A. Dean, D. D. Strong, W. E. Zimmer, Nuclear entry of nonviral vectors. *Gene Therapy* (2005) *12*, 881-890.

[13] C. W. Pouton, K. M. Wagstaff, D. M. Roth, G. W. Moseley, D. A. Jans, Targeted delivery to the nucleus. *Advanced Drug Delivery Reviews* (2007) *59*, 698-717.

[14] M. Molas, R. Bartrons, J. C. Perales, Single stranded DNA condensed with poly-L-lysine results in nanometric particles that are significantly smaller, more stable in physiological ionic strengthfluids and afford higher efficiency of gene delivery than their double-stranded counterparts. *Biochimica et Biophysica Acta* (2002) *1572*, 37-44.

[15] Y. H. Choi, F. Liu, J. S. Kim, Y. K. Choi, J. S. Park, S. W. Kim, Polyethylene glycol-
      grafted poly-L-lysine as polymeric gene carrier. *Journal of Controlled Release*
      (1998) *54*, 39-48.

[16] G. Liu, M. Molas, G. A. Grossmann, M. Pasumarthy, J. C. Perales, M. J. Cooper, R. W.
      Hanson, Biological properties of Poly-L-lysine-DNA Complexes Generated by
      Cooperative Binding of the Polycation. *Journal of Biological Chemistry* (2001)
      276, 34379-34387.

[17] J. Wang, H. Q. Mao, K. W. Leong, A Novel Biodegradable Gene Carrier Based on
      Polyphosphoester. *Journal of the American Chemical Society* (2001) *123*, 9480-
      9481.

[18] Y. B. Lim, C. H. Kim, K. Kim, S. W. Kim, J. S. Park, Development of a Safe Gene
      Delivery system Using Biodegradable Polymer, Poly[α-(4-aminobutyl)-L-glycolic
      acid]. *Journal of the American Chemical Society* (2000) *122*, 6524-6525.

[19] J. S. Remy, B. Abdallah, M. A. Zanta, O. Boussif, J. P. Behr, B. Demeneix, Gene transfer
      with lipospermines and polyethyleneimines. *Advanced Drug Delivery Reviews*
      (1998) *30*, 85-95.

[20] R. Kircheis, L. Wightman, E. Wagner, Design and gene delivery activity of modified
      polyethylenimines. *Advanced Drug Delivery Reviews* (2001) *53,* 341-358.

[21] M. Neu, D. Fischer, T. Kissel, Recent advances in rational gene design based on
      poly(ethylene imine) and its derivatives. *Journal of Gene Medicine* (2005) *7*, 992-
      1009.

[22] U. Lungwitz, M. Breunig, R. Liebl, T. Blunk, A. Goepferich, Gene delivery with low
      molecular weight linear polyethylenimines. *European Journal of Pharmaceutics
      and Biopharmaceutics* (2008) *69*, 134-1298.

[23] M. Breunig, U. Lungwitz, R. Liebl, C. Fonatanari, J. Klar, A. Kurtz, T. Blunk, A.
      Goepferich. Gene delivery with low molecular weight linear polyethylenimines,
      Journal of Gene Medicine (2005) *7*, 1287-1298.

[24] J. M. Dang, K. W. Leong, Natural polymers for gene delivery and tissue engineering.
      Advanced Drug Delivery Reviews (2006) *58*, 487-499.

[25] S. Kommareddy, M. Amiji, Preparation and Evaluation of Thiol-modified Gelatin
      Nanoparticles for Intracellular DNA Delivery in Response to Glutathione.
      Bioconjugate Chemistry (2005) *16*, 1423-1432.

[26] A. Bernkop-Schnürch, M. Hornof, D. Guggi, Thiolated chitosans. *European Journal of
      Pharmaceutics and Biopharmaceutics* (2004) *57*, 9-17.

[27] T. Sato, T. Ishii, Y. Okahata, In vitro gene delivery mediated by chitosan. Effect of pH,
      serum and molecular weight on the transfection efficiency. *Biomaterials* (2001)
      22, 2075-2080.

[28] V. L. Truong-Le, S. M. Walsh, E. Schweibert, H. Q. Mao, J. T. Guggino, J. T. August, K. W. Leong, Gene Transfer by DNA-Gelatin Nanospheres. *Archives of Biochemistry and Biophysics* (1999) *361*, 47-56.

[29] A. Kim, D. M. Checkla, P. Dehazya, W. Chen, Characterization of DNA-hyaluronan matrix for sustained gene transfer. *Journal of Controlled Release* (2003) *90*, 81-95.

[30] Y. H. Yun, D. J. Goetz, P. Yellen, W. Chen, Hyaluronan microspheres for sustained gene delivery and site-specific targeting. *Biomaterials* (2004) *25*, 147-157.

[31] R. E. Samuel, C. R. Lee, S. C. Ghivizzani, C. H. Evans, I. V. Yannas, B. R. Olsen, M. Spector, Delivery of Plasmid DNA to Articular Chondrocytes via Novel Collagen-Glycosaminoglycan Matrices. *Human Gene Therapy* (2002) *13*, 791-802.

[32] Y. Tabata, Y. Ikada, Protein release from gelatin matrices. *Advanced Drug Delivery Reviews* (1998) *31*, 287-301.

[33] T. C. Laurent, J. Fraser, Hyaluronan. *FASEB Journal* (1992) *6*, 2397-2404.

[34] K. W. Leong, H.-Q. Mao, V. L. Truong-Le, K. Roy, S. M. Walsh, J. T. August, DNA-polycation nanospheres as non-viral gene delivery vehicles. *Journal of Controlled Release* (1998) *53*, 183-193.

[35] W. Friess, Collagen - biomaterial for drug delivery. *European Journal of Pharmaceutics and Biopharmaceutics* (1998) *45*, 113-136.

[36] X. Guo, F. C. Szoka, Chemical Approaches to Triggerable Lipid Vesicles for Drug and Gene Delivery. *Accounts of Chemical Research* (2003) *36*, 335-341.

[37] M. Voinea, M. Simionescu, Designing of "intelligent" liposomes for efficient delivery of drugs. *Journal of Cellular and Molecular Medicine* (2002) *6*, 465-474.

[38] D. D. Lasic, N. S. Templeton, Liposomes in gene therapy. *Advanced Drug Delivery Reviews* (1996) *20*, 221-266.

[39] L. P. Brewster, E. M. Brey, H. P. Greisler, Cardiovascular gene delivery: The good road is awaiting. *Advanced Drug Delivery Reviews* (2006) *58*, 604-629.

[40] M. D. Kofron, C. T. Laurencin, Bone tissue engineering by gene delivery. *Advanced Drug Delivery Reviews* (2006) *58*, 555-576.

[41] B. Nussenbaum, P. H. Krebsbach, The role of gene therapy for craniofacial and dental tissue engineering. *Advanced Drug Delivery Reviews* (2006) *58*, 577-591.

[42] A. Saraf, A. G. Mikos, Gene delivery strategies for cartilage tissue engineering. *Advanced Drug Delivery Reviews* (2006) *58*, 592-603.

[43] J. Bonadio, Tissue engineering via local gene delivery: Update and future prospects for enhancing the technology. *Advanced Drug Delivery Reviews* (2000) *44*, 185-194.

[44] J. Bonadio, Tissue engineering via local gene delivery. *Journal of Molecular Medicine* (2000) *78*, 303-311.

[45] K. R. Cutroneo, Gene Therapy for Tissue Regeneration. *Journal of Cellular Biochemistry* (2003) *88*, 418-425.

[46] L. A. Chandler, D. L. Gu, A. M. Ma, J. Gonzalez, T. Doukas, T. Nguyen, G. F. Pierce, M. L. Phililips, Matrix-enabled gene transfer for cutaneous wound repair. *Wound Repair and Regeneration* (2000) *8*, 473-479.

[47] J.-H. Jang, T. L. Houchin, L. D. Shea, Gene delivery from polymer scaffolds for tissue engineering. *Expert Reviews Medical Devices* (2004) *1*, 127-138.

[48] L. D. Shea, E. Smiley, J. Bonadio, D. J. Mooney, DNA delivery from polymer matrices for tissue engineering. *Nature Biotechnology* (1999) *17*, 551-554.

[49] N. Giannoukakis, A. W. Thomson, P. D. Robbins, Gene therapy in transplantation. *Gene Therapy* (1999) *6*, 1499-1511.

[50] J. Bonadio, E. Smiley, P. Patil, S. Goldstein, Localized, direct plasmid gene delivery *in vivo*: prolonged therapy results in reproducible tissue regeneration. *Nature Medicine* (1999) *5*, 753-759.

[51] M. Egermann, E. Schneider, C. H. Evans, A. W. Baltzer, The potential of gene therapy for fracture healing in osteoporosis. *Osteoporosis International* (2005) *16*, S120-S128.

[52] J. Fang, Y. Y. Zhu, E. Smiley, J. Bonadio, J. P. Rouleau, S. A. Goldstein, L. K. McCauley, B. Davidson, B. J. Roessler, Stimulation of new bone formation by direct transfer of osteogenic plasmid genes. *Proceedings of the National Academy of Sciences of the United States of America* (1996) *93*, 5753-5758.

[53] J. Bonadio, S. A. Goldstein, R. J. Levy, Gene therapy for tissue repair and regeneration. *Advanced Drug Delivery Reviews* (1998) *33*, 53-69.

[54] H. Petite, V. Viateau, W. Bensaid, A. Meunier, C. de Pollak, M. Bourguignon, K. Oudina, L. Sedel, G. Guillemin, Tissue-engineered bone regeneration. *Nature Biotechnology* (2000) *18*, 959-963.

[55] L. V. Christensen, C. W. Chang, J. W. Yockman, R. Conners, H. Jackson, Z. Zhong, J. Feijen, D. A. Bull, S. W. Kim, Reducible poly(amido ethylenediamine) for hypoxia-inducible VEGF delivery. *Journal of Controlled Release* (2007) *118*, 254-263.

[56] D. Trentin, H. Hall, S. Wechsler, J. A. Hubbell, Peptide-Matrix-mediated gene transfer of an oxygen-insensitive hypoxia-inducible factor-1α variant for local induction of angiogenesis. *Proceedings of the National Academy of Sciences of the United States of America* (2006) *103*, 2506-2511.

[57] A. Napoli, M. Valentini, N. Tirelli, M. Muller, J. A. Hubbell, Oxidation-responsive polymeric vesicles. *Nature Materials* (2004) *3*, 183-189.

[58] T. Segura, J. A. Hubbell, Synthesis and in Vitro Characterization of an ABC Triblock Copolymer for siRNA Delivery. *Bioconjugate Chemistry* (2007) *18*, 736-745.

[59] M. C. Garnett, Targeted drug conjugates: principles and progress. *Advanced Drug Delivery Reviews* (2001) *53*, 171-216.

[60] S. Ganta, H. Devalapally, A. Shahiwala, M. Amiji, A review of stimuli-responsive nanocarriers for drug and gene delivery. *Journal of Controlled Release* (2008) *126*, 187-204.

[61] M. Ou, X. L. Wang, R. Xu, C. W. Chang, D. A. Bull, S. W. Kim, Biodegradable Poly(disulfide amine)s for Gene Delivery with High Efficiency and Low Cytotoxicity. *Bioconjugate Chemistry* (2008) *19*, 626-633.

[62] M. Morille, C. Passirani, A. Vonarbourg, A. Clavreul, J. P. Benoit, Progress in developing cationic vectors for non-viral systemic gene therapy against cancer. *Biomaterials* (2008) *29*, 3477-3496.

[63] D. Lechardeur, A. S. Verkman, G. L. Lukacs, Intracellular routing of plasmid DNA during non-viral gene transfer. *Advanced Drug Delivery Reviews* (2005) *57*, 755-767.

[64] R. Bausinger, K. von Gersdorff, K. Braeckmans, M. Ogris, E. Wagner, C. Bräuchle, A. Zumbusch, The Transport of Nanosized Gene Carriers Unraveled by Live-Cell Imaging. *Angewandte Chemie International Edition English* (2006) *45*, 1568-1572.

[65] C. S. Pillay, E. Elliott, C. Dennison, Endolysosomal proteolysis and its regulation. *Biochemistry Journal* (2002) *363*, 417-429.

[66] T. Tagami, J. M. Barichello, H. Kikuchi, T. Ishida, H. Kiwada, The gene-silencing effect of siRNA in cationic lipoplexes is enhanced by incorporating pDNA in the complex. *International Journal of Pharmaceutics* (2007) *333*, 62-69.

[67] A. W. Wong, S. J. Scales, D. E. Reilly, DNA Internalized via Caveolae Requires Microtubule-dependent, Rab7-independent Transport to the Late Endocytic Pathway for Delivery to the Nucleus. *Journal of Biological Chemistry* (2007) *282*, 22953-22963.

[68] A. Akinc, R. Langer, Measuring the pH environment of DNA delivered using nonviral vectors: Implications for lysosomal trafficking. *Biotechnology and Bioengineering* (2002) *78*, 503-508.

[69] W. C. Shen, H. J. Ryser, L. LaManna, Disulfide spacer between methotrexate and poly(D-lysine). A probe for exploring the reductive process in endocytosis. *Journal of Biological Chemistry* (1985) *260*, 10905-10908.

[70] G. Saito, J. A. Swanson, K. D. Lee, Drug delivery strategy utilizing conjugation via reversible disulfide linkages: role and site of cellular reducing activities. *Advanced Drug Delivery Reviews* (2003) *55*, 199-215.

[71] S. Takae, K. Miyata, M. Oba, T. Ishii, N. Nishiyama, K. Itaka, Y. Yamasaki, H. Koyama, K. Kataoka, PEG-Detachable Polyplex Micelles Based on Disulfide-Linked Block

Catiomers as Bioresponsive Nonviral Gene Vectors. *Journal of the American Chemical Society* (2008) *130*, 6001-6009.

[72] C. D. Austin, X. Wen, L. Gazzard, C. Nelson, R. H. Scheller, S. J. Scales, Oxidizing potential of endosomes and lysosomes limits intracellular cleavage of disulfide-based antibody-drug conjugates. *Proceedings of the National Academy of Sciences of the United States of America* (2005) *102*, 17987-17992.

[73] E. P. Feener, W. C. Shen, H. J. Ryser, Cleavage of disulfide bonds in endocytosed macromolecules. A processing not associated with lysosomes or endosomes. *Journal of Biological Chemistry* (1990) *265*, 18780-18785.

[74] F. Q. Schafer, G. R. Buettner, Redox environment of the cell as viewed through the redox state of the glutathione disulfide/glutathione couple. *Free Radical Biology and Medicine* (2001) *30*, 1191-1212.

[75] J. Yang, H. Chen, I. R. Vlahov, J. X. Cheng, P. S. Low, Evaluation of disulfide reduction during receptor-mediated endocytosis by using FRET imaging. *Proceedings of the National Academy of Sciences of the United States of America* (2006) *103*, 13872-13877.

[76] D. S. Manickam, D. Oupicky, Polyplex gene delivery modulated by redox potential gradients. *Journal of Drug Targeting* (2006) *14*, 519-526.

[77] H. R. López-Mirabal, J. R. Winther, Redox characteristics of the eukaryotic cytosol. *Biochimica et Biophysica Acta (BBA) - Molecular Cell Research* (2008) *1783*, 629-640.

[78] D. S. Manickam, A. Hirata, D. A. Putt, L. H. Lash, F. Hirata, D. Oupicky, Overexpression of Bcl-2 as a proxy redox stimulus to enhance activity of non-viral redox-responsive delivery vectors. *Biomaterials* (2008) *29*, 2680-2688.

[79] J. Sastre, F. V. Pallardo, J. Viña, Glutathione, in *Reactions, Processes*, Springer, Berlin/Heidelberg (2005) 91-108.

[80] E. Fenouillet, R. Barbouche, I. M. Jones, Cell Entry by Enveloped Viruses: Redox Considerations for HIV and SARS-Coronavirus. *Antioxidants & Redox Signaling* (2007) *9*, 1009-1034.

[81] G. Saito, G. L. Amidon, K. D. Lee, Enhanced cytosolic delivery of plasmid DNA by a sulfhydryl-activatable listeriolysin O/protamine conjugate utilizing cellular reducing potential. *Gene Therapy* (2003) *10*, 72-83.

[82] D. S. Collins, E. R. Unanue, C. V. Harding, Reduction of disulfide bonds within lysosomes is a key step in antigen processing. *Journal of Immunology* (1991) *147*, 4054-4059.

[83] U. T. Phan, B. Arunachalam, P. Cresswell, Gamma-Interferon-inducible Lysosomal Thiol Reductase (GILT). MATURATION, ACTIVITY, AND MECHANISM OF ACTION, *Journal of Biological Chemistry* (2000) *275*, 25907-25914.

[84] D. Gainey, S. Short, K. L. McCoy, Intracellular location of cysteine transport activity correlates with productive processing of antigen disulfide. *Journal of Cellular Physiology* (1996) *168*, 248-254.

[85] B. Arunachalam, U. T. Phan, H. J. Geuze, P. Cresswell, Enzymatic reduction of disulfide bonds in lysosomes: Characterization of a Gamma-interferon-inducible lysosomal thiol reductase (GILT). *Proceedings of the National Academy of Sciences of the United States of America* (2000) *97*, 745-750.

[86] J. Yang, H. Chen, I. R. Vlahov, J. X. Cheng, P. S. Low, Characterization of the pH of Folate Receptor-Containing Endosomes and the Rate of Hydrolysis of Internalized Acid-Labile Folate-Drug Conjugates. *Journal of Pharmacoogy and. Experimental Therapeutics* (2007) *321*, 462-468.

[87] S. K. Lai, K. Hida, S. T. Man, C. Chen, C. Machamer, T. A. Schroer, J. Hanes, Privileged delivery of polymer nanoparticles to the perinuclear region of live cells via a non-clathrin, non-degradative pathway. *Biomaterials* (2007) *28*, 2876-2884.

[88] J. P. Tam, C.-R. Wu, W. liu, J.-W. Zhang, Disulfide Bond Formation in Peptides by Dimethyl sulfoxide. Scope and Applications. *Journal of the American Chemical Society* (1991) *113*, 6657-6662.

[89] D. Oupicky, A. L. Parker, L. W. Seymour, Laterally Stabilized Complexes of DNA with Linear Reducible Polycations: Strategy for Triggered Intracellular Activation of DNA Delivery Vectors. *Journal of the American Chemical Society* (2002) *124*, 8-9.

[90] Y. Lee, H. Koo, G. Jin, H. Mo, M. Y. Cho, J. Y. Park, J. S. Choi, J. S. Park, Poly(ethylene oxide sulphide): New Poly(ethylene glycol) Derivatives Degradable in Reductive Conditions. *Biomacromolecules* (2005) *6*, 24-26.

[91] K. H. Sun, Y. S. Sohn, B. Jeong, Thermogelling poly(ethylene oxide-b-propylene oxide-b-ethylene oxide) Disulfide Multiblock Copolymer as a Thiol-Sensitive Degradable Polymer. *Biomacromolecules* (2006) *7*, 2871-2877.

[92] A. Napoli, N. Tirelli, G. Kilcher, A. Hubbell, New Synthetic Methodologies for Amphiphilic Multiblock Copolymers of Ethylene Glycol and Propylene Sulfide. *Macromolecules* (2001) *34*, 8913-8917.

[93] C. Woghiren, B. Sharma, S. Stein, Protected Thiol-Polyethylene Glycol: A New Activated Polymer for Reversible Protein modifications, *Bioconjugate Chemistry* (1993) *4*, 314-318.

[94] V. Ghetie, E. Vitetta, Chemical Construction of Immunotoxins. *Molecular Biotechnology,* (2001) *18*, 251-268.

[95] G. T. Hermanson, *Bioconjugate Techniques*, Academic Press, San Diego (2005).

[96] T. P. King, Y. Li, L. Kochoumian, Preparation of Protein Conjugates via Intramolecular Disulfide Bond Formation. *Biochemistry* (1978) *17*, 1499-1506.

[97]   T. Masuko, A. Minami, N. Iwasaki, T. Majima, S.-I. Nishimura, Lee Y.C, Thiolation of Chitosan: Attachment of Proteins via Thioether Formation. *Biomacromolecules* (2005) *6*, 880-884.

[98]   R. R. Traut, A. Bollen, T.-T. Sun, J. W. B. Hershey, J. Sundberg, L. R. Pierce, Methyl 4-Mercaptobutyrimidate as a Cleavable Cross-Linking Reagent and its Application to the *Escherichia coli* 30S Ribosome. *Biochemistry* (1973) *12*, 3266-3273.

[99]   D. A. Goff, S. F. Carroll, Substituted 2-Iminothiolanes: Reagents for the Preparation of Disulfide Cross-Linked Conjugates with Increased Stability. *Bioconjugate Chemistry* (1990) *1*, 381-386.

[100] S. F. Carroll, S. L. Bernhard, D. A. Goff, R. J. Bauer, W. Leach, A. H. C. Kung, Enhanced Stability in Vitro and in Vivo of Immunoconjugates Prepared with 5-Methyl-2-iminothiolane. *Bioconjugate Chemistry* (1994) *5*, 248-258.

[101] R. Benesch, R. E. Benesch, Formation of Peptide Bonds by Aminolysis of Homocysteine Thiolactones. *Proceedings of the National Academy of Sciences of the United States of America* (1958) *44*, 848-853.

[102] R. Benesch, R. E. Benesch, Thiolation of Proteins. *Journal of the American Chemical Society* (1956) *78*, 1597-853.

[103] Q. Peng, Z. Zhong, R. Zhuo, Disulfide Cross-Linked Polyethylenimines (PEI) Prepared via Thiolation of Low Molecular Weight PEI as Highly Efficient Gene Vectors. *Bioconjugate Chemistry* (2008) *19*, 499-506.

[104] I. M. Klotz, R. E. Heiney, Introduction of Sulfhydryl Groups into Proteins Using Acetylmercaptosuccinic Anhydride. *Archives of Biochemistry and Biophysics* (1962) *96*, 605-612.

[105] R. J. Duncan, P. D. Weston, R. Wrigglesworth, A New reagent Which May Be Used to Introduce Sulfhydryl Groups into Proteins, and Its Use in the Preparation of Conjugates for Immunoassay. *Anaytical. Biochemistry* (1983) *132*, 68-73.

[106] L. L. Chen, J. J. Rosa, S. Turner, R. B. Pepinsky, Production of Multimeric Forms of CD4 Through a Sugar-based Cross-linking Strategy. *Journal of Bioogical Chemistry* (1991) *266*, 18237-18243.

[107] S. Y. Huang, S. Pooyan, J. Wang, I. Choudhury, M. J. Leibowitz, S. Stein, Polyethylene Glycol Copolymer for Carrying and Releasing Multiple Copies of Cysteine-Containing Peptides. *Bioconjugate Chemistry* (1998) *9*, 612-617.

[108] W. K. Miskimins, N. Shimizu, Synthesis of a cytotoxic insulin cross-linked to diphtheria toxin fragment A capable of recognizing insulin receptors. *Biochemical and Biophysical Research Commununications* (1979) *91*, 143-151.

[109] N. Shimizu, W. K. Miskimins, Y. Shimizu, A cytotoxic epidermal growth factor cross-linked to diphtheria toxin-A fragment. *FEBS Letters* (1980) *118*, 274-278.

[110] D. G. Gilliland, R. J. Collier, J. M. Moehring, T. J. Moehring, Chimeric toxins: Toxic, disulfide-linked conjugate of concanavalin A with fragment A from diphtheria

toxin. *Proceedings of the National Academy of Sciences of the United States of America* (1978) *75*, 5319-5323.

[111] A. J. Lomant, G. Fairbanks, Chemical Probes of Extended Biological Structures: Synthesis and Properties of the Cleavable Preotein Cross-linking Reagent [^{35}S] Dithiobis(succinimidyl propionate). *Journal of Molecular Biology* (1976) *104*, 234-261.

[112] K. Wang, F. M. Richards, An Approach to Nearest Neighbor Analysis of Membrane Proteins, *Journal of Biological Chemistry* (1974) *249*, 8005-8018.

[113] L. V. Christensen, C. W. Chang, W. J. Kim, S. W. Kim, Z. Zhong, C. Lin, J. F. J. Engbersen, J. Feijen, Reducibel Poly(amido amine)s Designed for Triggered Intracellular Gene Delivery. *Bioconjugate Chemistry* (2006) *17*, 1233-1240.

[114] J. Hoon Jeong, L. V. Christensen, J. W. Yockman, Z. Zhong, J. F. J. Engbersen, W. Jong Kim, J. Feijen, S. Wan Kim, Reducible Poly(amido amine) directed to enhance RNA interference. *Biomaterials* (2007) *28*, 1912-1917.

[115] G. Mattson, E. Conklin, S. Desai, G. Nielander, M. D. Savage, S. Morgensen, A practical approach to crosslinking. *Molecular Biology Reports* (1993) *17*, 167-183.

[116] J. Carlsson, H. Drevin, R. Axen, Protein Thiolation and Reversible Protein-Protein Conjugation N-Succinimidyl 3-(2-Pyridyldithio)propionate, a new heterobifunctional reagent. *Biochemical Journal* (1978) *173*, 723-737.

[117] P. E. Thorpe, A. N. F. Brown, W. C. J. Ross, A. J. Cumber, S. I. Detre, D. C. Edwards, A. J. S. Davies, F. Stirpe, Cytotoxicity Acquired by Conjugation of an Anti-Thy$_{1.1}$ monoclonal Antibody and the Ribosome-Inactivating Protein, Gelonin. *European Journal of Biochemistry* (1981) *116*, 447-454.

[118] P. E. Thorpe, P. M. Wallace, P. P. Knowles, M. G. Relf, A. N. F. Brown, G. J. Watson, R. E. Knyba, E. J. Wawrzynczak, D. C. Blakey, New Coupling Agents for the Synthesis of immunotxins Containing a Hindered Disulfide Bond with Improved Stability *in Vivo. Cancer Research* (1987) *47*, 5924-5931.

[119] S. Arpicco, F. Dosio, P. Brusa, P. Crosasso, L. Cattel, New Coupling Reagents for the Preparation of Disulfide Cross-Linked Conjugates with Increased Stability. *Bioconjugate Chemistry* (1997) *8,* 327-337.

[120] L. Delprino, M. Giacomotti, F. Dosio, P. Brusa, M. Ceruti, G. Grosa, L. Cattel, Toxin-Targeted Design for Anticancer Therapy. I: Synthesis and Biological Evaluation of New Thioimidate Heterobifunctional Reagebts. *Journal of Pharmaceutical Sciebces* (1993) *82*, 506-512.

[121] L. Greenfield, W. Bloch, M. Moreland, Thiol-Containing Cross-Linking Agent with Enhanced Steric Hindrance. *Bioconjugate Chemistry* (1990) *1*, 400-410.

[122] J. J. Zara, R. D. Wood, P. Boon, C. H. Kim, N. Pomato, R. Bredehorst, C. W. Vogel, A Carbohydrate-Directed Heterobifunctional Cross-Linking Reagent for te Synthesis of Immunoconjugates. *Analytical Biochemistry* (1991) *194*, 156-162.

[123]   A.-G. Gao, W. A. Frazier, Identification of a Receptor Candidate fort he Carboxyl-terminal Cell Binding Domain of Thrombospondins. *Journal of Biological Chemistry* (1994) *269*, 29650-29657.

[124]   D. Dey, D. E. Bochkariov, G. G. Jokhadze, R. R. Traut, Cross-linking of Selected Residues in the N- and C-terminal Domains of *Escherichia coli* Protein L7/L12 to Other Ribosomal Proteins and the Effect of Elongation Factor Tu. *Journal of Biological Chemistry* (1998) *273*, 1670-1676.

[125]   G. Cavallaro, M. Campisi, M. Licciardi, M. Ogris, G. Giammona, Reversibly stable thiopolyplexes for intracellular delivery of genes. *Journal of Controlled Release* (2006) *115*, 322-334.

[126]   M. Neu, J. Sitterberg, U. Bakowsky, T. Kissel, Stabilized Nanocarriers for Plasmids Based Upon Cross-Linked Poly(ethylene imine). *Biomacromolecules* (2006) *7*, 3428-3438.

[127]   C. P. Chen, J. Kim, E. Steenblock, D. Liu, K. G. Rice, Gene Transfer with Poly-Melittin Peptides. *Bioconjugate Chemistry* (2006) *17*, 1057-1062.

[128]   T. Schmitz, I. Bravo-Osuna, C. Vauthier, G. Ponchel, B. Loretz, A. Bernkop-Schnürch, Development and in vitro evaluation of a thiomer-based nanoparticulate gene delivery system. *Biomaterials* (2007) *28*, 524-531.

[129]   R. C. Adami, K. G. Rice, Metabolic Stability of Glutaraldehyde Cross-Linked Peptide DNA Condensates. *Journal of Pharmaceutical Sciences* (1999) *88*, 739-746.

[130]   C. Chittimalla, L. Zammut-Italiano, G. Zuber, J. P. Behr, Monomolecular DNA Nanoparticles for Intravenous Delivery of Genes. *Journal of the American Chemical Society* (2005) *127*, 11436-11441.

[131]   T. Blessing, J. S. Remy, J. P. Behr, Monomolecular collapse of plasmid DNA into stable virus-like Particles. *Proceedings of the National Academy of Sciences of the United States of America* (1998) *95*, 1427-1431.

[132]   V. S. Trubetskoy, V. G. Budker, L. J. Hanson, P. M. Slattum, J. A. Wolff, J. E. Hagstrom, Self-assembly of DNA-polymer complexes using template polymerization. *Nucleic Acids Research* (1998) *26*, 4178-4185.

[133]   V. S. Trubetskoy, A. Loomis, P. M. Slattum, J. E. Hagstrom, V. G. Budker, J. A. Wolff. Caged DNA does not aggregate under high ionic strength solutions, *Bioconjugate Chemistry* (1999) *10*, 624-628.

[134]   F. Tang, J. A. Hughes, Introduction of a Disulfide Bond into a Cationic Lipid Enhances Transgene Expression of Plasmid DNA. *Biochemical and Biophysical Research Communications* (1998) *242*, 141-145.

[135]   P. S. Ajmani, F. Tang, S. Krishnaswami, E. M. Meyer, C. Sumners, J. A. Hughes, Enhanced transgene expression in rat brain cell cultures with a disulfide-containing cationic lipid. *Neuroscience Letters* (1999) *277*, 141-144.

[136] F. Tang, J. A. Hughes, Use of Dithioglycolic Acid as a Tether for Cationic Lipids Decreases the Cytotoxiciy and Increases Transgene Expression of Plasmid DNA *in Vitro. Bioconjugate Chemistry* (1999) *10*, 791-796.

[137] D. Lee, W. Zhang, S. Shirley, X. Kong, G. Hellermann, R. Lockey, S. Mohapatra, Thiolated Chitosan/DNA Nanoparticles Exhibit Enhanced and Sustained Gene Delivery. *Pharmaceutical Research* (2007) *24*, 157-167.

[138] D. L. McKenzie, K. Y. Kwok, K. G. Rice, A potent New Class of Reductively Activated Peptide Gene Delivery Agents. *Journal of Biological Chemistry* (2000) *275*, 9970-9977.

[139] K. Y. Kwok, Y. Park, Y. Yang, D. L. McKenzie, Y. Liu, K. G. Rice, In Vivo Gene Transfer Using Sulfhydryl Cross-Linked PEG/Glycopeptide DNA Co-Condensates. *Journal of Pharmaceutical Sciences* (2003) *92*, 1174-1185.

[140] D. L. McKenzie, E. Smiley, K. Y. Kwok, K. G. Rice, Low Molecular Weight Cross Linking Peptides as Nonviral Gene Delivery Carriers. *Bioconjugate Chemistry* (2000) *11*, 901-909.

[141] Y. Park, K. Y. Kwok, C. Boukarim, K. G. Rice, Synthesis of Sulfhydryl Cross-linking Poly(Ethylene Glycol)-Peptides and Glycopeptides as Carriers for Gene Delivery. *Bioconjugate Chemistry* (2002) *13*, 232-239.

[142] D. Trentin, J. Hubbell, H. Hall, Non-viral gene delivery for local and controlled DNA release. *Journal of Controlled Release* (2005) *102*, 263-275.

[143] S. J. Lee, Cytokine Delivery and Tissue Engineering. *Yonsei Medical Journal* (2000) *41*, 704-719.

[144] C. Pichon, E. LeCam, B. Guerin, D. Coulaud, E. Delain, P. Midoux, Poly[Lys-(AEDTP)]: A Cationic Polymer That Allows Dissociation of pDNA/Cationic Polymer Complexes in a Reductive Medium and Enhances Polyfection. *Bioconjugate Chemistry* (2002) *13*, 76-82.

[145] D. Oupicky, R. C. Carlisle, L. W. Seymour, Triggered intracellular activation of disulfide crosslinked polyelectrolyte gene delivery complexes with extended systemic circulation in vivo. *Gene Therapy* (2001) *8*, 713-724.

[146] M. A. Gosselin, W. Guo, R. J. Lee, Incorporation of Reversibly Cross-Linked Polyplexes into LPDH Vectors for Gene Delivery. *Bioconjugate Chemistry* (2002) *13*, 1044-1053.

[147] M. Neu, O. Germershaus, S. Mao, K. H. Voigt, M. Behe, T. Kissel, Crosslinked nanocarriers based upon poly (ethylene imine) for systemic plasmid delivery: In vitro characterization and in vivo studies in mice. *Journal of Controlled Release (*2007) *118*, 370-380.

[148] H. Lee, H. Mok, S. Lee, Y. K. Oh, T. G. Park, Target-specific intracellular delivery of siRNA using degradable hyaluronic acid nanogels. *Journal of Controlled Release* (2007) *119*, 245-252.

[149] M. Greindl, A. Bernkop-Schnürch, Development of a Novel Method for the Preparation of Thiolated Polyacrylic Acid Nanoparticles. *Pharmaceutical Research* (2006) *23*, 2183-2189.

[150] A. N. Zelikin, J. F. Quinn, F. Caruso, Disulfide Cross-Linked Polymer Capsules: En Route to Biodeconstructible Systems. *Biomacromolecules* (2006) *7*, 27-30.

[151] J. Chen, S.-W. Huang, W.-H. Lin, R.-X. Zhuo, Tunable Film Degradation and Sustained Release of Plasmid DNA from Cleavable Polycation/Plasmid DNA Multilayers under Reductive Conditions. *Small* (2007) *3*, 636-643.

[152] J. Blacklock, Y. Z. You, Q. H. Zhou, G. Mao, D. Oupicky, Gene delivery in vitro and in vivo from bioreducible multi-layered polyelectrolyte films of plasmid DNA. *Biomaterials* (2009) *30*, 939-950.

[153] M. Ogris, S. Brunner, S. Schuller, R. Kircheis, E. Wagner, PEGylated DNA/transferrin-PEI complexes: reduced interaction with blood components, extended circulation in blood and potential for systemic gene delivery. *Gene Therapy* (1999) *6*, 595-605.

[154] D. Oupicky, K. A. Howard, C. Konak, P. R. Dash, K. Ulbrich, L. W. Seymour, Steric Stabilization of poly-L-Lysine/DNA Complexes by the Covalent Attachment of Semitelechelic poly[N-(2-Hydroxypropyl)methacrylamide]. *Bioconjugate Chemistry* (2000) *11*, 492-501.

[155] M. Lee, S. W. Kim, Polyethylene Glycol-Conjugated Copolymers for Plasmid DNA Delivery. *Pharmaceutical Research* (2005) *22*, 1-10.

[156] Y. Kakizawa, A. Harada, K. Kataoka, Glutathione-Sensitive Stabilization of Block Copolymer Micelles Composed of Antisense DNA and Thiolated Poly(ethylene glycol)-block-poly(L-Lysine): A Potential Carrier for Systemic Delivery of Antisense DNA. *Biomacromolecules* (2001) *2*, 491-497.

[157] H. Mok, T. G. Park, PEG-Assisted DNA Solubilization in Organic Solvents for Preparing Cytosol Specifically Degradable PEG/DNA Nanogels. *Bioconjugate Chemistry* (2006) *17*, 1369-1372.

[158] T. Ishida, M. J. Kirchmeier, E. H. Moase, S. Zalipsky, T. M. Allen, Targeted delivery and triggered release of liposomal doxorubicin enhances cytotoxicity against human B lymphoma cells. *Biochimica et Biophysica Acta* (2001) *1515*, 144-158.

[159] D. Kirpotin, K. Hong, N. Mullah, D. Papahadjopoulos, S. Zalipsky, Liposome with detachable polymer coating: destabilization and fusion of dioleoylphosphatidylethanolamine vesicles triggered by cleavage of surface-grafted poly(ethylene glycol). *FEBS Letters* (1996) *388*, 115-118.

[160] M. Neu, O. Germershaus, M. Behe, T. Kissel, Bioreversibly crosslinked of PEI and high molecular weight PEG show extended circulation times in vivo. *Journal of Controlled Release* (2007) *124*, 69-80.

[161] R. C. Carlisle, T. Etrych, S. S. Briggs, J. A. Preece, K. Ulbrich, L. W. Seymour, Polymer-coated polyethylenimine/DNA complexes designed for triggered activation by intracellular reduction. *Journal of Gene Medicine* (2004) *6*, 33-344.

[162] K. Miyata, Y. Kakizawa, N. Nishiyama, A. Harada, Y. Yamasaki, H. Koyama, K. Kataoka, Block Catiomer polyplexes with Regulated Densities of Charge and Disulfide Cross-Linking Directed To Enhance Gene Expression. *Journal of the American Chemical Society* (2004) *126*, 2355-2361.

[163] J. Kloeckner, E. Wagner, M. Ogris, Degradable gene carriers based on oligomerized polyamines, *European Journal of Pharmaceutical Sciences* (2006) *29*, 414-425.

[164] Y. Kakizawa, A. Harada, K. Kataoka, Environment-Sensitive Stabilization of Core-Shell Structured Polyion Complex Micelle by Reversible Cross-Linking of the Core through Disulfide Bond. *Journal of the American Chemical Society* (1999) *121*, 11247-11248.

[165] K. Miyata, Y. Kakizawa, N. Nishiyama, Y. Yamasaki, T. Watanabe, M. Kohara, K. Kataoka, Freeze-dried formulations for in vivo gene delivery of PEGylated polyplex micelles with disulfide crosslinked cores to the liver. *Journal of Controlled Release* (2005) *109*, 15-23.

[166] A. G. Schatzlein, Non-viral vectors in cancer gene therapy: principles and progress, *Journal of Biomedicine and Biotechnology* (2003) 149-158.

[167] V. Russ, E. Wagner, Cell and Tissue Targeting of Nucleic Acids for Cancer Gene Therapy. *Pharmaceutical Research* (2007) *24*, 1047-1057.

[168] A. Muratovska, M. R. Eccles, Conjugates for efficient delivery of short interfering RNA (siRNA) into mammalian cells, *FEBS Letters* (2004) *558*, 63-68.

[169] S. B. Rajur, C. M. Roth, J. R. Morgan, M. L. Yarmush, Covalent Protein-Oligonucleotide Conjugates for Efficient Delivery of Antisense Molecules, *Bioconjugate Chemistry* (1997) *8*, 935-940.

[170] E. Bonfils, C. Depierreux, P. Midoux, N. T. Thuong, M. Monsigny, A. C. Roche, Drug targeting: synthesis and endocytosis of oligonucleotide-neoglycoprotein conjugates, *Nucleic Acids Research* (1992) *20*, 4621-4629.

[171] E. Wagner, Application of membrane-active peptides for nonviral gene delivery, *Advanced Drug Delivery Reviews* (1999) *38*, 279-289.

[172] J.-P. Behr, The Proton Sponge: a Trick to enter Cells the Viruses did not exploit. *Chimia* (1997) *51*, 34-38.

[173] M. Ogris, R. C. Carlisle, T. Bettinger, L. W. Seymour, Melittin Enables Efficient Vesicular Escape and Enhanced Nuclear Access of Nonviral Gene Delivery Vectors. *Journal of Biological Chemistry* (2001) *276*, 47550-47556.

[174] M. Meyer, A. Philipp, R. Oskuee, C. Schmidt, E. Wagner, Breathing Life into Polycations: Functionalization with pH-Responsive Endosomolytic Peptides and Polyethylene

Glycol Enables siRNA Delivery. *Journal of the American Chemical Society* (2008) *130*, 3272-3273.

[175] M. Meyer, A. Zintchenko, M. Ogris, E. Wagner, A dimethylmaleic acid-melittin-polylysine conjugate with reduced toxicity, pH-triggered endosomolytic activity and enhanced gene transfer potential. *Journal of Gene Medicine* (2007) 797-805.

[176] M. Oishi, T. Hayama, Y. Akiyama, S. Takae, A. Harada, Y. Yamasaki, F. Nagatsugi, S. Sasaki, Y. Nagasaki, K. Kataoka, Supramolecular Assemblies for the Cytoplasmatic Delivery of Antisense Oligodeoxynucleotides: Polyion Complex (PIC) Micelles Based on Poly(ethylene glycol)-SS-Oligodeoxynucleotide Conjugate. *Biomacromolecules* (2005) *6*, 2449-2454.

[177] M. Breunig, U. Lungwitz, R. Liebl, A. Goepferich, Breaking up the correlation between efficacy and toxicity for nonviral gene delivery. *Proceedings of the National Academy of Sciences of the United States of America* (2007) *104*, 14454-14459.

[178] Y. Lee, H. Mo, H. Koo, J. Y. Park, M. Y. Cho, G. Jin, J. S. Park, Visualization of the Degradation of a Disulfide Polymer, Linear Poly(ethylenimine sulfide), for Gene Delivery. *Bioconjugate Chemistry* (2007) *18*, 13-18.

[179] M. A. Gosselin, W. Guo, R. J. Lee, Efficient Gene Transfer Using Reversibly Cross-Linked Low Molecular Weight Polyethylenimine. *Bioconjugate Chemistry* (2001) *12*, 989-994.

[180] C. Lin, C. J. Blaauboer, M. M. Timoneda, M. C. Lok, M. van Steenbergen, W. E. Hennink, Z. Zhong, J. Feijen, J. F. J. Engbersen, Bioreducible poly(amido amine)s with oligoamine side chains: Synthesis, characterization, and structural effects on gene delivery. *Journal of Controlled Release (*2008) *126*, 166-174.

[181] D. Soundara Manickam, H. S. Bisht, L. Wan, G. Mao, D. Oupicky, Influence of TAT peptide polymerization on properties and transfection activity of TAT/DNA polyplexes. *Journal of Controlled Release, (*2005) *102*, 293-306.

[182] S. L. Lo, S. Wang, An endosomolytic TAT peptide produced by incorporation of histidine and cysteine as a nonviral vector for DNA transfection. *Biomaterials* (2008) *29*, 2408-2414.

[183] S. Huth, F. Hoffmann, K. von Gersdorff, A. Laner, D. Reinhardt, J. Rosenecker, C. Rudolph, Interaction of polyamine gene vectors with RNA leads to the dissociation of plasmid DNA-carrier complexes. *Journal of Gene Medicine* (2006) *8*, 1416-1424.

[184] B. Lucas, K. Remaut, N. N. Sanders, K. Braeckmans, S. C. DeSmedt, J. Demeester, Studying the Intracellular Dissociation of Polymer-Oligonucleotide Complexes by Dual Color Fluorescence Fluctuation Spectroscopy and Confocal Imaging. *Biochemistry* (2005) *44*, 9905-9912.

[185] M. Bertschinger, G. Backliwal, A. Schertenleib, M. Jordan, D. L. Hacker, F. M. Wurm, Disassembly of polyethylenimine-DNA particles in vitro: Implications for polyethylenimine-mediated DNA delivery. *Journal of Controlled Release* (2006) *116*, 96-104.

[186] J. P. Clamme, J. Azoulay, Y. Mely, Monitoring of the Formation and Dissociation of Polyethylenimine/DNA Complexes by Two Photon Fluorescence Correlation Spectroscopy. *Biophysical Journal* (2003) *84*, 1960-1968.

[187] M. Breunig, C. Hozsa, U. Lungwitz, K. Watanabe, I. Umeda, H. Kato, A. Goepferich, Mechanistic investigation of poly(ethylene imine)-based siRNA delivery: Disulfide bonds boost intracellular release of the cargo. *Journal of Controlled Release* (2008) *130*, 57-63.

[188] C. Lin, Z. Zhong, M. C. Lok, X. Jiang, W. E. Hennink, J. Feijen, J. F. J. Engbersen, Novel Bioreducible Poly(amido amine)s for Highly efficient Gene Delivery. *Bioconjugate Chemistry* (2007) *18*, 138-145.

[189] T. Reschel, C. Konak, D. Oupicky, L. W. Seymour, K. Ulbrich, Physical properties and in vitro transfection efficiency of gene delivery vectors based on complexes of DNA with synthetic polycations. *Journal of Controlled Release* (2002) *81*, 201-217.

[190] X. L. Wang, R. Jensen, Z. R. Lu, A novel environment-sensitive biodegradable polydisulfide with protonatable pendants for nucleic acid delivery. *Journal of Controlled Release* (2007) *120*, 250-258.

[191] M. L. Read, S. Singh, Z. Ahmed, M. Stevenson, S. S. Briggs, D. Oupicky, L. B. Barrett, R. Spice, M. Kendall, M. Berry, J. A. Preece, A. Logan, L. W. Seymour, A versatile reducible polycation-based system for efficient delivery of a broad range of nucleic acids. *Nucleic Acids Research* (2005) *33*, e86, 1-16.

[192] G. Byk, B. Wetzer, M. Frederic, C. Dubertret, B. Pitard, G. Jaslin, D. Scherman, Reduction Sensitive Lipopolyamines as a Novel Nonviral Gene Delivery System for Modulated Release of DNA with Improved Transgene Expression. *Journal of Medicinal Chemistry* (2000) *43*, 4377-4387.

[193] V. P. Torchilin, Multifunctional nanocarriers. *Advanced Drug Delivery Reviews* (2006) *58*, 1532-1555.

[194] S. Ganta, H. Devalapally, A. Shahiwala, M. Amiji, A review of stimuli-responsive nanocarriers for drug and gene delivery. *Journal of Controlled Release (*2008) *126*, 187-204.

[195] W. Li, C. Nesselmann, Z. Zhou, L.-L. Ong, F. Öri, G. Tang, A. Kaminski, K. Lützow, A. Lendlein, A. Liebhold, C. Stamm, J. Wang, N. Ma, Gene delivery to the heart by magnetic nanobeads. *Journal of Magnetism and Magnetic Materials* (2007) *311*, 336-341.

[196] C. Alexander, K. M. Shakesheff, Responsive Polymers at the Biology/Materials Science Interface, *Advanced Materials* (2006) *18*, 3321-3328.

[197] T. Maeda, K. Fujimoto, A reduction-triggered delivery by a liposomal carrier possessing membrane-permeable ligands and a detachable coating. *Colloids and Surfaces B: Biointerfaces* (2006) *49*, 15-21.

[198] N. Murthy, J. Campbell, N. Fausto, A. S. Hoffman, P. S. Stayton, Bioinspired pH-
        Responsive Polymers for the Introcellular Delivery of Biomolecular Drugs.
        Bioconjugate Chemistry, 2003, *14*, 412-418.

[199] N. Murthy, J. Campbell, N. Fausto, A. S. Hoffman, P. S. Stayton, Design and Synthesis
        of pH-responsive polymeric carriers that target uptake and enhance the
        intracellular delivery of oligonucleotides. *Journal of Controlled Release,* 2003, *89,*
        365-374.

[200] V. Bulmus, M. Woodward, L. Lin, N. Murthy, P. Stayton, A. Hoffman, A new pH-
        responsive and glutathione-reactive, endosomal membrane-disruptive polymeric
        carrier for intracellular delivery of biomolecular drugs. *Journal of Controlled
        Release (*2003) *93*, 105-120.

[201] N. Raghunand, R. A. Gatenby, R. J. Gillies, Microenvironmental and cellular
        consequences of altered blood flow in tumours. *British Journal of Radiology*
        (2003) *76*, 11-22.

[202] V. Sethuraman, M. Lee, Y. Bae, A Biodegradable pH-sensitive Micelle System for
        Targeting Acidic Solid Tumors. *Pharmaceutical Research* (2008) *25,* 657-666.

Chapter 2

Goals of the thesis

The delivery of nucleic acids is a promising strategy for the modulation of gene expression inside cells. It offers both, the opportunity to insert therapeutic genes by the application of DNA and the chance to inhibit the expression of non-functional or harmful proteins by the use of therapeutic RNA. These two approaches each pave the way for the treatment of inherited or acquired diseases as well as the regeneration of defective tissue. But safe and efficient carrier systems for these therapies are still needed. While viral carriers are generally considered to be most efficient, they bear considerable risks such as infectiousness and insertional oncogenesis. Thus, scientists focused on the development of non-viral, polymeric carrier systems. The most prominent polymer among these systems is poly(ethylene imine) (PEI). It masters the most important steps in the delivery of nucleic acids: it condenses its payload into small particles, protects it from degradation and facilitates endosomal uptake. In the endosome it achieves endosomolysis and thereafter releases its cargo. Despite these advantages its broad use is hampered by the tendency of PEI particles to agglomerate and the strong correlation between transfection efficiency and toxicity. Thus, the first aim of the thesis was the development of new strictly linear PEI copolymers with lower toxicity and enhanced stability in the extracellular environment due to the attachment of a shielding moiety. In a second step copolymers responsive to a specific trigger -the change in redox potential upon cell entry- were developed and investigated.

First of all the delivery of nucleic acids via disulfide based carrier systems is reviewed. Therefore, the biological rationale for the exploitation of the large intra-/extracellular redox gradient was explained. Thereafter examples for the generation of disulfides were given, followed by a section which dealt with examples for carrier systems bearing disulfides. Finally, examples for redox active systems in the field of tissue engineering were given (**Chapter 1**).

Chapter 3 deals with the synthesis and modification of PEI. Compared to the standard synthesis for linear PEI, an attempt was taken to insert a thiol group at the chain end instead of the

common hydroxy group. This thiol group was introduced to selectively build a bridge between the chain end of PEI and the chain end of a second polymer resulting in strictly linear copolymers. For this modification different reaction conditions were tested. Furthermore, since the resulting thiol group is known to be unstable, different methods for its reactivation and storage were examined. Afterwards it was tested via an ethidium bromide exclusion assay whether the 13 obtained thiol-modified polymers with a molecular weight ranging from 1.5 kDa to 10.8 kDa were able to form particles with pDNA. Moreover, the hydrodynamic diameters and zeta potentials were determined.

After the synthesis of 13 different thiol-modified PEIs two attempts were taken towards the formation of strictly linear copolymers made from PEI and the shielding moiety poly(ethylene glycol) (PEG). The first copolymer series aimed at the formation of noncleavable thioether-connected copolymers with different molecular weights of both PEI and PEG for an analysis of structure-activity-relationships later on. But first these copolymers were examined for their complexation ability for such different nucleic acids as pDNA and siRNA by an ethidium bromide exclusion assay and size measurement of the particles made from the polymers and nucleic acids (polyplexes). The second copolymer series was intended for the triggered degradation of the disulfide bond which connected PEI with PEG (PEI-SS-PEG). Therefore, a thioacetate-modified PEG was synthesized, the conditions for its cleavage were examined and PEI-SS-PEG copolymers were synthesized (**Chapter 4**).

Chapter 5 aims at the performance of structure-function-relationships for the library of thioether connected copolymers. It was hypothesized that this library would allow a systematic study of the influence of the PEG moiety on the physicochemical properties and the biological activity of the polyplexes formed with pDNA. Thus, sizes and zeta potentials were measured under different conditions in order to obtain information about the compactness of the polyplexes, the extent of the PEG shielding and the influence of different pH values. The size measurements

were further supported by electron micrographs. Furthermore, a quenching assay was introduced for the determination of the strength of interaction between the nucleic acids and the PEI homo- or copolymers. In order to study the effects of different copolymer compositions in cell culture transfection experiments were performed as well as uptake studies. The polyplex uptake was also observed with the confocal microscope. The results of all these experiments were used to draw structure-activity-relationships.

Last, but not least, the series of thiol-connected copolymers was tested for its physicochemical and transfection characteristics. The cleavage of the disulfide bond connecting the PEI and the PEG chain is very important because the detachment of the PEG part is thought to be needed for the restoration of PEIs transfection efficiency which is generally reduced after the addition of a shielding moiety. Thus, the special focus of **Chapter 6** lay on the reductive cleavage of the connecting disulfide bond which was examined in detail. Size and zeta potential measurements were performed under non-reductive and reductive conditions in order to work out the influence of the molecular weights of both, PEG and PEI, on the cleavability. In order to support these experiments cellular uptake and transfection studies were also performed. The second main point of this chapter was the determination of the influence of the PEG shielding on the mobility of the polyplexes in a model matrix. This was investigated with the help of FRAP (fluorescence recovery after photobleaching) experiments. Since this method needed special fluorescently labeled copolymers, a synthesis route for fluoresceine labeled copolymers was developed and FRAP experiments were performed with these copolymers.

Chapter 3

Synthesis and characterization of thiol modified low molecular weight linear poly(ethylene imine)s

Abstract

Poly(ethylene imine) 25 kDa (PEI 25k) is the gold standard in nonviral gene delivery. This high molecular weight polymer efficiently transfects cells but it is also rather toxic. Generally, transfection efficiency and toxicity of PEI strongly correlate. Thus, it is not astounding that linear PEI with low molecular weight appeared to be a promising gene carrier which transfects cells and is rather nontoxic. Here we report on the synthesis of linear low molecular weight PEI with a thiol group at the chain end. This thiol group is intended for further modifications. We synthesized a library of 13 different PEIs with a molecular weight ranging from 1.5 to 10.8 kDa and introduced a sophisticated synthesis route leading to activated and at the same time storable PEI thiol derivatives. This multistep synthesis was investigated in detail. After successful synthesis the resulting carriers were tested for their ability to condense plasmid DNA into particles and to exclude ethidium bromide from the intercalation with the nucleic acid. Thus, the resulting polymers seem to be ideally suited for the attachment of further moieties such as a shielding polyethylene glycol chain for further improvement of the gene carrier.

Introduction

The decoding of the human genome in 2001 was a milestone [1] and greatly improved the understanding of hereditary diseases. It seemed to be possible to replace defective genes and cure diseases which were untreatable by state-of-the-art medicine. Unfortunately, applying naked genes is impossible mostly because they are not effectively taken up by cells due to their large size, which exceeds the upper uptake limit by far. Moreover, they carry negative charges and are prone to degradation by nucleases. Thus, carrier systems are needed, which condense nucleic acids into small particles. In nature basic polyamines such as spermine or spermidine interact with the DNA within a cell [2,3] and pack this DNA into small particles arranged next to each other like pearls in a necklace. These aliphatic polyamines are important for gene expression, enzyme activity and cell proliferation as well as differentiation [4,5]. But most importantly, they protect DNA from external agents. Having this in mind researchers examined these natural polycations in detail [6-8], used them as guideline and looked for other basic polymers as DNA condensing agents. The most prominent representative of these polycations is poly(ethylene imine) (PEI) [9]. It exists in two different forms, branched and linear, and both of them contain a high number of basic amines. These amines account for typical properties such as high buffering capacity, the ability to escape from endosomes and high protonation level at physiologic pH [10,11]. Due to its high efficiency branched PEI 25 kDa (bPEI 25k) has become the gold standard in gene delivery efficiency, the so called transfection. Unfortunately, the polymer exhibits at the same time cytotoxicity which correlates especially with the molecular weight and the branching degree [12,13]. Thus, linear PEI (lPEI) appeared to be an alternative to bPEI. In *in vitro* and in *in vivo* experiments long chain lPEI (22 kDa and 25 kDa) outperformed bPEI 25k concerning its transfection [14,15]. But toxicity of high molecular weight PEI was still an issue. This inspired our group to investigate the performance of lPEIs with lower molecular weight. In a series of 12 different lPEIs with a molecular weight ranging from 1 to 10 kDa we could show that the toxicity and transfection efficiency correlated with the molecular weight of the polymer [16].

This finding encouraged us to keep the approach of low molecular weight PEIs. We synthesized a library of low molecular weight PEIs with a thiol group at the end of the polymer chain because we wanted to further improve these gene vectors by attaching additional moieties such as shielding components or targeting ligands either stably by thioethers or degradably via disulfides. For this purpose we synthesized and tested a library of 13 different PEIs. But we varied the underlying synthesis scheme compared to the known synthesis which yielded a hydroxyl group at the chain end. We sticked to the living polymerization of 2-ethyl-2-oxazoline by methyl toluenesulfonate (Figure 1, **1**) but we inserted a substitution step in order to gain a thioacetate group as thiol precursor **(2)** which in turn had to be cleaved **(3)** and activated **(4)** before use. Thus, the synthesis was a multistep procedure according to Figure 1 resulting in polymers that were on the one hand suited for the formation of polyplexes (the complexes made
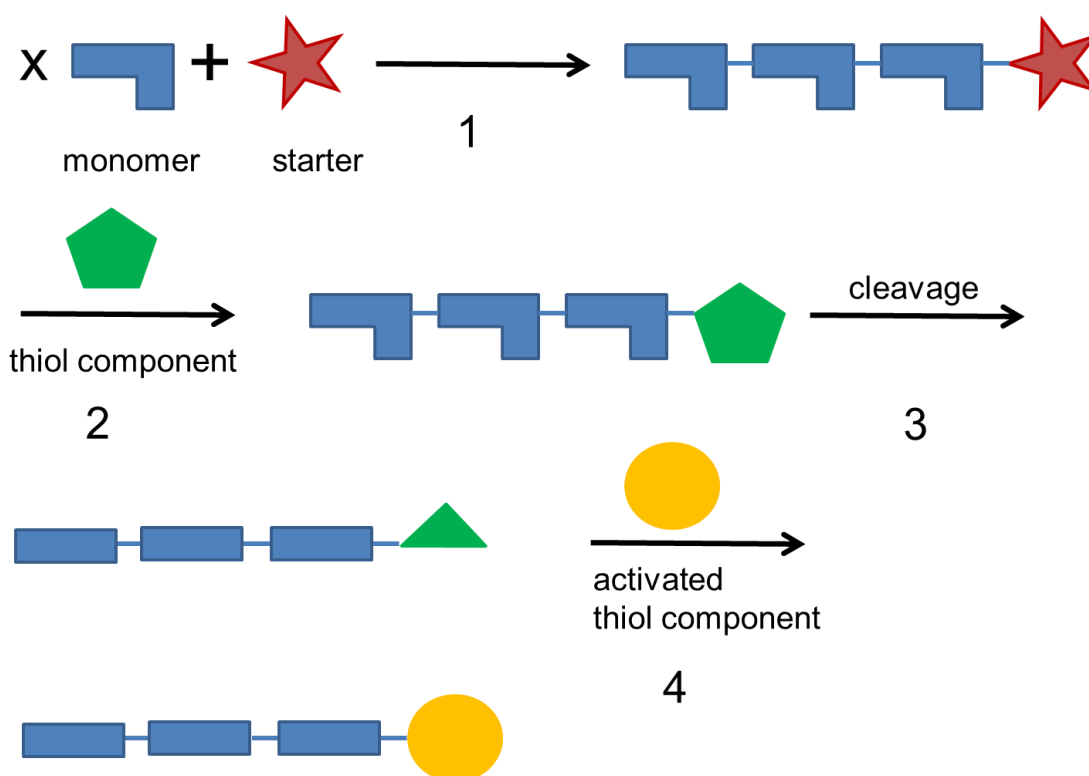

Figure 1. *Schematic drawing of the multistep synthesis yielding activated lPEI-SH.*

from nucleic acids and polymeric carriers) from the homopolymers and on the other hand suited for the attachment of a second moiety.

Materials and methods

All chemicals and materials were from Merck KGaA (Germany), Acros Organics (Belgium), Sigma-Aldrich Chemie GmbH (Germany), J.T. Baker (The Netherlands) or IRIS Biotech (Germany). Acetonitrile, dimethylformamide (DMF) and 2-ethyl-2-oxazoline were distilled over calciumhydride. Methyl-p-toluene sulfonate was dried in vacuo before use. All other chemicals were used as received.

The plasmid DNA encoding enhanced green fluorescent protein (EGFP) (pEGFP-N1, Clontech, Germany) was used as reporter gene and isolated from E. coli JM 109 strain using a Qiagen Plasmid Maxi Kit (Qiagen, Germany).

Polymer synthesis poly(2-ethyl-2-oxazoline)-thioacetate/ linear poly(ethylene imine) thiol

poly(2-ethyl-2-oxazoline) (pEtOXZ) was synthesized by cationic ring opening polymerization of 2-ethyl-2-oxazoline in acetonitrile at 90°C. The polymerization was conducted in dried glass ware in which dry acetonitrile, 2-ethyl-2-oxazoline and varying amounts of methyl-p-toluene sulfonate were converted. The amounts of methyl-p-toluene sulfonate were chosen depending on the desired molecular weight (MW) of PEI (typical amounts are listed in Table 1). The reaction apparatus was set under a nitrogen atmosphere and was heated to 90°C for several days (3 to 6 days, depending on the calculated MW of PEI). Afterwards the reaction was cooled down to rt and the MW of the resulting polymer was determined by ^{1}H-NMR. Then, 7.5 equivalents (eq., corresponding to the MW of PEI) of sodium thioacetate in DMF were added and the reaction mixture was stirred for 4 hours (h). After this the solvent was removed, the residue was dissolved in chloroform and the solution was washed 3 times with water. The raw product, poly(2-ethyl-2-oxazoline)-thioacetate (pEtOXZ-SAc) , was precipitated in ice cooled diethyl ether,

filtrated and dried in vacuo. In the next step, pEtOXZ-SAc was hydrolyzed in fuming HCl at 95°C for one day. After distilling off the HCl, the product PEI-SH was dissolved in water, precipitated with NaOH, washed with water until the supernatant became neutral and dried in vacuo.

Table 1. *Overview of the reaction educts for the polymerization.*

MW (pEtOXZ)	MW (lPEI)	V (OXZ) [ml]	n (Tos) [mmol]	m (Tos) [mg]	n (SAc) [mmol]	m (SAc) [mg]
22790	10000	6.25	0.266	50	2.00	228
19372	8500	6.25	0.313	58	2.35	268
15953	7000	6.25	0.380	71	2.85	325
13622	5977	6.25	0.445	83	3.34	381
11395	5000	6.25	0.532	99	3.99	456
10256	4500	6.25	0.592	110	4.44	507
9114	3999	6.25	0.666	124	5.00	570
8415	3655	6.25	0.731	136	5.48	626
7938	3483	6.25	0.764	142	5.73	654
6860	3010	6.25	0.884	165	6.63	757
5684	2494	6.25	1.067	199	8.00	914
4606	2021	6.25	1.317	245	9.88	1128
3465	1500	6.25	1.751	326	13.13	1500

The third step was the activation of the PEI derivative with 30 eq. $NaBH_4$ at pH 8.5 for 20 minutes (min), then the reaction mixture was acidified to pH 1 in order to destroy unreacted $NaBH_4$. This was followed by the adjustment of the pH to 4, the addition of 2.5 eq. 2,2`-dithio dipyridine (DTDP) and stirring overnight. On the next day the reaction mixture was slightly concentrated and dialysed against water excessively. Then the product was dried in vacuo.

Successful conversion was monitored by ^{1}H-NMR. ^{1}H-NMRs were recorded on an Avance 300 spectrometer (300 MHz, Bruker BioSpin GmbH, Germany). Afterwards the polymers were dissolved in 150 mM NaCl, and the pH was adjusted to 7.0.

NMR analysis

Estimation of the molecular weight of the polymer pEtOXZ

In order to estimate the molecular weight of the polymer NMRs were recorded of the oxazolinium salt species (Figure 2, **3**). The peaks assigned to the aromatic protons of the tosylate starter were set to 2 and the protons of the backbone peaks were calculated according to this first setting. These peaks corresponded to the propionyl side chains (0.81-1.41 ppm and 2.18-2.64 ppm) and to the methylene groups of the polymer backbone (3.13-3.92 ppm) and accounted for 3, 2 or 4 protons, respectively.

Conversion into pEtOXZ-thioacetate

The backbone peaks of the polymer (Figure 2, **4**) were set to the number of protons calculated from the precursor NMR of the oxazolinium salt polymer (Figure 2, **3**). The area of the only visible peak for the thioacetate at 2.92-2.97 ppm was used for the calculation of the conversion rate. The ratio of the resulting peak area to the theoretical area of 2 protons was the basis for the calculation of the conversion.

Conversion of lPEI-SH into lPEI-SS-pyr

In the ^{1}H-NMRs one backbone peak for lPEI can be seen as well as the aromatic peaks for the pyridyl conjugate. The area of the backbone peak was set to the expected value calculated from the molecular weight estimation after the first synthesis step. All other peaks resulted from this setting. The ratio of the obtained peak areas compared to the theoretical value of 1 gave the conversion into PEI-SS-pyr.

Investigation of the influence of reaction conditions on the polymer conversion

In order to determine the best reaction conditions for the conversion of the pEtOXZ intermediate into the thioacetate a series of different reaction conditions was tested. One series investigated the influence of reaction temperature and reaction time while the other series concentrated on reaction time and amount of added potassium thioacetate.

In both cases the polymerization was performed as described in the former section.

For the examination of the influence of time and temperature the reaction was divided into 3 parts after a reaction time of 4 days. One part was cooled down to 0°C, the other one was cooled down to rt while the third part was kept at 95°C. To each part 10 equ. of potassium thioacetate were added. After 1, 3 and 5 days samples were taken, the solvent was removed and the residue was dissolved in chloroform. This solution was washed three times with water and the resulting raw product was precipitated in diethyl ether. After filtration the product was dried in vacuo and the conversion degree was determined by ^{1}H-NMR as described before.

The investigation of the influence of time and excess of potassium thioacetate on the conversion rate followed the same scheme. First the polymerization was started. After 4 days reaction time the reaction was cooled down to room temperature, split into 4 parts and different amounts of potassium thioacetate (corresponding to 5 eq., 7.5 eq., 10 eq. and 15 eq.) were added. Again samples were taken at different time points (1h, 3h, 5h and 1day) and were worked up as described above. Also the conversion degree was calculated by ^{1}H-NMR as described above.

Determination of reduction/activation conditions

The determination of the best reaction conditions focused on the pH and reaction time during the reduction step on the one hand and on the same parameters during the activation step with 2,2`dithio dipyridine (DTDP).

Three different samples were prepared. For these samples three different starting pH´s were chosen (pH 7.5, pH 8 and pH 9). Each sample contained 0.545 mmol of the obtained lPEI-derivative dissolved in water and 0.48 ml alkaline $NaBH_4$ solution pH 7.5 (70% w/V) were added to every reaction vessel. The mixtures were stirred at rt. After 5 different time points (15 min, 30 min, 60 min, 90 min and 120 min) samples were taken. These samples were treated with 0.1 ml hexanol and 0.75 ml 6M HCl for 2 min and then further split in 3 parts. Part 1 had a pH of 4; part 2 was adjusted to pH 6 and part 3 was adjusted to pH 7. After this adjustment 0.0045 mmol DTDP were added and all samples were stirred. After different time points (15 min, 30 min, 60 min and overnight) samples were taken which were measured on a TitertekPlus Microplate Reader (Bartolomey Labortechnik, Germany) at 343 nm. This resulted in 180 different reaction conditions which were all measured in sextuplets. The concentrations were determined using cysteine standards reacted with DTDP. The outcome was visualized with MODDE (Umetrix, Umea, Sweden).

NTSB-Assay

The NTSB assay was adopted from [17]. The assay stock solution was prepared by dissolving 0.1 g 5,5`-dithio-bis-(2-nitrobenzoic acid) (DTNB) in 10 ml 1M Na_2SO_3 solution. This mixture was then heated to 38°C and oxygen was bubbled through the solution for 45 min. For the preparation of the assay solution the stock solution was further diluted 1:100 with a solution containing 0.605 g tris(hydroxymethyl)aminomethane (TRIS), 0.315 g Na_2SO_3 and 28 mg ethylene diamine tetra acetate (EDTA) pH 9,5. 300 µl assay solution were then mixed with 10 µl sample, pipetted into a 96 well plate and incubated for 10 min. Thereafter the absorbance was detected on a TitertekPlus Microplate Reader (Bartolomey Labortechnik, Germany) at 412 nm. All samples were measured three times. The concentration was determined using cysteine solutions as standards.

Ellman assay

For the Ellman assay the supplier´s instruction was transferred to a 96 well plate protocol. In brief, a pH 8 reaction buffer consisting of 0.1 M sodium phosphate and 1 mM EDTA was prepared. The Ellman reagent solution was made by mixing 4 mg Ellman´s reagent (5,5`-dithio-bis-(2-nitrobenzoic acid)) with 1 ml reaction buffer. All samples were reduced to thiols before analysis. Therefore, the pH of the PEI solutions was adjusted to pH 8-9, 5 eq. of $NaBH_4$ were added and the reaction mixtures were stirred at rt. After 20 min pH 1 was adjusted using 6M HCl and the solution was again stirred for 2 min. Then the pH was again adjusted, this time to pH 7. 25 µl of these solutions were mixed with 250 µl reaction buffer and 5 µl Ellman´s reagent. After incubation for 15 min at rt the absorbance was measured on a TitertekPlus Microplate Reader (Bartolomey Labortechnik, Germany) at 412 nm. All samples were measured 3 times and the concentration was determined using cysteine standards.

DTDP assay

The assay of Riener et al. [18] was modified for the use in a well plate format. The buffer for the DTDP-Assay (2,2`-dithio-dipyridine assay) consisted of 100 mM NaH_2PO_4 and 0.2 mM EDTA at pH 7. The assay solution was prepared by dissolving 88 mg DTDP in 100 µl fuming HCl and 3 ml water. This solution was diluted to 100 ml with DTDP buffer. All samples were reduced to thiols before analysis. Therefore, the pH of the PEI solutions was adjusted to pH 8-9, 5 eq. of $NaBH_4$ were added and the reaction mixtures were stirred at rt. After 20 min pH 1 was adjusted using 6M HCl and the solution was again stirred for 2 min. Then the pH was again adjusted, this time to pH 7. 4 µl samples were taken and mixed with 300 µl reaction buffer and 12.5 µl assay solution. After incubation at rt for 5 min the absorbance was measured on a TitertekPlus Microplate Reader (Bartolomey Labortechnik, Germany) at 343 nm. All samples were measured in triplicate and the concentrations were determined relative to cysteine standards.

Formation of polyplexes

The polyplexes of plasmid DNA and polymer were prepared at different N/P ratios (ratio of nitrogens in polymer to phosphates in DNA). The polymer and plasmid DNA were each diluted in equal volumes of 150 mM NaCl. The polymer solution was added to the DNA solution, the mixture was vortexed for 20 seconds and then incubated for 20 min before use. The amount of plasmid DNA and the total volume of the polyplex solution are given in each section.

Ethidium bromide quenching assay

The polyplexes were prepared at different N/P ratios ranging from 0.5 to 3 by diluting 1 µg of plasmid DNA in a final volume of 100 µl. After incubation for 20 min the polyplexes were pipetted in a 96-well plate and mixed with 2.5 µl of a 0.1 µg/µl ethidium bromide (EtBr) solution. The fluorescence of EtBr was excited at 518 nm and recorded at 605 nm using a LS 55 fluorescence spectrometer (Perkin Elmer, Germany) and expressed as relative fluorescence compared to uncomplexed plasmid DNA. Measurements were performed in quadruplet. The relative fluorescence loss was calculated as follows:

relative fluorescence loss = relative fluoresence$_{PEG-PEI-polyplexes}$/relative fluorescence$_{PEI-polyplexes}$.

Hydrodynamic diameter and zeta potential measurements

The hydrodynamic diameter was measured using a Zetasizer Nano-ZS from Malvern Instruments (Malvern, Germany) at 25°C. A 4 mW He-Ne laser at a wavelength of 633 nm was used as the light source. The measurement position was at 4.65 mm with automated laser attenuation. Scattered light was detected at an angle of 173° backscatter. The viscosity and refractive index of the dispersant were used as follows: 150 mM NaCl: 0.90 mm^2/s and 1.33, respectively. Three measurements with 10 sub-runs were performed for each sample. Data were analyzed by the general purpose mode and expressed as mean ± standard deviation (SD).

Polyplexes were formed by mixing 2 µg DNA and varying amounts of polymer to achieve different N/P ratios in a final volume of 500 µl.

Statistics

Results are shown as mean (± SD). Experiments were performed in triplicate if not otherwise indicated. Significance between the mean values of the pDNA and different polyplexes was calculated using one-way ANOVA analysis followed by Bonferroni t-test. A p-value of 0.05 was considered to be significant. Analysis was performed with Sigma Plot (Version 12.2, Systat Software, Chicago, IL, USA).

Results and discussion

Synthesis of pEtOXZ-SAc

The synthesis was a multistep procedure according to Figure 2. The first step comprised the polymerization of 2-ethyl-2-oxazoline **(1),** which was started by methyl-p-toluenesulfonate **(2)** and terminated by potassium thioacetate. The resulting poly-2-ethyl-2-oxazoline thioacetate (pEtOXZ-SAc, **4**) was cleaved yielding linear polyethylene imine thiol (lPEI-SH, **5**). This was further modified resulting in lPEI pyridyl disulfide (lPEI-SS-pyr, **6**).

We applied this polymerization reaction because of its living character where one monomer after the other is added to the growing polymer chain [19-21]. The growth is much slower than the increase in molecular weight gained by a radical polymerization. Thus, the addition is much more uniform and the size distribution is very narrow. This narrow size distribution was needed in order to properly characterize the resulting polymers and draw correlations between their molecular weight and their physicochemical and transfection characteristics. We chose 2-ethyl-2-oxazoline **(1)** as starting material for the formation of poly-2-ethyl-2-oxazoline (pEtOXZ) among
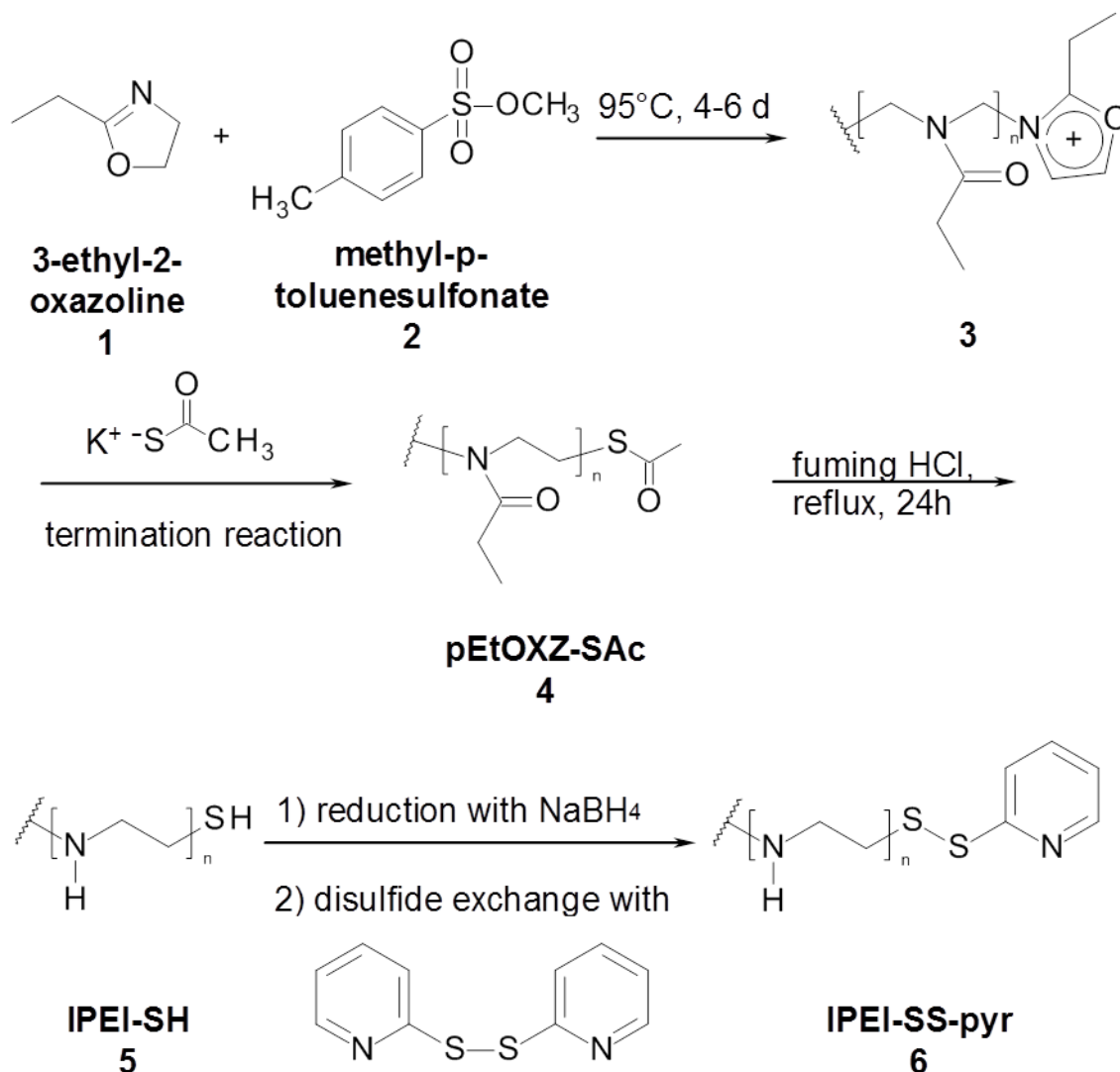
Figure 2. *Overview over the synthesis route of IPEI-SS-pyr.*

a lot of possible different cyclic imino ethers [22-24] because this 5-membered cyclic imino ether possesses high polymerizability. This is caused by both the thermodynamically favorable isomerization of the imino ether group to the amide and factors concerning ring strain [25]. In the case of the polymerization of 2-ethyl-2-oxazoline methyl-p-toluenesulfonate **(2)** has been shown to be perfectly suited as a starter since it decomposes fast when heated and, thus, the polymerization of each polymer strand is initiated at nearly the same time [26]. Furthermore, according to literature acetonitrile was used as solvent [26-29] and the reaction times were set to
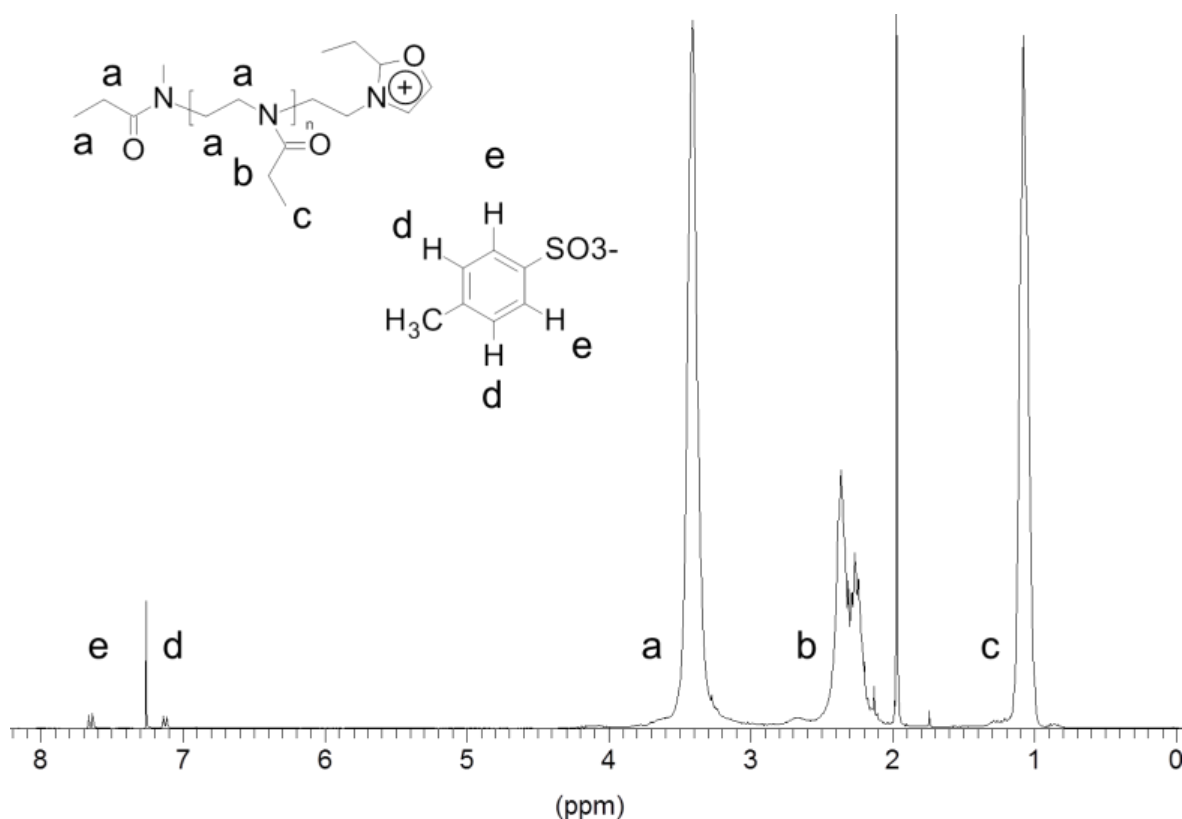
Figure 2. ^{1}H-NMR of the intermediate oxazolinium tosylate recorded in CDCl$_3$. The molecular weight of the polymer was estimated from the ratio of peaks (a), (b) and (c) to peaks (d) and (e). Peaks (d) and (e) were both set to 2 and peaks (a), (b) and (c) were calculated according to this setting.

4-6 days which guaranteed for complete conversion [26,30]. After this polymerization time samples were taken and the molecular weight of the resulting polymers was analyzed by ^{1}H-NMR according to [26]. The ratios of the calculated number of protons to the protons per molecule part allowed for an estimation of the molecular weight. This procedure was also possible because of the living nature of the polymerization [20,31] where all growing pEtOXZ-chains are terminated by a oxazolinium tosylate end **(3)**. As seen from Table 2 the calculated molecular weights of the obtained polymers were in good agreement with the theoretical values.

Table 2. *Overview of the theoretical and calculated molecular weight (MW) of the synthesized polymers.*

Polymer		MW pEtOXZ theory [g/mol]	MW pEtOXZ calculated [g/mol]	MW lPEI theory [g/mol]	MW lPEI calculated [g/mol]	designated
PEI	1	3456	3456	1501	1501	PEI 1.5
PEI	2	4606	4752	2001	2064	PEI 2.1
PEI	3	5648	5346	2453	2322	PEI 2.3
PEI	4	6860	6831	2980	2967	PEI 3.0
PEI	5	7938	8019	3448	3483	PEI 3.5
PEI	6	8415	8811	3655	3827	PEI 3.8
PEI	7	9114	9108	3959	3956	PEI 4.0
PEI	8	10256	9405	4455	4085	PEI 4.1
PEI	9	11389	11385	4947	4945	PEI 4.9
PEI	10	13622	15518	5917	6740	PEI 6.7
PEI	11	19372	18612	8414	8084	PEI 8.1
PEI	12	21285	20790	9245	9030	PEI 9.0
PEI	13	22790	24849	9899	10793	PEI 10.8

After analyzing polymer **3** (Figure 2), the oxazolinium salt species was used as activated intermediate for the attachment of a new functional group [21]. In this case potassium thioacetate was used to insert the precursor of the thiol group at the polymer chain end. This one step procedure proved to be faster and yielded higher conversion rates than the classical activation of hydroxyl groups with tosylates and their further substitution with thioacetates. High conversion rates are indispensable for further reactions because purification of polymers which differ only in their functional end group is very difficult. This is due to the fact that the polymer backbone is mainly responsible for the behavior of the molecule while the end group has just a minor influence. Thus, the optimization of the reaction yield was highly important and the 1-step
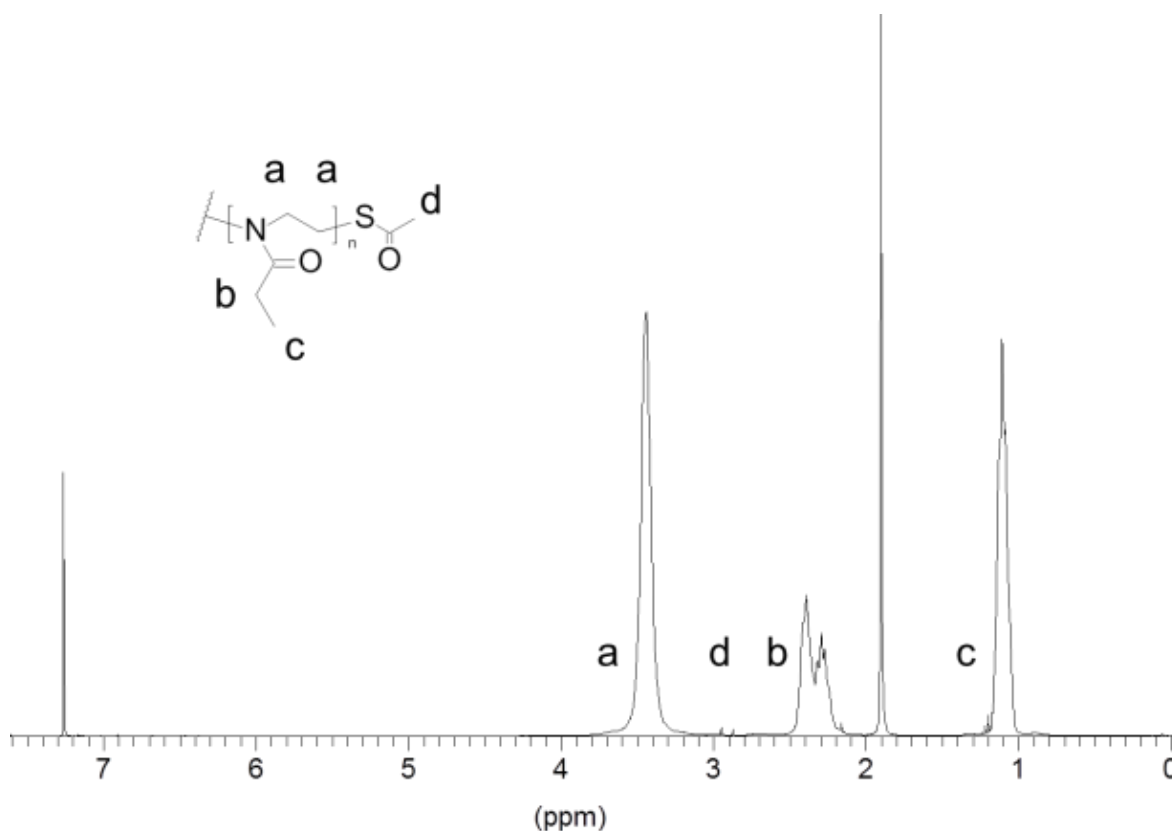
Figure 3. ^{1}H-NMR of pEtOXZ-SAc recorded in CDCl$_3$. The backbone peaks (a), (b) and (c) were set to the number of protons calculated from the precursor NMR of the oxazolinium salt polymer. The area of peak (d) was used for the calculation of the conversion rate. The conversion was calculated from the ratio of the resulting peak area to the theoretical area of 2 protons.

approach needed to be examined in detail concerning the reaction temperature, the excess of thioacetate as well as the reaction time. After different times samples were taken and all of them were analyzed by ^{1}H-NMR in order to determine the conversion into the thioacetate. It can be seen from Figure 4 that the differences between the conditions were not huge, just for a reaction at 95°C for 3 days higher yields were obtained. But further prolonging the reaction time had adverse effects and the reaction was never brought to completeness.
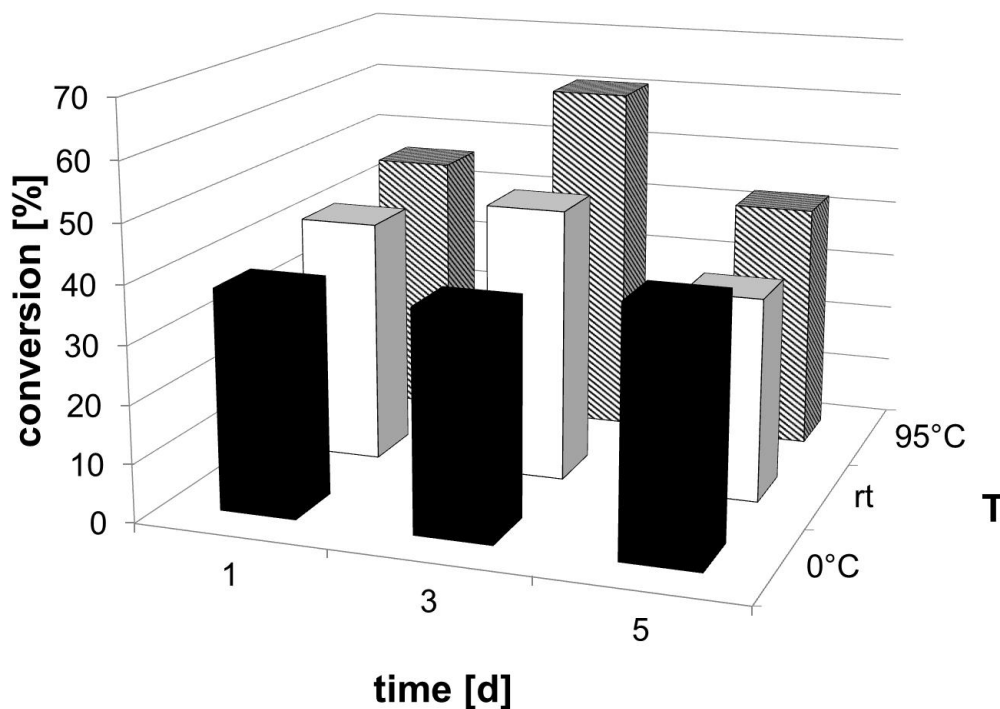
Figure 4. *Investigation of the influence of reaction time and reaction temperature on the conversion rate. The reaction time is given on the x-axis and the reaction temperature on the z-axis. The y-axis corresponds to the conversion rate.*

Thus, in a second approach the influence of the amount of thioacetate was investigated. Since the conversion differences obtained in the first assay were not high and reactions at rt are easier to handle this investigation was conducted at rt and the amounts of thioacetate were varied. This time also the reaction times were shortened since the thioacetate seemed to be cleaved if the reaction lasted too long. The samples were analyzed by ^{1}H-NMR again.

Interestingly, best results were obtained when 7.5 eq. thioacetate were used and when the reaction time was rather short. Hence reaction conditions were chosen according to these results.
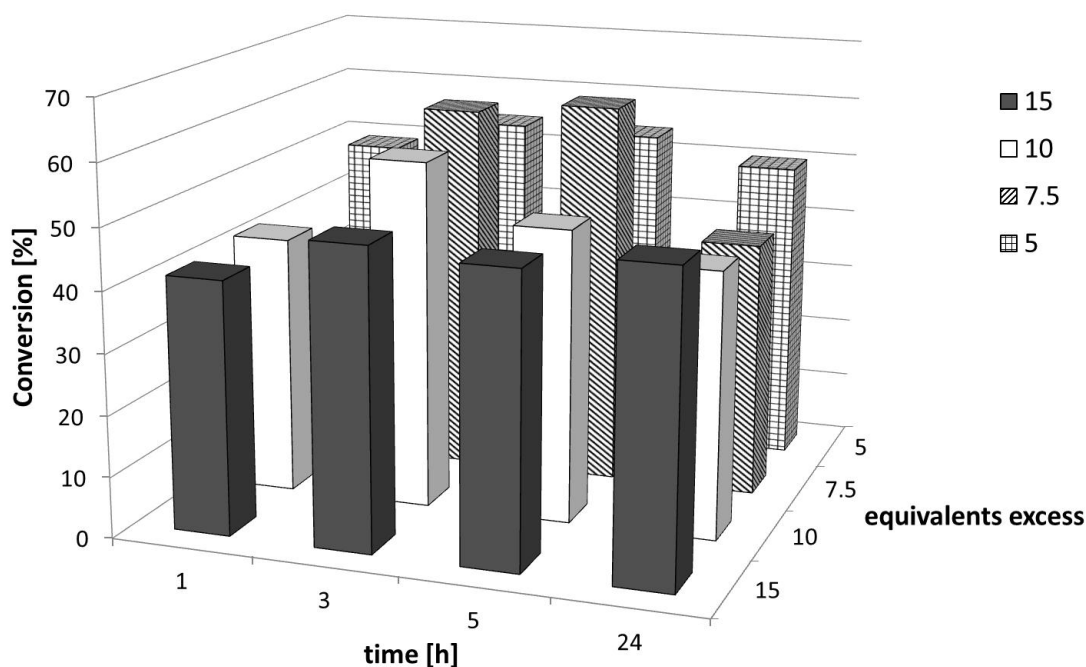
Figure 5. *Investigation of the influence of reaction time and thioacetate excess on the conversion rate. The reaction time is given on the x-axis. The thioacetate excess is on the z-axis and the y-axis accounts for the conversion rate.*

Synthesis and activation of lPEI-SH

The second synthesis step comprised the acidic cleavage of pEtOXZ-SAc (Figure 2, **4**) and the subsequent activation with 2,2´-dithio-dipyridine (DTDP). According to literature [26,27,32] the pEtOXZ-SAc was cleaved by acidic hydrolysis yielding the corresponding low molecular weight lPEI-SH (Figure 2, **5**). Fuming HCl and reflux for 1 d were chosen to guarantee for complete cleavage of the amide bonds [27]. The subsequent purification comprised a very basic work-up step. This proved to be rather problematic since thiols were instable at this basic pH and formed disulfides fast. In consequence a reduction procedure after this work up had to be established as well as a step that generates stable thiol forms for storage. Thus, downstream the work up

another 2-step reaction had to be introduced which eliminated the problem of disulfide formation during work-up and storage by reduction and subsequent thiol modification.

For the reduction a lot of different agents are known. The most important ones are tris(2-carboxyethyl)phosphine (TCEP) [33-37] dithiothreitol (DTT) [34,38,39], mercaptoethanol [40,41] and NaBH$_4$ [42-44]. Their features are summarized in Table 3.

Table 3. *Characteristics of the most common disulfide reductants.*

Reductant	*Tris(2-carboxy ethyl)phos-phine*	*Cleland´s reagent (dithiothreitol)*	*β-Mercapto-ethanol*	*Sodium borohydride*
Solubility	Water soluble			
Abbreviation	TCEP	DTT	β-ME	NaBH$_4$
Application	Stoichiometric	Minor excess	Vast excess	Variable
Reduction driving force	Thermodynamic forces	Thiol-disulfide exchange favour-ed by ring strain	Thiol-disulfide exchange	High S-nucleo-philicity of the borohydride ion
Removal	Precipitation and filtration; Dialysis		Dialysis; Removal in vacuo	Decomposition into gaseous components after addition of acetone or acid
Theoretical suitability for PEI	Precipitation unsuitable, dialysis possible		Removal in vacuo impossible Dialysis possible;	Possible
Suitability	Unsuitable (Disulfide reformation possible due to long dialysis time)			Well suited due to fast decom-position in acidic environment pre-venting disulfide reformation

These two steps (the reduction and the activation) had to be performed immediately after each other because reformation of disulfides could occur if too much time between the two steps passed. Furthermore, the reaction had to be performed in aqueous solutions due to the solubility of the obtained PEI derivative. Unfortunately, $NaBH_4$ is known to be instable in aqueous solutions. Thus, in order to obtain a good conversion the reaction series needed a fine tuning concerning reaction times and reaction pH´s for both steps. Therefore, a series of reactions was analyzed. In the first step different pHs were chosen as well as different reaction times. The values were chosen to be a compromise between PEI solubility on the one hand and $NaBH_4$ degradation on the other hand. Also the reaction times were a balance between sufficient time for the reduction and reoxidation of the generated thiols. After deletion of $NaBH_4$ the samples were split and 3 other pH values were adjusted. The reason for this was that DTDP is known to react in acidic pH, while disulfides are formed more eagerly under less acidic conditions. The samples were then allowed to react for 15 min, 30 min, 60 min or overnight and the amount of DTDP conversion was measured spectrophotometrically. The results for a reaction time of 2 h for the second step are given in Figure 6.

From the reddish colors in the single diagrams of Figure 6 it can be seen that pH 4 for the second step has the biggest influence on the conversion rate. For the first step a rather short reaction time (about 15 min) and the highest adjusted pH proved to be best. Thus, these reaction conditions were used for further experiments.
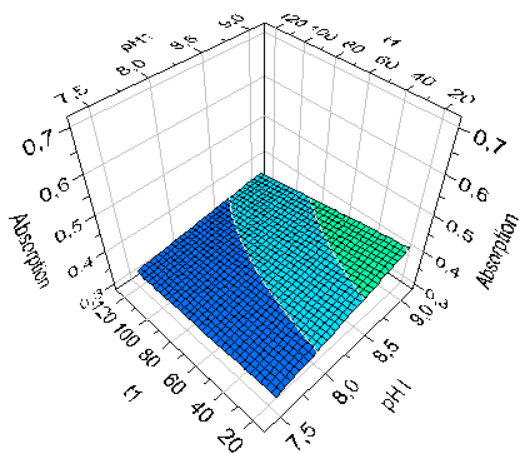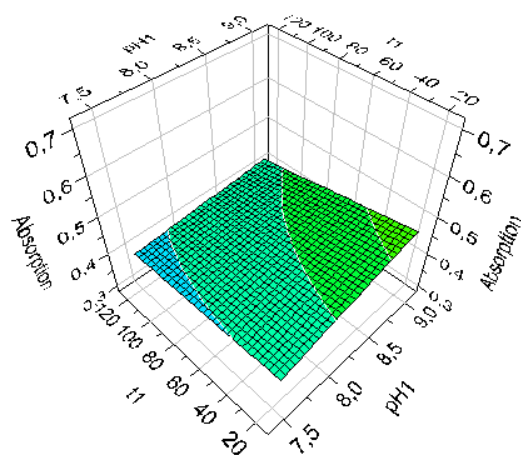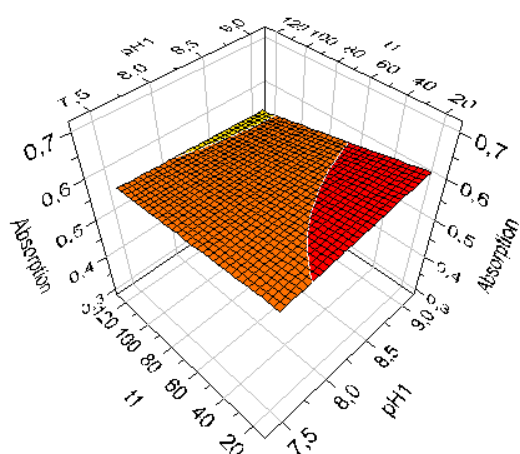
pH of 2nd reaction step:

4

pH of 2nd reaction step:

7

pH of 2nd reaction step:

8

Figure 6. Investigation of the influence of different parameters (pH 1, t 1, pH 2, t 2) on the conversion rate of the overall reaction sequence (measured as absolute absorbance of the resulting pyridyl disulfide derivative). Shown are the values for a reaction time of 2h for the second step (t 2=2h). t 1 is given on the y-axis, pH 1 is on the z-axis while the x-axis shows the measured absorption and, thus, corresponds to the conversion rate. Bluish colors indicate minor conversion while red colors denote high conversions.

The results of the UV measurements of the obtained lPEI-SS-pyr could also be confirmed by ^{1}H-NMR. The conversion rates were in most cases about 80%.
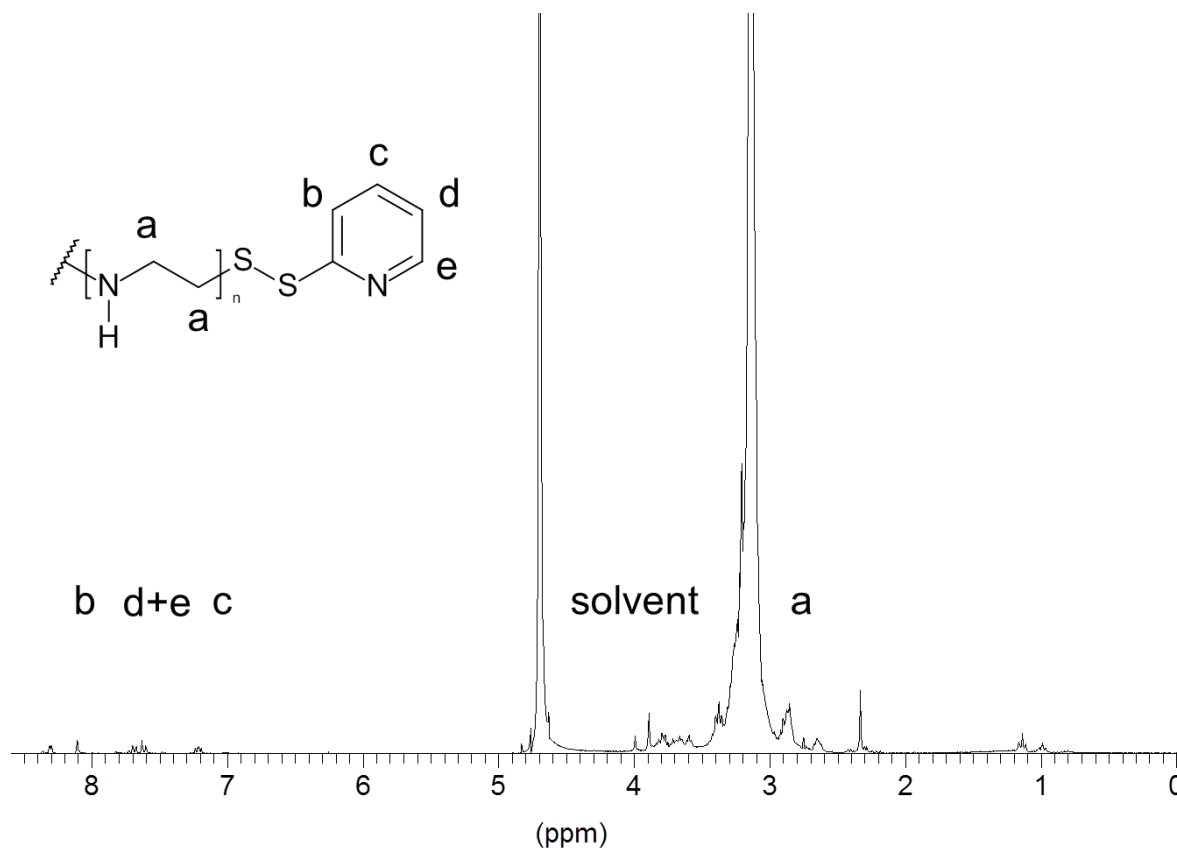

Figure 7. ^{1}H-NMR of lPEI-SS-pyr recorded in D$_2$O. The area of the backbone peak (a) was set to the expected value calculated from the molecular weight estimation after the first synthesis step. The ratio of the obtained peak areas compared to the theoretical value of 1 gave the conversion into PEI-SS-pyr.

Determination of thiol content

Knowledge about the thiol concentration of a sample is desirable in order to have a controlling device for the synthesis outcome and the improvement of the reaction conditions. This is

particularly important in the case of the synthesis of the thioether linked copolymers created here. Since the coupling step is performed without any further activation it is indispensable to calculate the appropriate net weight needed for the synthesis. The thioacetate/thiol content can be assayed at the stage of pEtOXZ or PEI. For pEtOXZ the thioacetate conversion can be assayed by ^{1}H-NMR. In the case of PEI the thiol content can be determined immediately after reduction by a lot of different assays [47,48] which are normally used for protein analytics. The most common ones are the Ellman assay [18, 36, 44, 49,50], the NTSB assay [51] and the DTDP assay [18, 42, 52, 53]. Figure 8 records the results of all these assays and the results from ^{1}H-NMR measurements. In most cases, the NTSB assay shows the highest amount of thiols, which is probably due to the fact that it has the power to analyze both species -thiols and disulfides- at once. Despite this big advantage of double detection, the hitch of this method was that the assay needed pH 9.5 which was not suitable for all tested PEIs. The longer the PEI chain was, the higher was the probability of polymer precipitation which hampered the readout of the assay. The Ellman and the DTDP assay gave lower concentrations than the NTSB assay in many cases which can be ascribed to the single detection of thiols. If the upstream reduction step cannot comprise all disulfides the resulting calculated conversion rate is lower than the finding of the NTSB assay. But both assays were more suitable for the higher molecular weight PEIs because they needed a pH which was beneficial for complete PEI solubility. The results of the NMR were somewhere in between which was due to the fact that the integral setting was not always clear. Thus, the NTSB assay was most suited for the detection of the whole thiol content of a PEI sample as long as the molecular weight of PEI was not too high. Assays such as the Ellman or DTDP assay were more appropriate for high molecular weight samples since they required less basic pHs in which PEI was completely soluble. While integral setting for PEI thioacetate was sometimes spurred ^{1}H-NMR offered the possibility to quickly check the purity of the product giving valuable information about the success of the work-up procedure.
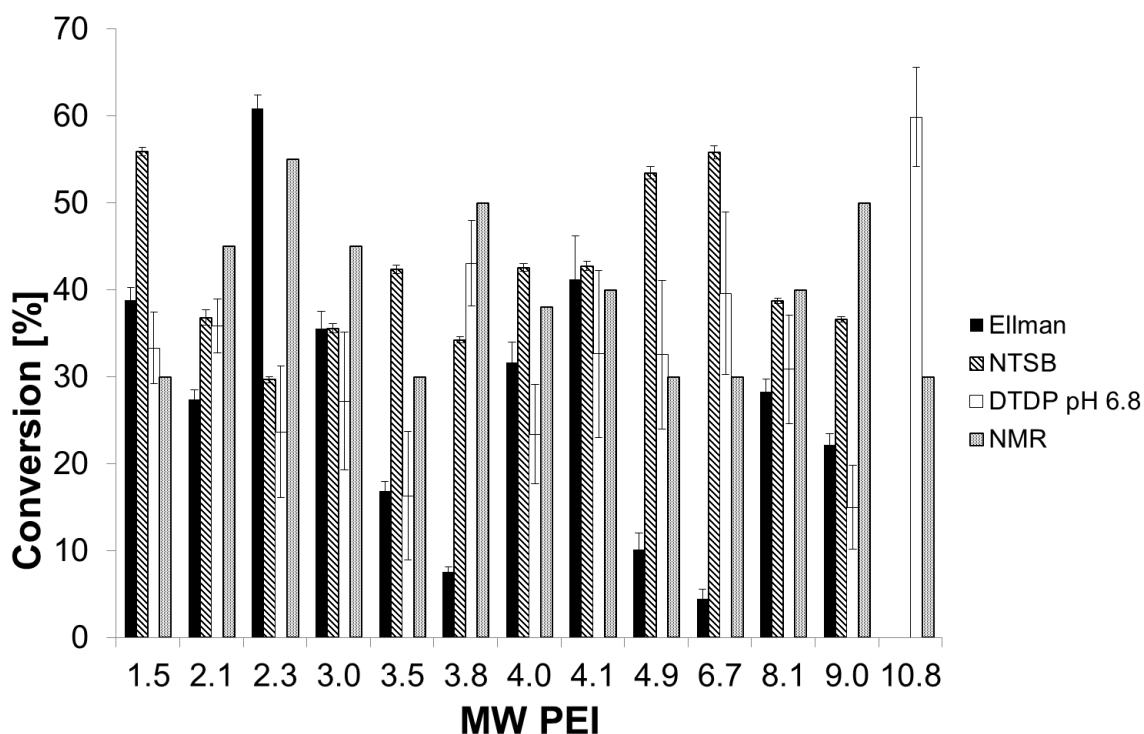
Figure 8. *Thiol-/thioacetate conversion of lPEI measured by Ellman´s assay, NTSB assay, DTDP assay at pH 6.8 or ^{1}H-NMR. The x-axis gives the molecular weight of the polymer PEI and the y-axis gives the determined conversion into thiols (Ellman assay, NTSB assay, DTDP assay) or thioacetates (^{1}H-NMR), respectively.*

Characterization of physicochemical properties

After successful synthesis the polymers had to proof themselves suitable for gene delivery applications. One very important prerequisite for a carrier system is its ability to complex nucleic acids into particles and to protect its payload from degradation and displacement from the carrier. In order to test the polymers condensation of the cargo an ethidium bromide (EtBr) exclusion assay was performed. A carrier is well suited if it excludes EtBr from the intercalation with pDNA which indicates strong interaction between the carrier and the payload. It can be seen in Figure 9 that the exclusion of EtBr became more efficient with higher N/P ratio (the ratio

between the protonatable amines in the carrier and the negative charges along the backbone of the nucleic acid). Also a trend concerning the molecular weight of PEI was observed. The longer the chain became the more efficient was the displacement of EtBr from the pDNA double strand. So, these polymers fulfilled their most important task- the complexation of the nucleic acid- very well.
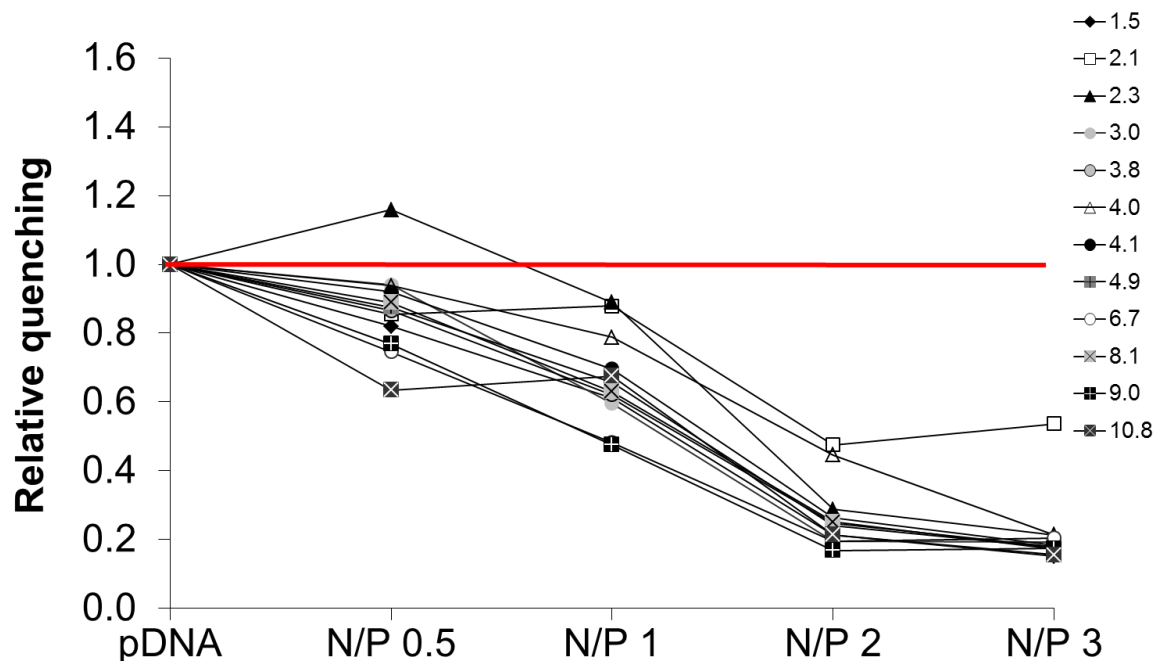

Figure 9. *Relative fluorescence loss of EtBr after complexation of plasmid DNA with PEI at different N/P ratios compared to the fluorescence of pure plasmid DNA. The N/P ratio is indicated at the x-axis, while the molecular weight of PEI is given in the legend. The relative fluorescence of all polymers at different N/P ratios was statistically different from the fluorescence of pDNA alone with p<0.005. The only exception was PEI 3.0.*

The complexation into particles was also analyzed by measuring the hydrodynamic size of the polyplexes. It can be seen from Figure 10 that the higher the N/P ratio became the larger the polyplexes got. However, the chain length seemed to play only a minor important role for the size of polyplexes. Nevertheless, all polymers were able to complex pDNA into particles which

made them suitable for gene delivery applications. Furthermore, the polydispersity indices of these polyplexes were all below 0.4 (data not shown) which indicated a quite homogenous size distribution. These rather uniform size distributions are desirable for gene delivery because it is easier to derive structure-activity relations if the particles in the collective are equal-sized.
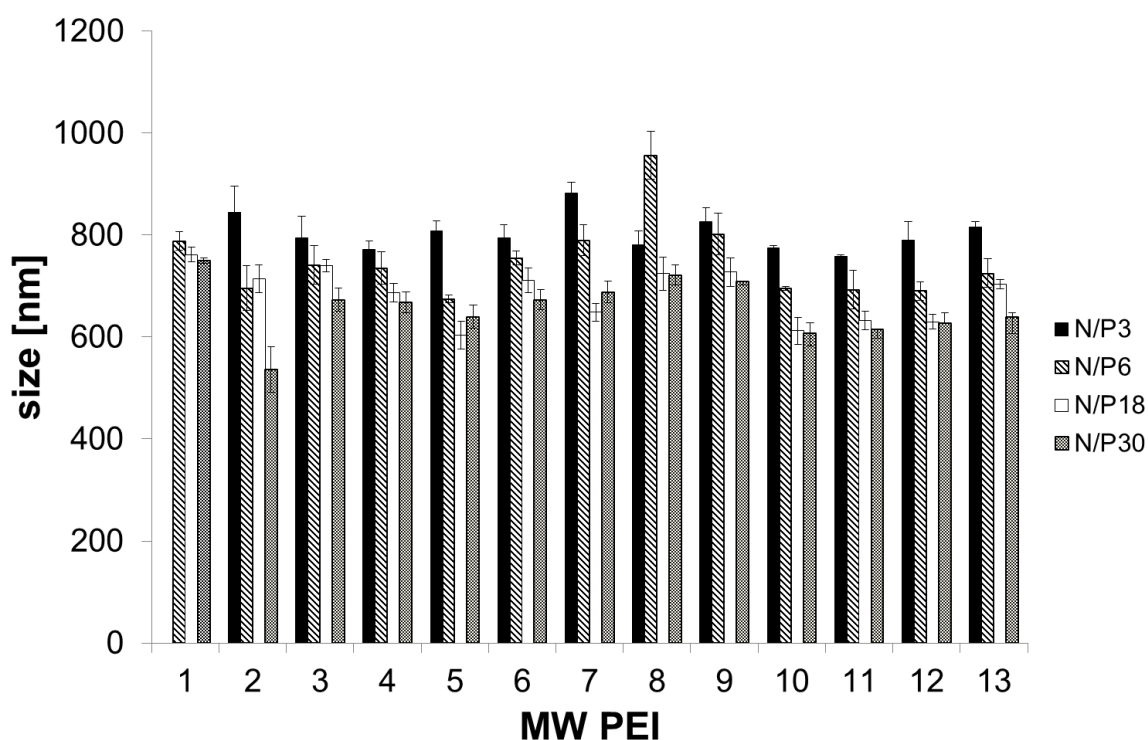

Figure 10. *Size of the polyplexes built from plasmid DNA and PEI at different N/P ratios. The x-axis indicates the molecular weight of and the legend gives the used N/P ratios.*

Conclusion

We successfully synthesized a library of 13 end group functionalized lPEI derivatives which can be employed for copolymer synthesis resulting in both stable thioether connected copolymers and cleavable disulfide linked copolymers. For this purpose we altered the polymerization sequence reported by [26] and [27] in such a way that a thioacetate group instead of a hydroxyl group terminated the polymer chain. In order to guarantee for the highest possible conversion rate we investigated the influence of different reaction conditions such as time, temperature and amount of terminating agent. This was essential since purification of polymers differing only in the terminal group is very difficult and impure products hamper further syntheses. Furthermore, we eliminated the problem of premature disulfide formation by introducing a reaction sequence which consisted of a reduction step and the formation of a stable storage form. For this procedure comprehensive investigations of reaction conditions such as pH and time were performed. Moreover, we introduced different assays for the determination of the thiol/disulfide content of the polymers in order to have a controlling device for the synthesis outcome and to get information about the polymer amounts needed for further copolymer synthesis. Beside these synthetic improvements we also checked the complexation ability of the thiol-modified polymers. As shown by an EtBr exclusion assay and the measurement of the polyplex sizes all polymers were able to form particles with plasmid DNA. Thus, they met the most important prerequisite for an efficient gene carrier and could be used for further modifications improving their characteristics.

References

[1] J. C.Venter et al., The Sequence of the Human Genome. *Science.* 291 (2001) 5507, 1304–1351.

[2] Tabor. Polyamines. *Annual Reviews of Biochemistry* (1984) 749-790.

[3] L. C. Gosule, J. A. Schellman, Compact form of DNA induced by spermidine. *Nature.* 259 (1976) 5541, 333–335.

[4] A. E. Pegg, Polyamine Metabolism and Its Importance in Neoplastic Growth and as a Target for Chemotherapy. *Cancer Research.* 48 (1988) 4, 759-774.

[5] O. Heby, Role of Polyamines in the Control of Cell Proliferation and Differentiation. *Differentiation.* 19 (1981) 1-3, 1-20.

[6] H. Deng, Structural basis of polyamine–DNA recognition: spermidine and spermine interactions with genomic B-DNAs of different GC content probed by Raman spectroscopy. *Nucleic Acids Research.* 28 (2000) 17, 3379-3385.

[7] A. A. Ouameur, H.-A. Tajmir-Riahi, Structural Analysis of DNA Interactions with Biogenic Polyamines and Cobalt(III)hexamine Studied by Fourier Transform Infrared and Capillary Electrophoresis. *Journal of Biological Chemistry.* 279 (2004) 40, 42041-42054.

[8] M. Saminathan, Ionic and Structural Specificity Effects of Natural and Synthetic Polyamines on the Aggregation and Resolubilization of Single-, Double-, and Triple-Stranded DNA. *Biochemistry.* 38 (1999) 12, 3821-3830.

[9] O. Boussif, A versatile vector for gene and oligonucleotide transfer into cells in culture and in vivo: polyethylenimine. *Proceedings of the National Academy of Sciences.* 92 (1995) 16, 7297-7301.

[10] W. T. Godbey, K. K. Wu, A. G.Mikos, Poly(ethylenimine) and its role in gene delivery. *Journal of Controlled Release.* 60 (1999) 2-3, 149-160.

[11] J. Suh, H. J. Paik, B. K. Hwang, Ionization of Poly(ethylenimine) and Poly(allylamine) at Various pH's. *Bioorganic Chemistry.* 22 (1994) 3, 318-327.

[12] W. T. Godbey, K. K. Wu, A. G.Mikos, Size matters: Molecular weight affects the efficiency of poly(ethylenimine) as a gene delivery vehicle. *Journal of Biomedical Materials Research.* 45 (1999) 3, 268-375.

[13] K. Kunath, A. von Harpe, D. Fischer , H. Petersen, U. Bickel, K. Voigt, T. Kissel, Low-molecular-weight polyethylenimine as a non-viral vector for DNA delivery: comparison of physicochemical properties, transfection efficiency and in vivo distribution with high-molecular-weight polyethylenimine. *Journal of Controlled Release.* 89 (2003) 1, 113-125.

[14] J. W. Wiseman, C. A. Goddard, D. McLelland, W. H. Colledge, A comparison of linear and branched polyethylenimine (PEI) with DCChol//DOPE liposomes for gene delivery to epithelial cells in vitro and in vivo. *Gene Therapy.* 10 (2003) 19, 1654-1662.

[15] L. Wightman, R. Kircheis, V. Rössler, S. Carott , R. Ruzicka, M. Kursa, Different behavior of branched and linear polyethylenimine for gene delivery in vitro and in vivo. *The Journal of Gene Medicine.* 3 (2001) 4, 362-372.

[16] M. Breunig, U. Lungwitz, R. Liebl C. Fontanari, J. Klar , A. Kurtz, T. Blunk, A. Goepferich, Gene delivery with low molecular weight linear polyethylenimines. *The Journal of Gene Medicine.* 7 (2005) 10, 1287-1298.

[17] T. W. Thannhauser, Y. Konishi, H. A.Scheraga, Sensitive quantitative analysis of disulfide bonds in polypeptides and proteins. *Analytical Biochemistry.* 138 (1984) 1, 181-188.

[18] C. Riener, G. Kada, H. Gruber, Quick measurement of protein sulfhydryls with Ellman's reagent and with 4,4'-dithiodipyridine. *Analytical and Bioanalytical Chemistry.* 373 (2002) 4, 266-276.

[19] T. Saegusa, H. Ikeda, H. Fujii, Isomerization Polymerization of 2-Oxazoline. IV. Kinetic Study of 2-Methyl-2-oxazoline Polymerization. *Macromolecules.* 5 (1972) 4, 359-362.

[20] J. E. McAlvin, S. B. Scott, C. L. Fraser, Synthesis of Thermochromic Iron(II) Tris(bipyridine)-Centered Star-Shaped Polyoxazolines and Their Bipyridine-Centered Macroligand Counterparts. *Macromolecules.* 33 (2000) 19, 6953-6964.

[21] M. Miyamoto, K. Naka, M. Tokumizu, T. Saegusa, End capping of growing species of poly(2-oxazoline) with carboxylic acid: a novel and convenient route to prepare vinyl- and carboxy-terminated macromonomers. *Macromolecules.* 22 (1989) 4, 1604-1607.

[22] T. Saegusa, Y. Hashimoto, S. Matsumoto, Ring-Opening Polymerization of Oxacyclobutane by Boron Trifluoride. Concentration of Propagating Species and Rate of Propagation. *Macromolecules.* 4, 1971, 1-3.

[23] R. Tanaka, I. Ueoka, Y. Takaki, K. Kataoka, S. Saito, High molecular weight linear polyethylenimine and poly(N-methylethylenimine). *Macromolecules.* 16 (1983) 6, 849-853.

[24] T. Saegusa, A. Yamada, H. Taoada, S. Kobayashi, Linear Poly(N-alkylethylenimine)s. *Macromolecules.* 11 (1978) 2, 435-436.

[25] K. Aoi, M. Okada, Polymerization of oxazolines. *Progress in Polymer Science.* 21 (1996) 1, 151-208.

[26] B. Brissault, A. Kichler, C. Guis, C. Leborgne, O. Danos, H. Cheradame, Synthesis of Linear Polyethylenimine Derivatives for DNA Transfection. *Bioconjugate Chemistry.* 14 (2003) 3, 581-587.

[27} U. Lungwitz, S. Drotleff, A. Goepferich, Synthesis and Characterization of poly(2-ethyl-2-oxazoline) and linear polyethylenimine, in U. Lungwitz. *Poly(ethylenimine)-derived gene carriers and their complexes with plasmid DNA- Design, Synthesis and Characterization.* Thesis, Regensburg (2006).

[28] O. Nuyken, P. Persigehl, R. Weberskirch, Amphiphilic poly(oxazoline)s – synthesis and application for micellar catalysis. *Macromolecular Symposia.* 177 (2002) 1, 163-174.

[29] G. Hochwimmer, O. Nuyken, U. Schubert, S. 6,6′-Bisfunctionalized 2,2′-bipyridines as metallo-supramolecular initiators for the living polymerization of oxazolines. *Macromolecular Rapid Communications.* 19 (1998) 6, 309-313.

[30] R. Hoogenboom, M. W. Fijten, C. Brändli, J. Schroer, U. Schubert, Automated Parallel Temperature Optimization and Determination of Activation Energy for the Living Cationic Polymerization of 2-Ethyl-2-oxazoline. *Macromolecular Rapid Communications.* 24 (2003) 1, 98-103.

[31] T. Saegusa, H. Ikeda, H. Fujii, Isomerization Polymerization of 2-Oxazoline. IV. Kinetic Study of 2-Methyl-2-oxazoline Polymerization. *Macromolecules.* 5 (1972) 4, 359-362.

[32] K. M. Kem, Kinetics of the hydrolysis of linear poly[(acylimino)-ethylenes]. *Journal of Polymer Science: Polymer Chemistry Edition.* 17 (1979) 7, 1977-1990.

[33] J. A. Burns, J. C. Butler, J. Moran., G. M. Whitesides, Selective reduction of disulfides by tris(2-carboxyethyl)phosphine. *Journal of Organic Chemistry.* 56 (1991) 8, 2648-2650.

[34] E.B. Getz, M. Xiao, T. Chakrabarty, R. Cooke, P.R. Selvin, A Comparison between the Sulfhydryl Reductants Tris(2-carboxyethyl)phosphine and Dithiothreitol for Use in Protein Biochemistry. *Analytical Biochemistry.* 273 (1999) 1, 73-80.

[35] W. R. Gray, Disulfide structures of highly bridged peptides: A new strategy for analysis. Protein Science. 2 (1993) 10, 1732-1748.

[36] J. C. Han, G. Y. Han, A Procedure for Quantitative Determination of Tris(2-Carboxyethyl)phosphine, an Odorless Reducing Agent More Stable and Effective Than Dithiothreitol. *Analytical Biochemistry.* 220 (1994) 1, 5-10.

[37] K. Tyagarajan, E. Pretzer, J. E. Wiktorowicz, Thiol-reactive dyes for fluorescence labeling of proteomic samples. *ELECTROPHORESIS.* 24 (2003) 14, 2348-2358.

[38] W. W. Cleland, Dithiothreitol, a New Protective Reagent for SH Groups. *Biochemistry.* 3, (1964) 4, 480-482.

[39] K. Iyer Subramonia , W. A. Klee, Direct Spectrophotometric Measurement of the Rate of Reduction of Disulfide Bonds. *Journal of Biological Chemistry.* 248 (1973) 2, 707-710.

[40] M. Svoboda, W. Meister, W. Vetter, A method for counting disulfide bridges in small proteins by reduction with mercaptoethanol and electrospray mass spectrometry. *Journal of Mass Spectrometry.* 30 (1995) 11, 1562-1566.

[41] L.-O. Andersson, Reduction and reoxidation of the disulfide bonds of bovine serum albumin. *Archives of Biochemistry and Biophysics.* 133 (1969) 2, 277-285.

[42] R. E. Hansen, H. Ostergaard, P. Norgaard, J. R. Winther, Quantification of protein thiols and dithiols in the picomolar range using sodium borohydride and 4,4′-dithiodipyridine. *Analytical Biochemistry.* 363 (2007) 1, 77-82.

[43] M. B. Mathews, The reductionn of cozymase by sodium borohydride. *Journal of Biological Chemistry.* 176 (1948) 1, 229-232.

[44] A. F. S. A. Habeeb, A sensitive method for localization of disulfide containing peptides in column effluents. *Analytical Biochemistry.* 56 (1973) 1, 60-65.

[45] S.-Y. Huang, S. Pooyan, J. Wang, I. Choudhury, M.J. Leibowitz, S. Stein, A Polyethylene Glycol Copolymer for Carrying and Releasing Multiple Copies of Cysteine-Containing Peptides. *Bioconjugate Chemistry.* 9 (1998) 5, 612-617.

[46] T. P. King, Y. Li, L. Kochoumian, Preparation of protein conjugates via intermolecular disulfide bond formation. *Biochemistry.* 17 1978) 8, 1499-1506.

[47] R. E.Hansen, J. R. Winther, An introduction to methods for analyzing thiols and disulfides: Reactions, reagents, and practical considerations. *Analytical Biochemistry.* 394, 2009, 2, 147-158.

[48] H. Cui, J. Leon, E. Reusaet, A. Bult, Selective determination of peptides containing specific amino acid residues by high-performance liquid chromatography and capillary electrophoresis. *Journal of Chromatography A.* 704 (1995) 1, 27-36.

[49] N. I. Escobar, A. Morales, G. Núñez, Micromethod for quantification of SH groups generated after reduction of monoclonal antibodies. *Nuclear Medicine and Biology.* 23 (1996) 5, 641-644.

[50] P. Eyer, F. Worek, D. Kiderlen, G. Sinko, A. Stuglin, V. Simeon-Rudolf, Molar absorption coefficients for the reduced Ellman reagent: reassessment. *Analytical Biochemistry.* 312 (2003) 2, 224-227.

[51] M. Neu, J. Sitterberg, U. Bakowski, T. Kissel, Stabilized Nanocarriers for Plasmids Based Upon Cross-linked Poly(ethylene imine). *Biomacromolecules.* 7 (2006) 12, 3428-2438.

[52] D. R. Grassetti, J. F.Murray [JR.], Determination of sulfhydryl groups with 2,2′- or 4,4′-dithiodipyridine. *Archives of Biochemistry and Biophysics.* 119 (1967) 41-49.

[53] J. Bai, B. Acan, A. Ghahary, B. Ritchie, V. Somayaji, H. Uluda, Poly(ethyleneimine)/arginine–glycine–aspartic acid conjugates prepared with N-succinimidyl 3-(2-pyridyldithio)propionate: An investigation of peptide coupling and conjugate stability. *Journal of Polymer Science Part A: Polymer Chemistry.* 42 (2004) 23, 6143-6156.

Chapter 4

Synthesis of libraries of poly(ethylene glycol)-poly(ethylene imine) copolymers connected via stable thioether and degradable disulfide bonds

Abstract

The development of safe and efficient gene therapy methods strongly demands well characterised nonviral carrier systems. Some very promising carriers are based on poly(ethylene imine) (PEI) supported by a shielding moiety such as poly(ethylene glycol) (PEG). Unfortunately, most known copolymers are not well defined. Here, we report on the synthesis of two PEG-PEI copolymer libraries where every PEI molecule is just connected with one PEG molecule at the chain end. Thus, these copolymers meet the requirement of good definition. We synthesized copolymers with both stable thioether bonds and degradable disulfide linkages in order to obtain structure-activity-relationships from the thioethers and to test if the degradable carriers are superior compared to the nondegradable copolymers. The complexation ability of the thioether connected copolymers was tested for different nucleic acids. Efficient exclusion was found for both nucleic acids. Furthermore all polymers generated small particles when complexed with small interfering RNA. The situation was somewhat different in the case of plasmid DNA. The polyplexes of pDNA and PEI or PEI-PEG 2 kDa generally resulted in rather large polyplexes whereas the polyplexes built from PEI-PEG 5 kDa or PEI-PEG 10 kDa were significantly smaller. To conclude, all our copolymers were equally suited for the complexation of siRNA while the copolymers with longer PEG chains were better suited for pDNA than those without or with only a small PEG chain.

Introduction

A lot of novel drugs such as proteins and antibodies or drug carriers such as micelles and polyplexes (complexes made from polymers and nucleic acids) experience severe limitations. This is due to their short half-life times and their cytotoxicity which is associated with their positive surface charge. In order to enhance the half-lives and mask these charges, shielding moieties can be attached which inhibit the interactions. A lot of different polymers can be employed for this task such as poly(acrylamide), poly(vinylpyrrolidone), poly(ethyl-oxazoline), dextranes or poly(ethylene glycol) (PEG) [1, 2].The most commonly used polymer is PEG (for review see [3-8]) and numerous strategies for PEG attachment exist [9-14]. ADAGEN, PEGASYS, Pegintron or Oncaspar are some of the PEGylated drugs on the market which proof the effectiveness of this approach [8]. But PEGylation is not only restricted to these protein modifications. The circulation time of carrier systems such as micelles or polyplexes could be improved, too. Among the plethora of different carriers also poly(ethylene imine) (PEI), the gold standard in nonviral gene therapy, was equipped with PEG. Grafted or star-like copolymers with linear or branched PEG moieties of different molecular weight were synthesized [15-27]. All of them share a reduced zeta potential, improved colloidal stability and lower toxicity as well as longer circulation times in vivo. But product mixtures of different PEG-PEI copolymers are possible due to the way of their synthesis. Furthermore, if the PEG moiety is not clearly separated from the PEI moiety the shielding moiety may interfere with the complex formation resulting in less stable polyplexes. Thus, we hypothesized that the synthesis of strictly linear PEG-PEI copolymers would be beneficial for the formation of stronger polyplexes and the drawing of structure activity correlations. We synthesized a library of non degradable PEG-PEI copolymers connected via a thioether bond for the analysis of the physicochemical characteristics as well as the performance in cell culture which results only from the copolymer structure. But since the stably attached PEG moiety could also hamper the endosomal escape and the subsequent processing of the polyplexes [28] we prepared a second set of degradable

polymers. Here, we report on the synthesis of both the stable and the cleavable copolymers and the suitability of the thioether connected copolymers for the formation of polyplexes with plasmid DNA (pDNA) as well as small interfering RNA (siRNA).

Materials

All chemicals and materials were from Merck KGaA (Germany), Acros Organics (Belgium), Sigma-Aldrich Chemie GmbH (Germany), J.T. Baker (The Netherlands) or IRIS Biotech (Germany).

The plasmid DNA encoding enhanced green fluorescent protein (EGFP) (pEGFP-N1, Clontech, Germany) was used as reporter gene and was isolated from E. coli JM 109 strain using a Qiagen Plasmid Maxi Kit (Qiagen, Germany).

Synthesis poly(ethylene glycol)-S-poly(ethylene imine)

Uncleavable PEI-S-PEG copolymers were obtained by coupling reactive lPEI-SH (description of the synthesis in chapter PEI synthesis) with a PEG maleimide (MW 2, 5 or 10 kDa). For this purpose the lPEI derivative was dissolved in water and the pH was adjusted to 8-9. Then 30 eq. $NaBH_4$ were added and the mixture was stirred at room temperature (rt) for 20 min. Thereafter unreacted $NaBH_4$ was destroyed by the addition of fuming HCl which resulted in pH 1. After 2 min the pH was again raised to 7.2, the PEG maleimide was added and the mixture was stirred under a nitrogen atmosphere overnight at rt. The crude product was purified by extensive dialysis against water and then lyophilized. Afterwards ^{1}H-NMRs were recorded in D_2O. The NMRs only showed the two backbone peaks of the polymers (2,65-3,08 ppm $-CH_2-O-CH_2-$; 3,49-3,75 ppm $CH_2-NH-CH_2$) . These peaks were used to calculate the purity of the product. The ratio of the peak areas corrected for the molecular weights of each polymer were used for the analysis of the purity.

Formation of polyplexes

The polyplexes of plasmid DNA (pDNA) or shirt interfering RNA (siRNA) and polymer were prepared at different N/P ratios (ratio of nitrogens in polymer to phosphates in the backbone of the nucleic acid). The polymer and the nucleic acid were each diluted in equal volumes of 150 mM NaCl. The polymer solution was added to the nucleic acid solution, the mixture was vortexed for 20 seconds and then incubated for 20 min before use. The amount of plasmid DNA or siRNA and the total volume of the polyplex solution are given in each section.

Ethidium bromide quenching assay

The polyplexes were prepared at a N/P ratio of 3 by diluting 1 µg of pDNA in a final volume of 100 µl. After incubation for 20 min the polyplexes were pipetted in a 96-well plate and mixed with 2.5 µl of a 0.1 µg/µl ethidium bromide (EtBr) solution. The fluorescence of EtBr was excited at 518 nm and recorded at 605 nm using a LS 55 fluorescence spectrometer (Perkin Elmer, Germany) and expressed as relative fluorescence compared to uncomplexed plasmid DNA or siRNA, respectively. Measurements were performed in quadruplet. The relative fluorescence loss was calculated as follows:

relative fluorescence loss = relative fluoresence$_{PEG\text{-}PEI\text{-}polyplexes}$/relative fluorescence$_{PEI\text{-}polyplexes}$.

Hydrodynamic diameter and zeta potential measurements

The hydrodynamic diameter and the zeta potential of the polyplexes was measured using a Zetasizer Nano-ZS from Malvern Instruments (Germany) at 25°C. A 4 mW He-Ne laser at a wavelength of 633 nm was used as the light source. For the determination of the size, the measurement position was at 4.65 mm with automated laser attenuation. Scattered light was detected at an angle of 173° backscatter. The viscosity and refractive index of the dispersant were used as follows: 150 mM NaCl: 0.90 mm^2/s and 1.33, respectively. Three measurements with 10 sub-runs were performed for each sample. Data were analyzed by the general purpose

mode and expressed as mean ± standard deviation (SD). The zeta potential of the polyplexes was measured at 25°C. Three measurements with 10 sub-runs were performed for each sample. Data were processed in the monomodal mode which guarantees for good sample stability due to short measurement duration and then expressed as mean (± SD). For size measurements, polyplexes were formed by mixing 2 µg pDNA or siRNA and varying amounts of polymer to achieve different N/P ratios in a final volume of 500 µl, while for zeta potential measurements the polyplexes were built with 4 µg pDNA or siRNA in a final volume of 1000 µl.

Synthesis of methoxyPEG-thioacetate

methoxy PEGthioacetate (mPEG-SAc) , was prepared in a 2-step procedure: for the synthesis of mPEG-tosylate dry methoxy PEG-OH (2 or 5 kDa) was reacted with   0.5 eq of 4-dimethylaminopyridine (DMAP), 1.5 eq. of p-toluene sulfonate and 2.0 eq. of triethylamine. The reaction mixture was dissolved in dichloromethane and stirred overnight at rt, followed by the replacement of the dichloromethane by chloroform and washing the crude product 3 times with water and 2 times with 0.1 M HCl. The resulting mPEG-tosylate was dried over magnesium sulfate and in vacuo.^{1}H-NMRs were recorded in CDCl$_3$ on a Avance 300spectrometer (300MHz, Bruker BioSpin GmbH, Germany). The aromatic tosylate protons could be seen at 7.75-7.85 ppm and 7.30-7.40 ppm as well as the adjacent methyl group at 2.35-2.50 ppm. Furthermore, the PEG backbone peak is visible at 3.45-3.80 ppm and the peaks for the methoxy group are at 3.35-3.44 ppm. For the determination of the conversion degree the peak for the methoxy group of PEG was set to 3 and the area of the tosylate protons was calculated according to this setting. The conversion degree was calculated from the ratio of the theoretical area of 2 for each aromatic tosylate peak and the area determined by ^{1}H-NMR.

 The second step involved the exchange of the tosylate group by the thioacetate gruop. Here, 2.5 eq. of potassium thioacetate were added to the mPEG-tosylate in DMF and the mixture was stirred for 8 h at rt. The mixture was concentrated, poured into a 10 fold volume of water and

washed with chloroform 3 times. The organic phase was dried over magnesium sulfate and evaporated to dryness yielding mPEG-SAc. As for the former step the methoxy peak from 3.35-3.44 ppm was used for scaling and was set to 3. Two other peaks could be used for the determination of the conversion degree: the methyl peak of the thioacetate (2.30-2.35 ppm) and the peak of the methylene group between the PEG chain and the thioacetate at 3.05-3.12 ppm. These peaks accounted for 3 or 2 protons, respectively. The conversion degree was again determined as the ratio of the theoretical values and the gained peak areas.

Thioacetate cleavage conditions

In order to determine suitable reaction conditions for the thioacetate cleavage 3 different solvents and 10 different reaction times were tested. For this purpose PEG thioacetate was dissolved either in 0.1M methanolic HCl or a 1:1 mixture of methanol and water which was acidified with 8 drops fuming HCl. In the case of methanolic HCl one sample was heated to 95°C, while the other one was stirred at rt. The water-methanol-mixture was heated to 95°C. At predetermined time points (0.5, 1, 2 ,3, 4, 5, 6, 7, 8 and 18 h). samples of 1 ml were taken, diluted with 4 ml water and mixed with 125 µl 2,2`-dithio dipyridine (DTDP) assay solution. This assay solution was prepared by dissolving 88 mg DTDP in 100 µl fuming HCl and 3 ml water and further dilution to 100 ml with a solution of 100 mM NaH_2PO_4 and 0.2 mM EDTA at pH 7.

After incubation at rt for 5 min the absorbance was measured on a TitertekPlus Microplate Reader (Bartolomey Labortechnik, Germany) at 343 nm. All samples were measured 3 times and the concentrations were determined relative to cysteine standards.

Synthesis PEI-SS-PEG

For the synthesis of PEG-SS-PEI, lPEI-SS-pyr and PEG-SH were needed. PEG-SH was obtained by cleavage of PEG thioacetate in situ. Here mPEG thioacetate (mPEG-SAc) was dissolved in a 1:1 mixture of water and methanol which was acidified with 8 drops fuming HCl. This mixture was heated to 90°C for 8 h. After that time 1 thiol eq. of the activated PEI (lPEI-SS-pyr, description of the synthesis in chapter 3) was added and the mixture was stirred overnight. This was followed by excessive dialysis against water and lyophilisation. Afterwards ^{1}H-NMRs were recorded in D_2O on a Avance 300 spectrometer (300MHz, Bruker BioSpin GmbH, Germany) In the NMRs the two backbone peaks for the PEI and the PEG chains were clearly visible (2.82-3.30 ppm CH_2-NH-CH_2, 3.51-3.65 ppm CH_2-O-CH_2). Unfortunately, the methoxy peak of PEG was no longer clearly separated from the PEG backbone. Thus, scaling was performed according to the results of the previous ^{1}H-NMRs. The purity of the product was determined as the ratio of the peaks for PEG and PEI corrected for the molecular weight of each polymer.

Statistics

Results are shown as mean (± SD). Experiments were performed in triplicate if not otherwise indicated. Significance between two groups was tested using a one-tailed Student's t-test. A p-value < 0.01 was considered to be significant. Significance between the mean values of the homopolymer and copolymer polyplexes was calculated using one-way ANOVA analysis followed by Bonferroni t-test. A p-value of 0.05 was considered to be significant. Analysis was performed with Sigma Plot (Version 12.2, Systat Software, Chicago, IL, USA).

Results and discussion

The goal of the syntheses was to couple the PEG moiety directly to the functionalized end of the PEI chain. As can be seen from Figure 1 two different synthesis strategies for the attachment of a shielding moiety onto PEI were employed. The difference between the two synthesis routes was that the first one yielded nondegradable copolymers (Figure 1, component 6) which were synthesized with the help of maleimides while the second one resulted in reductively degradable copolymers connected via disulfide bonds (Figure 1, component 9). The advantage of this strategy was that it only allowed for the formation of linear copolymers where one PEI was attached to one PEG chain. Product mixtures or multiple graftings were excluded. Furthermore,
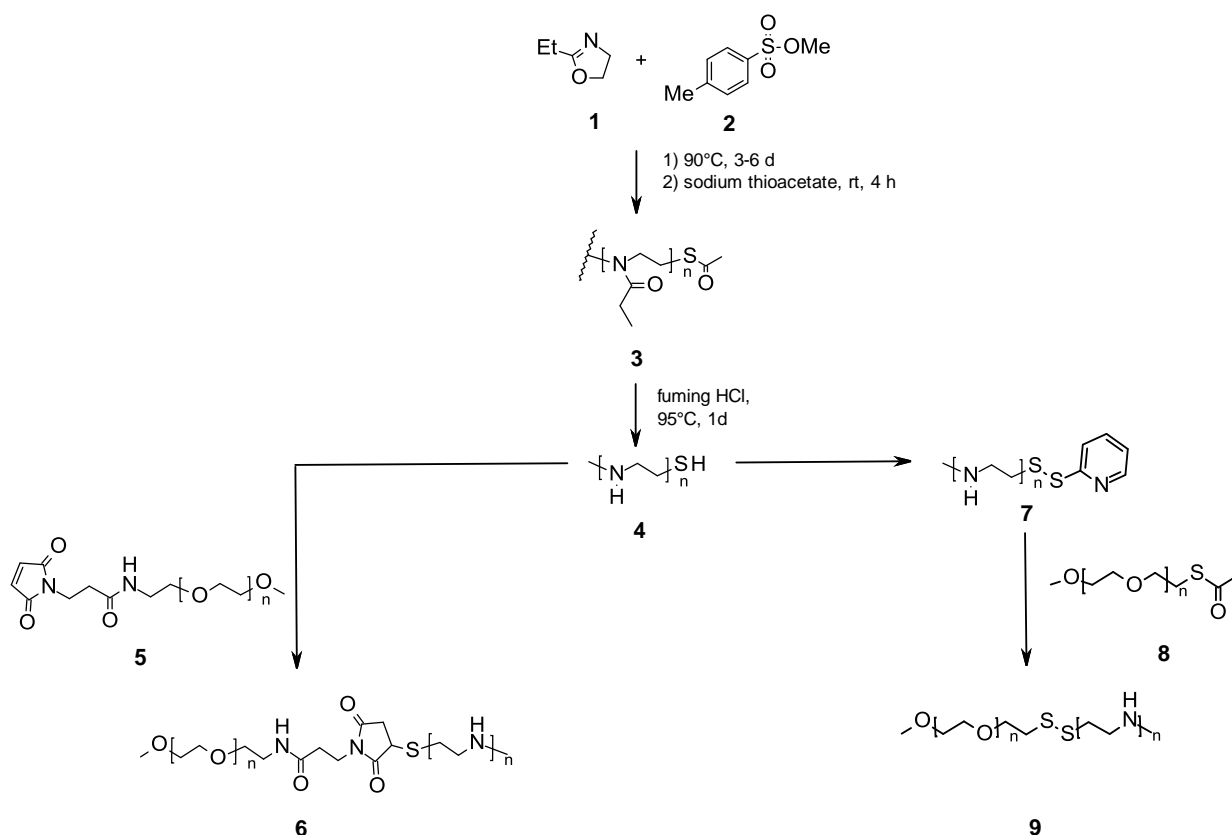

Figure 1. *Synthesis scheme for both copolymers synthesis routes yielding stable thioether bonds (left side) or degradable disulfides (right side).*

both segments were strictly separated which reduced the probability of interference of the PEG chain with the polyplex formation. The library of stable polymers was used to deduce the influence of PEGylation and PEI chain length on the physiochemical characteristics and the performance in cell culture. In a second step cleavable copolymers were synthesized for a comparison between stable and cleavable copolymers.

Synthesis of PEI-S-PEG

The first synthetic approach aimed at the formation of non cleavable copolymers which were connected via thioether bonds. These polymers were synthesized by adding a solution of lPEI-
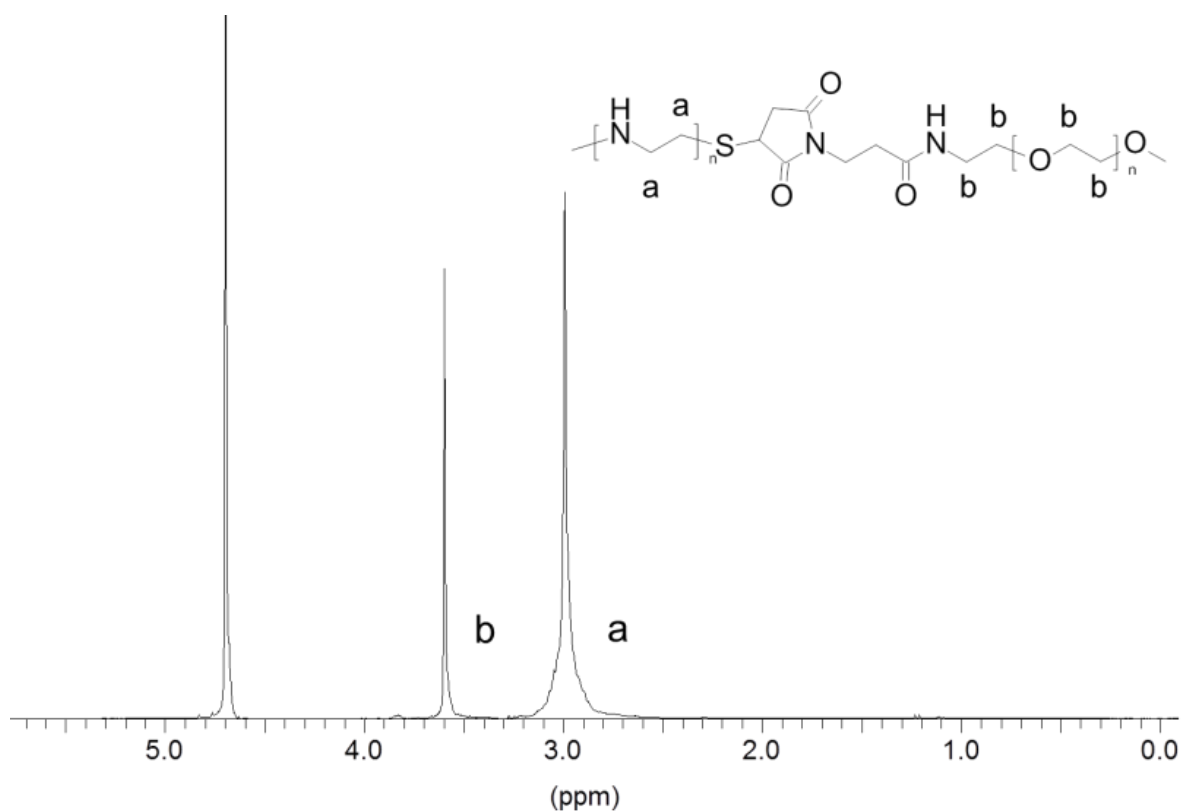

Figure 2. ^{1}H-NMR of PEG-S-PEI copolymer recorded in D$_2$O. The NMRs showed the two backbone peaks (a) and (b) of the polymers. The ratio of the peak areas corrected for the molecular weights of each polymer were used for the analysis of the purity.

thiol to commercially available mPEG-maleimide (Figure 1, left side).

In the first step the PEI part was reduced with NaBH$_4$ generating thiol ends in situ. Then it was mixed with mPEG-maleimide, the pH was adjusted to 7.2 according to the manufacturer´s instructions as well as literature [29] and the mixture was stirred overnight. After excessive dialysis and subsequent lyophilisation the product was dissolved in D$_2$O and analyzed by ^{1}H-NMR (Figure 2).

Characterization of the complexation ability

The resulting non cleavable copolymers had to proof their performance as compacting agents for nucleic acids. They were tested for their complexation ability for the different demands of large, flexible pDNA with a molecular weight of several kilo base pairs as well as the requirements of short, stiff siRNA made from 21-23 base pairs [30-32]. The two main parameters which were screened were the complex formation monitored by polyplex size as well as the stability of the polyplexes examined by an ethidium bromide (EtBr) exclusion assay. In both cases different N/P ratios (the ratio between the number of protonatable amines of the carrier and negatively charged phosphates in the nucleic acid backbone) were examined. The analysis of polplexes built from pDNA at N/P 3 gave clear differences between the polyplexes built from homo- and copolymers. The polyplexes with pure PEI were very large (up to 900 nm) whereas the copolymers with longer PEG chains formed smaller polyplexes (Figure 3). In many cases a short PEG chain of 2 kDa was not enough to completely shield the nucleic acids and, thus, the resulting polyplexes aggregated and were nearly as large as the polyplexes from the homopolymer PEI. If PEIs with a molecular weight (MW) of up to 4.9 kDa were used the sizes of the polyplexes with 5 kDa as well as 10 kDa PEG chains were small (about 100 nm). If the MW of PEI increased then the shielding effect of PEG seemed to be diminished, especially for the PEG 5 kDa polyplexes. Thus, there was a clear trend: the longer the PEG chain was the smaller

were the resulting polyplexes. A similar tendency could also be observed for the polydispersity indices (Pdis) (data not shown). They are a measure for the homogeneity of the polyplex sizes. The smaller the Pdi the more homogene is the sample. The smallest values were obtained for copolymers with PEG 10 kDa while the highest values were characteristic for polyplexes from pDNA and unmodified PEI.
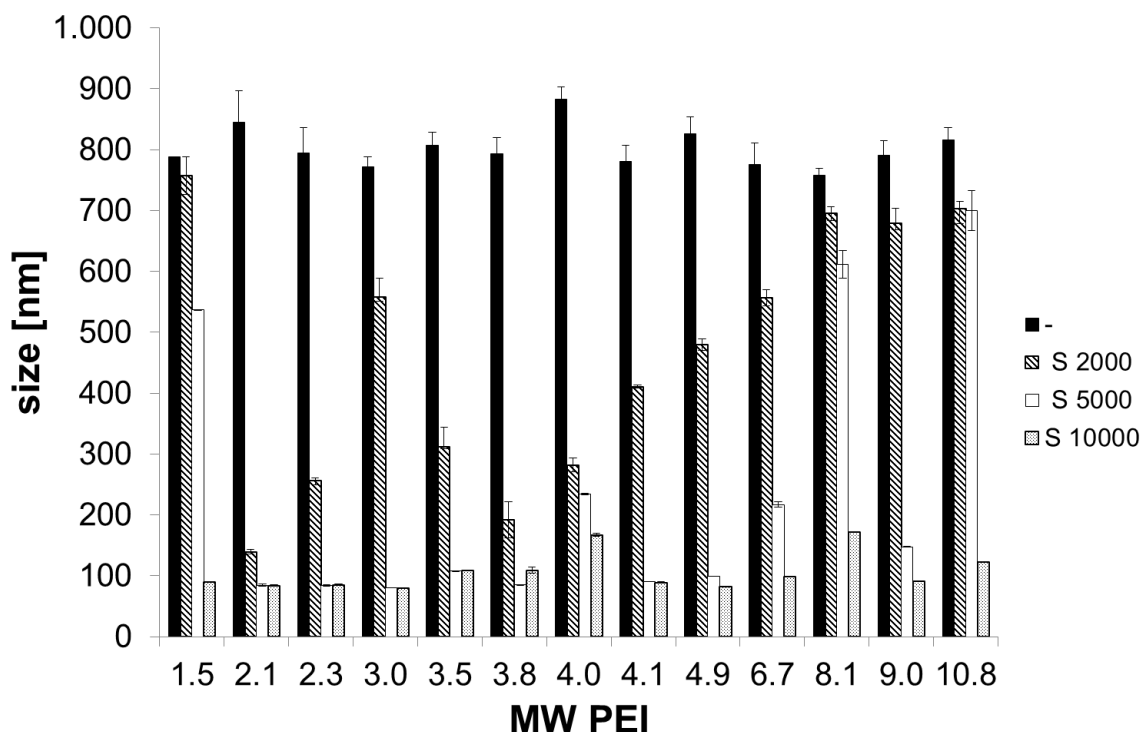

Figure 3. *Polyplex size for polyplexes built from PEI-S-PEG copolymers and pDNA at a N/P ratio of 3 in 150 mM NaCl. The molecular weight of PEI is presented on the x-axis, while the legend gives the molecular weight of the PEG part of the copolymers. "-" indicates unmodified PEI. The hydrodynamic diameter of all copolymer polyplexes was significantly different from PEI-polyplexes with p>0.05. The only exception was PEI 6.7-S-PEG 2000.*

Compared to pDNA siRNA generally formed smaller polyplexes with every polymer (Figure 4). Again if the PEI MW was not higher than 4.9 kDa the polyplexes were not larger than 250 nm. If

the molecular weight of PEI increased then the polyplexes grew up to about 400 nm. But there were no big differences in size if the polyplexes from pure PEI and the copolymers were compared. Only the polyplexes with the PEG 10 kDa showed slightly reduced sizes but not as distinct as in the case of pDNA. The same was true for the Pdis (data not shown). All of them were small (0.05-0.30) indicating homogenous polyplexes.
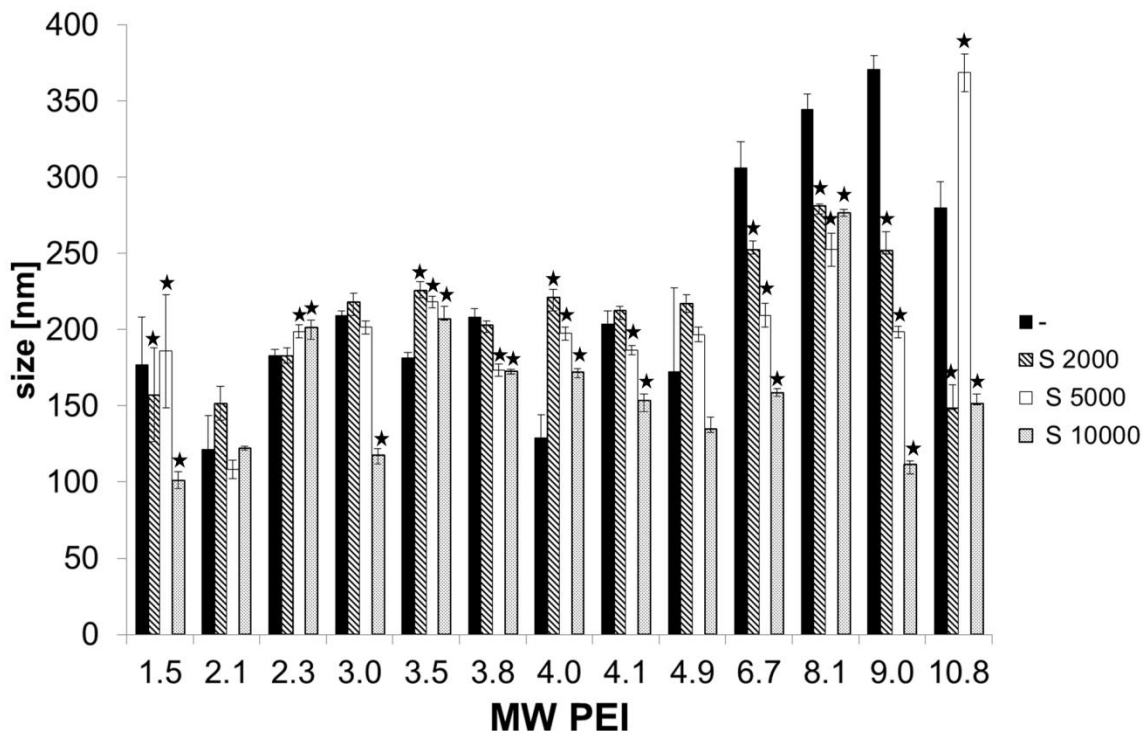

Figure 4. *Polyplex size for polyplexes built from PEI-S-PEG copolymers and siRNA at a N/P ratio of 3 in 150 mM NaCl. The molecular weight of PEI is presented on the x-axis, while the legend gives the molecular weight of the PEG part of the copolymers. "-" indicates unmodified PEI. Whenever the hydrodynamic diameter of the polyplexes made from copolymers was statistically different from the polyplexes with PEI (p<0.05) it is indicated with ★.*

Beside polyplex sizes we also investigated the ability to exclude EtBr from the intercalation with nucleic acids. In order to directly compare the homo- and copolymers, the relative fluorescence of EtBr in PEG-PEI polyplexes was related to PEI polyplexes and the relative quenching was

plotted. Most polyplexes from copolymers and pDNA quenched EtBr better than polyplexes made from PEI alone (Figure 5). The better EtBr is prevented from the intercalation with the nucleic acid the stronger is the interaction between the polymer and its payload and, thus, the more stable is the whole complex resulting in relative quenching values below 1. In most cases the polyplex stability seemed to profit from the PEG attachment. Only sometimes longer PEG chains seemed to be obstructive.
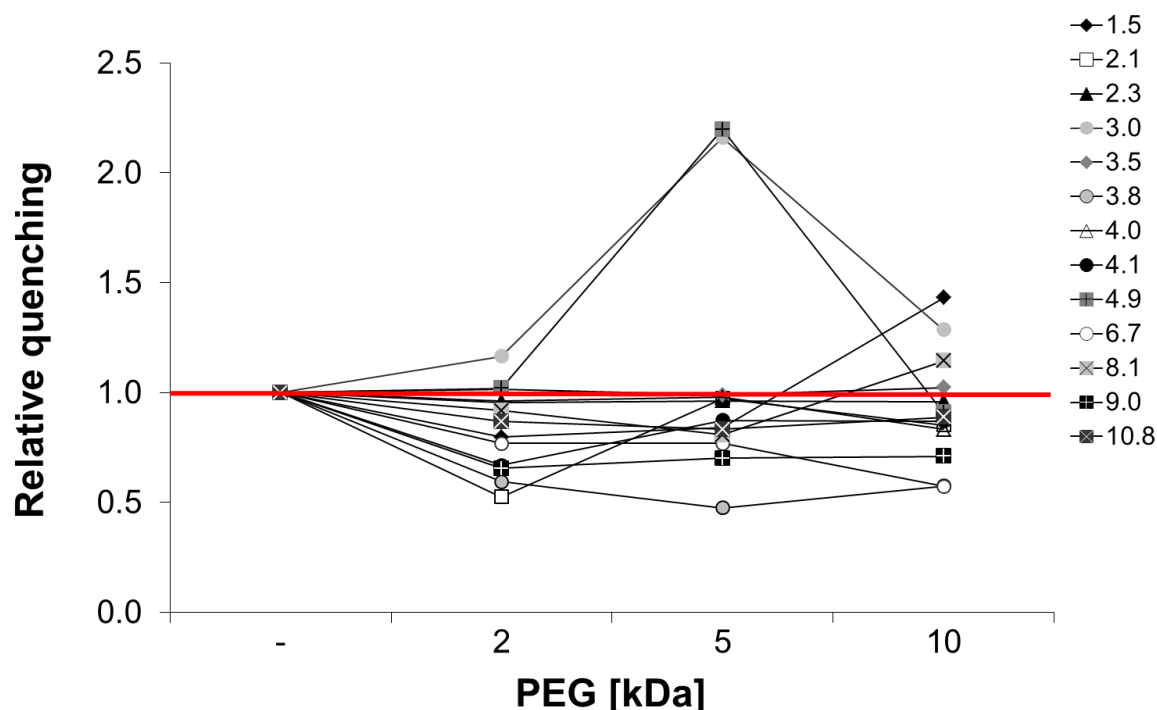

Figure 5. *Relative fluorescence loss of EtBr after complexation of pDNA with PEI and the corresponding PEG-S-PEI copolymers at a N/P ratio of 3. The MW of PEG is indicated on the x-axis ("-" indicates the homopolymer), while the MW of PEI is given in the legend. Statistically significant differences between the polyplexes from copolymers and those from PEI were found for all copolymers (p<0.05).*

In the case of siRNA the differences in fluorescence loss was not as pronounced as for pDNA and these differences were not always significant (especially for the copolymers with PEG 2 kDa). But it can be seen from the small quenching ratio compared to polyplexes from pure PEI

that especially polyplexes with PEG 5 kDa were very stable (Figure 6). The next best performing

polyplexes were those from polymers with PEG 10 kDa. In the case of PEG 2 kDa large

differences in the quenching ability of the copolymers were obtained. It seemed that there was a

lower PEI molecular weight limit for beneficial complexation performance especially with siRNA.

Furthermore, PEG chains normally did not interfere with complex formation but even boosted

complex formation independently of the nucleic acid used. The small performance differences

between pDNA and siRNA were probably due to the different structures of the nucleic acids.

Although it is known that not all carriers which are suitable for pDNA delivery perform well for

siRNA [33-34] our copolymers seemed to be suitable carriers for both nucleic acids. So copolymers

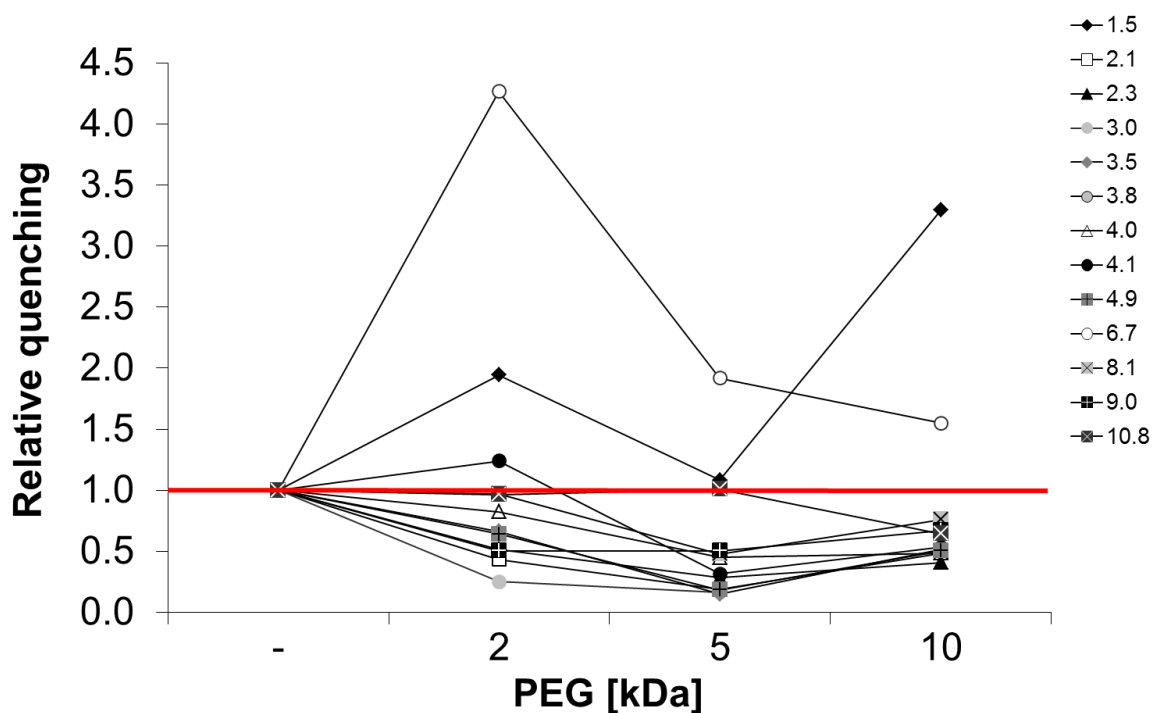with strictly linear assembly allow for the condensation of large and flexible DNAs as well as for

Figure 6. *Relative fluorescence loss of EtBr after complexation of siRNA with PEI and the corresponding PEG-S-PEI copolymers at N/P 3.The MW of PEG is indicated on the x-axis ("-" indicates the homopolymer), while the MW of PEI is given in the legend.*

the short and stiff RNAs. By fine-tuning of the PEG-PEI ratio superior condensing agents can be obtained. Thus, our results suggest that PEG chains with a molecular weight above 2 kDa are needed for the formation of stable polyplexes- independent of the nucleic acid used.

Synthesis of PEI-SS-PEG

For the synthesis of the degradable copolymers (Figure 1, component 9) two different components were needed: On the one hand the activated PEI-SS-pyr (Figure 1, component 7, see chapter 3 for the description of the synthesis) and on the other hand a PEG with a thiol end or a group which could be converted into a thiol in situ such as the thioacetate (Figure 1, component 8, PEG synthesis depicted in Figure 7).
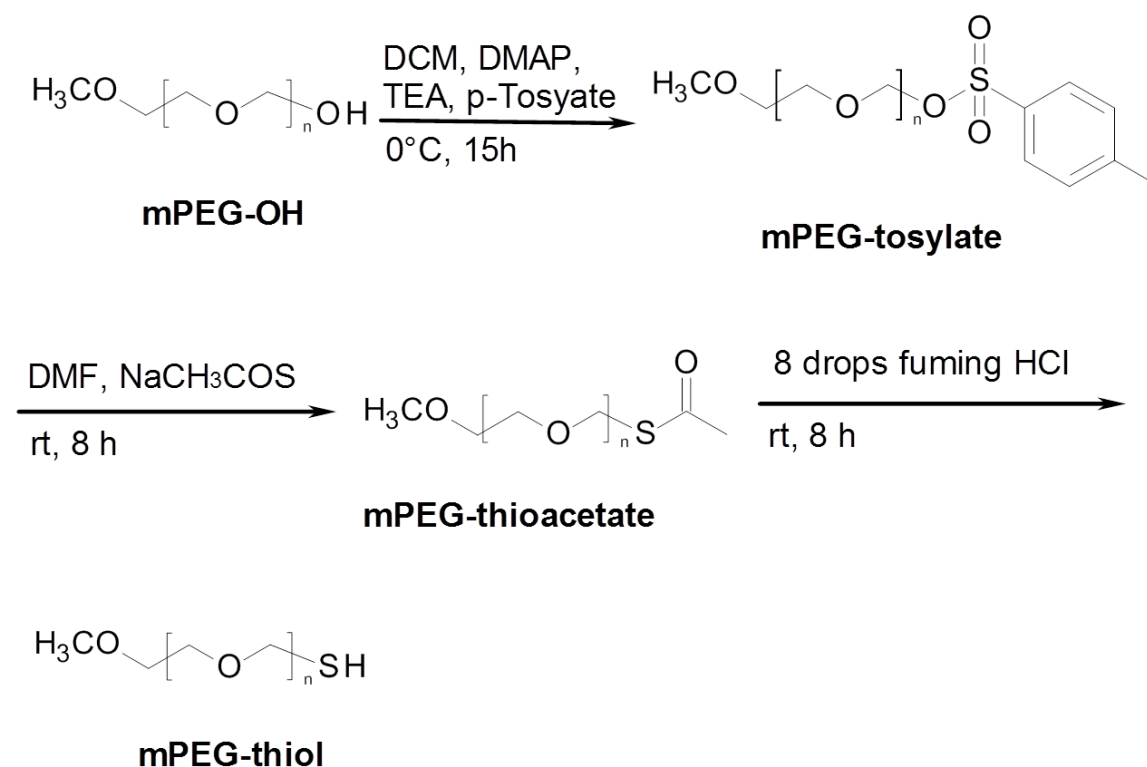

Figure 7. *Synthesis scheme for the conversion of mPEG-OH into mPEG-SH.*

As seen for the PEI synthesis in the previous chapter it was again important to create thiols in situ in order to avoid their oxidation forming PEG-SS-PEG copolymers. The best suited functional group for this task is the thioacetate group which can be cleaved in acidic as well as basic media and whose cleavage by-product acetic acid can be easily removed by evaporation or dialysis. A convenient starting material for all syntheses with PEG is the commercially available methoxyPEG-OH (mPEG-OH).

Since the hydroxyl group is not very eager to react it has to be activated first. This is commonly performed by tosylation replacing the hydroxyl group by a good leaving group [35-38].
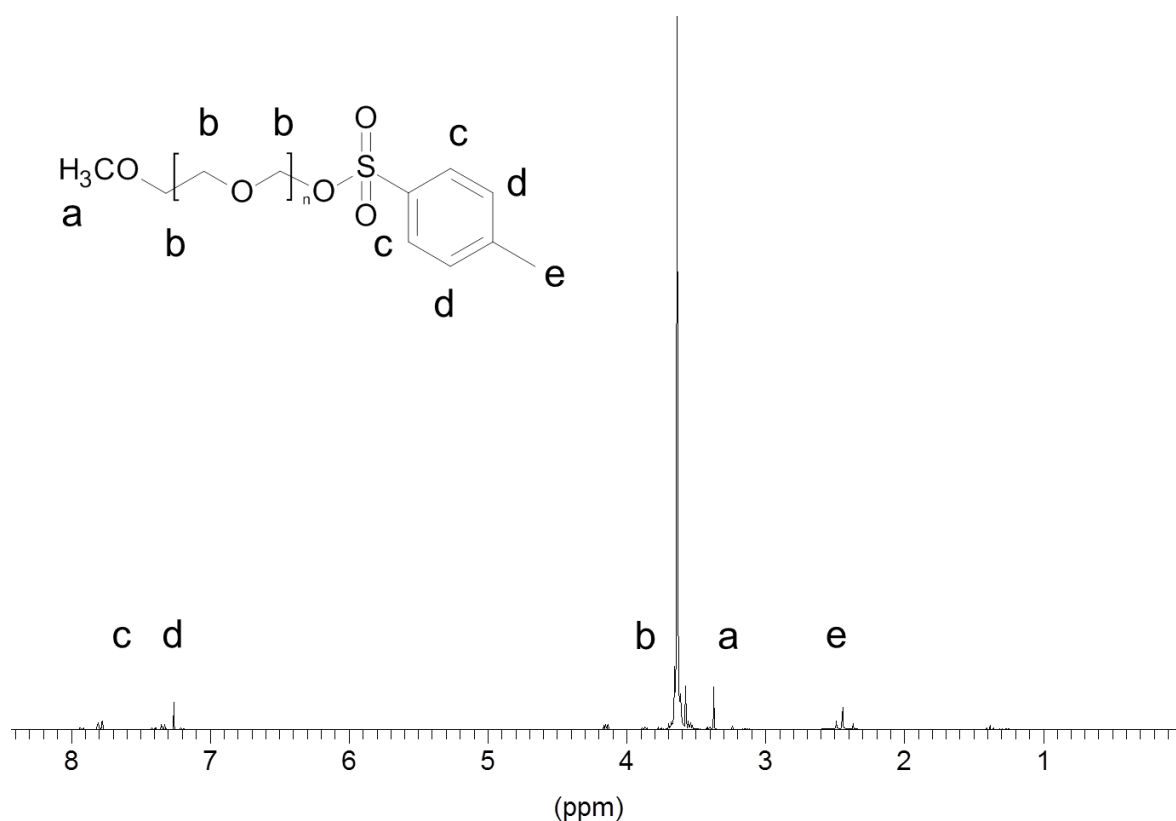

Figure 8. ^{1}*H-NMR of mPEG-tosylate recorded in CDCl$_3$. The peak for the methoxy group of PEG (a) was set to 3 and the area of the tosylate protons (c) and (d) was calculated according to this setting. The conversion degree was calculated from the ratio of the theoretical area of 2 for each aromatic tosylate peak and the area determined by ^{1}H-NMR.*

With the help of DMAP as catalyst and triethylamine as base the tosylate was added to the PEG end (Figure 7). The successful conversion could be monitored by ^{1}H-NMR (Figure 8). Typical conversion degrees were about 90%.

According to Figure 7 the second step of the synthesis involved the substitution of the tosylate by a thioacetate which was the precursor for the thiol. Once more the successful conversion was monitored by ^{1}H-NMR (Figure 9). Typical overall conversation degrees were about 80-85%.
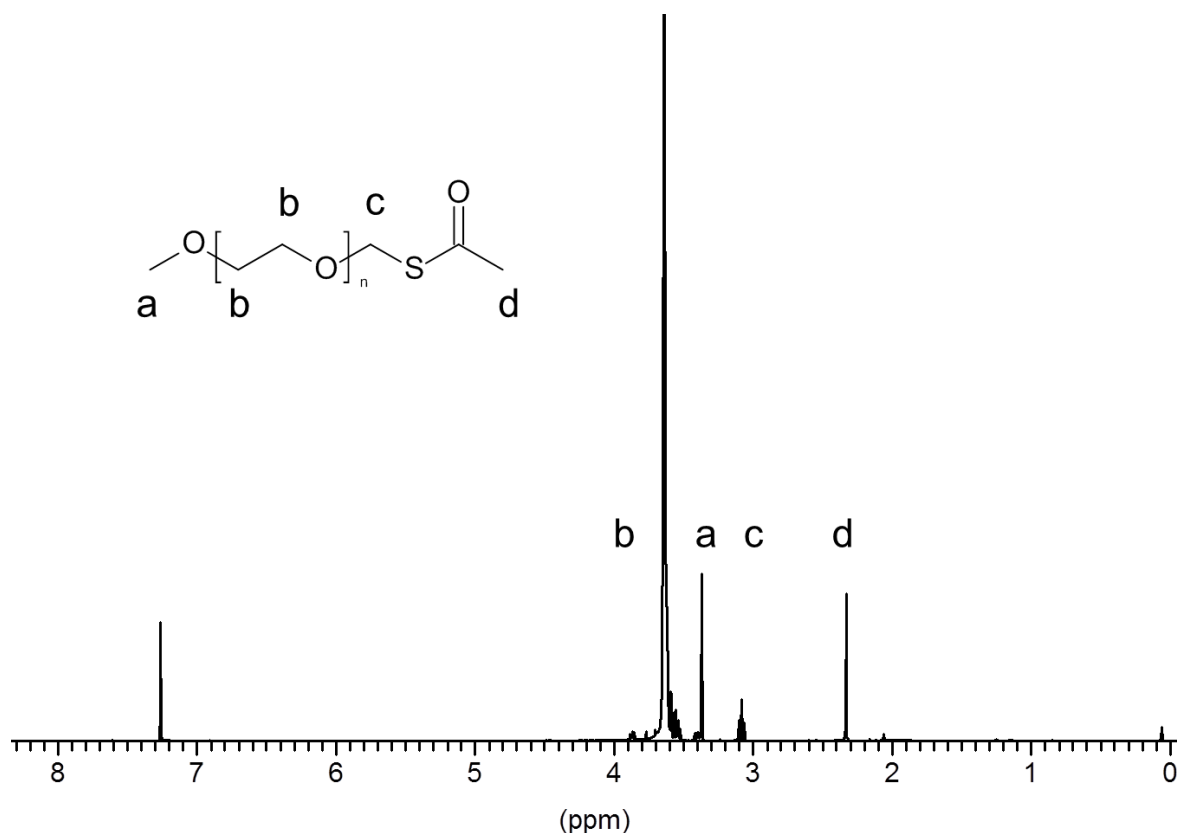

Figure 9. [1]*H-NMR of mPEG-SAc recorded in CDCl₃. The methoxy peak (a) was used for scaling and was set to 3. The methyl peak of the thioacetate (d) and the peak of the methylene group between the PEG chain (b) and the thioacetate (c) accounted for 3 or 2 protons, respectively. The conversion degree was determined as the ratio of the theoretical values and the obtained peak areas.*

In the following step the obtained thioacetate had to be cleaved in order to gain the requested thiol (Figure 7). Due to the instability of this thiol which prohibited any time-consuming analyses it was important to find suitable reaction conditions for the thioacetate cleavage. So three different cleavage conditions were tested, namely stirring the PEG in 0.1M HCl in methanol at 95°C or at rt [39] or boiling it at 95°C in a 1:1 mixture of water and methanol which was acidified with fuming HCl [40]. At different times samples were taken and mixed with DTDP assay solution. The DTDP reacted with the available thiols forming a mixed disulfide between PEG and DTDP which could be analyzed spectrophotometrically after 5 min incubation time. The maximum amount of thiol was calculated from the initial weight of PEG and its conversion degree which was determined by ^{1}H-NMR. It can be seen from Figure 10 that the amount of thiol increased with longer reaction times for all three cleavage conditions. The reaction at rt was the

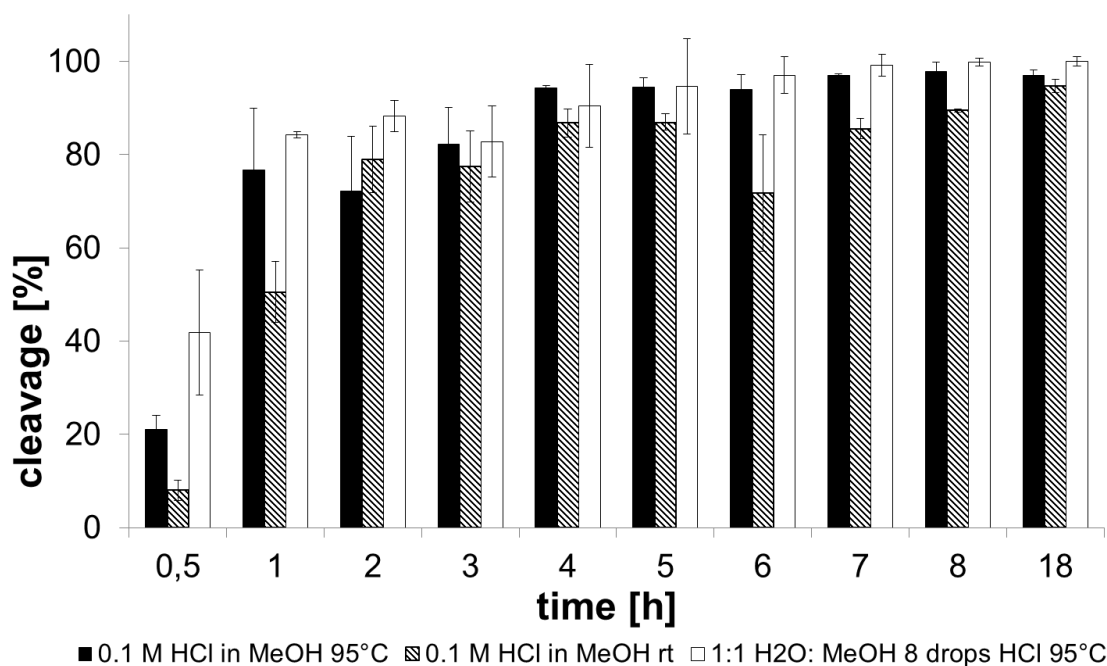■ 0.1 M HCl in MeOH 95°C   ▨ 0.1 M HCl in MeOH rt   □ 1:1 H2O: MeOH 8 drops HCl 95°C

Figure 10. Influence of different reaction conditions and reaction times on the cleavage of the thioacetate moiety. The reaction time is given on the x-axis, while the percentage of cleavage is indicated by the y-axis. The reaction conditions can be found in the legend.

slowest reaction and was only after the longest reaction time (18 h) comparable with the two other conditions. The cleavage in boiling 0.1M HCl in methanol reached a plateau after about 4 h. In contrast, the acidified mixture of water and methanol needed about 7 h until it reached its plateau but this condition resulted in the highest cleavage rates. Thus, to guarantee for the best cleavage rate for further syntheses the thioacetate was boiled in the acidified water methanol mixture for 8 h.

For the coupling of the two polymers 1 thiol eq. of the activated lPEI-SS-pyr was added to the acidified PEG-SAc solution after the cleavage time of 8 h and the mixture was stirred overnight. Subsequently, the product was analyzed by ^{1}H-NMR in D_2O (Figure 11).
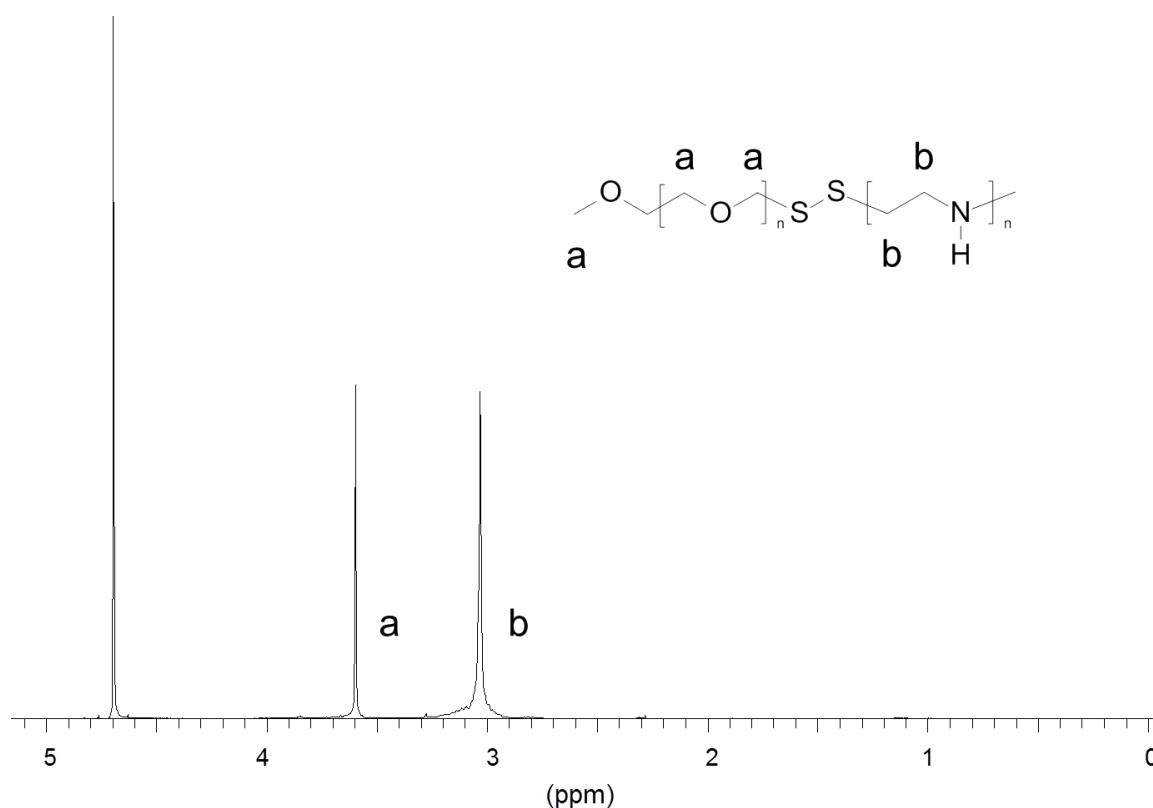

Figure 11. *^{1}H-NMR of a PEG-SS-PEI copolymer recorded in D_2O. The two backbone peaks for the PEI (b) and the PEG chains (a) were used for scaling. The purity of the product was determined as the ratio of the peaks for PEG and PEI corrected for the molecular weight of each polymer.*

The resulting library of copolymers was analyzed for its complexation ability as well as for its transfection efficiency. The results of these investigations are given in Chapter 5.

Conclusion

We successfully synthesized libraries of both stable thioether connected and degradable disulfide linked PEG-PEI copolymers. The library of stable thioethers was built from PEI and mPEG maleimide. The obtained copolymers were used for a first test of the complexation abilities for pDNA and siRNA carried out by an EtBr exclusion assay and determination of polyplex sizes. In the case of pDNA the measured polyplex sizes revealed a distinct division. While homopolymers and polymers with a short 2 kDa PEG chain built rather large polyplexes (up to 900 nm), the particles from copolymers with longer PEG chains (5 kDa and 10 kDa) gave much smaller sizes (commonly below 150 nm) and their size distribution was more uniform. In contrast, the polyplexes assembled from siRNA were all comparably small (about 100-350 nm). Furthermore, the quenching assay proved better complexation ability for siRNA as well as pDNA for nearly all copolymers compared to the homopolymers. This makes the PEG-PEI copolymers very promising carriers for such structurally diverse nucleic acids as siRNA and pDNA. For the synthesis of degradable copolymers a thiol-functionalized PEG was created. Here we established a reaction were thiols were formed in situ and instantly coupled the PEI moiety to the PEG chains. The resulting library can be used for an investigation of structure-activity-relationships as well as intracellular processing of the cleavable copolymers.

References

[1] V. P. Torchilin, V. S. Trubetskoy, Which polymers can make nanoparticulate drug carriers long-circulating? *Advanced Drug Delivery Reviews.* 16 (1995) 2-3, 141-155.

[2] V. Toncheva, M. A. Wolfert, P. A. Dash, D. Oupicky, K. Ulbrich, L. W. Seymour, Novel vectors for gene delivery formed by self-assembly of DNA with poly(l-lysine) grafted with hydrophilic polymers. *Biochimica et Biophysica Acta (BBA) - General Subjects.* 1380 (1998) 3, 354-368.

[3] M. J. Roberts, M. D. Bentley, J. M. Harris, Chemistry for peptide and protein PEGylation. *Advanced Drug Delivery Reviews.* 54 (2002) 4, 459-476.

[4] J. M. Harris, R. B. Chess, Effect of pegylation on pharmaceuticals. *Nature Reviews Drug Discovery* 2 (2003) 3, 214-221.

[5.] F. M. Veronese, Peptide and protein PEGylation: a review of problems and solutions. *Biomaterials.* 22 (2001) 5, 405-417.

[6] D. E. Owens III, N. A. Peppas, Opsonization, biobistribution and pharmacokinetics of polymeric nanoparticles. *International Journal of Pharmaceutics.* 307 (2006) 1, 93-102.

[7] B. Romberg, W. Hennink, G. Storm, Sheddable Coatings for Long-Circulating Nanoparticles. *Biomaterials.* 22 (2001) 5, 405-417.

[8] F. M. Veronese, G. Pasut, PEGylation, successful approach to drug delivery. *Drug Discovery Today.* 10 (2005) 21, 1451-1458.

[9] M. S. Thompson, T. P. Vadala, M.L. Vadala, Y. Lin, J. S. Riffle, Synthesis and applications of heterobifunctional poly(ethylene oxide) oligomers. *Polymer.* 49 (2008) 2, 345-373.

[10] S. Herman, J. Loccufier, E. Schacht, End-group modification of α-hydro-ω-methoxypoly(oxyethylene), 3. Facile methods for the introduction of a thiol-selective reactive end-group. *Macromolecular Chemistry and Physics.* 195 (1994) 1, 203-209.

[11] M. J. Roberts, M. D. Bentley, J. M. Harris, Chemistry for peptide and protein PEGylation. *Advanced Drug Delivery Reviews.* 54 (2002) 4, 459-476.

[12] G. Hooftman, S. Herman, E. Schacht, Poly(Ethylene Glycol)s with Reactive Endgroups. II. Practical Consideration for the Preparation of Protein-PEG Conjugates. *Journal of Bioactive and Compatible Polymers.* 11 (1996) 2, 135-159.

[13] S. Zalipsky, Chemistry of polyethylene glycol conjugates with biologically active molecules. *Advanced Drug Delivery Reviews.* 16 (1995) 2-3, 157-182.

[14] S. Zalipsky. Functionalized Poly(ethylene glycols) for Preparation of Biologically Relevant Conjugates. *Bioconjugate Chemistry.* 6 (1995) 2, 150-165.

[15] M. Zheng, S. R. Pan, H. Hu, G.-F. Wu, M. Feng, W. Zhang, Poly(ethylene oxide) Grafted with Short Polyethylenimine Gives DNA Polyplexes with Superior Colloidal

Stability, Low Cytotoxicity, and Potent In Vitro Gene Transfection under Serum Conditions. *Biomacromolecules.* 13 (2012) 3, 881-888.

[16] H. Petersen, P. M. Fechner, A. L. Martin, K. Kunath, S. Stolnik, C.J . Roberts, D. Fischer, M. C. Davies, T. Kissel, Polyethylenimine-graft-Poly(ethylene glycol) Copolymers: Influence of Copolymer Block Structure on DNA Complexation and Biological Activities as Gene Delivery System. *Bioconjugate Chemistry.* 13 (2002) 4, 845-854.

[17] V. Knorr, M. Ogris, E. Wagner, An Acid Sensitive Ketal-Based Polyethylene Glycol-Oligoethylenimine Copolymer Mediates Improved Transfection Efficiency at Reduced Toxicity. *Pharmaceutical Research.* 25 (2008) 12, 2937-2945.

[18] M. R. Park, K. O. Han, K. I. Han, M.H. Cho, J. W. Nah, Y. J. Choi, C. S. Cho, Degradable polyethylenimine-alt-poly(ethylene glycol) copolymers as novel gene carriers. *Journal of Controlled Release.* 105 (2005) 3, 367-380.

[19] C.-H. Ahn, S. Y. Chae, Y. H. Bae, S. W. Kim, Biodegradable poly(ethylenimine) for plasmid DNA delivery. *Journal of Controlled Release.* 80 (2002) 1-3, 273-282.

[20] S. Patnaik, S. K. Tripathi, R. Goyal, A. Arora, K. Mitra, A. Villaverde, Polyethylenimine-polyethyleneglycol-bis(aminoethylphosphate) nanoparticles mediated efficient DNA and siRNA transfection in mammalian cells. *Soft Matter.* 7 (2011) 13, 6103-6112.

[21] H. Petersen, K. Kunath, A. L. Martin, S. Stolnik, C. J. Roberts, M. C. Davies, T. Kissel, Star-Shaped Poly(ethylene glycol)-block-polyethylenimine Copolymers Enhance DNA Condensation of Low Molecular Weight Polyethylenimines. *Biomacromolecules.* 3 (2002) 5, 926-936.

[22] H. Petersen, P. M. Fechner, D. Fischer, T. Kissel, Synthesis, Characterization, and Biocompatibility of Polyethylenimine-graft-poly(ethylene glycol) Block Copolymers. *Macromolecules.* 35 (2002)18, 6867-6874.

[23] X. Zhang, S. R. Pan, H.-M. Hu, G.-F. Wu, M. Feng, W. Zhang, Poly(ethylene glycol)-block-polyethylenimine copolymers as carriers for gene delivery: Effects of PEG molecular weight and PEGylation degree. *Journal of Biomedical Materials Research Part A.* 84 (2008) 3, 789-804.

[24] M. Kursa, G. F. Walker, V. Roessler, M. Ogris, W. Roedl, R. Kircheis, E. Wagner, Novel Shielded Transferrin−Polyethylene Glycol−Polyethylenimine/DNA Complexes for Systemic Tumor-Targeted Gene Transfer. *Bioconjugate Chemistry.* 14 (2002) 1, 222-231.

[25] S-J. Sung, S. H. Min, K. Y. Cho, S. Lee, Y.-J. Min, Y. I. Yeom, J.-K. Park, Effect of Polyethylene Glycol on Gene Delivery of Polyethylenimine. *Biological and Pharmaceutical Bulletin.* 26 (2003). 4, 492-300.

[26] M. Neu, O. Germershaus, , M. Behe, T. Kissel, Bioreversibly crosslinked polyplexes of PEI and high molecular weight PEG show extended circulation times in vivo. *Journal of Controlled Release.* 124 (2007) 1-2, 69-80.

[27] H. Petersen, A. L. Martin, S. Stolnik, C. J. Roberts, M. C. Davies, T. Kissel, The Macrostopper Route: A New Synthesis Concept Leading Exclusively to Diblock Copolymers with Enhanced DNA Condensation Potential. *Macromolecules.* 35 (2002) 27, 9854-9856.

[28] E. Salcher, E. Wagner, Chemically Programmed Polymers for Targeted DNA and siRNA Transfection. *Nucleic Acid Transfection (*2010) 296, 227-249.

[29] G. T. Hermanson, *Bioconjugate Techniques 2nd edition.* : Academic Press, 2008. p 184.

[30] D. J. Gary, N. Puri, Y-Y. Won, Polymer-based siRNA delivery: Perspectives on the fundamental and phenomenological distinctions from polymer-based DNA delivery. *Journal of Controlled Release.* 121 (2007) 1-2, 64-73.

[31] C. Scholz, E. Wagner, Therapeutic plasmid DNA versus siRNA delivery: Common and different tasks for synthetic carriers. *Journal of Controlled Release.* 161 (2012) 2, 554-565.

[32] K. A. Howard, Delivery of RNA interference therapeutics using polycation-based nanoparticles. *Advanced Drug Delivery Reviews.* 61 (2009) 9, 710-720.

[33] A. Richards Grayson, A. Doody, D. Putnam, Biophysical and Structural Characterization of Polyethylenimine-Mediated siRNA Delivery in Vitro. *Pharmaceutical Research.* 23 (2006) 8, 1868-1876.

[34] S. Mao, M. Neu, O. Germershaus, O. Merkel, J. Sitterberg, U. Bakowsky, T. Kissel, Influence of Polyethylene Glycol Chain Length on the Physicochemical and Biological Properties of Poly(ethylene imine)-graft-Poly(ethylene glycol) Block Copolymer/SiRNA Polyplexes. *Bioconjugate Chemistry.* 17 (2006) 5, 1209-1218.

[35] Z. Zhong, J. Feijen, M. C. Lok, W. E. Hennink, I. V. Christensen, J. W.Yockman, Low Molecular Weight Linear Polyethylenim ine-b-poly(ethylene glycol)-b-polyethylenimine Triblock Copolymers: Synthesis, Characterization, and in Vitro Gene Transfer Properties. *Biomacromolecules.* 6 (2005) 6, 3440-3448.

[36] Y. Lee, H. Koo, G.-W. Jin, H. Mo, M. Y. Cho, J.-Y. Park,.Poly(ethylene oxide sulfide): New Poly(ethylene glycol) Derivatives Degradable in Reductive Conditions. *Biomacromolecules.* 6 (2004) 1, 24-26.

[37] M. J. Stefanko, Y. K. Gun´ko, D. K. Rai, P. Evans, Synthesis of functionalised polyethylene glycol derivatives of naproxen for biomedical applications. *Tetrahedron.* 64 (2008) 44, 10132-10139.

[38] H. Koo, G.-W. Jin, H. Kang, Y. Lee, H.-Y. Nam, H.-S. Jang, A new biodegradable crosslinked polyethylene oxide sulfide (PEOS) hydrogel for controlled drug release. *International Journal of Pharmaceutics.* 374 (2009) 1-2, 58-65.

[39] C. Pale-Grosdemange, E. S. Simon, K. L. Prime, G. M. Whitesides, Formation of self-assembled monolayers by chemisorption of derivatives of oligo(ethylene glycol) of structure HS(CH2)11(OCH2CH2)mOH on gold. *Journal of the American Chemical Society.* 113 (1991) 1, 12-20.

[40] Y.-Y. Luk, M. L. Tingey, D. J. Hall, B. A. Israel, C. J. Murphy, P. J. Bertics, Using Liquid Crystals to Amplify Protein−Receptor Interactions: Design of Surfaces with Nanometer-Scale Topography that Present Histidine-Tagged Protein Receptors. *Langmuir.* 19 (2003) 5, 1671-1680.

Chapter 5

A library of strictly linear poly(ethylene glycol)-poly(ethylene imine) diblock copolymers to perform structure-function-relationship of non-viral gene carriers

Abstract

A library of 39 strictly linear poly(ethylene glycol)-poly(ethylene imine) (PEG-PEI) diblock copolymers was synthesized for the delivery of plasmid DNA using PEG of 2, 5 or 10 kDa in combination with linear PEI with a molecular weight (MW) ranging from 1.5 to 10.8 kDa. In contrast to other approaches, the copolymers demonstrated a clear separation between the hydrophilic PEG and the nucleic acid condensing PEI moieties. Hence, the hypothesis was that PEG may not sterically counteract the interaction between the nucleic acid and PEI and that consequently, the copolymers are perfectly suited to build small and stable polyplexes. Analysis of the polyplexes revealed structure-function relationships and a general guideline was that the PEG domain had a greater influence on the physicochemical properties of the polyplexes than PEI. A PEG content higher than 50% led to small (< 150 nm), nearly neutral polyplexes with favorable stability. The transfection efficacy of these polyplexes was significantly reduced compared to the PEI homopolymer, but restored by the application of the corresponding degradable copolymer, which involved a redox triggerable PEG domain. In conclusion, valuable design criteria for the optimization of gene delivery carriers, which is only possible through the screening of such a large library, was gained.

Introduction

The development of efficient and safe carriers for the delivery of nucleic acids would be an outstanding achievement for the treatment of genetic disorders as well as cancer [1,2]. Since its introduction in 1995 [3], poly(ethylene imine) (PEI) has asserted its position as one of the most intensively investigated polymer-based non-viral gene carriers [4,5]. The favorable properties of PEI allow for condensation and protection of the genetic material in the extracellular environment, and also achieve endosomolysis and subsequent release of the nucleic acid into the cell interior [4,5]. Despite these advantages, the broad use of PEI experiences severe limitations because the transfection efficacy and toxicity of PEI-polyplexes (polyelectrolyte complexes built of PEI and nucleic acids) are strongly correlated [6-9]. Moreover, PEI-polyplexes tend to aggregate under physiological conditions [4,5], which may be particularly counterproductive for in vivo application [5,10].

A common approach to address these shortcomings is to shield the positive surface charge of PEI-polyplexes by the covalent attachment of a hydrophilic, protective polymer layer using poly(ethylene glycol) (PEG) [4,5,11], a strategy also called PEGylation. Different types of PEG-PEI copolymers have been synthesized with block, alternating, or statistical composition arranged in linear, branched, graft, or star topology and varying molecular weight (MW) of PEG [11-17]. The PEG moiety of these copolymers is generally believed to provide for polyplexes with reduced surface charge and a lower tendency towards aggregation [18,19]. In contrast, the effect of PEG on the transfection efficacy is controversially discussed [11]. Depending on the degree of PEGylation, a reduced transfection rate was reported [20,21], while other studies revealed a similar or even higher transfection efficacy of PEGylated versus non-PEGylated polyplexes [14,16,17,22,23]. Reasons for this controversy are manifold and may be returned to the following limitations: First, many of these PEG-PEI copolymers bear a PEG moiety that is not clearly separated from the PEI moiety. Consequently, PEG may sterically counteract the interaction between the DNA and the

140

polycation [11,24], thereby interfering with the particle formation process and the polyplex stability. Second, the synthesis routes proposed for these PEG-PEI copolymers lead to a product mixture because one PEI molecule is not connected to a defined number of PEG molecules. This makes the experimental readout difficult to interpret.

We hypothesized that strictly linear PEG-PEI diblock copolymers may overcome these limitations. Therefore, we connected linear PEI with a MW ranging from 1.5 to 10.8 kDa via a thioether bond to PEG with a MW of 2, 5 or 10 kDa. This resulted in a library of 39 copolymers (PEG-S-PEI), which were compared to the respective homopolymers. To screen for the optimal copolymer composition, the size, zeta potential, stability and biological activity of the polyplexes were analyzed. Additionally, since the PEG moiety may hamper the endosomal escape and further intracellular processing of the polyplexes [25], we synthesized a set of reductively degradable copolymer counterparts (PEG-SS-PEI). The intention was that these degradable polymers would shed off the PEG domain in the intracellular environment thereby restoring the transfection efficacy. The detailed correlation of the copolymer composition with the physicochemical properties and biological activity of the polyplexes will reveal structure-function relationship and give key features for the design of future gene carriers.

Materials and Methods

Materials

2-ethyl-2-oxazoline, methyl-p-toluene sulfonate, sodium borohydride (NaBH$_4$), 2,2`-dithio dipyridine (DTDP), methoxy-PEG-OH, 4-dimethylaminopyridine (DMAP), triethylamine, magnesium sulfate, potassium thioacetate, ethidium bromide (EtBr), propidium iodide, calcium hydride, Tris, heparin, Ham´s F12 and MEM-Eagle medium were from Sigma-Aldrich Chemie GmbH (Steinheim, Germany). Acetonitrile, diethyl ether, fuming HCl, NaOH, chloroform were purchased from Merck KGaA (Darmstadt, Germany). Dimethylformamide (DMF), dichlormethane were obtained from Acros Organics (Belgium). PEG-maleimides of various MW were from or IRIS Biotech GmbH (Martkredwitz, Germany). Trypsin, PBS buffer, YOYO-1 and CellMask^{TM} deep red plasma membrane stain were received from Life Technologie GmbH (Darmstadt, Germany). CDCl$_3$ and D$_2$O were purchased from Deutero GmbH (Kastellaun, Germany). µ-silde 8 well ibiTreat microscopy chambers were from Ibidi GmbH (Martinsried, Germany). Acetonitrile, DMF and 2-ethyl-2-oxazoline were distilled over calciumhydride. Methyl-p-toluene sulfonate was dried in vacuo before use. All other chemicals were used as received. The plasmid DNA encoding enhanced green fluorescent protein (EGFP) (pEGFP-N1, Clontech) was used as reporter gene and isolated from E. coli JM 109 strain using a Qiagen Plasmid Maxi Kit (Qiagen, Hilden, Germany). When indicated, plasmid DNA was stained with the intercalating dye YOYO-1. The labeling reaction was carried out with a molar ratio of 1 dye molecule per 300 base pairs at room temperature (rt) in the dark. CHO-K1 cells (ATCC No. CCL-61) and HeLa cells (ATCC No. CCL-2) were grown in 75 ml culture flasks in a 5% CO$_2$ atmosphere at 37°C as adherent culture to 90% confluency before seeding. CHO-K1 cells were cultivated in Ham´s F-12 and HeLa cells in MEM-Eagle medium containing pyruvate. Both culture media were supplemented with 10% fetal bovine serum (Biochrom AG, Berlin, Germany).

Polymer synthesis

An overview of the synthesis of the PEG-S-PEI and PEG-SS-PEI copolymers is given in Figure 1. The process began with the cationic ring opening polymerization of 2-ethyl-2-oxazoline (**1**) (6.25 ml) in acetonitrile (25 ml) using varying amounts of methyl-p-toluene sulfonate (**2**), depending on the desired MW of PEI. After polymerization under a nitrogen atmosphere at 90°C for several days (3 to 6 days, depending on the calculated MW of PEI), the reaction was cooled down to rt and the MW of the resulting polymer was determined by ^{1}H-NMR. Thereafter, 7.5 eq. (corresponding to the MW of PEI) of sodium thioacetate in DMF (10 ml) were added and the reaction mixture stirred for 4 hours (h). The solvent was then removed, the residue dissolved in chloroform and the solution washed 3 times with water. The raw product, poly(2-ethyl-2-oxazoline)-thioacetate (pEtOXZ-SAc) (**3**), was precipitated in ice cooled diethyl ether, filtrated and dried in vacuo (yield: ~80%). In the next step, **3** was hydrolyzed in fuming HCl (100 ml) at 95°C for one day. After removing the HCl, the product PEI-SH (**4**) was dissolved in water, precipitated with NaOH, washed with water until the supernatant became neutral and dried in vacuo (yield: ~95%). The third step was the activation of component **4** with NaBH$_4$ at pH 8.5 for 20 minutes (min), then the reaction mixture was acidified to pH 1 in order to destroy unreacted NaBH$_4$. Subsequently, each PEI derivative was coupled with methoxy PEG-maleimide (**5**) with a MW of 2, 5 or 10 kDa at pH 7.2 overnight at rt yielding PEG-S-PEI (**6**) (yield: ~80%). Unreacted components were removed by dialysis against water (48 h, dialysis medium was changed twice).

For the synthesis of PEG-SS-PEI (**9**), component **4** was activated with NaBH$_4$ as described above. 3 eq. of DTDP were added to the reaction mixture at pH 4 and stirred overnight. The crude product, PEI-pyridyl disulfide (PEI-SSpyr, **7**), was dialysed against water and lyophilized. The second component, methoxy PEG-SAc (**8**), was synthesized in a 2-step procedure: dry methoxy PEG-OH (5 g) was tosylated using 0.5 eq. of DMAP, 1.5 eq. of p-toluene sulfonate and 2.0 eq. of triethylamine. The reaction mixture was dissolved in dichloromethane (30 ml) and

stirred overnight at rt, followed by the replacement of the dichloromethane by chloroform and washing the crude product 3 times with water and 2 times with 0.1 M HCl. The resulting mPEG-tosylate was dried over magnesium sulfate and in vacuo (yield: ~90%). In the second step, 2.5 eq. of potassium thioacetate were added to the mPEG-tosylate (5 g) in DMF (25 ml) and the mixture was stirred for 8 h at rt. The mixture was concentrated, poured into a 10 fold volume of water and washed with chloroform 3 times. The organic phase was dried over magnesium sulfate and evaporated to dryness yielding mPEG-SAc (**8**) (yield: ~80-90%). Component **8** (1g) was then dissolved in a mixture of water and methanol (1:1, 10 ml), acidified with 5 drops fuming HCl and brought to reflux for 8 h. After cooling to rt and adjusting the pH to 4, component **7** was added and stirred overnight. The product, PEG-SS-PEI (**9**) (yield: ~80%), was dialyzed against water (48 h, dialysis medium was changed twice) and lyophilized.

Successful conversion was monitored by ^{1}H-NMR. ^{1}H-NMR spectra were recorded on an Avance 300 spectrometer (300MHz, Bruker BioSpin GmbH, Germany). Typical chemical shift were as follows: ^{1}H-NMR (CDCl$_3$, 300 MHz) compound **3** (pEtOXZ-SAc): δ_H (ppm) = 0.8-1.4 (br s, 3H NCO-CH$_2$-*CH$_3$*), 2.2-2.6 (br m, 2H, NCO-*CH$_2$*-CH$_3$), 2.9-3.0 (t, 3H, SCO-*CH$_3$*) 3.1-3.9 (br s, 4H, -N(COEt)*CH$_2$-CH$_2$*-); ^{1}H-NMR (D$_2$O, 300 MHz) compound **6** (PEI-S-PEG): δ_H (ppm) = 2.6-3.1 (br s, 4H, *CH$_2$*-O-*CH$_2$*), 3.5-3.8 (br s, 4H, *CH$_2$*-NH-*CH$_2$*); ^{1}H-NMR (D$_2$O, 300 MHz) compound **7** (PEI-SSpyr): δ_H (ppm) = 2.6-3.0 (br s, 4H, -*CH$_2$*-NH-*CH$_2$*-), 7.0 (t, 1H, C$_{Ar}$), 7.5 (d, 1H, C$_{Ar}$), 7.7 (t, 1H, C$_{Ar}$), 7.8 (d, 1H, C$_{Ar}$); ^{1}H-NMR (D$_2$O, 300 MHz) compound **9** (PEI-SS-PEG): δ_H (ppm) = 2.8-3.3 (br s, 4H, -*CH$_2$*-NH-*CH$_2$*-), 3.5-3.7 (br s, 4H, -*CH$_2$*-O-*CH$_2$*-)

Formation of polyplexes

The polyplexes of plasmid DNA (pDNA) and polymer were prepared at different N/P ratios (ratio of nitrogens in polymer to phosphates in DNA). The polymer and plasmid DNA were each diluted in equal volumes of 150 mM NaCl. The polymer solution was added to the DNA solution, the

mixture was vortexed for 20 seconds and then incubated for 20 min before use. The amount of plasmid DNA and the total volume of the polyplex solution are given in each section.

Particle and zeta potential measurements

The hydrodynamic diameter and the zeta potential of the polyplexes was measured using a Zetasizer Nano-ZS from Malvern Instruments (Malvern, Germany) at 25°C. A 4 mW He-Ne laser at a wavelength of 633 nm was used as the light source. For the determination of the size, the measurement position was at 4.65 mm with automated laser attenuation. Scattered light was detected at an angle of 173° backscatter. The viscosity and refractive index of the dispersants were used as follows: 150 mM NaCl: 0.90 mm^2/s and 1.33, respectively; culture medium: 0.90 mm^2/s and 1.681, respectively. Three measurements with 10 sub-runs were performed for each sample. Data were analyzed by the general purpose mode and expressed as mean ± standard deviation (SD). The zeta potential of the polyplexes was measured at 25°C. Three measurements with 10 sub-runs were performed for each sample. Data were processed in the monomodal mode which guarantees for good sample stability due to short measurement duration and then expressed as mean (± SD). For size measurements, polyplexes were formed by mixing 2 μg DNA and varying amounts of polymer to achieve different N/P ratios in a final volume of 500 μl, while for zeta potential measurements the polyplexes were built with 4 μg plasmid DNA in a final volume of 1000 μl. For transmission electron microscopy (TEM), the polyplex solution was pipetted onto carbon coated copper grids, and the counterstaining was performed with an uranyl acetate solution (2% w/w). Images were taken at 120 keV using a Philips CM12 microscope (FEI, Eindhoven, The Netherlands). As an indirect measurement for the protonation capacity, the zeta potential of the polyplexes was measured after dilution in Tris buffer at a final pH of 5.5, 6.5 and 7.4, respectively.

Ethidium bromide quenching assay

The polyplexes were prepared at a N/P ratio of 1 and 6 by diluting 1 µg of plasmid DNA in a final volume of 100 µl. After incubation for 20 min the polyplexes were pipetted in a 96-well plate and mixed with 2.5 µl of a 0.1 µg/µl ethidium bromide (EtBr) solution. The fluorescence of EtBr was excited at 518 nm and recorded at 605 nm using a LS 55 fluorescence spectrometer (Perkin Elmer, Germany) and expressed as relative fluorescence compared to uncomplexed plasmid DNA. Measurements were performed in quadruplet. The relative fluorescence loss was calculated as follows: relative

fluorescence loss = relative fluoresence$_{PEG-PEI-polyplexes}$/relative fluorescence$_{PEI-polyplexes}$.

Stability of the polyplexes

The polyplex solution (500 µl) containing 2 µg of pDNA was incubated over a time period of 10 h and the hydrodynamic diameter of the polyplexes was recorded every 10 min as described above. Alternatively, the polyplexes of plasmid DNA and polymer were prepared at a N/P ratio of 6 using 2 µg pDNA in a final volume of 100 µl. The polyplex solution was then diluted with 400 µl HAM´s F12 culture medium and the hydrodynamic diameter of the polyplexes was measured as described above.

Transfection studies

HeLa or CHO-K1 cells were seeded in 24-well plates at a density of 40,000 or 38,000 cells per well 24 h prior to transfection. 2 µg of plasmid DNA was used to prepare the polyplexes with the appropriate amount of polymer to yield different N/P ratios in a final volume of 100 µl. The cells were washed with PBS, then 900 µl of serum free culture medium and 100 µl of polyplex solution was added. After 4 h the transfection medium was removed and cells were incubated for an additional 20 h with culture medium containing serum. After detachment of the cells from the surface by trypsin, extensive washing with PBS and the addition of propidium iodide

(1µg/ml), the analysis of the EGFP expression and cell viability was performed by flow cytometry using a FACSCalibur (Becton-Dickinson, Germany). EGFP was excited at 488 nm and the fluorescence was detected using a 515 - 545 nm bandpass filter, whereas the propidium iodide emission was measured with a 670 nm longpass filter. The data were analyzed using WinMDI 2.8 software by J. Trotter. To exclude doublets and cellular debris, cells were appropriately gated in forward/sideward scatter plots with 20,000 events per sample. The percentage of cells that was positive for EGFP indicated the transfection efficacy [%] and was expressed as means (± SD) from three independent samples. Cells that were negative for propidium iodide accounted for the cell viability [%]. Cells treated with 150 mM NaCl were used as control, they had a threshold value of 1%. The relative transfection was calculated as follows:

relative transfection = transfection efficacy [%]$_{PEG-PEI-polyplexes}$/transfection efficacy [%]$_{PEI-polyplexes}$.

Cellular uptake

80,000 CHO-K1 cells per well were seeded in a 24-well plate. The polyplexes were prepared at a N/P ratio of 6 in 100 µl using 2 µg of YOYO-1 labeled pDNA. The cells were then treated as described in the previous section, but detached from the surface after 4 h by trypsin that was supplemented with 20 mM sodium azide. Cells were analyzed by flow cytometry as described above, YOYO-1 was excited with a 488 nm argon laser and detected with a 515 - 545 nm bandpass filter. The mean fluorescence intensity (MFI) of 20,000 gated cells was recorded as a measure for the amount of internalized plasmid DNA. The values were expressed as means (± SD) from three independent samples.

Confocal laser scanning microscopy was performed using a Zeiss Axiovert 200 M microscope coupled to a Zeiss LSM 510 scanning device (Carl Zeiss Co. Ltd., Germany). CHO-K1 cells were plated in µ-slide 8 well ibiTreat microscopy chambers at a density of 20,000 cells per well and incubated with YOYO-1 labeled polyplexes. After 2 h the cell membranes were stained with CellMask^{TM} deep red plasma membrane stain as indicated by the supplier. The fluorophores

were then excited with 488 and 633 nm and the fluorescence was recorded with a 505 - 530 bandpass filter and a longpass filter of 650nm. The measurements were performed using a Plan-Apochromat 63x/1.4 oil objective at 37°C and the thickness of the optical sections was 1.1 µm.

Toxicity

The MTT toxicity assay was performed according to Mosmann [26] with slight modifications. Briefly, HeLa cells were seeded at a density of 10,000 per well into 96-well plates 24 h before testing. The cells were incubated for 4 hours with polymer dilutions in serum-free cell culture medium or cell culture medium only as a control. Then, the medium was replaced with culture medium containing serum. After an additional 20 h, 200 µl of [3-(4,5-dimethylthiazol-2-yl)-2,5-diphenyl tetrazolium bromide] (MTT) (0.6 mg/ml) was added to the cells for 4 h. Unreacted dye was removed and 110 µl of a 10 % SDS solution were added to each well for a further 22 h. The optical density (OD) of each well was determined on a TitertekPlus Microplate Reader (Bartolomey Labortechnik, Germany) with 570 nm as test wavelength and 690 nm as reference wavelength. Each polymer concentration was tested in sextuplet. The relative viability was calculated by $OD_{test}/OD_{control}$ x 100%. The IC50 values were determined by fitting the calculated values in a four parameter logistic curve using Sigma Plot (Version 12.2, Systat Software, Chicago, IL, USA).

Statistics

Results are shown as mean (± SD). Experiments were performed in triplicate if not indicated otherwise. Significance between two groups was tested using a one-tailed Student's t-test. A p-value < 0.01 was considered to be significant. Significance between the mean values of the homopolymer and copolymer polyplexes was calculated using one-way ANOVA analysis followed by Bonferroni t-test. A p-value of 0.05 was considered to be significant. Analysis was performed with Sigma Plot (Version 12.2, Systat Software, Chicago, IL, USA).

Results

Synthesis of the PEG-PEI copolymers

The library of PEG-PEI copolymers was prepared in a multi-step procedure starting with the polymerization and the activation of the PEI block, followed by the coupling of PEI and PEG either via a thioether or disulfide bond yielding non-degradable PEG-S-PEI or degradable PEG-SS-PEI copolymers, respectively (Figure 1).
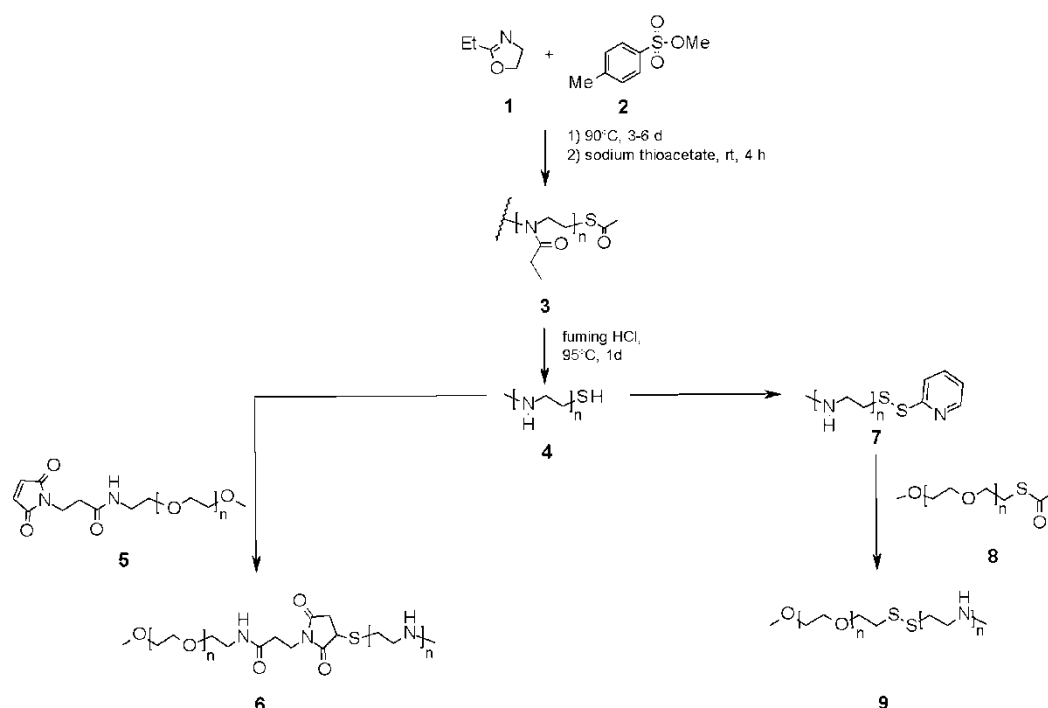

Fig. 1. *Synthesis scheme for PEG-S-PEI and PEG-SS-PEI block copolymers.*

To this end, 13 different linear PEI derivatives with a molecular weight (MW) ranging from 1.5 to 10.8 kDa were polymerized in a parallel approach. Their MW was controlled by the ratio of the monomer 3-ethyl-2-oxazoline (**1**) and the starter methyltosylate (**2**) and was determined by ^{1}H-NMR (see Supporting Information, Figure S1 and Table S1). The reactive group was then introduced by stopping the reaction with a thioacetate, producing poly(2-ethyl-2-oxazoline)-thioacetate (pEtOXZ-SAc) (**3**) (see Supporting Information for ^{1}H-NMR, Figure S2), which was

hydrolysed to thiolated PEI (**4**). Each PEI derivative was then coupled to methoxy PEG-maleimide (**5**) of 2, 5, or 10 kDa, leading to the final PEG-S-PEI (**6**) copolymers (see Supporting Information for ^{1}H-NMR, Figure S3). According to Figure 2, the synthesis resulted in a library of 39 co- and 13 homopolymers which are denoted as follows: PEG(x)-S-PEI(y) or PEI(y), where x represents the MW of the PEG and y the MW of the PEI. The PEG content of the copolymers covered a range of about 15 to 90%.
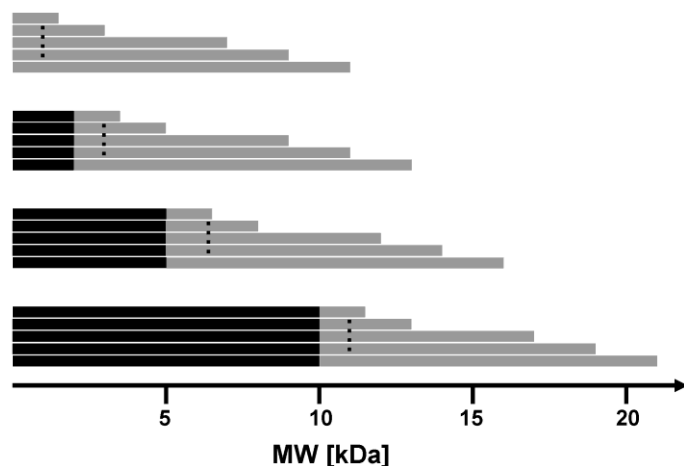

Fig. 2. *Composition of the PEG-S-PEI block copolymers. The MW of PEG (black bars) was 2, 5 or 10 kDa and is indicated as received by the manufacturer. The PEI MW (gray bars) ranged from about 1.5 to 10.8 kDa and was determined by ^{1}H-NMR. Because the MW of PEG and PEI were determined by two different methods (gel permeation chromatography and ^{1}H-NMR, respectively), they can not be directly compared, and one should be aware that the MW is a distribution around an average value. The black dots indicate that more homo- and copolymers were synthesized than shown in the Figure.*

Additionally, a set of reductively degradable counterparts (PEG-SS-PEI, **9**) was synthesized. In this case, component **4** reacted in a disulfide exchange reaction to form PEI-pyridyl disulfide (PEI-SSpyr, **7**), which was thereafter coupled to mPEG-SAc (**8**) with a MW of 5 kDa. The PEG-SS-PEI copolymers are denoted analogously to the PEG-S-PEI block copolymers. The synthesis

route only allowed for the coupling of one PEG to PEI molecule as proposed in Figure 1, and uncoupled PEG and PEI were removed by dialysis of the copolymers. The composition of the copolymers was calculated using the appropriate signals in ^{1}H-NMR spectra as well as the PEG and PEI content of the copolymers (data not shown), and was in good agreement with theoretical values.

Physicochemical characterization of the polyplexes

Polyplexes of PEG-S-PEI copolymers and plasmid DNA were formed under physiological salt concentrations at a N/P ratio of 6 to study the influence of the copolymer composition on the size of the polyplexes (for other N/P ratios see Supplementary Information, Figure S4). With increasing MW of PEG in the copolymer, the hydrodynamic diameter of the polyplexes decreased (Figure 3A). The hydrodynamic diameter of pure PEI-polyplexes ranged from about 650 to 950 nm, while polyplexes fabricated with PEG(10)-S-PEI were significantly smaller with hydrodynamic diameters from about 75 to 150 nm. Considering the polyplex size according to the PEG content of the copolymers, a minimum of about 50% PEG was necessary to form polyplexes smaller than 150 nm. In contrast, the influence of the PEI MW on the polyplex size was less pronounced. The polydispersity index (PI), which estimates the width of the size distribution of the polyplexes, showed a similar trend (Supplementary Information, Figure S5) indicating that polyplexes built with PEG(10)-S-PEI copolymers were more homogeneously distributed compared to the other ones. Transmission electron microscopy (TEM) images confirmed this trend. PEI-polyplexes were large and formed aggregates (Figure 3B), while PEG(10)-S-PEI-polyplexes were much smaller and had a spherical or elliptical morphology (Figure 3C).
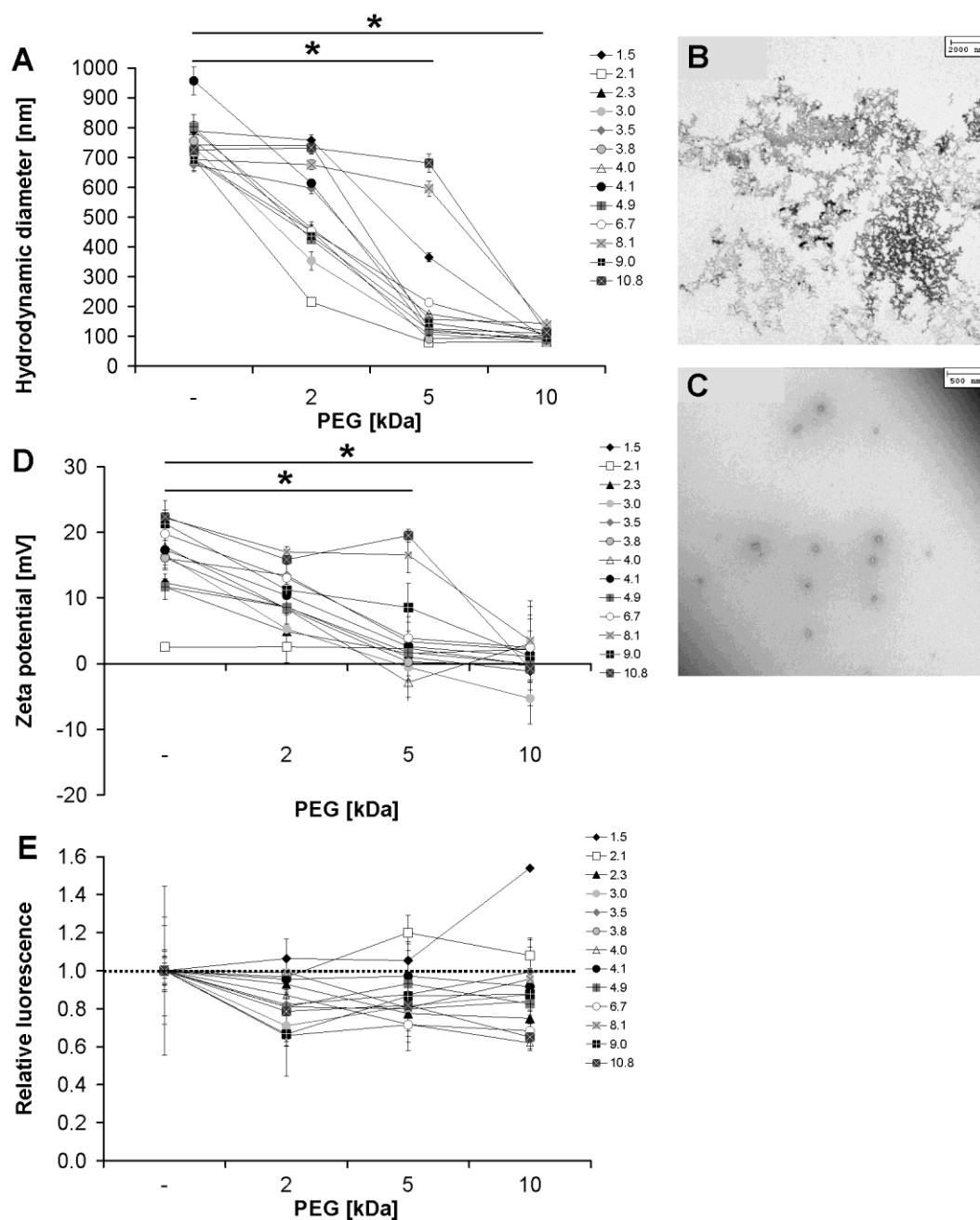
Fig. 3. *Physicochemical characterization of the polyplexes: (A) The hydrodynamic diameter of polyplexes assembled of plasmid DNA and PEG-S-PEI copolymers or PEI homopolymers at a N/P ratio of 6 in 150 mM NaCl as determined by dynamic light scattering. The MW of PEG [kDa] is presented on the x-axis ("-" indicates the homopolymer), while the MW of PEI [kDa] is given in the legend. The hydrodynamic diameter of PEG(5)-PEI- and PEG(10)-PEI-polyplexes were significantly different from PEI-polyplexes with p < 0.05, which is indicated by *. (B and C) are*

*electron micrographs of PEI(4.0)- and PEG(10)-PEI(4.0)-polyplexes, respectively. The size of PEI-polyplexes is larger than measured by dynamic light scattering, most likely due to aggregation artifacts during sample preparation. (D) The zeta potential of the polyplexes at a N/P ratio of 6. The MW of PEG [kDa] is presented on the x-axis ("-" indicates the homopolymer), while the MW of PEI [kDa] is given in the legend. The zeta potential of PEG(5)-PEI- and PEG(10)-PEI-polyplexes were significantly different from PEI-polyplexes with $p < 0.05$, which is indicated by *. Exceptions were the zeta potentials of PEI(2.1) and PEI(2.3). (E) shows the relative fluorescence of EtBr after complexation of plasmid DNA with PEG-S-PEI copolymers compared to pure PEIs at N/P 6. The MW of PEG [kDa] is presented on the x-axis ("-" indicates the homopolymer), while the MW of PEI [kDa] is given in the legend.*

The zeta potential is one of the most important factors determining the stability of the polyplexes as well as their interaction with cells. As expected, polyplexes built with pure PEI showed a positive zeta potential of about +10 to +25 mV, which decreased with the MW of the PEG in the PEG-S-PEI copolymers (Figure 3D). The zeta potential of polyplexes formed with PEG(10)-S-PEIs was particularly effectively reduced to values below ~ +3 mV, irrespective of the PEI derivative. Also at other N/P ratios, the PEG(10)-S-PEI polyplexes had a zeta potential around zero (see Supplementary Information, Figure S6). Considering again the polyplex properties with respect to the PEG content, copolymers with more than 50% PEG formed polyplexes with low zeta potential.

The DNA condensation ability of the co- and homopolymers was investigated by the quenching of EtBr fluorescence. In order to directly compare the homo- and copolymers, the relative fluorescence of EtBr in PEG-PEI-polyplexes was related to PEI-polyplexes and expressed as "relative fluorescence" (Figure 3E). All PEG-PEI-polyplexes displayed a lower relative

fluorescence compared to the PEI-polyplexes, exceptions were PEG-S-PEI(1.5) and PEG-S-PEI(2.1).

To evaluate the stabilizing effect of PEG on the polyplexes, the complex size was monitored over a time period of 10 h (Figure 4). As expected, the hydrodynamic diameter of polyplexes built with pure PEI and with PEG(2)-PEI copolymers increased up to 4 fold. For PEG(5)-PEI or PEG(10)-PEI, the stability of the polylplexes depended on the PEG content in the copolymer. Copolymers with >50% PEG allowed for excellent stability of the corresponding polyplexes (Figure 4A and B). In contrast, a PEG content below 50% lead to aggregation or only limited stability (Figure 4C). The favorable stability of PEGylated polyplexes bearing a PEG content > 50% was also confirmed by measuring the size of the polyplexes after dilution in cell culture medium (Supporting Information, Table S2). Similar results were obtained by challenging the polyplex stability using the extracellular matrix component heparin (see Supporting Information, Figure S7)
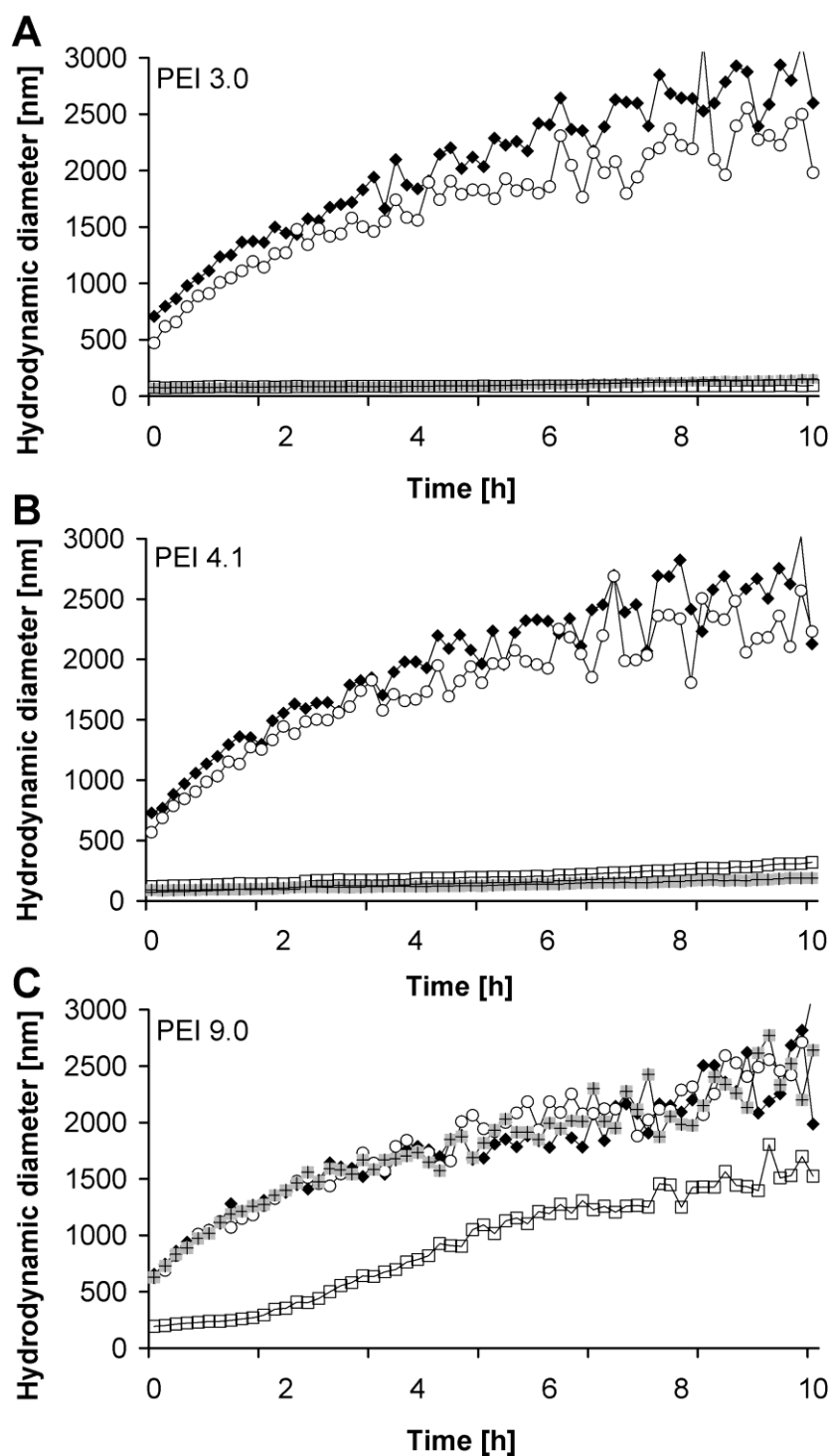
Fig. 4. *Hydrodynamic diameter of polyplexes at a NP ratio of 6 built with PEI of 3.0 (A), 4.1 (B) and 9.0 (C) kDa (◆) and the corresponding PEG(2)-S-PEI (○), PEG(5)-S-PEI (▦) and PEG(10)-S-PEI (□) copolymers as determined by dynamic light scattering over a time period of 10 h.*

If PEG is attached to the surface of a nanoparticle in low density, it will take the mushroom conformation and presumably not provide for a good colloidal stability [27]. At higher packing density, the PEG chains are more extended and found in the brush conformation, and are consequently leading to a much better colloidal stability [27]. We roughly estimated, which conformation PEG may take on the surface of the polyplexes depending on the MW of PEG and PEI. These considerations were in very good agreement with polyplex stability data (Supporting Information, Table S3).

Biological activity of the polyplexes

The transfection efficacy of the PEI- and PEG-S-PEI-polyplexes at N/P 6 was determined by measuring the expression of EGFP in CHO-K1 cells (for other N/P ratios see Supplementary Information, Figure S8). The percentage of EGFP positive cells depended on the MW of PEG and PEI in the copolymers (Figure 5A). PEI with a MW of 4.9 kDa and lower yielded a moderate transfection efficacy, while PEIs with higher MW displayed very good transfection rates of about 40%. If PEG(2)-PEI copolymers were used, no specific trend was observed compared to the corresponding PEI homopolymers. In contrast, the transfection was reduced for most PEG(5)-PEI- and especially for PEG(10)-PEI-copolymers. The effect of PEG 10 kDa on the transfection efficacy of polyplexes became even more evident when the relative transfection, which is defined as the transfection efficacy of the PEG-PEI-polyplexes related to the PEI-polyplexes, was considered. Figure 5B impressively shows that the relative transfection rate of PEG(10)-PEI-polyplexes was significantly lower than that of the PEI-polyplexes. The transfection results in HeLa cells were similar, and the polyplexes also provided for transfection under serum-containing culture conditions (Supplementary Information, Figure S9 and S10, respectively).
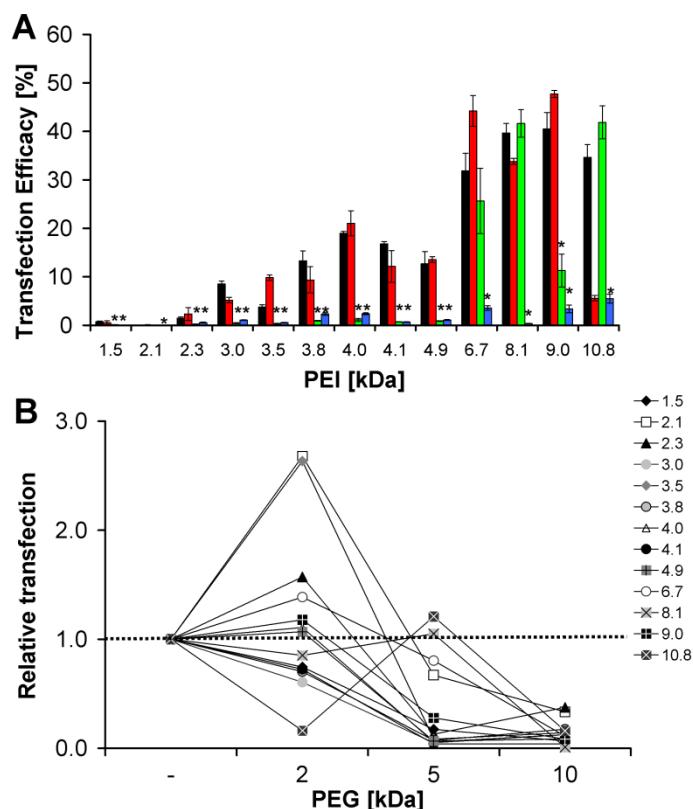
Fig. 5. *Transfection efficacy of polyplexes at a N/P ratio of 6 built with PEI (▇) and the*

corresponding PEG(2)-S-PEI (▇), PEG(5)-S-PEI (▇) and PEG(10)-S-PEI (▇) copolymers (A) in

CHO-K1 cells. The MW of PEI [kDa] is indicated on the x-axis. Statistically significant differences

of PEG(5)- and PEG(10)-PEI-polyplexes from PEI-polyplexes are indicated by * (p < 0.05).

Additionally, the values of the transfection efficacy of the PEG-PEI-polyplexes were related to

the corresponding PEI-polyplexes and expressed as relative transfection (B). Here, the MW of

PEG [kDa] is shown on the x-axis ("-" indicates the homopolymer), while the MW of PEI [kDa] is

given in the legend.

The reason for the suppression of the transfection by the application of the copolymers may be

manifold. First, PEG(10)-PEI-polyplexes with zeta potential close to zero may be hindered from

electrostatic interaction with cells, consequently leading to a reduced cellular uptake of the

polyplexes and transfection rate. Alternatively, the polyplexes may still be taken up by the cells,

but the endosomal escape or other intracellular events may be prevented due to PEG. To test these possibilities, we first measured the cellular uptake of fluorescently-labeled polyplexes. Flow cytometry analysis revealed that there were only slight differences in the cellular uptake between polyplexes built with PEG-S-PEI copolymers and their corresponding PEI homopolymer (Supporting Information, Figure S11). To get a deeper insight into the process of cellular uptake, fluorescently-labeled polyplexes were incubated with CHO-K1 cells and observed by confocal laser scanning microscopy (Figure 6). The images illustrated that PEI- and PEG(2)-PEI-polyplexes were much larger than PEG(5)-PEI- and PEG(10)-PEI-polyplexes. In addition, it was evident that more of the smaller polyplexes than the larger ones were internalized. However, a detailed image analysis revealed that despite the difference in the size and number of the
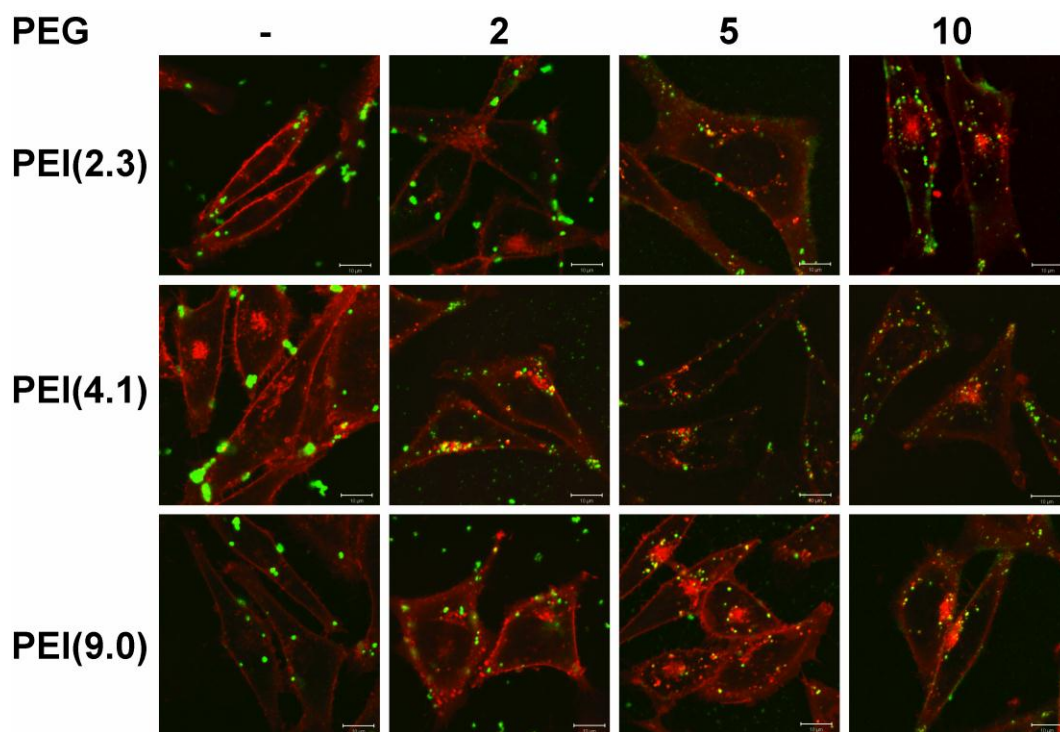

Fig. 6. The cellular uptake of fluorescently-labeled polyplexes was observed by confocal laser scanning microscopy. The polyplexes are shown in green, while the cell membranes of HeLa cells are stained with CellMask^TM deep red plasma membrane stain and displayed in red. The bar indicates 10 μm.

polyplexes inside cells, the overall amount of plasmid DNA per cell was in the same range (data not shown) which corroborated the results from the flow cytometry measurements.

To investigate the alternative possibility that PEG-S-PEI copolymers may be hampered by a limited intracellular processing, a set of reductively degradable PEG-SS-PEI copolymers was synthesized. As an example, 5 copolymers were chosen with a PEG moiety of 5 kDa and a PEI moiety of 2.3, 3.5, 4.0, 4.9 or 6.7 kDa. Both the PEG(5)-SS-PEI and the corresponding PEG(5)-S-PEI copolymers were applied for transfection studies. Figure 7 clearly shows that the relative transfection was not only restored using PEG(5)-SS-PEI copolymers, but exceeded the relative transfection of PEG(5)-S-PEI-polyplexes by a factor 1.2 to 4.5.
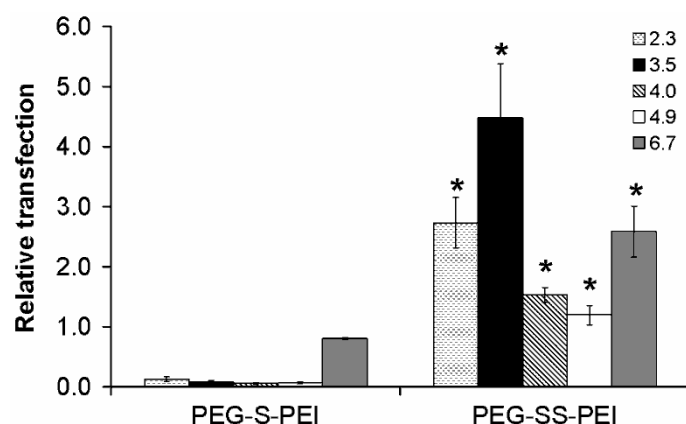

Fig. 7. *Relative transfection of PEG(5)-S-PEI- and PEG(5)-SS-PEI-polyplexes at a N/P ratio of 6 as determined by flow cytometry analysis. The MW of PEI is indicated in the legend. The relative transfection of degradable polyplexes was significantly different from non degradable polyplexes and is indicated by * (p < 0.001).*

To examine the reason for a limited intracellular processing in more detail, the endosomal escape capacity of the polyplexes was investigated. To follow up this goal, the protonation capacity of the polyplexes, which can be estimated by measuring their zeta potential as a function of pH, was determined. Figure 8 shows that the pH had no huge influence on the zeta
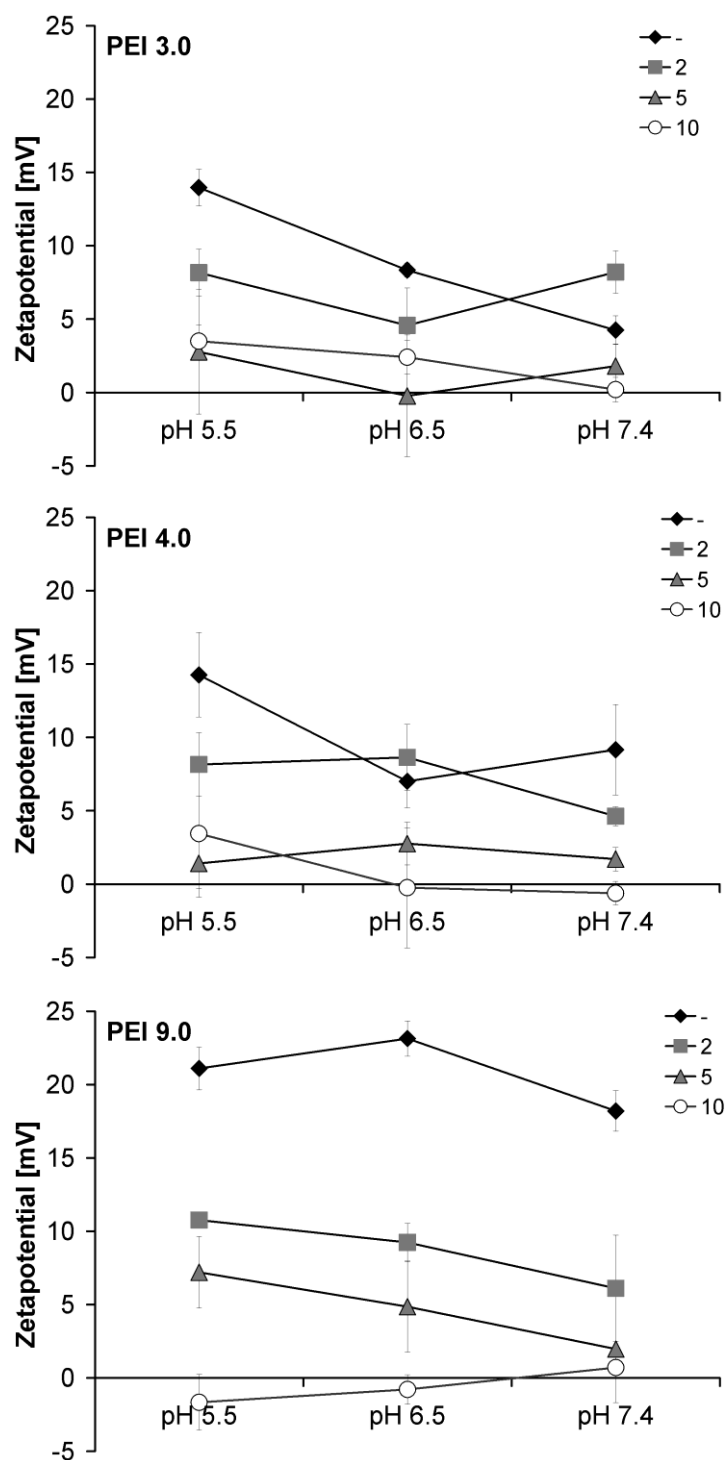
159

Fig. 8. *The zeta potential of polyplexes assembled of plasmid DNA and PEG-S-PEI copolymers*

or PEI homopolymers at a N/P ratio of 6. The measurements were performed in Tris buffer at pH

5.5, 6.5 and 7.4, respectively. The MW of PEI was 3.0, 4.0 and 9.0 kDa, and the MW of PEG

[kDa] is given in the legend.

potential of the polyplexes. Though, as expected, the zeta potential of PEI-polyplexes tended to be slightly higher than for PEG-PEI-polyplexes at pH 5.5. This result was supported by an erythrocyte leakage assay (Supporting Information, Figure S12).

The toxicity of the pure polymers was tested using the MTT assay. The IC_{50} values depended both on the MW of PEI and PEG. As expected, the IC_{50} values increased with decreasing MW of PEI and increasing MW of PEG (Figure 9). It was also remarkable that there was not a significant difference between pure PEIs and PEG(2)-PEI copolymers. Additionally, the viability of cells after treatment with polyplexes was evaluated using a propidium iodide staining. The results demonstrate that the polyplexes were not toxic to cells at the applied concentration (Supporting Information, Figure S13).
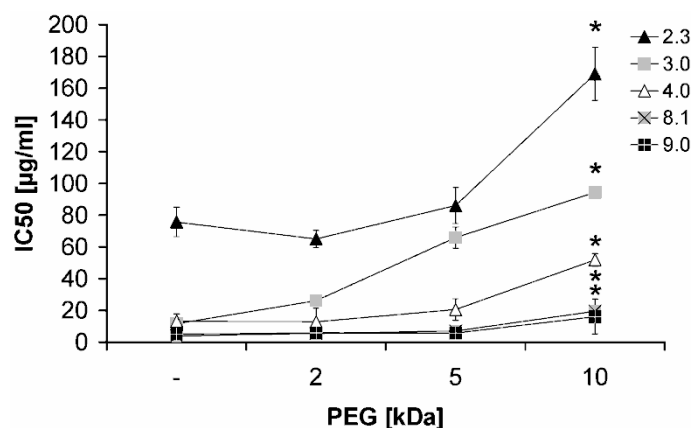

Fig. 9. IC_{50} value of PEG-PEI copolymers and PEI homopolymers as evaluated by the MTT assay. As an example, the IC_{50} values of a set of 5 PEI derivatives and the corresponding copolymers is shown. The MW of PEG [kDa] is indicated on the x-axis ("-" indicates the homopolymer), while the MW of PEI [kDa] is given in the legend. The IC_{50} values of PEG(10)-PEI polyplexes were significantly different from other PEI- and PEG-PEI polyplexes, which is indicated by * (p < 0.05).

Finally, as already highlighted, the library of PEG-S-PEI copolymers was perfectly suited to draw correlations between the copolymer composition and the physicochemical and biological activity of the polyplexes. Therefore, the PEG content of PEG-S-PEI copolymers was plotted against the hydrodynamic diameter of the polyplexes, their zeta potential and their transfection ability (Figure 10). A PEG content higher than 50% led to small polyplexes (Figure 10A) with a zeta potential lower than 5 mV (Figure 10B). Despite the low zeta potential, these polyplexes were taken up by cells, but completely lost their transfection efficacy (Figure 10C). Copolymers with a lower PEG content were regarded as less suitable for a potential clinical application because the polyplexes were large, had a positive zeta potential and formed aggregates. However, those polymers may be less hampered concerning the endosomal escape, thereby reaching higher transfection rates.
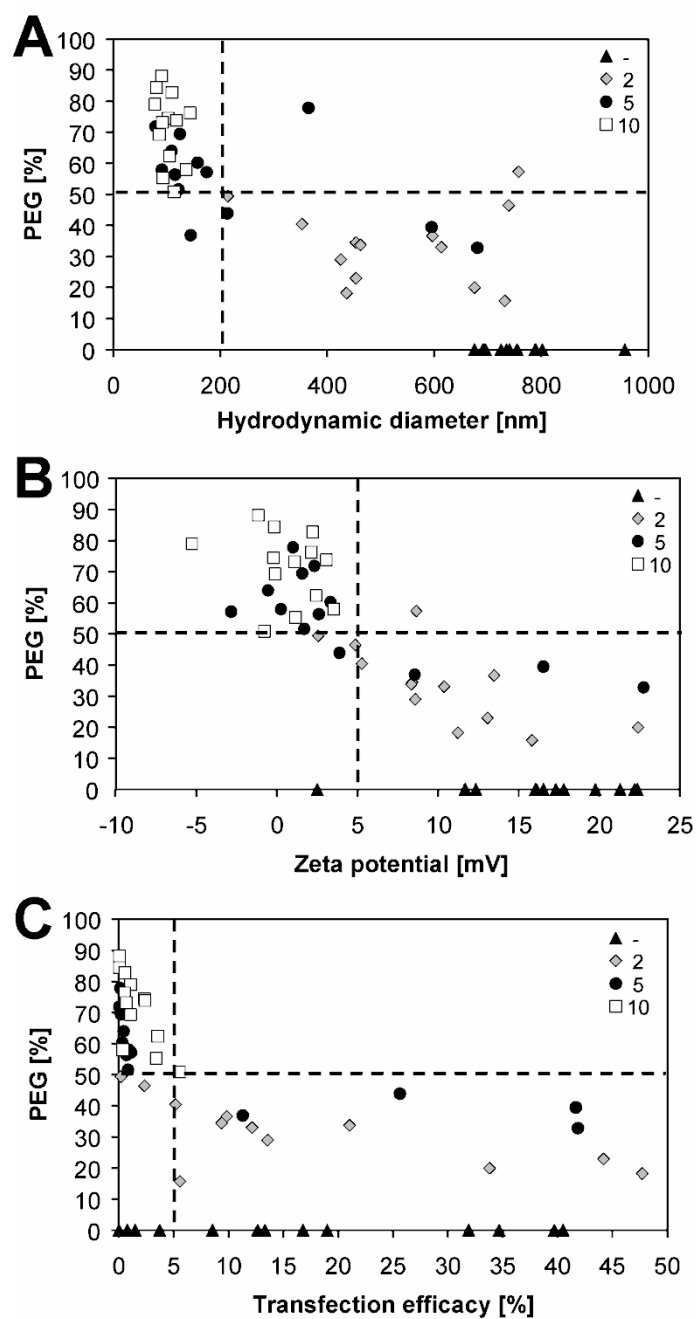
Fig. 10. *Correlation of the PEG content [%] of the polymers with the hydrodynamic diameter of the polyplexes (A), their zeta potential (B) as well as their transfection efficacy (C). The MW of PEG is given in the figure legend. For better clarity the standard deviations are omitted.*

Discussion

A new route for the synthesis of a library of well defined, linear PEG-PEI diblock copolymers forming polyplexes with plasmid DNA was successfully developed. These copolymers were prepared with the goal to elucidate the relationship between the polymer composition and the physicochemical properties as well as the biological activity of the polyplexes. To the best of our knowledge, such an extensive library of PEG-PEI copolymers with the approach to vary the MW of PEG and PEI has never been conducted before. The presented synthesis strategy was more time-consuming than other approaches leading to graft or statistical PEG-PEI copolymers [12,16,22], but the advantages outbalanced the alternative laborious procedure by far. First, a multiple addition of PEG to PEI was not possible. Consequently, the synthesis exclusively resulted in linear diblock copolymers. In order to determine how the polymer structure is related to the polyplex properties, it is necessary to produce such exactly defined PEG-PEI copolymers and not product mixtures. Second, in the presented linear diblock PEG-PEI copolymers the PEG moiety is clearly separated from the PEI moiety. PEG is supposed to act as a shell forming, hydrophilic block, counteracting aggregation and maintaining the stability of the polyplexes, and the cationic PEI block is intended for interaction with the nucleic acid, thereby building the core of the polyplex. In contrast, PEG-PEI copolymers of other topologies bear no segregated hydrophilic and cationic domains, and hence the PEG moiety may provide for steric hindrance to the polyelectrolyte interaction [11]. Although branched PEI derivatives seem to have stronger condensation capacity of the nucleic acids [5,28,29], which may guarantee for a favorable cellular uptake and transfection efficacy [29], linear PEI was applied as cationic block for the copolymer synthesis. One big advantage of linear PEI is its more defined structure compared to branched PEI. Additionally, linear PEI seems to support the intracellular disintegration of polyplexes, which is very beneficial for the subsequent release of the nucleic acid and a high gene expression [29,30]. Moreover, we used linear PEI of low MW because it is not toxic to cells at the applied concentrations and N/P ratio [8].

The physicochemical properties of polyplexes strongly determine their interaction with the biological system. Hence, the influence of PEG on these properties was of great interest. The size and zeta potential of the polyplexes strongly depended on the MW of PEG; they decreased with increasing PEG content in PEG-S-PEI copolymers. The shielding effect was particularly effective for PEG 10 kDa. PEG(10)-S-PEI copolymers produced polyplexes below 150 nm accompanied by a zeta potential close to zero, which is preferable for in vivo application [5,11,31]. In contrast, PEG with a MW of 2 kDa was most likely not properly oriented on the polyplex surface for a sufficient shielding, or long distance charge effects from the polyplex core were still dominating [32]. The zeta potentials of polyplexes that have been built with alternating PEG-PEI copolymers was not as efficiently reduced [14,16], and such a positive effect on the physicochemical properties of polyplexes has only been observed for triblock copolymers of PEG and PEI bearing an additional hydrophobic domain [33]. The favorable physicochemical properties of the presented PEG-PEI-polyplexes may indicate that the polyplex formation occurs in an oriented manner, with the PEG block squeezed away from the interaction between polymer and DNA [17,22,24]. An additional argument in favor of well-defined polyplexes was the quenching of the EtBr fluorescence, which was more efficient in copolymer- compared to homopolymer-polyplexes. This phenomenon was also observed for other types of copolymers with PEG presented in a diblock like fashion [34]. The assumption that the polyplexes may be formed in an oriented manner was also supported by the high stability of PEG(5)-S-PEI and PEG(10)-S-PEI copolymer polyplexes in cell culture medium as well as in the heparin exclusion assay. Only a hydrophilic PEG layer pointing towards the outer regions of the polyplex may guarantee for stability in cell culture medium over such a long time period or against extracellular matrix components, respectively. In this environment, PEG chains of 5 and 10 kDa may take an extended conformation thereby enabling stealth properties [35]. In contrast, PEG with 2 kDa may have lost its flexibility or inefficiently cover the surface thereby reducing the polyplex stability. These findings have only been observed for grafted PEG-PEI copolymers if the grafting density

was close to 1, thereby yielding grafted copolymers with diblock copolymer-like character [17,22] or a diblock PEG-PEI copolymer built with branched PEI [13]. The latter has unfortunately not been tested in cell culture. However, it should be noted that these experiments give merely a hint towards controlled formation of the polyplexes, but no direct evidence.

While there is a consensus about the intended influence of PEG on the physicochemical properties of the polyplexes, the biological activity of the polyplexes is still under debate [11]. To list some examples: a higher or similar transfection efficacy compared to the homopolymer was reported for grafted [17,22] or alternating [14,16] PEG-PEI copolymers, while a lower transfection ability was achieved in other studies with grafted PEG-PEI copolymers [20,21]. However, as these examples differ in the MW of PEG, the overall PEG content, the topology of the copolymer and the N/P ratio of the polyplexes and in the cell line used for transfection studies, it is hard to make comparisons between them. In the case of strictly linear PEG-S-PEI copolymer, the transfection rate of the polyplexes significantly decreased with increasing PEG content in the copolymer. Different reasons may be taken into account for this phenomenon and are discussed next. A change in the transfection rate upon PEGylation of polyplexes either to higher or lower levels is generally associated with changes in the cellular uptake of the polyplexes [25,36] and/ or due to limited intracellular processing [25]. However, both possibilities have not been systematically investigated for PEG-PEI copolymers to date. Surprisingly, the amount of plasmid DNA taken up by cells was similar for the PEG-PEI- and PEI-polyplexes and not suppressed by PEGylation of the polyplexes. Confocal microscopy supported these results, but additionally gave a deeper insight into the cellular uptake of polyplexes. PEI-polyplexes that were detected inside cells, were large and formed agglomerates, which was expected from the measurements of the size and stability. With increasing MW of PEG in the copolymers, the polyplexes inside cells became smaller. These findings suggested that the PEG moiety is very beneficial for producing small, nearly neutral polyplexes that can potentially experience cellular uptake. The exact mechanism of polyplex uptake is unclear and requires further investigation. An alternative explanation for the

166

reduced transfection efficacy of PEG-PEI-polyplexes may be that PEG may prevent further intracellular processing, as for example the endosomal escape of the polyplexes [25]. An argument in favor of the limited endosomal escape capacity of PEGylated polyplexes was their reduced protonation capacity compared to PEI-polyplexes at slightly acidic pH, which can be found in endosomes. Besides the reduced endosomal escape, other intracellular events may reduce the transfection efficacy of PEG-S-PEI-polyplexes: their higher stability may prevent an efficient intracellular disassembly of polyplexes, consequently leading to a limited intracellular release of plasmid DNA. A reversible PEG shielding that can be triggered upon a physiological stimulus has been proposed to restore the reduced transfection rate [11,37,38]. To follow up this goal, we introduced a disulfide bond between the PEG and PEI domain in the copolymer with the intention of triggering the PEG release due to the redox potential gradient between the extra- and intracellular environments [37]. As soon as the PEG layer would be shed off, the polyplexes would regain their higher endosomolytic properties and exhibit lower stability. Indeed, the introduction of a disulfide bond between the PEG and PEI moiety restored the reduced transfection efficacy. These results provide evidence that an intracellular mechanism could be involved in the limited transfection efficacy of non-degradable PEG-S-PEI copolymers.

The investigations concerning the cytotoxicity completed the picture of PEG-PEI copolymers and supported the beneficial effect of the PEGylation on the properties of the polyplexes. As expected [18,21,22], PEGylation reduced the toxic effects of PEI. The longer the PEG chains was in the copolymers, the higher the IC_{50} values were. An exception was PEG 2 kDa, which was not sufficient to exert a positive effect on the cell viability compared to pure PEI.

Conclusion

We successfully synthesized a library of strictly linear PEG-S-PEI copolymers. The hypothesis was that these copolymers would allow for systematic study of the influence of the PEG moiety on the physicochemical properties and biological activity of polyplexes formed with plasmid DNA. Non-degradable PEG-S-PEI copolymers with a PEG content higher than 50% led to small, nearly neutral polyplexes, eventually taking a kind of core-shell structure. The transfection ability of these polyplexes was lost, but restored by the application of degradable PEG-SS-PEI copolymer counterparts. This suggests that the intracellular cleavage of the PEG domain from the polyplex surface is a necessary prerequisite for the transfection process. Concerning the MW of the PEI moiety, two findings were relevant: first, a MW lower than 3 kDa was less suited to form compact and stable polyplexes. Moreover, it was evident that the transfection ability of the polyplexes increased with the chain length of PEI, but in the same order the toxicity also increased. Those toxic effects were at least partially reduced by the incorporation of a high MW PEG domain into the copolymer. We proved our hypothesis that strictly linear PEG-PEI copolymers are perfectly suited for performing structure property relationship and additionally gave new insights for the optimization of gene delivery carriers.

.

References

[1]   D.W. Pack, A.S. Hoffman, S. Pun, P.S. Stayton, Design and development of polymers for gene delivery, *Nature Reviews Drug Discovery*, 4 (2005) 581-593.

[2]   M.A. Mintzer, E.E. Simanek, Nonviral vectors for gene delivery, *Chemical Reviews*, 109 (2008) 259-302.

[3]   O. Boussif, F. Lezoualc'h, M.A. Zanta, M.D. Mergny, D. Scherman, B. Demeneix, J. Behr, A versatile vector for gene and oligonucleotide transfer into cells in culture and in vivo: polyethylenimine, *Proceedings of the National Academy of Sciences of the United States of America*, 92 (1995) 7297-7301.

[4]   U. Lungwitz, M. Breunig, T. Blunk, A. Goepferich, Polyethylenimine-based non-viral gene delivery systems, *European Journal of Pharmaceutics and Biopharmaceutics*, 60 (2005) 247-266.

[5]   M. Neu, D. Fischer, T. Kissel, Recent advances in rational gene transfer vector design based on poly(ethylene imine) and its derivatives, *Journal of Gene Medicine,* 7 (2005) 992-1009.

[6]   W.T. Godbey, K.K. Wu, A.G. Mikos, Size matters: molecular weight affects the efficiency of poly(ethylenimine) as a gene delivery vehicle, *Journal of Biomedical Materials Research*, 45 (1999) 268-275.

[7]   W.T. Godbey, K.K. Wu, A.G. Mikos, Poly(ethylenimine) and its role in gene delivery, *Journal of Controlled Release*, 60 (2001) 149-160.

[8]   M. Breunig, U. Lungwitz, R. Liebl, C. Fontanari, J. Klar, A. Kurtz, T. Blunk, A. Goepferich, Gene delivery with low molecular weight linear polyethylenimines, *Journal of Gene Medicine*, 7 (2005) 1287-1298.

[9]   M. Breunig, U. Lungwitz, R. Liebl, A. Goepferich, Breaking up the correlation between efficacy and toxicity for nonviral gene delivery, . *Proceedings of the National Academy of Sciences of the United States of America*, 104 (2007) 14454-14459.

[10] M. Ogris, P. Steinlein, M. Kursa, K. Mechtler, R. Kircheis, E. Wagner, The size of DNA/transferrin-PEI complexes is an important factor for gene expression in cultured cells, *Gene Therapy*, 5 (1998) 1425-1433.

[11] Y. Vachutinsky, K. Kataoka, PEG-based polyplex design for gene and nucleotide delivery, *Israel Journal of Chemistry*, 50 (2010) 175-184.

[12] H. Petersen, P.M. Fechner, D. Fischer, T. Kissel, Synthesis, characterization, and biocompatibility of polyethylenimine-graft-poly(ethylene glycol) block copolymers, *Macromolecules*, 35 (2002) 6867-6874.

[13] H. Petersen, A.L. Martin, S. Stolnik, C.J. Roberts, M.C. Davies, T. Kissel, The macrostopper route: a new synthesis concept leading exclusively to diblock copolymers with enhanced DNA condensation potential, *Macromolecules*, 35 (2002) 9854-9856.

[14] M.R. Park, K.O. Han, I.K. Han, M.H. Cho, J.W. Nah, Y.J. Choi, C.S. Cho, Degradable polyethylenimine-alt-poly(ethylene glycol) copolymers as novel gene carriers, *Journal of Controlled Release*, 105 (2005) 367-380.

[15] H. Petersen, K. Kunath, A.L. Martin, S. Stolnik, C.J. Roberts, M.C. Davies, T. Kissel, star-shaped poly(ethylene glycol)-block-polyethylenimine copolymers enhance DNA condensation of low molecular weight polyethylenimines, *Biomacromolecules*, 3 (2002) 926-936.

[16] C.H. Ahn, S.Y. Chae, Y.H. Bae, S.W. Kim, Biodegradable poly(ethylenimine) for plasmid DNA delivery, *Journal of Controlled Release,* 80 (2002) 273-282.

[17] H. Petersen, P.M. Fechner, A.L. Martin, K. Kunath, S. Stolnik, C.J. Roberts, D. Fischer, M.C. Davies, T. Kissel, Polyethylenimine-graft-poly(ethylene glycol) copolymers: influence of copolymer block structure on DNA complexation and biological activities as gene delivery system, *Bioconjugate Chemistry*, 13 (2002) 845-854.

[18] M. Ogris, S. Brunner, S. Schuller, R. Kircheis, E. Wagner, PEGylated DNA/transferrin-PEI complexes: reduced interaction with blood components, extended circulation in blood and potential for systemic gene delivery, *Gene Therapy*, 6 (1999) 595-605.

[19] D. Edinger, E. Wagner, Bioresponsive polymers for the delivery of therapeutic nucleic acids, *Wiley Interdisciplinary Reviews: Nanomedicine and Nanobiotechnology*, 3 (2011) 33-46.

[20] H.K. Nguyen, P. Lemieux, S.V. Vinogradov, C.L. Gebhart, N. Guerin, G. Paradis, T.K. Bronich, V.Y. Alakhov, A.V. Kabanov, Evaluation of polyether-polyethylenimine graft copolymers as gene transfer agents, *Gene Therapy*, 7 (2000) 126-138.

[21] S.J. Sung, S.H. Min, K.Y. Cho, S. Lee, Y.J. Min, Y.I. Yeom, J.K. Park, Effect of polyethylene glycol on gene delivery of polyethylenimine, *Biological and Pharmaceutical Bulletin*, 26 (2003) 492-500.

[22] M. Neu, O. Germershaus, M. Behe, T. Kissel, Bioreversibly crosslinked polyplexes of polyethylenimine and high molecular weight polyethylene glycol show extended circulation times in vivo, *Journal of Controlled Release*, 124 (2007) 69-80.

[23] X. Zhang, S.R. Pan, H.M. Hu, G.F. Wu, M. Feng, W. Zhang, X. Luo, Poly(ethylene glycol)-block-polyethylenimine copolymers as carriers for gene delivery: effects of PEG molecular weight and PEGylation degree, *Journal of Biomedical Materials Research*, 84A (2008) 795-804.

[24] V. Toncheva, M.A. Wolfert, P.R. Dash, D. Oupicky, K. Ulbrich, L.W. Seymour, E.H. Schacht, Novel vectors for gene delivery formed by self-assembly of DNA with poly(l-lysine) grafted with hydrophilic polymers, *Biochimica et Biophysica Acta*, 1380 (1998) 354-368.

[25] E. Salcher, E. Wagner, Chemically Programmed Polymers for Targeted DNA and siRNA Transfection, in: W. Bielke and C. Erbacher (Eds.), Nucleic Acid Transfection*,* Springer Berlin / Heidelberg, 2010, pp. 227-249.

[26] T. Mosmann, Rapid colorimetric assay for cellular growth and survival: application to proliferation and cytotoxicity assays, *Journal of Immunological Methods*, 65 (1983) 55-63.

[27] L. Huang, Y. Liu, In vivo delivery of RNAi with lipid-based nanoparticles, *Annual Reviews of Biomedical Engineering*, 13 (2011) 507-530.

[28] D.D. Dunlap, A. Maggi, M.R. Soria, L. Monaco, Nanoscopic structure of DNA condensed for gene delivery, Nucleic Acids Res., 25 (1997) 3095-3101.

[29] Z. Dai, T. Gjetting, M.A. Mattebjerg, C. Wu, T.L. Andresen, Elucidating the interplay between DNA-condensing and free polycations in gene transfection through a mechanistic study of linear and branched PEI, *Biomaterials*, 32 (2011) 8626-8634.

[30] L. Wightman, R. Kircheis, V. Rossler, S. Carotta, R. Ruzicka, M. Kursa, E. Wagner, Different behavior of branched and linear polyethylenimine for gene delivery in vitro and in vivo, *Journal of Gene Medicine*, 3 (2001) 362-372.

[31] E.V.B. van Gaal, R. van Eijk, R.S. Oosting, R.J. Kok, W.E. Hennink, D.J.A. Crommelin, E. Mastrobattista, How to screen non-viral gene delivery systems in vitro?, *Journal of Controlled Release*, 154 (2011) 218-232.

[32] M.A. Wolfert, E.H. Schacht, V. Toncheva, K. Ulbrich, O. Nazarova, L.W. Seymour, Characterization of vectors for gene therapy formed by self-assembly of DNA with synthetic block co-polymers, *Human Gene Therapy*, 7 (1996) 2123-2133.

[33] D. Velluto, S.N. Thomas, E. Simeoni, M.A. Swartz, J.A. Hubbell, PEG-b-PPS-b-PEI micelles and PEG-b-PPS/PEG-b-PPS-b-PEI mixed micelles as non-viral vectors for plasmid DNA: Tumor immunotoxicity in B16F10 melanoma, *Biomaterials*, 32 (2011) 9839-9847.

[34] S. Venkataraman, W.L. Ong, Z.Y. Ong, S.C. Joachim Loo, P.L. Rachel Ee, Y.Y. Yang, The role of PEG architecture and molecular weight in the gene transfection performance of PEGylated poly(dimethylaminoethyl methacrylate) based cationic-polymers, *Biomaterials*, 32 (2011) 2369-2378.

[35] D.E. Owens III, N.A. Peppas, Opsonization, biodistribution, and pharmacokinetics of polymeric nanoparticles, *International Journal of Pharmaceutics*, 307 (2006) 93-102.

[36] S. Mishra, P. Webster, M.E. Davis, PEGylation significantly affects cellular uptake and intracellular trafficking of non-viral gene delivery particles, *European Journal of Cell Biology*, 83 (2004) 97-111.

[37] S. Bauhuber, C. Hozsa, M. Breunig, A. Goepferich, Delivery of nucleic acids via disulfide-based carrier systems, *Advanced Materials*, 21 (2009) 3286-3306.

[38] W. Sun, P.B. Davis, Reducible DNA nanoparticles enhance in vitro gene transfer via an extracellular mechanism, *Journal of Controlled Release*, 146 (2010) 118-127.

Supporting Information

Determination of the MW of the polymers

The polymerization of 2-ethyl-2-oxazoline proceeds according to a living process, and all polymer chains have tosylate counterions at the end. Consequently, the average molecular weight (MW) of poly(2-ethyl-2-oxazoline) (pEtOXZ) was estimated by the ratio of the aromatic protons of the tosylate starter to the protons of the PEtOXZ backbone peaks (Figure S1) [1]. In detail, the aromatic protons **d** and **e** were each set to 2, while the methylene groups (**a**) and the propionyl side chain protons (**b** and **c**) and accounted for 4, 2 and 3 protons, respectively. This procedure allowed for the calculation of the amount of monomer units per molecule and finally for the estimation of the polymer MW. The theoretical and calculated MW of the polymers is given in Table S1.
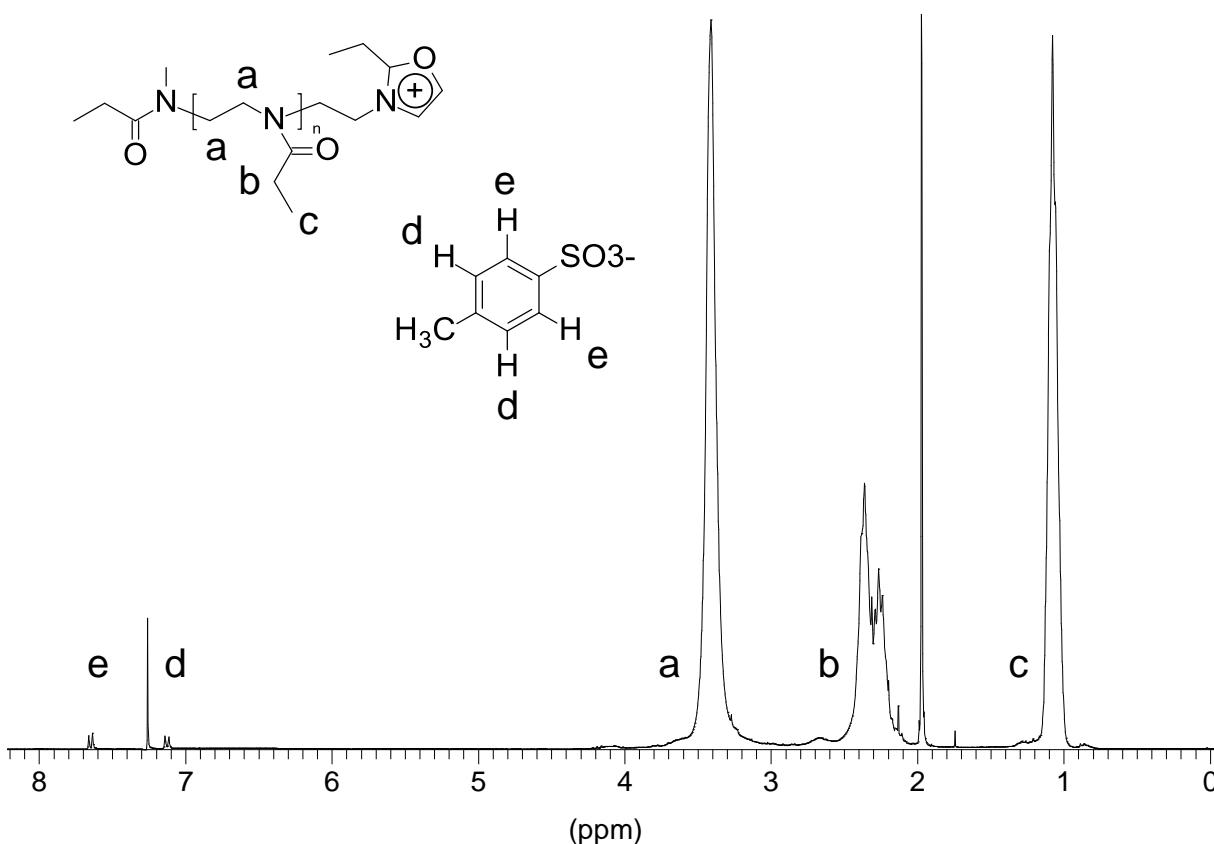

Fig. S1. Example of a ^{1}H-NMR spectrum of pEtOXZ recorded in CDCl$_3$.

Tab. S1. *The theoretical and calculated MW of the polymers.*

| Polymer		MW pEtOXZ theory [g/mol]	MW pEtOXZ calculated [g/mol]	MW PEI theory [g/mol]	MW PEI calculated [g/mol]	designated
PEI	1	3456	3456	1501	1501	PEI 1.5
PEI	2	4606	4752	2001	2064	PEI 2.1
PEI	3	5648	5346	2453	2322	PEI 2.3
PEI	4	6860	6831	2980	2967	PEI 3.0
PEI	5	7938	8019	3448	3483	PEI 3.5
PEI	6	8415	8811	3655	3827	PEI 3.8
PEI	7	9114	9108	3959	3956	PEI 4.0
PEI	8	10256	9405	4455	4085	PEI 4.1
PEI	9	11389	11385	4947	4945	PEI 4.9
PEI	10	13622	15518	5917	6740	PEI 6.7
PEI	11	19372	18612	8414	8084	PEI 8.1
PEI	12	21285	20790	9245	9030	PEI 9.0
PEI	13	22790	24849	9899	10793	PEI 10.8

^{1}H-NMR of poly(2-ethyl-2-oxazoline)-thioacetate (pEtOXZ-SAc)
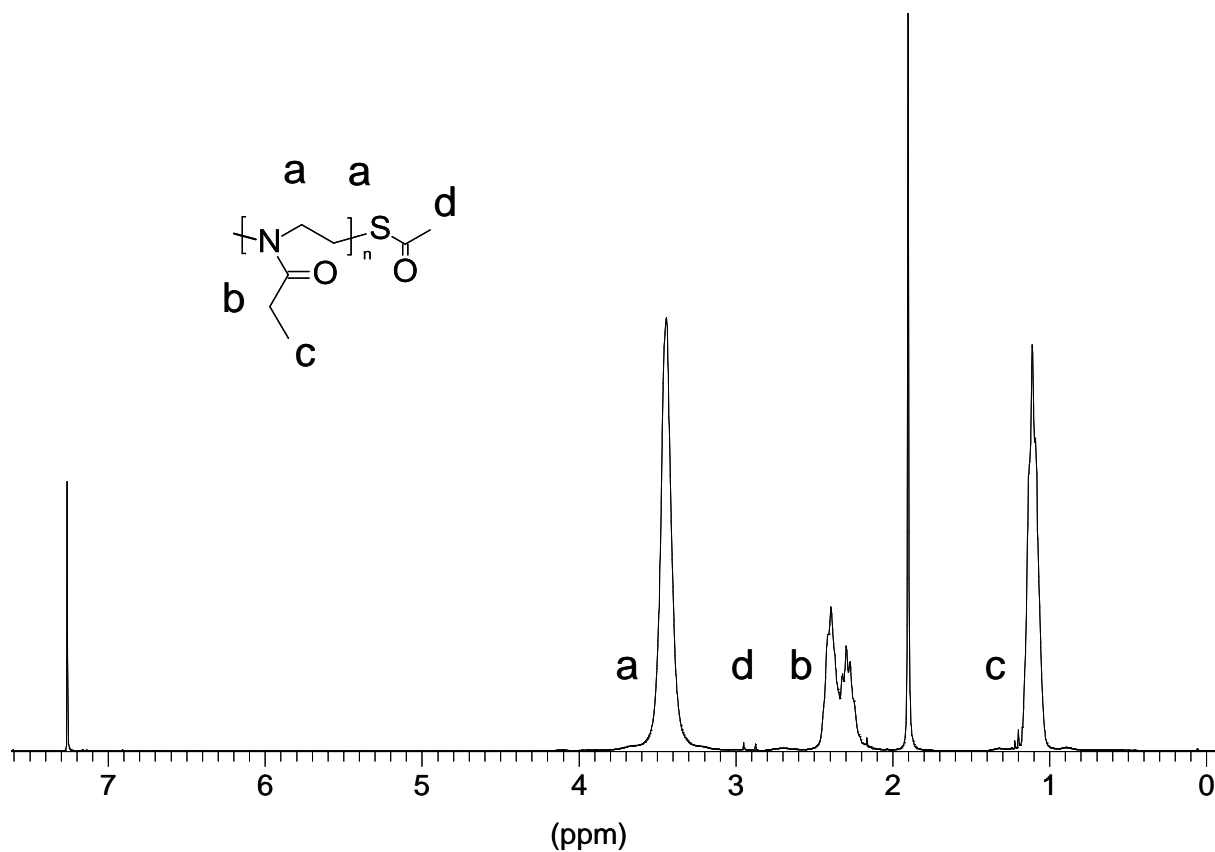
Fig. S2. Example of a ^{1}H-NMR spectrum of pEtOXZ-SAc recorded in CDCl₃.
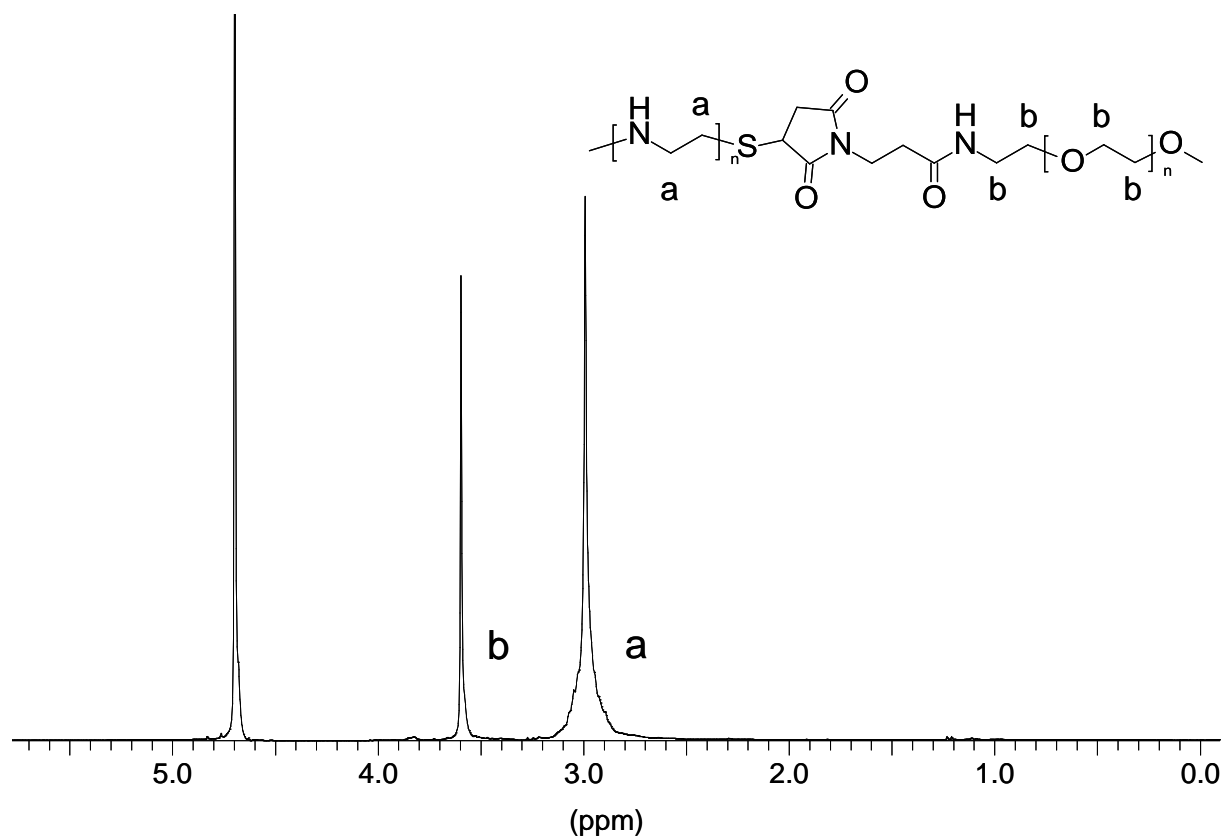
^{1}H-NMR of the PEG-S-PEI copolymer

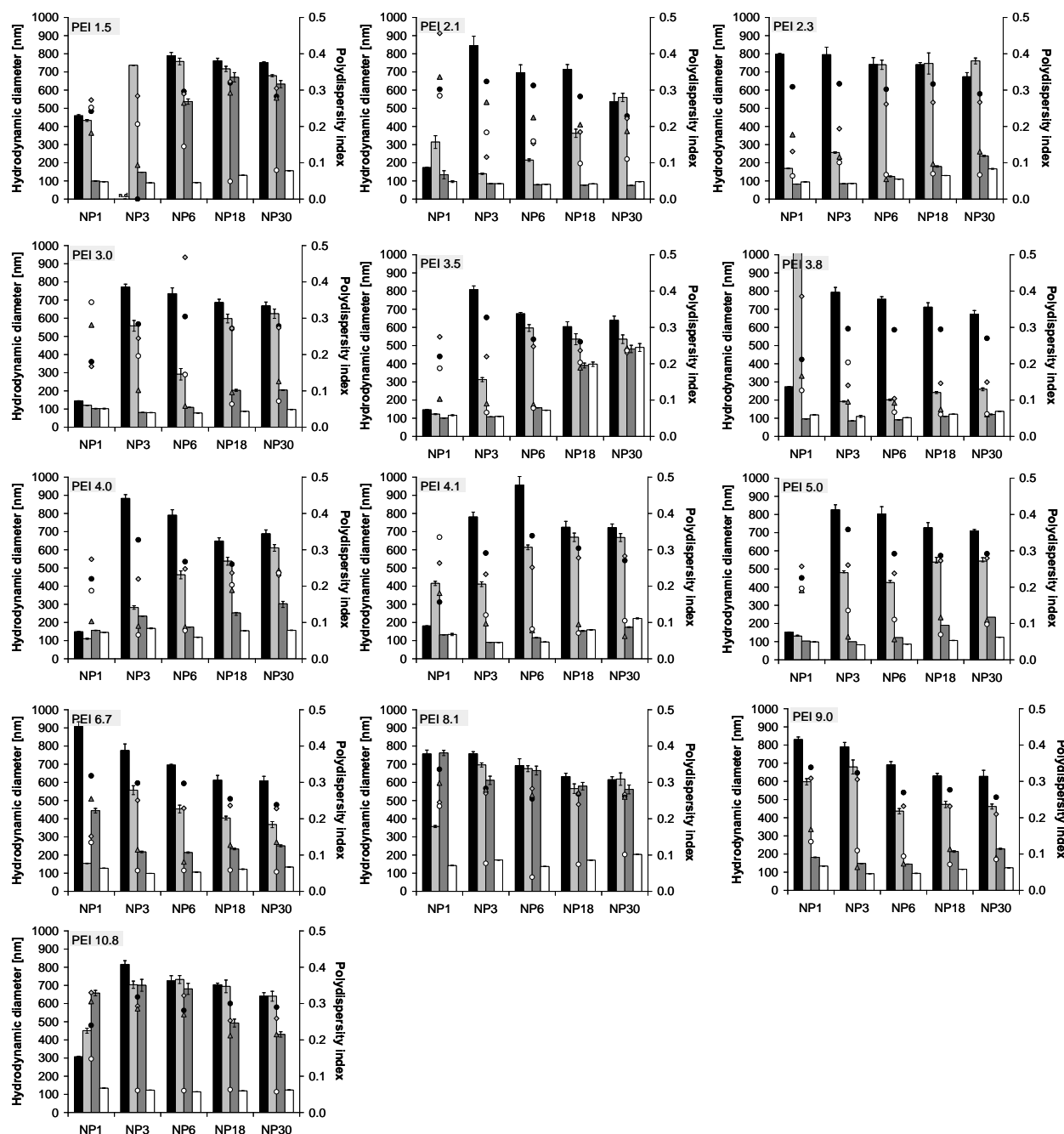*Fig. S3.* Example of a ^{1}H-NMR spectrum of PEG-S-PEI recorded in D_2O.

Fig. S4. *Hydrodynamic diameter of polyplexes assembled of plasmid DNA and PEI (■) or the corresponding PEG(2)-S-PEI (▨), PEG(5)-S-PEI (▨) and PEG(10)-S-PEI (□) copolymers. The MW of PEI is indicated in each graph. The polyplexes were built at various N/P ratios in 150 mM NaCl and measurements were performed by dynamic light scattering. Values are expressed as mean ± standard deviation (SD) of three measurements of one sample.*
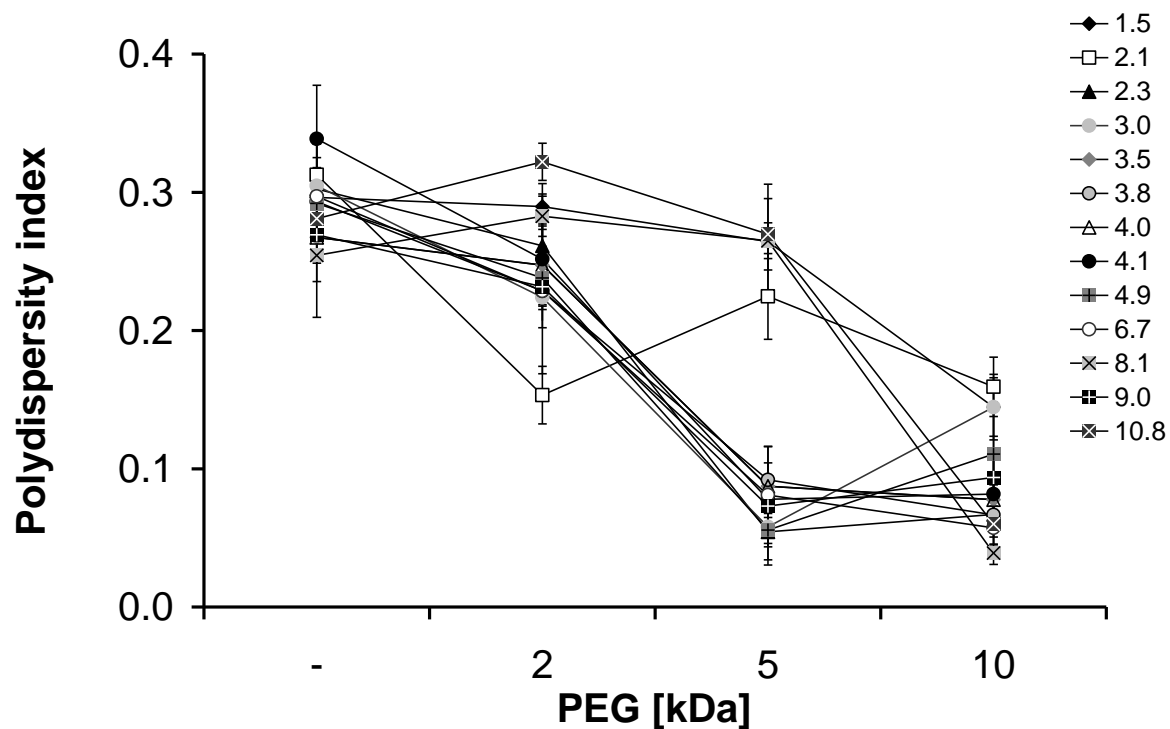
Fig. S5. *Polydispersity indices of polyplexes assembled of plasmid DNA and PEG-S-PEI*

copolymers or PEI homopolymers at a N/P ratio of 6 in 150 mM NaCl as determined by dynamic

light scattering. The MW of PEG [kDa] is presented on the x-axis ("-" indicates the

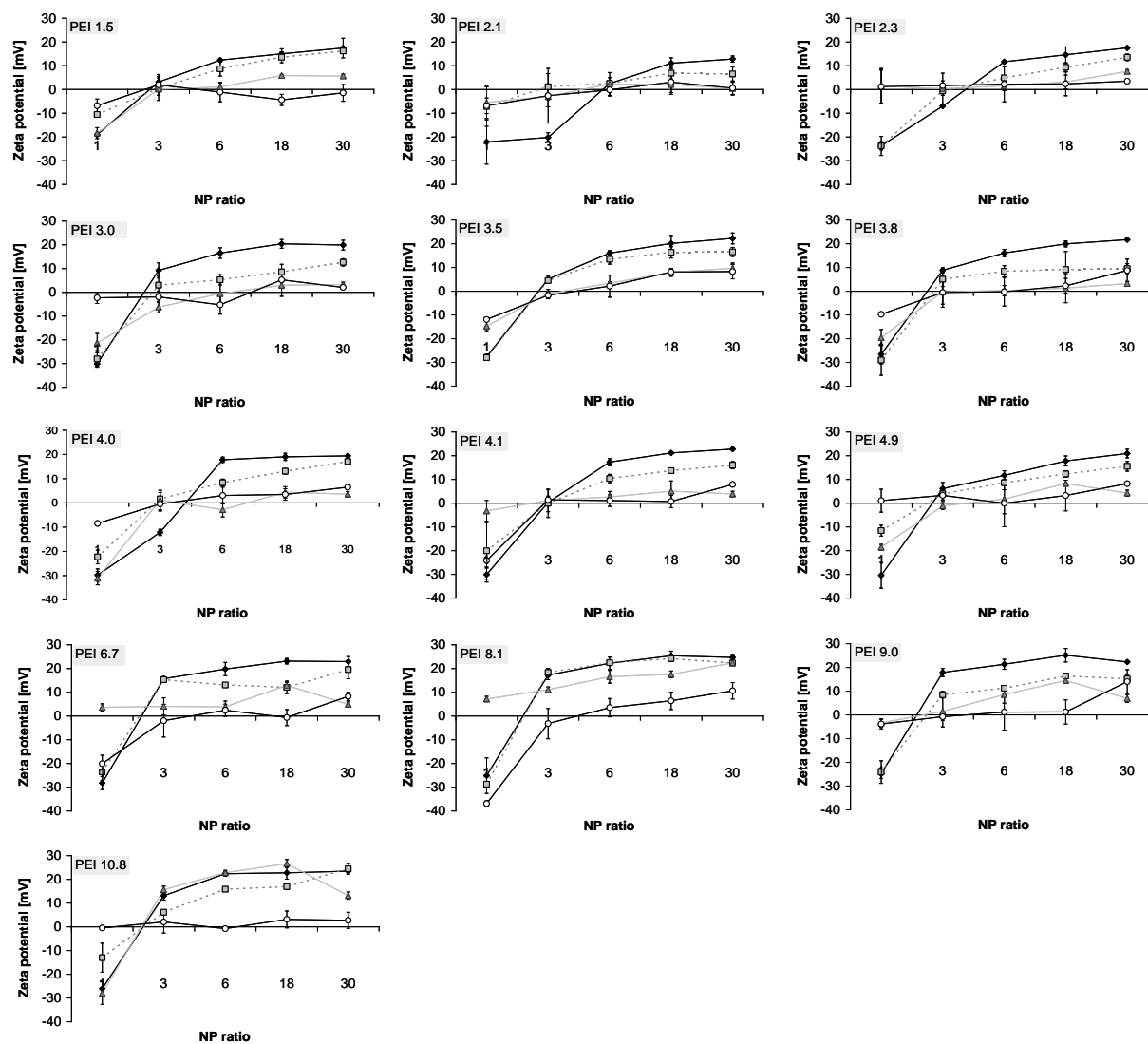*homopolymer), while the MW of PEI [kDa] is given in the legend.*

Fig. S6. *Zeta potential of polyplexes assembled of plasmid DNA and PEI (⬥——) or the corresponding PEG(2)-S-PEI (▫), PEG(5)-S-PEI (▲) and PEG(10)-S-PEI (○——) copolymers. The MW of PEI is indicated in each graph.*

PEI \ PEG	-	2	5	10
1.5				
2.1				+
2.3			+	+
3.0			+	+
3.5			+	+
3.8		+	+	+
4.0			+	+
4.1			+	+
4.9			+	+
6.7			+	+
8.1				+
9.0			+	+
10.8				+

Tab. S2. *Colloidal stability of polyplexes built with PEI derivatives of a MW ranging from 1.5 to 10.8 kDa and the corresponding PEG(2)-PEI, PEG(5)-PEI and PEG(10)-PEI copolymers after dilution in culture medium. Polyplexes that remained stable after dilution in cell culture medium are denoted by "+". They only slightly increased in the hydrodynamic diameter (less than 1.5 fold, data not shown). All other polyplexes rapidly aggregated and sedimented after dilution in culture medium, hence a measurement of the hydrodynamic diameter by dynamic light scattering was not possible.*
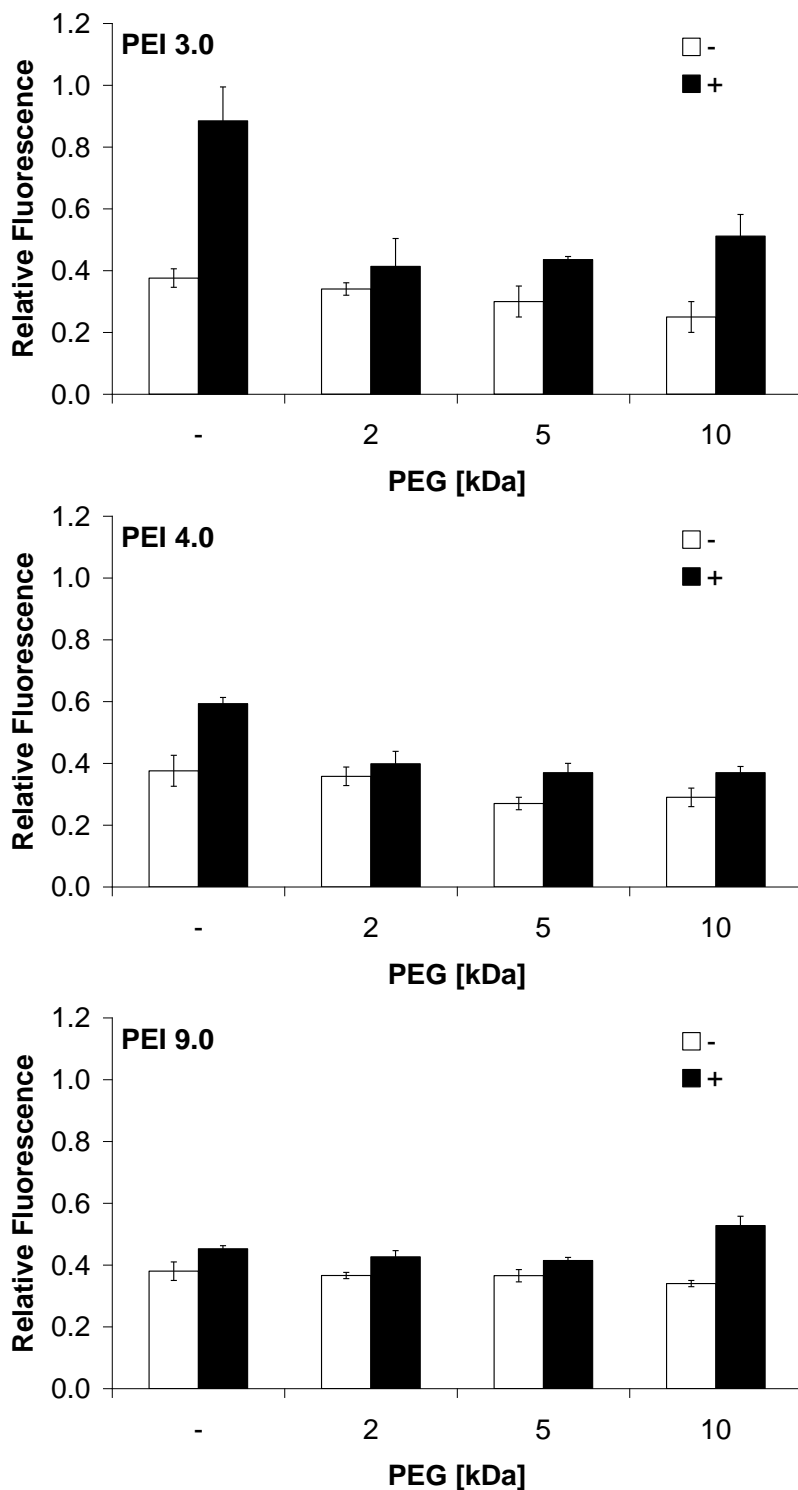
Heparin exclusion assay

Fig. S7. *The stability of the polyplexes was also examined by an heparin exclusion assay. To*

this end, polyplexes containing 2 µg plasmid DNA were prepared at N/P 6 in a final volume of 90

µl (n=3). Polyplexes were prepared with PEI(3.0), PEI(4.0) and PEI(9.0) and the corresponding copolymers. Subsequently, the polyplexes were incubated with 20 IU heparin (10µl) for 10 min at rt (■) and compared to polyplexes without heparin treatment (□). Then 2.5 µl of a 0.1 µg/µl ethidium bromide (EtBr) solution was added, and the plasmid DNA release was analyzed measuring the fluorescence of EtBr (excitation 518 nm, emission 605 nm, LS 55 fluorescence spectrometer (Perkin Elmer, Germany)). The fluorescence of plasmid DNA was related to the fluorescence of uncomplexed plasmid DNA and expressed as "relative fluorescence".

The release of plasmid DNA from polyplexes built with PEG-PEI(3.0) and PEG-PEI(4.0)-copolymers was much lower than from the corresponding homopolymer-polyplexes indicating a stabilizing effect of PEG on the polyplexes. PEI(9.0) allowed for a much lower release of plasmid DNA than the PEI derivatives of lower MW after heparin treatment. Consequently, the plasmid DNA release from PEG-PEI(9.0)-polyplexes was in a similar range as from the homopolymer-polyplexes indicating a similar stability against the extracellular matrix component heparin.

Estimation of the PEG conformation and stability of polyplexes

If PEG moieties are attached to a surface, they can take either the so-called brush or mushroom conformation [2]. In the mushroom conformation, the chains have a low packing density and are randomly oriented. Polyplexes bearing PEG chains in the mushroom conformation are most likely insufficiently protected and unstable. In the brush conformation, the PEG chains maintain a higher packing density and are more extended. Consequently, the polyplexes are most likely stable.

The conformation of PEG can be estimated as follows [2,3]: The number of PEG molecules on the surface of a polyplex allows for the determination of the packing density Γ and hence, the distance d_p between two PEG chains on the polyplex surface. Furthermore, the radius of the random coil form of PEG in solution is expressed by the Flory radius $R_F = aN^{3/5}$ (a: monomer size; N: degree of polymerization). The comparison of d_p and R_F allows for the determination of the conformation that PEG takes on the polyplex surface. If $d_p > 2\ R_F$, PEG takes the mushroom conformation. If the PEG chains form the brush conformation, then d_p is smaller than R_F.

For the calculation, the following assumptions were made: Complete charge neutralization of polyplexes is realized at N/P ~ 2.5 and according to [4] one polyplex contains about 3.5 plasmid DNA molecules. Furthermore, we assumed that PEI and plasmid DNA are located in the polyplex core with PEG forming a corona. The diameter of the polyplex core was calculated from the hydrodynamic diameter of the polyplexes at N/P 2.5 as measured by dynamic light scattering minus two times the Flory radius R_F of PEG. The PEG grafting density Γ arises from the number of PEG molecules per surface area and was calculated with $d_p = \Gamma^{-0.5}$.

Tab. S3. *Estimation of the distance of PEG chains on the polyplex surface at N/P 2.5. If $d_p > 2$ R_F, PEG should take the mushroom conformation, consequently producing unstable polyplexes.*

These polyplexes are indicated by the yellow color. These theoretical considerations and calculations are in quite good agreement with polyplex stability data.

PEG 10kDa, R_F = 9.08 nm

PEI [kDa]	PEG-PEI molecules/ polyplex	diameter polyplex [nm]	diameter polyplex core [nm]	surface polyplex core [nm^2]	PEG grafting density Γ	distance polymer chains d_p [nm]
1.5	2223	89	71	15764	0.1410	2.6
2.1	1588	84	66	13685	0.1160	2.9
2.3	1450	85	67	14180	0.1022	3.0
3.0	1112	80	62	11876	0.0936	3.2
3.5	953	109	91	26123	0.0365	5.1
3.8	878	110	91	26218	0.0335	5.3
4.0	834	167	149	69627	0.0120	8.9
4.1	813	89	71	15956	0.0510	4.3
4.9	681	82	64	12999	0.0524	4.2
6.7	498	99	80	20296	0.0245	6.2
8.1	412	172	154	74575	0.0055	13.1
9.0	371	91	73	16753	0.0221	6.5
10.8	309	123	105	34494	0.0090	10.3

PEG 5kDa, RF = 5.99 nm

PEI [kDa]	PEG-PEI molecules/ polyplex	diameter polyplex [nm]	diameter polyplex core [nm]	surface polyplex core [nm^2]	PEG grafting density Γ	distance polymer chains d_p [nm]
1.5	2223	148	136	57925	0.0384	5.0
2.1	1588	85	73	16564	0.0959	3.1
2.3	1450	84	72	16296	0.0890	3.3
3.0	1112	81	69	14773	0.0752	3.5
3.5	953	107	95	28590	0.0333	5.3
3.8	878	85	73	16712	0.0525	4.2
4.0	834	235	223	155526	0.0054	13.3
4.1	813	90	78	19232	0.0423	4.7
4.9	681	99	87	23764	0.0286	5.7
6.7	498	217	205	132072	0.0038	15.8
8.1	412	611	599	1127970	0.0004	50.8
9.0	371	148	136	57783	0.0064	12.1
10.8	309	700	688	1488121	0.0002	67.4

PEG 2kDa, RF = 3.34 nm

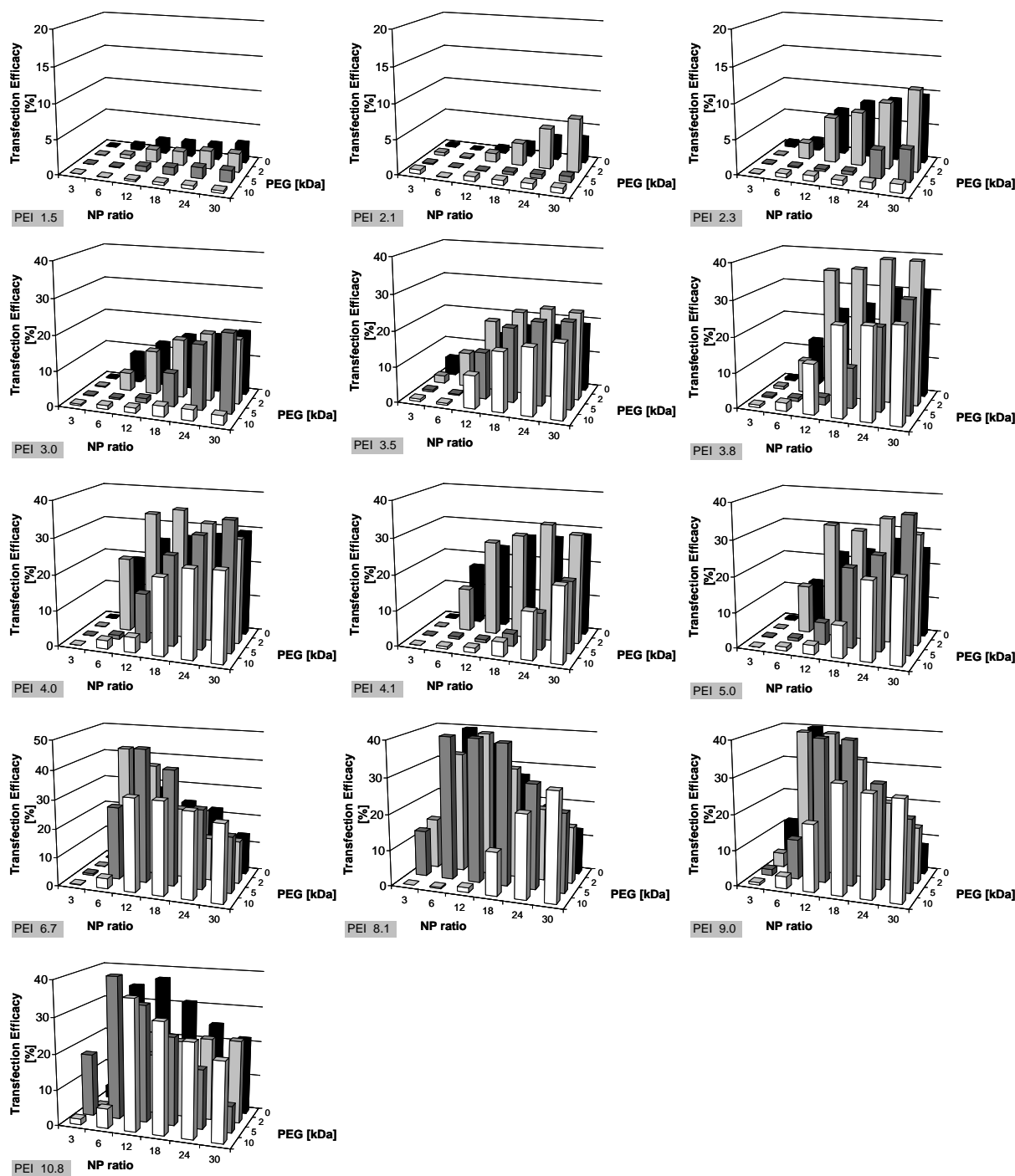| PEI [kDa]	PEG-PEI molecules/ polyplex	diameter polyplex [nm]	diameter polyplex core [nm]	surface polyplex core [nm^2]	PEG grafting density Γ	distance polymer chains d_p [nm]
1.5	2223	737	730	1673095	0.0013	26.6
2.1	1588	139	132	55033	0.0289	5.7
2.3	1450	256	249	195028	0.0074	11.3
3.0	1112	558	551	952917	0.0012	28.4
3.5	953	312	306	293097	0.0033	17.0
3.8	878	192	185	107336	0.0082	10.7
4.0	834	282	275	237901	0.0035	16.4
4.1	813	411	404	511452	0.0016	24.3
4.9	681	480	473	701581	0.0010	31.2
6.7	498	557	550	950382	0.0005	42.4
8.1	412	696	689	1491146	0.0003	58.4
9.0	371	679	672	1419187	0.0003	60.1
10.8	309	704	697	1524072	0.0002	68.2

Fig. S8. *Transfection efficacy of polyplexes at various N/P ratios with PEI (☐) and the corresponding PEG(2)-S-PEI (▨), PEG(5)-S-PEI (☐) and PEG(10)-S-PEI (■) copolymers in CHO-K1 cells. The MW of PEI is indicated in each graph. The number of EGFP positive cells was determined by flow cytometry.*
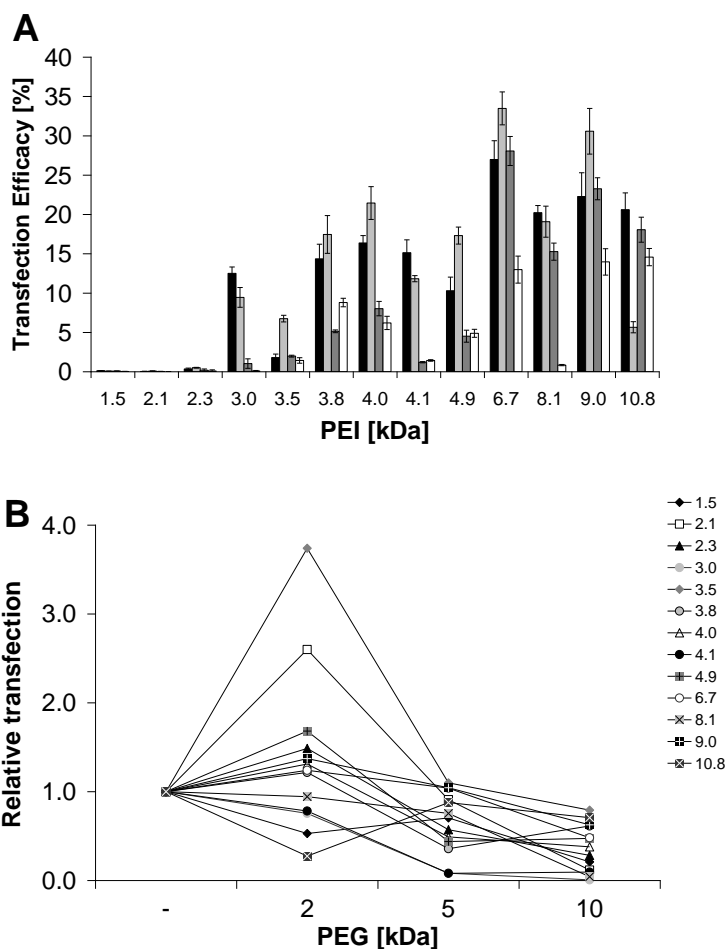
Fig. S9. *Transfection efficacy of polyplexes at a N/P ratio of 6 built with PEI (■) and the corresponding PEG(2)-S-PEI (▨), PEG(5)-S-PEI (▨) and PEG(10)-S-PEI (□) copolymers (A) measured in HeLa cells. The MW of PEI [kDa] is indicated on the x-axis. Additionally, the values of the transfection efficacy of the PEG-PEI-polyplexes were related to the corresponding PEI-polyplexes and expressed as relative transfection (B). Here, the MW of PEG [kDa] is shown on the x-axis ("-" indicates the homopolymer), while the MW of PEI [kDa] is given in the legend.*
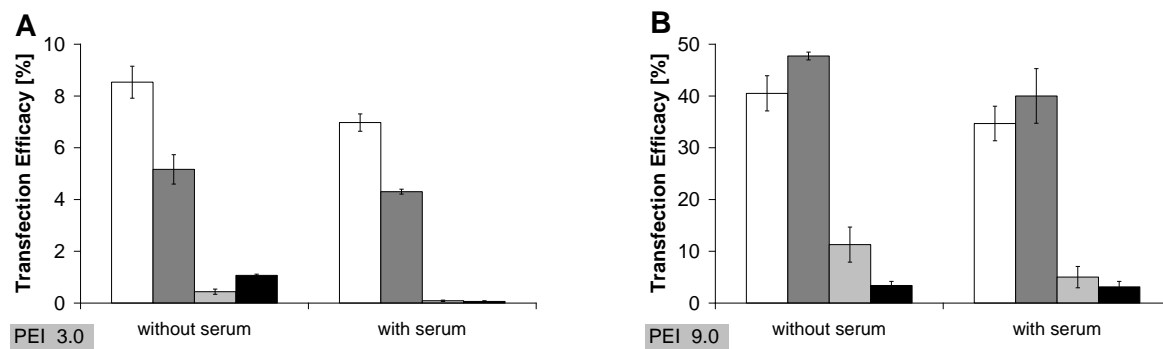
Fig. S10. *Transfection efficacy of polyplexes in serum-free versus serum-containing culture conditions at a N/P ratio of 6 built with PEI (▢) and the corresponding PEG(2)-S-PEI (▨), PEG(5)-S-PEI (▢) and PEG(10)-S-PEI (■) copolymers (A) measured in CHO-K1 cells. The MW of PEI was (A) 3.0 and (B) 9.0 kDa.*
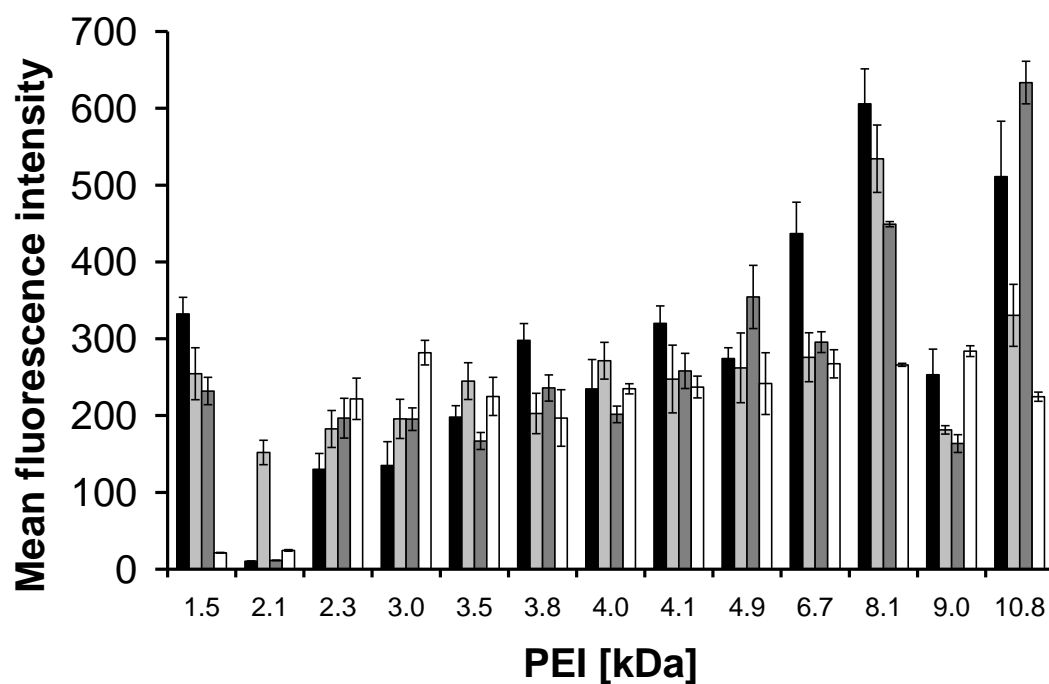
Fig. S11: *The cellular uptake of fluorescently-labeled polyplexes built with PEI (■) and the corresponding PEG(2)-S-PEI (▢), PEG(5)-S-PEI (▨) and PEG(10)-S-PEI (▢) copolymers into CHO-K1 cells was measured by flow cytometry. The mean fluorescence intensity is an indirect measure of the cellular uptake of the polyplexes. The MW of PEI [kDa] is indicated on the x-axis.*
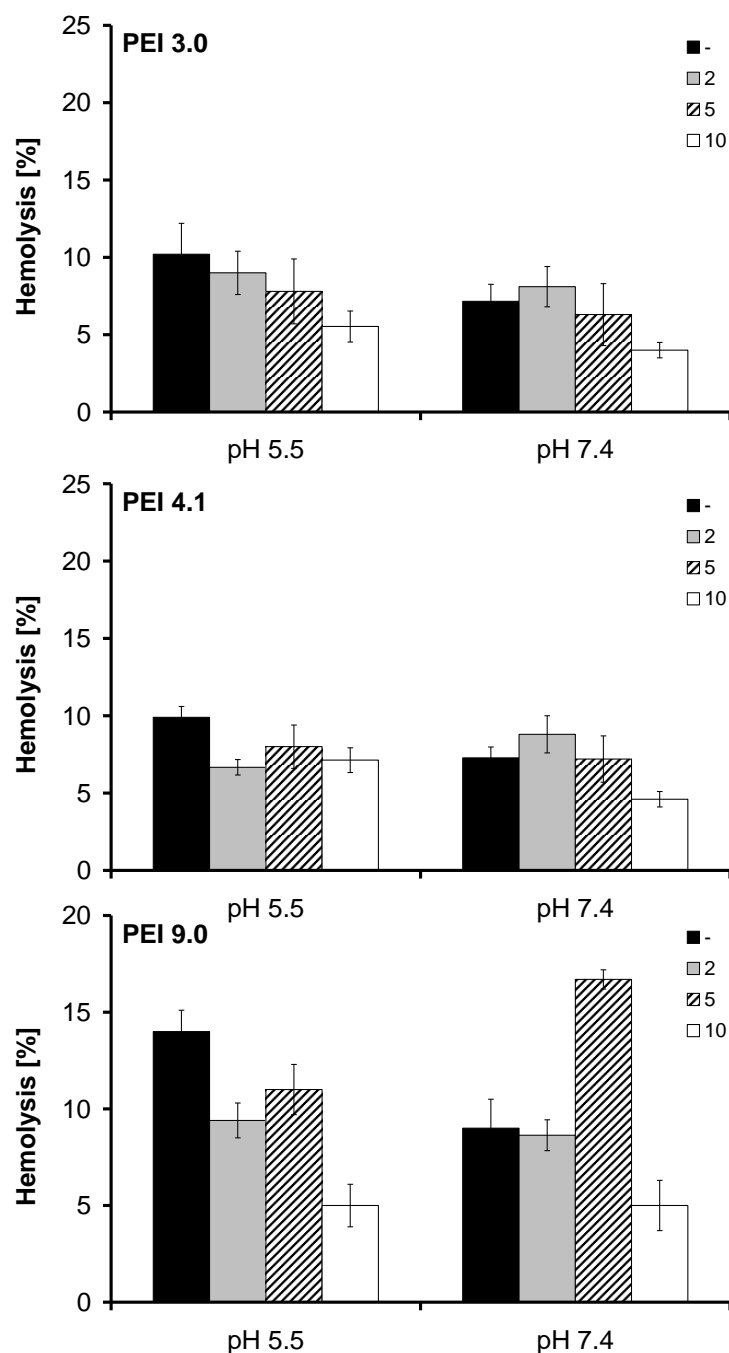
Erythrocyte leakage assay

Fig. S12. Human erythrocytes were isolated from heparin treated blood by centrifugation (800 g for 10 min at 4°C). Subsequently, the erythrocytes were washed in PBS buffer several times at 800 g for 10 min at 4°C. The erythrocytes were then diluted 1:10 in PBS. 500µl of the erythrocyte dilution was mixed with 500 µl polyplexes at pH 5.5 or 7.4 (Tris buffer), respectively,

188

and incubated on a shaker for 1 h at 37°C. The supernatant was measured for haemoglobin release at 405 nm using a TitertekPlus Microplate Reader (Bartolomey Labortechnik, Germany). Triton at a final concentration of 0.04% was applied as positive control, while erythrocytes treated with buffer only served as negative control. Polyplexes were prepared at N/P 6 using 30 µg plasmid DNA. Experiments were performed in triplicate. PEI with a MW of 3.0, 4.1 and 9.0 kDa was used, and the MW of PEG [kDa] is indicated in the Figure legend.

The pH had no huge influence on hemolysis induced by polyplexes. As expected, the hemolytic capacity of PEI-polyplexes was slightly higher than for PEG-PEI-polyplexes at pH 5.5.
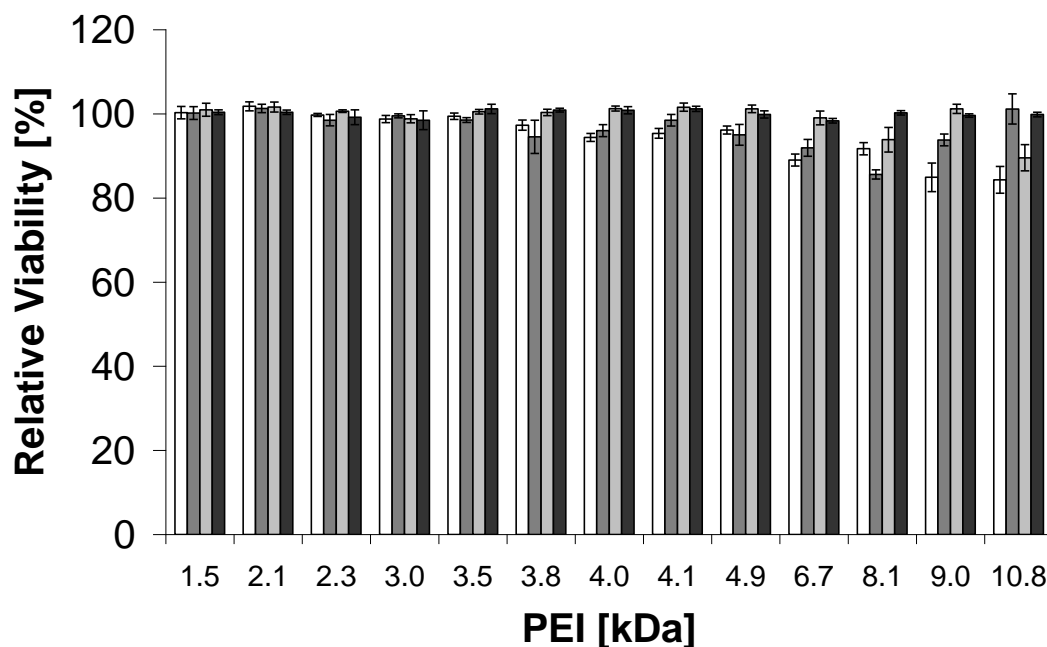
Fig. S13. *Relative cell viability of CHO-K1 cells after transfection with polyplexes at N/P 6 with PEI (☐) and the corresponding PEG(2)-S-PEI (◼), PEG(5)-S-PEI (☐) and PEG(10)-S-PEI (◼) copolymers in CHO-K1 cells. The MW of PEI is indicated on the x-axis. The number of viable cells was determined by flow cytometry after staining with propidium iodide.*

References

[1]   B. Brissault, A. Kichler, C. Guis, C. Leborgne, O. Danos, H. Cheradame, Synthesis of linear polyethylenimine derivatives for DNA transfection, *Bioconjugate Chemistry*, 14 (2003) 581-587.

[2]   L. Huang, Y. Liu, In vivo delivery of RNAi with lipid-based nanoparticles, Annual Review of Biomedical Engineering, 13 (2011) 507-530.

[3]   J. DeRouchey, C. Schmidt, G.F. Walker, C. Koch, C. Plank, E. Wagner, J.O. Raedler, Monomolecular assembly of siRNA and poly(ethylene glycol)/peptide copolymers, *Biomacromolecules*, 9 (2008) 724-732.

[4]   J.P. Clamme, J. Azoulay, Y. Mely, Monitoring of the formation and dissociation of polyethylenimine/DNA complexes by two photon fluorescence correlation spectroscopy, *Biophysical Journal*, 84 (2003) 1960-1968

Chapter 6

Linear disulfide-connected poly(ethylene imine)-poly(ethylene glycol) copolymers –
A library screening for their redox response

Abstract

Strictly linear reductively degradable poly(ethylene imine)-poly(ethylene glycol) diblock copolymers connected via a disulfide bond (PEI-SS-PEG) were synthesized from PEG 2 kDa and 5 kDa and 13 PEIs with a molecular weight ranging from 1.5 to 10.8 kDa as well as a set of fluorescently labeled copolymers with PEG 3 kDa, 5 kDa and 10 kDa. These polymers were intended for the formation of environment responsive polymeric carriers which deliver plasmid DNA (pDNA) to cells. Thus, the physicochemical properties of the complexes from pDNA and the polymers (the so called polyplexes) in response to a reductive trigger were examined and the performance in cell culture was studied. While polyplexes made from PEIs with short chains were generally rather instable and transfected poor, copolymers from PEIs of intermediate molecular weight were stable under nonreductive conditions, but degraded after addition of a reductant. Furthermore these degradable polyplexes performed well in cell culture. In contrast, copolymers with long chain PEIs could not be degraded under reductive conditions and differences in transfection performance between homo- and copolymers were not seen. So there is a small window of polymer molecular weight in which reductively degradable PEI-SS-PEG copolymers can be formed. If the PEI molecular weight is too low the resulting polyplexes are generally instable, while a PEI molecular weight which is too high results in nondegradable bonds.

Introduction

Although the last decades were characterized by a fast progress in medicine, there is still a need for efficient therapies for such severe diseases as genetic disorders and cancer. One very promising novel approach is the delivery of nucleic acids, but safe and efficient polymer-based carrier systems for their broad application are still needed. The probably most important polymer to fulfill this task is poly(ethylene imine) (PEI). It is the gold standard concerning transfection efficiency but unfortunately it is also rather toxic. This is due to its inherent positive charge which causes interactions with blood components and extracellular matrices. In order to overcome this problem shielding moieties such as poly(ethylene glycol) (PEG) have been attached to PEI -a widely used technique which is called PEGylation. This shield masked PEIs charge and lowered its toxicity [1, 2]. Up to now numerous different PEG-PEI copolymers are known which differ in their structure, grafting density and chain length. The first generation of copolymers was characterized by the formation of rigid, nondegradable bonds [1-7]. These copolymers efficiently enhanced colloidal stability [8, 9] and reduced the interference with blood components [8, 10], but the PEG moiety was permanently fixed to PEI. This possibly hampered intracellular events such as the endosomal escape of the vector (Figure 1) and, thus, the shielding sometimes led to reduced transfection efficiency [2, 3].

In order to improve this situation the carriers of the second generation were equipped with a labile bond connecting the PEI and PEG chains [11]. Researchers were looking for a special trigger upon which the copolymers degraded. One very prominent example is acidic pH because after cellular uptake the pH within endosomes drops during processing. Thus, copolymers connected by different esters [12, 13] or pyridylhydrazones [14-16] were synthesized. Depending on their exact structure the half-life of these copolymers varies a lot [17]. But as soon as these bonds come in contact with water they start to hydrolyze and this bears the risks of hydrolysis during storage or premature release in the bloodstream. If the linking bond is too stable the half time of hydrolysis may be too long and the carrier stays intact even inside cells, inhibiting the release of
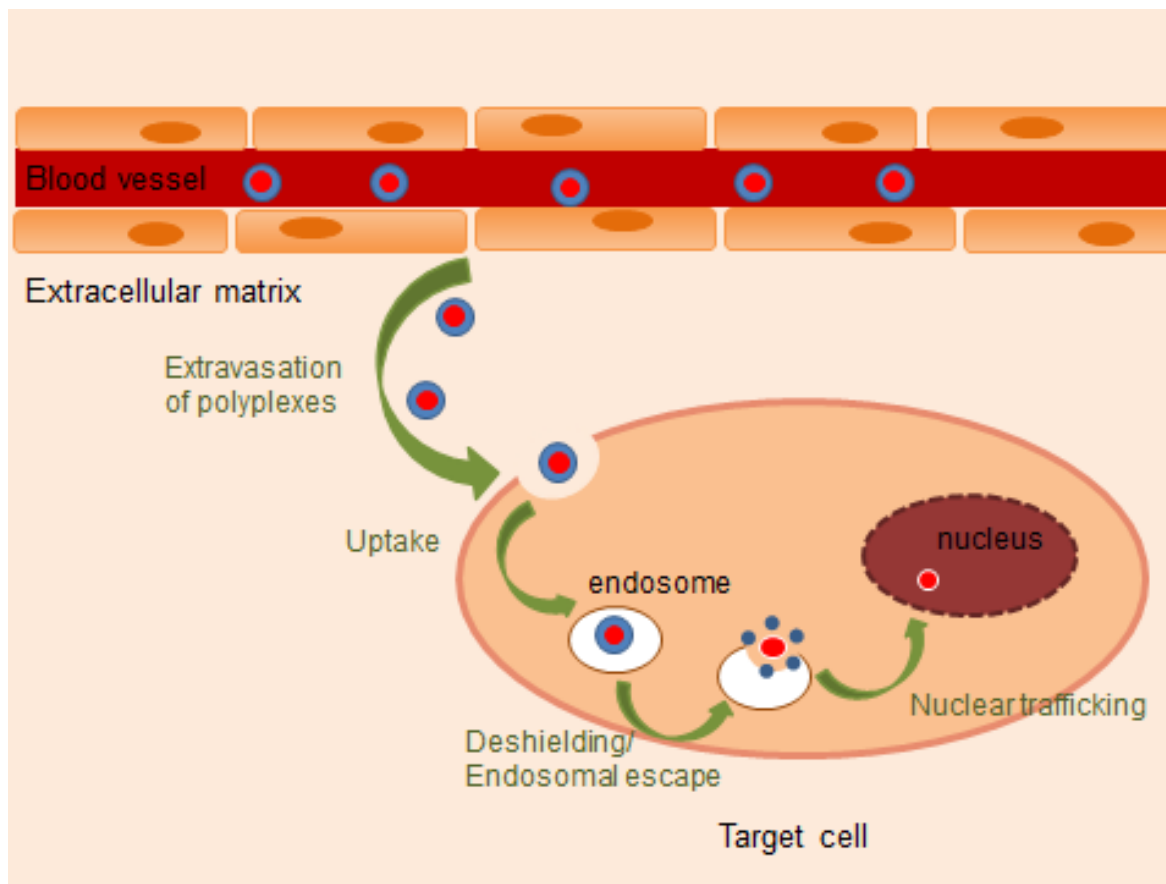
Figure 1. *The most important steps in gene delivery. After transport with the bloodstream the polyplex must be extravasated and then be taken up by a target cell. Thereafter the PEG shielding must be removed and the polyplex has to escape from the endosome before it can be transported to the nucleus. If the carrier is not deshielded its further processing is hampered and the transfection efficiency is severely affected.*

the cargo at the target site. So another more specific trigger would be beneficial such as the difference in the redox potential between the extracellular and intracellular compartments. It is known that the intracellular glutathione concentration is much higher than that of the extracellular space (roughly 1-10 mM to 10 μM, respectively) [18]. This sudden, huge difference could be used to cause polymer degradation and was exploited for polymeric carriers with disulfides in the backbone [19-25]. The rationale behind this was that high molecular weight polymers are generally known to achieve higher transfection rates than low molecular weight polymers, but they are

194

more toxic at the same time. So researchers tried to build high molecular weight polymers from low molecular weight parts by linking them through disulfide bonds. And in fact, these carriers combined the high transfection efficiency of high molecular weight polymers with the reduced toxicity of the low molecular weight fragments in which they could be degraded after exposure to reductive environment [19-25]. While this approach gained much attention only little is known about the triggered detachment of shielding moieties which were connected with the polymeric carrier via disulfide bonds [26-28]. This is astounding because it is generally acknowledged that the issue of shielding detachment is one of the most important steps in non-viral gene delivery. Since the redox trigger has not been exploited thoroughly so far, we synthesized a library of strictly linear, redox active PEI-SS-PEG copolymers. Our intention was to investigate the mobility of the copolymer particles in matrices and the possibility to cleave the labile bonds within these particles. Our focus lay on the cleavage under physiologic conditions and the deduction of structure-activity-relationships as to the chain length of both the PEG and the PEI part. Thus, we investigated the cleavage of the polyplexes (the complexes made from pDNA and polymers) under reductive conditions and performed uptake and transfection studies elucidating the usefulness of our approach.

Materials

All chemicals and materials were from Merck KGaA (Germany), Acros Organics (Belgium), Sigma-Aldrich Chemie GmbH (Germany), J.T. Baker (The Netherlands) or IRIS Biotech (Germany). Acetonitrile, dimethylformamide (DMF) and 2-ethyl-2-oxazoline were distilled over calciumhydride. Methyl-p-toluene sulfonate was dried in vacuo before use. All other chemicals were used as received.

The pDNA encoding enhanced green fluorescent protein (EGFP) (pEGFP-N1, Clontech, Germany) was used as reporter gene and isolated from E. coli JM 109 strain using a Qiagen Plasmid Maxi Kit (Qiagen, Germany). When indicated, plasmid DNA was stained with the intercalating dye YOYO-1 (Invitrogen/ Molecular Probes, The Netherlands). The labeling reaction was carried out with a molar ratio of 1 dye molecule per 300 base pairs at room temperature (rt) in the dark.

CHO-K1 cells (ATCC No. CCL-61) and HeLa cells (ATCC No. CCL-2) were grown in 75 ml culture flasks in a 5% CO_2 atmosphere at 37°C as adherent culture to 90% confluency before seeding. CHO-K1 cells were cultivated in Ham´s F-12 and HeLa cells in MEM-Eagle medium containing pyruvate. Both culture media were supplemented with 10% fetal bovine serum (Biochrom AG, Germany).

Polymer synthesis (Synthesis of PEI-SS-PEG and fluorescently labelled PEI-SS-PEG)

The synthesis started with the cationic ring opening polymerization of 2-ethyl-2-oxazoline (**1**) in acetonitrile using varying amounts of methyl-p-toluene sulfonate (**2**), depending on the desired moleculr weight (MW) of PEI. After polymerization under a nitrogen atmosphere at 90°C for several days (3 to 6 days, depending on the calculated MW of PEI), the reaction was cooled down to rt and the MW of the resulting polymer was determined by ^{1}H-NMR. Thereafter, 7.5 equivalents (eq. corresponding to the MW of PEI) of sodium thioacetate in DMF were added and

the reaction mixture stirred for 4 hours (h). The solvent was then removed, the residue dissolved in chloroform and the solution washed 3 times with water. The raw product was precipitated in ice cooled diethyl ether, filtrated and dried in vacuo. In the next step, **3** was hydrolyzed in fuming HCl at 95°C for one day. After removal of the HCl, the product was dissolved in water, precipitated with NaOH, washed with water until the supernatant became neutral and dried in vacuo. The third step was the activation of this component with $NaBH_4$ at pH 8.5 for 20 minutes (min), then the reaction mixture was acidified to pH 1 in order to destroy unreacted $NaBH_4$. The pH was adjusted to 4 and 3 eq. of 2,2`-dithiodipyridine (DTDP) were added to the reaction mixture. After stirring at overnight at rt the crude product, lPEI-SSpyr was dialysed against water and lyophilized.

For the synthesis of mPEG-SS-PEI, methoxy PEG-thioacetate (mPEG-SAc) (**6**) had to be synthesized in a 2-step procedure: dry methoxy PEG-OH was tosylated using 0.5 eq. of 4-dimethylaminopyridine (DMAP), 1.5 eq. of p-toluene sulfonate and 2.0 eq. of triethylamine. The reaction mixture was dissolved in dichloromethane and stirred overnight at rt, followed by the replacement of the dichloromethane by chloroform and washing the crude product 3 times with water and 2 times with 0.1 M HCl. The resulting mPEG-tosylate was dried over magnesium sulfate and in vacuo. In the second step, 2.5 eq. of potassium thioacetate were added to the mPEG-tosylate in DMF and the mixture was stirred for 8 h at rt. The mixture was concentrated, poured into a 10 fold volume of water and washed with chloroform 3 times. The organic phase was dried over magnesium sulfate and evaporated to dryness yielding mPEG-SAc . This component was then dissolved in a mixture of water and methanol (1:1), acidified with 5 drops fuming HCl and brought to reflux for 8 h. After cooling to rt and adjusting the pH to 4, the activated PEI component was added and stirred overnight. The product, mPEG-SS-PEI (**7**), was dialyzed against water and lyophilized.

For the synthesis of the fluorescein labelled copolymer PEI-SS-PEG-Fl (**9**), HS-PEG-NH-Boc (**8**) and IPEI-SS-pyr (**5**) were dissolved in water and the pH was adjusted to 4. The mixture was stirred overnight under nitrogen atmosphere at rt. Unreacted components were removed by dialysis and the resulting product was lyophilized. In the next step the Boc protection group was removed by stirring the copolymer in 2 M HCl at 40°C for 30 min. Subsequently the solvent was removed and the product dialysed against water and dried in vacuo. For the following labelling procedure the copolymer was dissolved in 0.05 M potassium phosphate buffer pH 8 and a solution of fluorescein-5-EX (Invitrogen/ Molecular Probes, The Netherlands) in DMF was added. This mixture was stirred for 2 h and afterwards dialysed against water. The resulting product was dried in vacuo. Successful conversion was monitored by ^{1}H-NMR. All ^{1}H-NMRs were recorded on an Avance 300 spectrometer (300MHz, Bruker BioSpin GmbH, Germany). The polymers were dissolved in 150 mM NaCl, and the pH was adjusted to 7.0.

Formation of polyplexes

The polyplexes of plasmid DNA and polymer were prepared at different N/P ratios (ratio of nitrogens in polymer to phosphates in DNA). The polymer and plasmid DNA were each diluted in equal volumes of 150 mM NaCl. The polymer solution was added to the DNA solution, the mixture was vortexed for 20 seconds and then incubated for 20 min before use. The amount of pDNA and the total volume of the polyplex solution are given in each section.

Fluorescence recovery after photobleaching (FRAP)

For the investigation of the mobility of polyplexes in extracellular matrices polyplexes of plasmid DNA and polymer were prepared with 2 µg pDNA at an N/P ratio of 6. The polymer and plasmid DNA were each diluted in 25 µl of 5% glucose. The polymer solution was added to the DNA solution, the mixture was vortexed for 20 seconds and then incubated for 20 min before use. Subsequently, the polyplex solution was mixed with 200 µl matrigel (BD Matrigel™ basement membrane matrix phenol red free, BD Biosciences, Europe) and transferred into Lab-Tek

Chambered Cover glass (Thermo Fisher Scientific, Germany). The FRAP experiments were performed at an Zeiss Axiovert 200 M microscope (Carl Zeiss, Jena, Germany). A Plan-Neofluar 10x objective lens with a numerical aperture of 0.30 was used and the confocal pinhole was opened completely. The bleaching experiments were performed with the 488 nm-line of a 30mW Argon laser which operated at full power. A time-series of 800 images with a resolution of 128x256 pixel and a laser beam with 0.15% transmission was recorded for each sample. 5 pictures were recorded ahead of the bleaching. Then the sample was bleached (200 iterations) and pictures were recorded immediately after the end of the bleaching procedure without any delay between the single pictures. The fluorescence recovery curve and the fractions of mobile and immobile phase were calculated with the Zeiss FRAP tool.

Cellular uptake

80,000 CHO-K1 cells per well were seeded in a 24-well plate. The polyplexes were prepared at a N/P ratio of 6 in 100 µl using 2 µg of YOYO-1 labeled plasmid DNA. The cells were washed with PBS, then 900 µl of serum free culture medium and 100 µl of polyplex solution was added. After 4 h the transfection medium was removed and the cells were detached from the surface by trypsin that was supplemented with 20 mM sodium azide. Cells were analyzed by flow cytometry using a FACSCalibur (Becton-Dickinson, Germany). YOYO-1 was excited with a 488 nm argon laser and detected with a 515 - 545 nm bandpass filter. The mean fluorescence intensity (MFI) of 20,000 gated cells was recorded as a measure for the amount of internalized plasmid DNA. The values were expressed as means (± SD) from three independent samples.

Hydrodynamic diameter and zeta potential measurements

The hydrodynamic diameter and the zeta potential of the polyplexes was measured using a Zetasizer Nano-ZS from Malvern Instruments (Malvern, Germany) at 25°C. A 4 mW He-Ne laser at a wavelength of 633 nm was used as the light source. For the determination of the size, the measurement position was at 4.65 mm with automated laser attenuation. Scattered light was

detected at an angle of 173° backscatter. The viscosity and refractive index of the dispersants were used as follows: 150 mM NaCl: 0.90 mm^2/s and 1.33, respectively; 5% glucose: 0,98 mm^2/s and 1.33, respectively. Three measurements with 10 sub-runs were performed for each sample. Data were analyzed by the general purpose mode and expressed as mean ± standard deviation (SD). The zeta potential of the polyplexes was measured at 25°C. Three measurements with 10 sub-runs were performed for each sample. Data were processed in the monomodal mode which guarantees for good sample stability due to short measurement duration and then expressed as mean (± SD). For size measurements, polyplexes were formed by mixing 2 µg DNA and varying amounts of polymer to achieve different N/P ratios in a final volume of 500 µl, while for zeta potential measurements the polyplexes were built with 4 µg pDNA in a final volume of 1000 µl.

For the determination of the polyplex stability under reducing conditions polyplexes were prepared at an N/P ratio of 6 in HBG buffer pH 7.4 which consisted of 20 mM 4-(2-hydroxyethyl)-1-piperazineethanesulfonic acid and 5% glucose. 2 µg pDNA were mixed with the corresponding amount of polymer yielding a volume of 450 µl. After 20 min incubation 50 µl of a 150 mM DTT stock solution were added. The polyplexes were measured all 15 min over a period of 10 h. The measurement of the zeta potential under reducing conditions was performed with polyplexes built in 900 µl HBG buffer pH 7.4 at an N/P ratio of 6 from 4 µg pDNA and various amounts of polymer. The polyplexes were incubated for 20 min at rt and then 100 µl of a 150mM DTT solution was added. The samples were measured only once either directly after addition of DTT or after 2 h, 8 h or 24 h, respectively. Three measurements with 10 sub-runs were performed for each sample.

Transfection studies

HeLa cells were seeded in 24-well plates at a density of 40,000 cells per well 24 h prior to transfection. 2 µg of pDNA was used to prepare the polyplexes with the appropriate amount of

polymer to yield different N/P ratios in a final volume of 100 µl. The cells were washed with PBS, then 900 µl of serum free culture medium and 100 µl of polyplex solution was added. After 4 h the transfection medium was removed and cells were incubated for an additional 20 h with culture medium containing serum. After detachment of the cells from the surface by trypsin and extensive washing with PBS, the analysis of the EGFP expression of cells was performed by flow cytometry using a FACSCalibur (Becton-Dickinson, Germany). EGFP was excited at 488 nm and the fluorescence was detected using a 515 - 545 nm bandpass filter. The data were analyzed using WinMDI 2.8 software by J. Trotter. To exclude doublets and cellular debris, cells were appropriately gated in forward/sideward scatter plots with 20,000 events per sample. The percentage of cells that was positive for EGFP indicated the transfection efficacy [%] and was expressed as means (± SD) from three independent samples. The relative transfection was calculated as follows:

relative transfection = transfection efficacy $[\%]_{PEG\text{-}PEI\text{-}polyplexes}$/transfection efficacy $[\%]_{PEI\text{-}polyplexes}$.

Confocal microscopy

Confocal laser scanning microscopy was performed using a Zeiss Axiovert 200 M microscope coupled to a Zeiss LSM 510 scanning device (Carl Zeiss Co. Ltd., Germany). HeLa cells were plated in 1µ-Slide 8 well ibiTreat microscopy chambers (ibidi, Germany) at a density of 20,000 cells per well. pDNA was labelled with TO-PRO dye as indicated by the supplier. Polyplexes were built from TO-PRO labelled pDNA and fluorescein labelled polymers. Cells were incubated with polyplexes for 2 h, washed and examined under the microscope. The fluorophores were then excited with 488 and 633 nm and the fluorescence was recorded with a 505–530 nm bandpass filter and a longpass filter of 650 nm. The measurements were performed using a Plan-Apochromat 63x/1.4 oil objective at 37°C and the thickness of the optical sections was 1.1 µm.

Results

Polymer synthesis

For the library of PEI-SS-PEG copolymers, PEG and PEI were prepared separately and subsequently coupled yielding redox active copolymers. The synthesis of PEI implied polymerization and activation steps (Fig. 2). 13 different linear PEI derivatives with a molecular weight ranging from 1.5 to 10.8 kDa were obtained in the polymerization step. The molecular weight was controlled by the ratio of the monomer 3-ethyl-2-oxazoline (**1**) and the starter methyltosylate (**2**) and was determined by ^{1}H-NMR. Subsequently, potassium thioacetate was added yielding poly(2-ethyl-2-oxazoline)-thioacetate (pEtOXZ-SAc) (**3**) which was thereafter hydrolysed to thiolated PEI (**4**). This component was further modified leading to PEI-pyridyl disulfide (PEI-SSpyr, **5**), which could be coupled to methoxyPEG thioacetate (mPEG-SAc) (**6**) with a molecular weight of 2 kDa or 5 kDa under acidic conditions. The PEG derivative mPEG-SAc was made by activation of mPEG with a tosylate in the first step and by a nucleophilic attack of potassium thioacetate in the second step.

Furthermore fluorescein modified copolymers (**9**) were synthesized in order to perform fluorescence recovery after photobleaching (FRAP) experiments and to detect polyplexes inside cell preparations. For this purpose, **5** was reacted with Boc-NH-PEG-thiol (**8**) at pH 4. The Boc-group was cleaved afterwards by addition of HCl. The freed amino group was then reacted with fluorescein-5-EX yielding PEI-SS-PEG-fluorescein (**9).**

 The overall synthesis route allowed for a selective coupling of only one PEG to one PEI molecule as proposed in Figure 2. Uncoupled PEG, PEI and fluorescein were removed by extensive dialysis of the copolymers. The composition of the copolymers was calculated by ^{1}H-NMR spectra and was in good agreement with theoretical values.
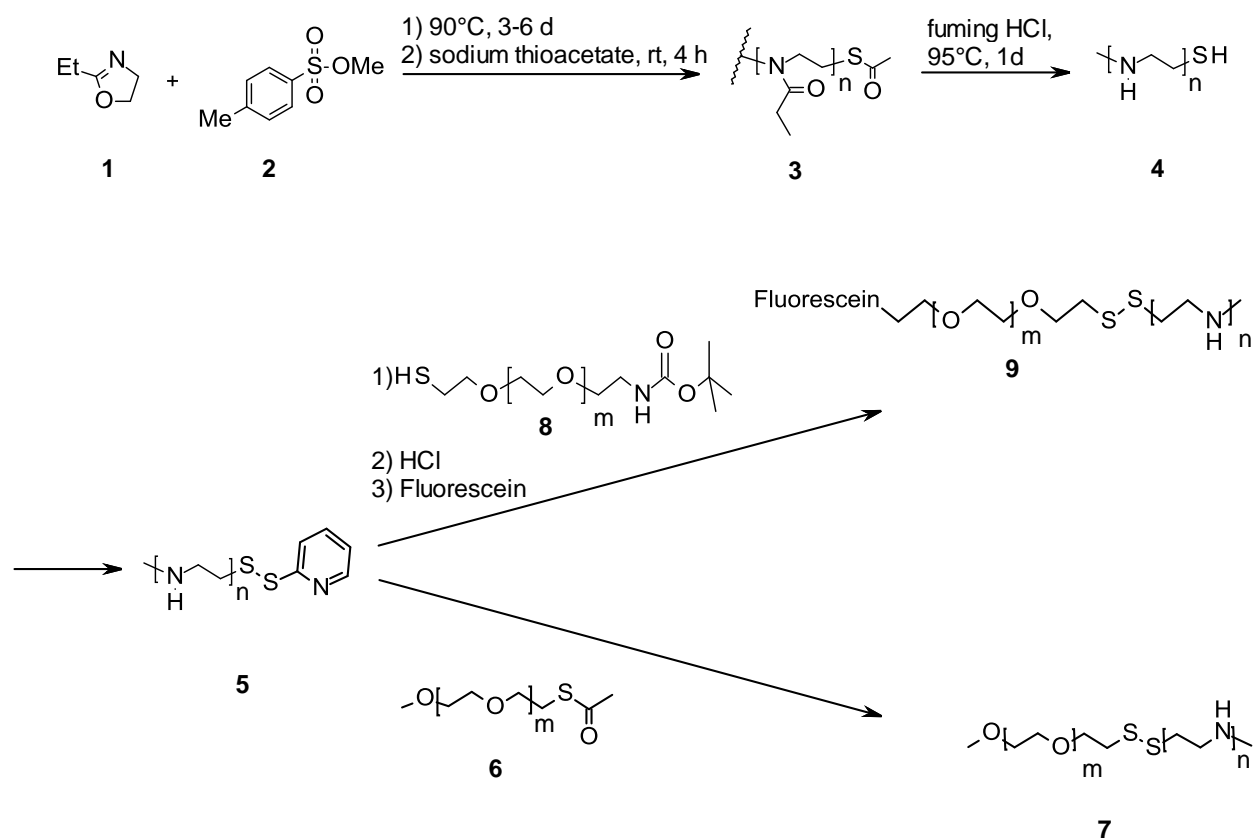
Figure 2. Synthesis of PEI-SS-PEG copolymers and their labeled counterparts PEI-SS-PEG-Fluorescein.

FRAP experiments

In order to determine if the polyplexes made from different fluorescently labelled polymers were able to diffuse through extracellular matrices, FRAP experiments were performed. This method allowed to determine the mobility of the polyplexes in a model matrix such as Matrigel™. Polyplexes made from pDNA and labelled PEI or PEI-SS-PEG copolymers were incorporated into Matrigel™ and their mobility after photobleaching was investigated. PEI 9.0 and its copolymers were chosen as an example. Figure 3 shows that the amount of mobile fraction was lowest for the polyplexes from the homopolymer PEI and pDNA and grew when the PEG chain of the copolymers became longer. While there was nearly no difference between PEI 9.0 and

PEI 9.0-SS-PEG 2, PEI 9.0-SS-PEG 5 exhibited better mobility and was even outperformed by

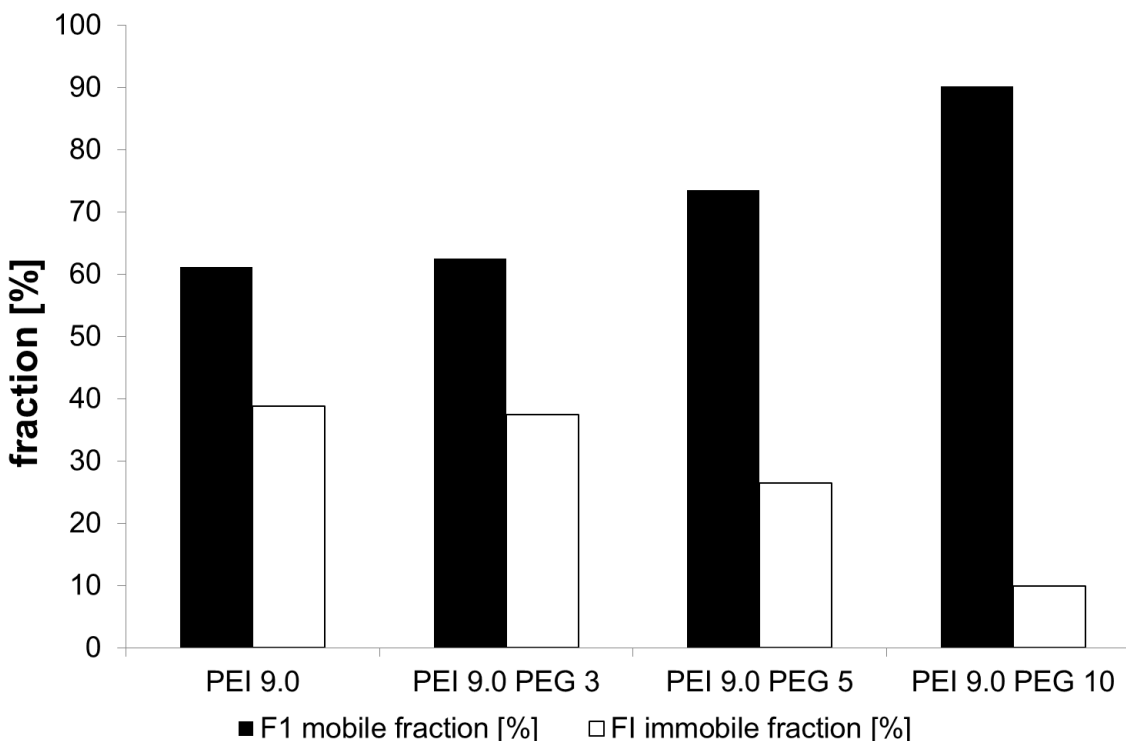PEI 9.0-SS-PEG 10 which showed the best mobility by far.

Figure 3. *Amounts of mobile (■) and immobile (□) polyplex fractions of a series of polyplexes made from PEI and three different copolymers (PEI 9.0-PEG 3, PEI 9.0-PEG 5, PEI 9.0-PEG 10) and pDNA at N/P 6 as determined by FRAP experiments.*

Uptake studies

After proving the mobility of the polyplexes in a model matrix, it was interesting to see if these

polyplexes could also achieve the next delivery step: the uptake by cells. For this purpose

particles were formed from YOYO labeled pDNA and different PEI or PEI-SS-PEG polymers.

Figure 4 shows the results of this experiment. The flow cytometry analysis demonstrated that all

polyplexes from PEGylated and unPEGylated polymers were taken up by CHO-K1 cells. Apart from some minor exceptions, only slight uptake differences were observed. Thus, all copolymers and most homopolymers were able to form polyplexes suitable for cellular uptake.
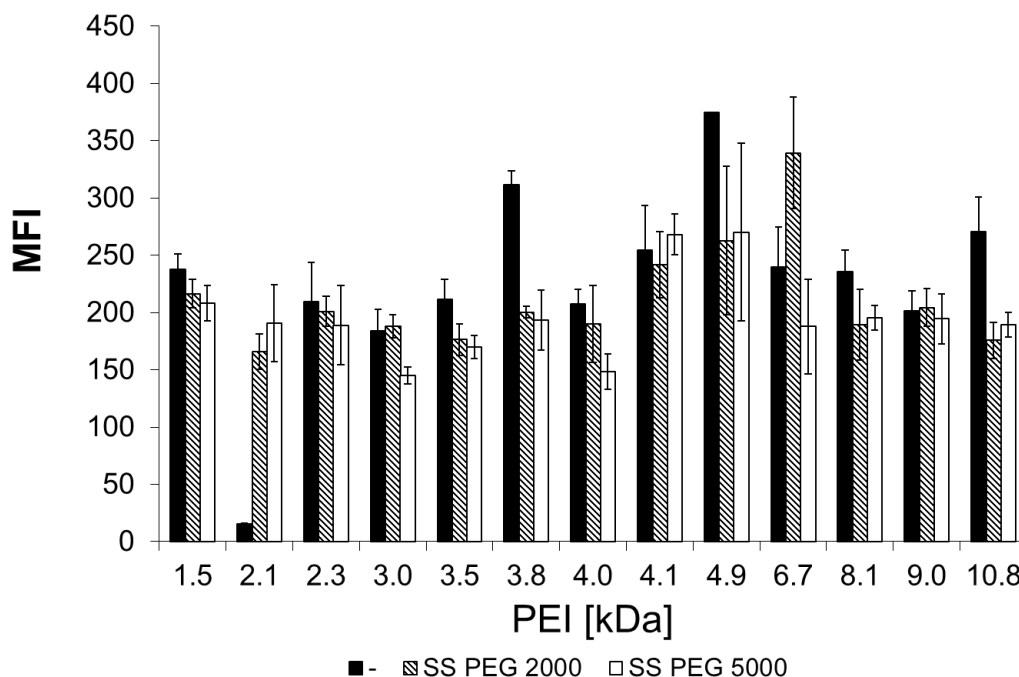

Figure 4. *The cellular uptake of fluorescently-labeled polyplexes built with PEI (■) and the corresponding PEI-SS-PEG 2 (▨) and PEI-SS-PEG 5 (▢) copolymers at N/P 6 into CHO-K1 cells was measured by flow cytometry. The mean fluorescence intensity (MFI) is an indirect measure of the cellular uptake of the polyplexes. The molecular weight of PEI [kDa] is indicated on the x-axis.*

Changes in size and zeta potential after incubation in reductive environment

After examining the diffusion ability and cellular uptake of our polyplexes a closer look at their response to external stimuli was important. It is a major prerequisite for every carrier to protect its payload from degradation as long as it has not reached its target site. But as soon as the

polyplex arrives at its destination, it has to release its cargo triggered by a specific stimulus such as a change in redox potential [29, 30]. Thus, the reductive environment inside cells was mimicked by incubating the polyplexes with dithiothreitol (DTT) which is a good substitute for the intracellularly occurring reductant glutathione. In a first experiment the zeta potentials of polyplexes after different incubation times was measured. Immediately after incubation with DTT the polyplexes made from the copolymers with PEG 2 kDa (Figure 5 A) as well as the polyplexes made from the copolymers with PEG 5 kDa (Figure 5B) exhibited a positive zeta potential ranging from about 25 mV to 35 mV for polyplexes with PEG 2 kDa and from about 10 mV to 40 mV for those with PEG 5 kDa, respectively. Despite of 3 exceptions all polyplexes showed reduced zeta potentials after 2 h of incubation compared to the beginning of the measurements. After 8 h and 24 h all polyplexes exhibited lower zeta potentials (around zero) than at the beginning of the measurement. This was also true for those polyplexes with slightly higher zeta potentials after 2 h.

Changes in the course of time were not only seen for the zeta potentials but could also be observed in measurements of the polyplex sizes. Again polyplexes were built at N/P 6 from different polymers and the polyplex sizes after incubation with and without DTT was measured by dynamic light scattering. In order to compare the absolute differences in the increase in size over time, size measurements of polyplexes incubated with or without DTT were set in relation and Figure 6 was built from these values. Compared to polyplexes without DTT all polyplexes incubated with DTT grew more in size over the observed time of 10 h than the polyplexes without DTT (Figure 6). The growth depended on the used polymers. In most cases the size increase was not higher than 5 fold. An extraordinary difference between starting and end point was observed for PEI 2.3-SS-PEG 2 and PEI 3.0-SS-PEG 2 with a 16 fold and 24 fold increase, respectively. The highest increase for copolymers made from PEG 5 kDa was found for PEI 5.0-SS-PEG 5 and PEI 6.7-SS-PEG 5 with 9 fold and 12 fold increase, respectively. In general, the increase in size was more pronounced for copolymers containing PEG 2 kDa.
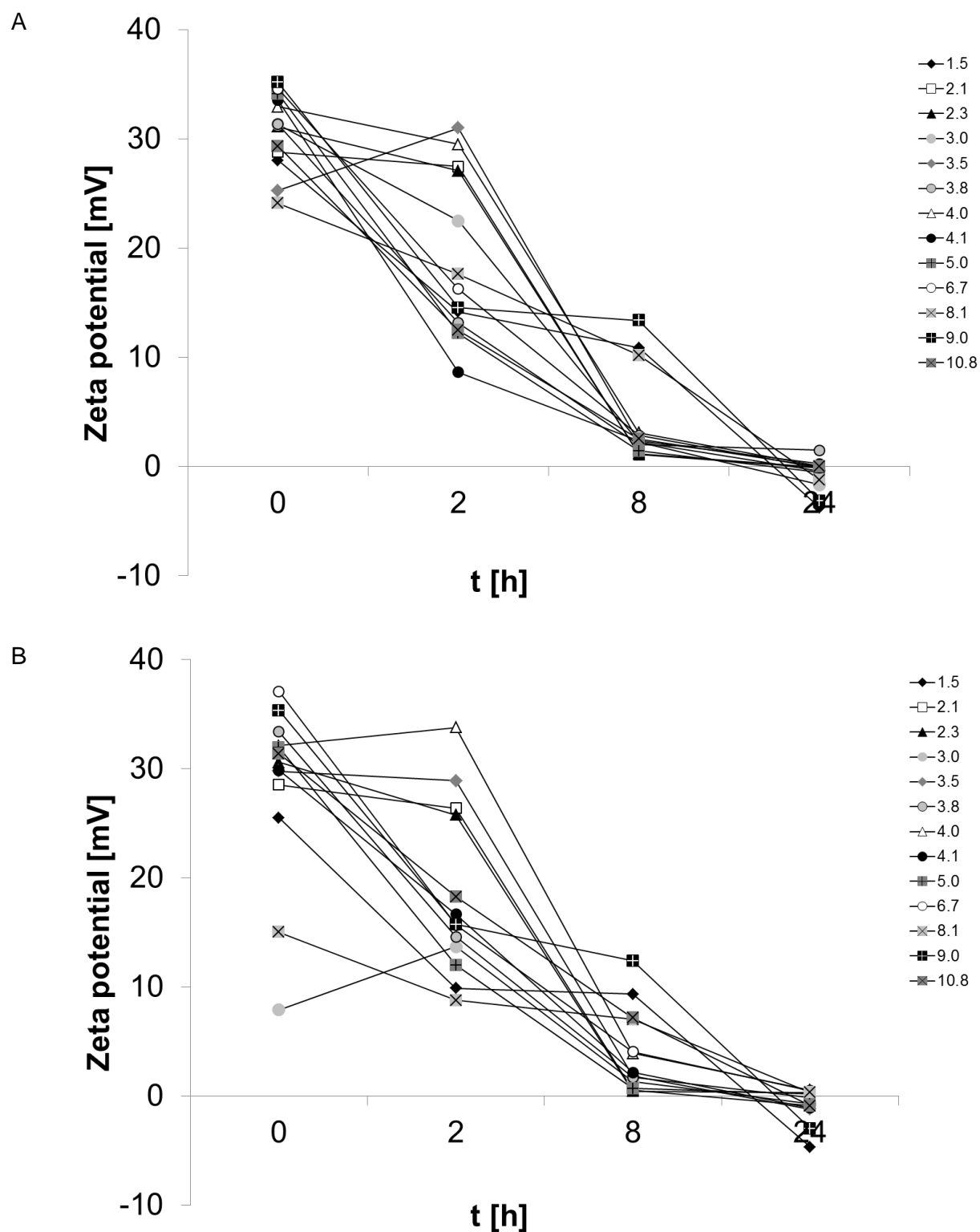
A

B

Figure 5. *Zeta potentials of polyplexes assembled of pDNA and copolymers with PEG 2 kDa (A)*

and copolymers with PEG 5 kDa (B) at N/P 6 after incubation with DTT at different time points.
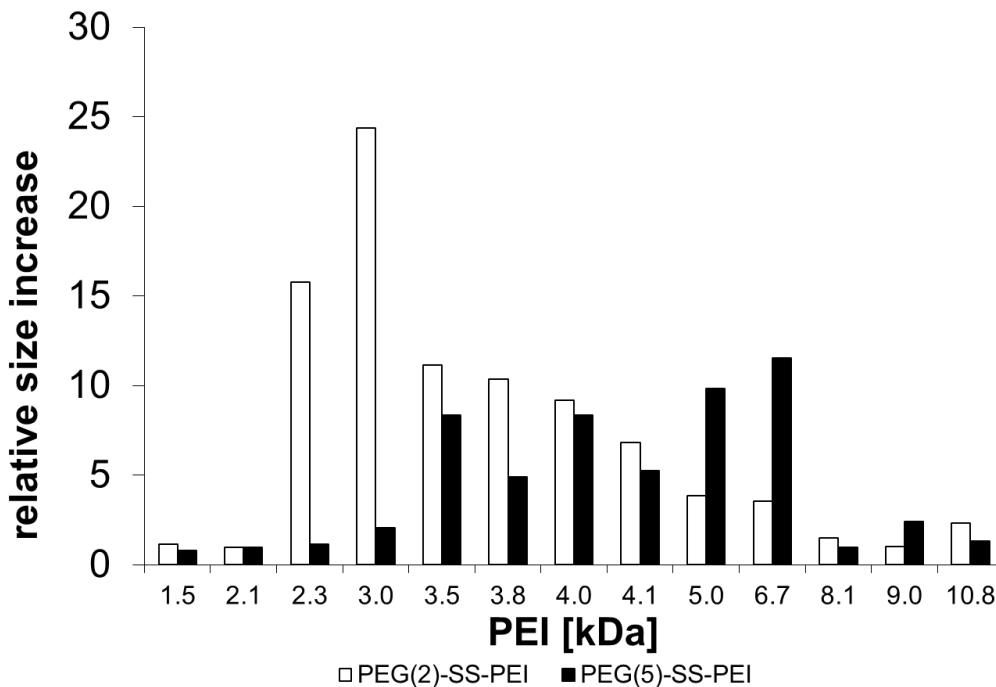
Figure 6. Relative increase in polyplex size after incubation with DTT compared to the increase in size without addition of DTT for polyplexes made from copolymers containing PEG 2 kDa (□) and PEG 5 kDa (■) and pDNA at N/P 6.

Beside the fact that the polyplexes responded to a reductive environment it was also very interesting to have a closer look at the polyplexes made from copolymers with different PEI chain length. A detailed analysis brought big differences between the polyplexes made from PEIs with different molecular weight to light (Figure 7). In the case of polyplexes made from PEI-SS-PEG copolymers with lower PEI molecular weight (Figure 7 A 1 and A 2) it could be seen that both the polyplexes incubated with DTT as well as the polyplexes without DTT became larger over the observed period of 10 h. Starting with a size of about 200 nm, they reached dimensions up to 2000 nm. Over the observed 10 h also their polydispersity indices (PdIs) grew steadily. For the polyplexes made from high molecular weight PEIs (Figure 7 C 1 and C 2) the situation was completely different. Although the polyplexes incubated with DTT gained a bit more in size over time than the non-treated polyplexes, it must be stated that both carriers

remained at rather constant small size (around 100-200 nm) with nearly unchanged PdIs. The balance between stability in non-reductive environment and cleavability under reducing conditions was best for the polyplexes made from PEIs of medium molecular weight (Figure 7 B 1and B 2). A huge difference between the DTT treated and untreated polyplexes could be seen. While the untreated carriers remained at constant size and PdI, the treated ones clearly gained in size combined with an increasing PdI.
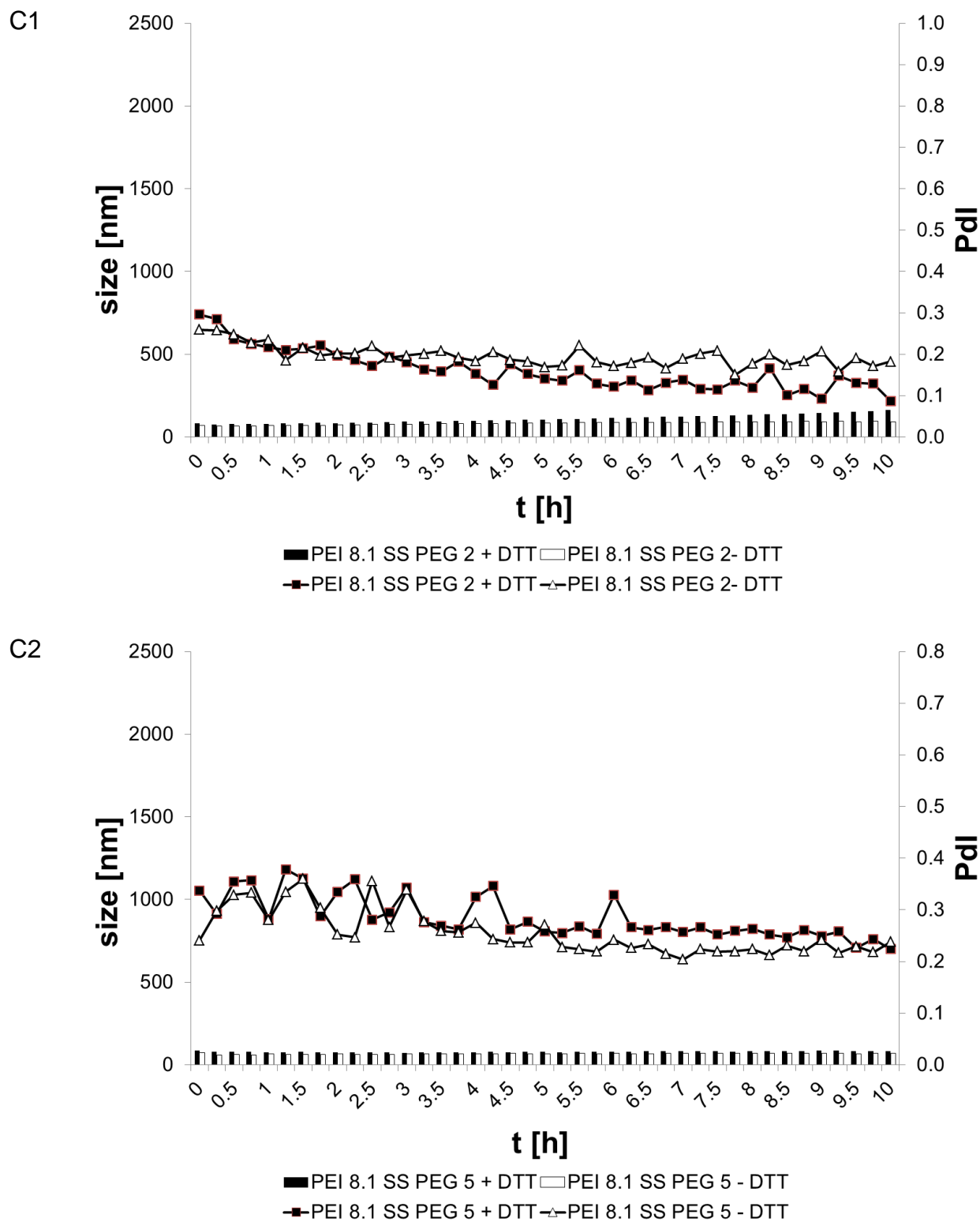
A1

A2
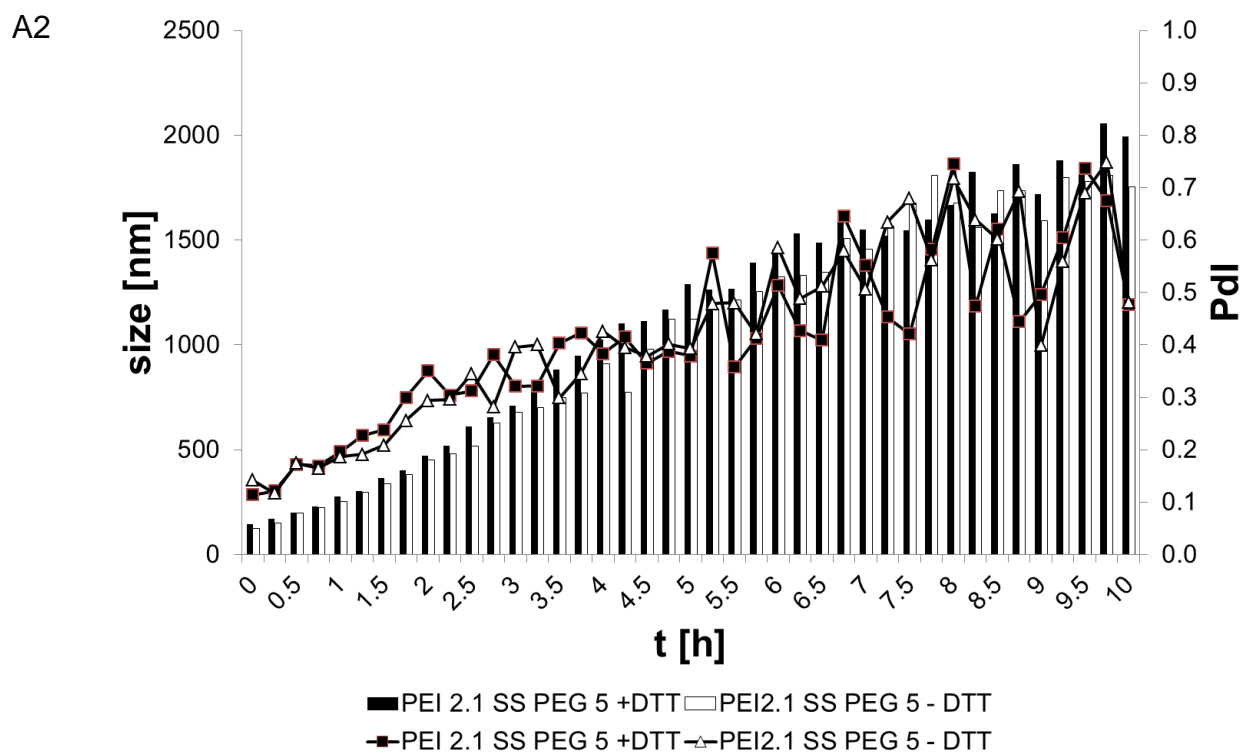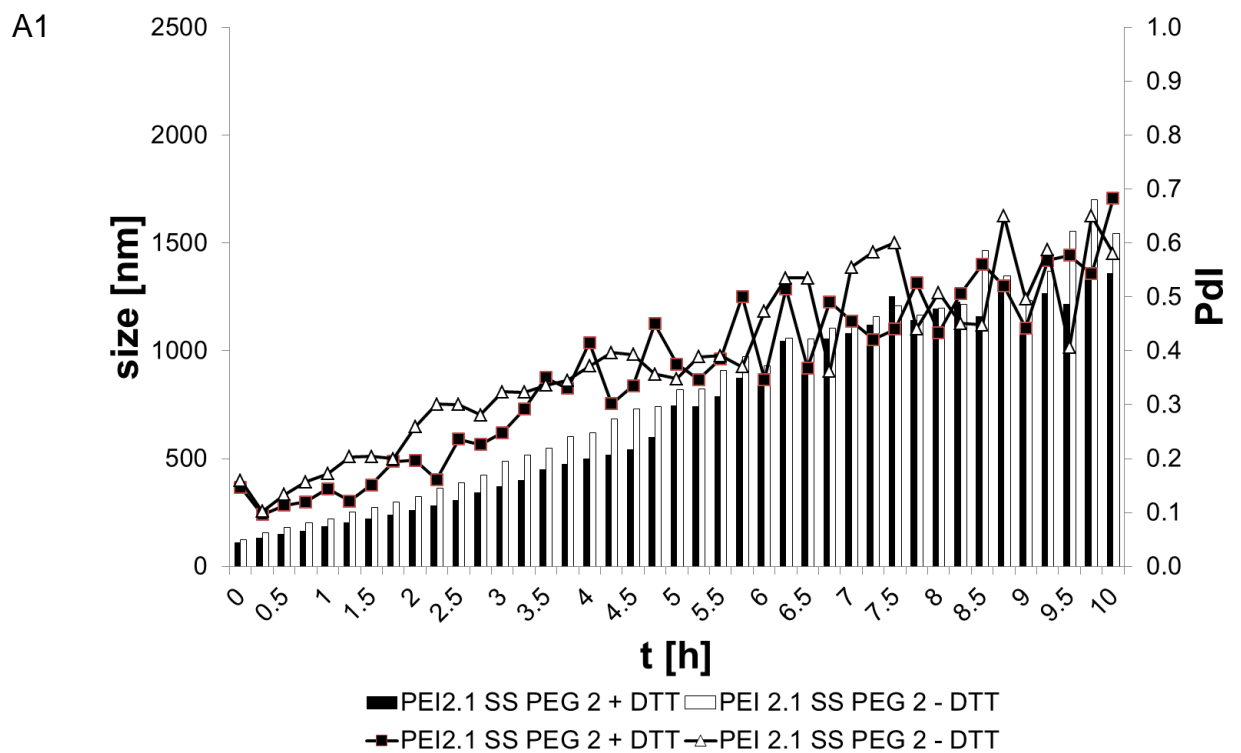
B1
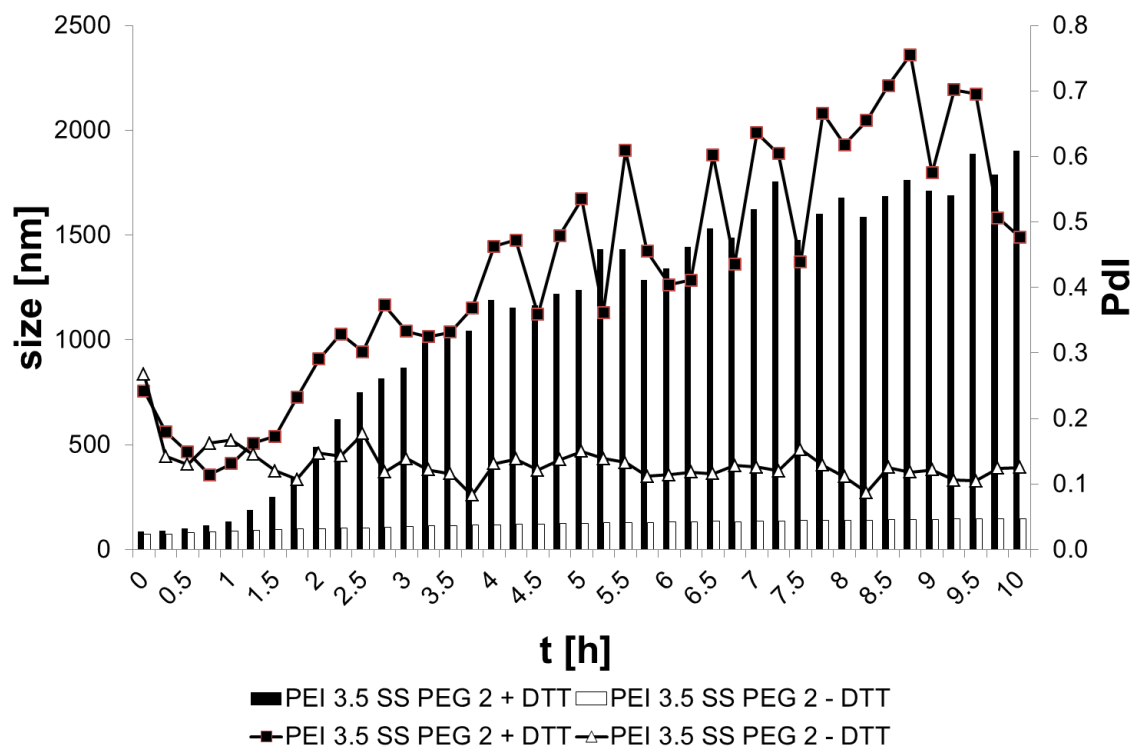
B2
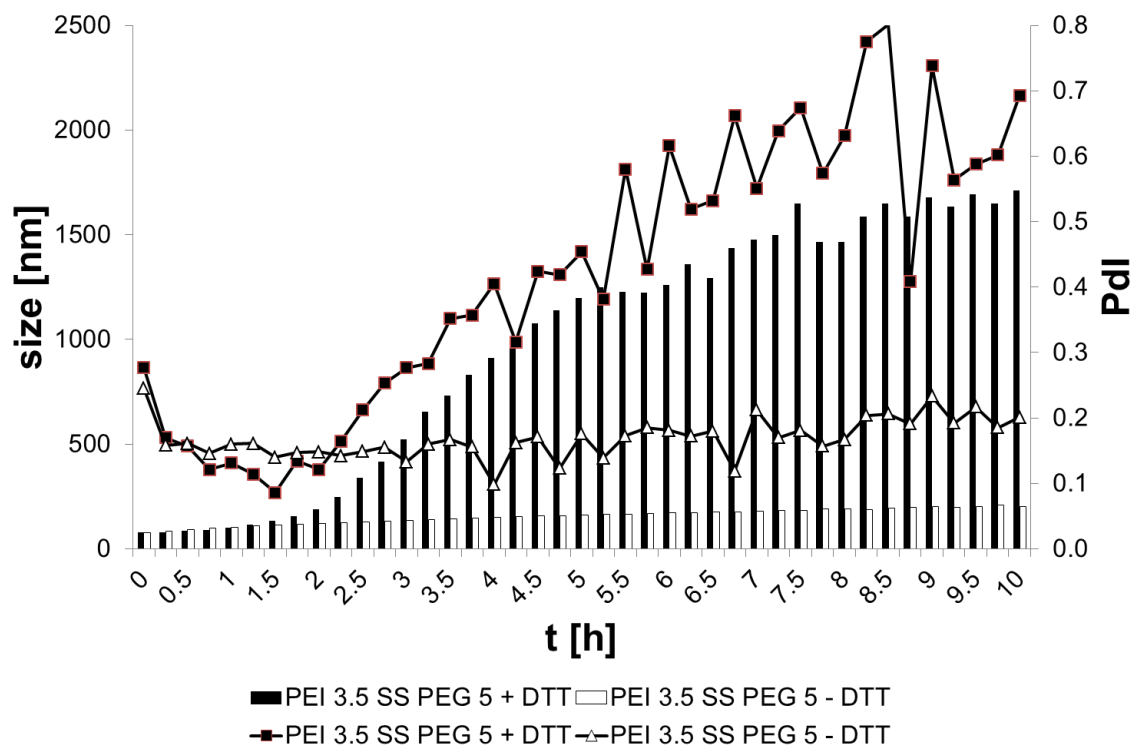
Figure 7. Hydrodynamic diameter and polydispersity indices (PdI) of polyplexes assembled of pDNA and PEI-SS-PEG copolymers at a N/P ratio of 6 in HBG buffer pH 7.4 as determined by

dynamic light scattering. The polyplexes were incubated with (■) and without DTT (□) and measurements were performed over 10 h. A1, B1 and C1 show polyplexes made from copolymers with PEG 2 kDa while A2, B2 and C2 show polyplexes made from copolymers with PEG 5 kDa. A shows polyplexes from PEI 2.3, B those with PEI 3.5 and C the polyplexes made from copolymers with PEI 8.1.

Transfection efficiency

Although stability and ability to diffuse in matrices are very important features of a gene carrier, the main criterion for a well suited gene delivery vehicle is its transfection ability. Thus, the transfection efficacy of all polymers was determined in HeLa cells by measuring the expression of EGFP. The amount of expressed EGFP depended mainly on the molecular weight of PEI (Figure 8). Polyplexes made from low molecular weight PEI such as PEI 1.5, PEI 2.1 or PEI 3.1 showed only very low EGFP expression (around 1%) while especially the polyplexes made from PEI of high molecular weight such as PEI 8.1, PEI 9.0 or PEI 10.8 exhibited a high transgene expression of about 40%. In most cases the EGFP expression mediated by polyplexes made from pDNA and PEI-SS-PEG copolymers exceeded the EGFP expression obtained by the corresponding polyplexes made from the PEI homopolymers. In order to simplify the comparison of the efficiency of different copolymer carriers, we calculated the relative transfection efficiency which relates the efficiency of the polyplexes made from PEI-SS-PEG copolymers to the efficiency of polyplexes made from PEI homopolymers. As seen before, all polyplexes made from copolymers except those from PEI 3.0-SS-PEG 5, PEI 5.0-SS-PEG 5 and PEI 9.0-SS-PEG 5 mediated higher transfection efficiency than the polyplexes from PEI alone (Figure 8). The overall differences in transfection efficiency were especially pronounced for the polyplexes from copolymers with low molecular weight PEIs since the basis for the calculation was a transfection efficacy below 1% for short chain PEIs. In such a case only a minor increase in transfection efficiency -such as for example 1%- results in very pronounced increases in trans-
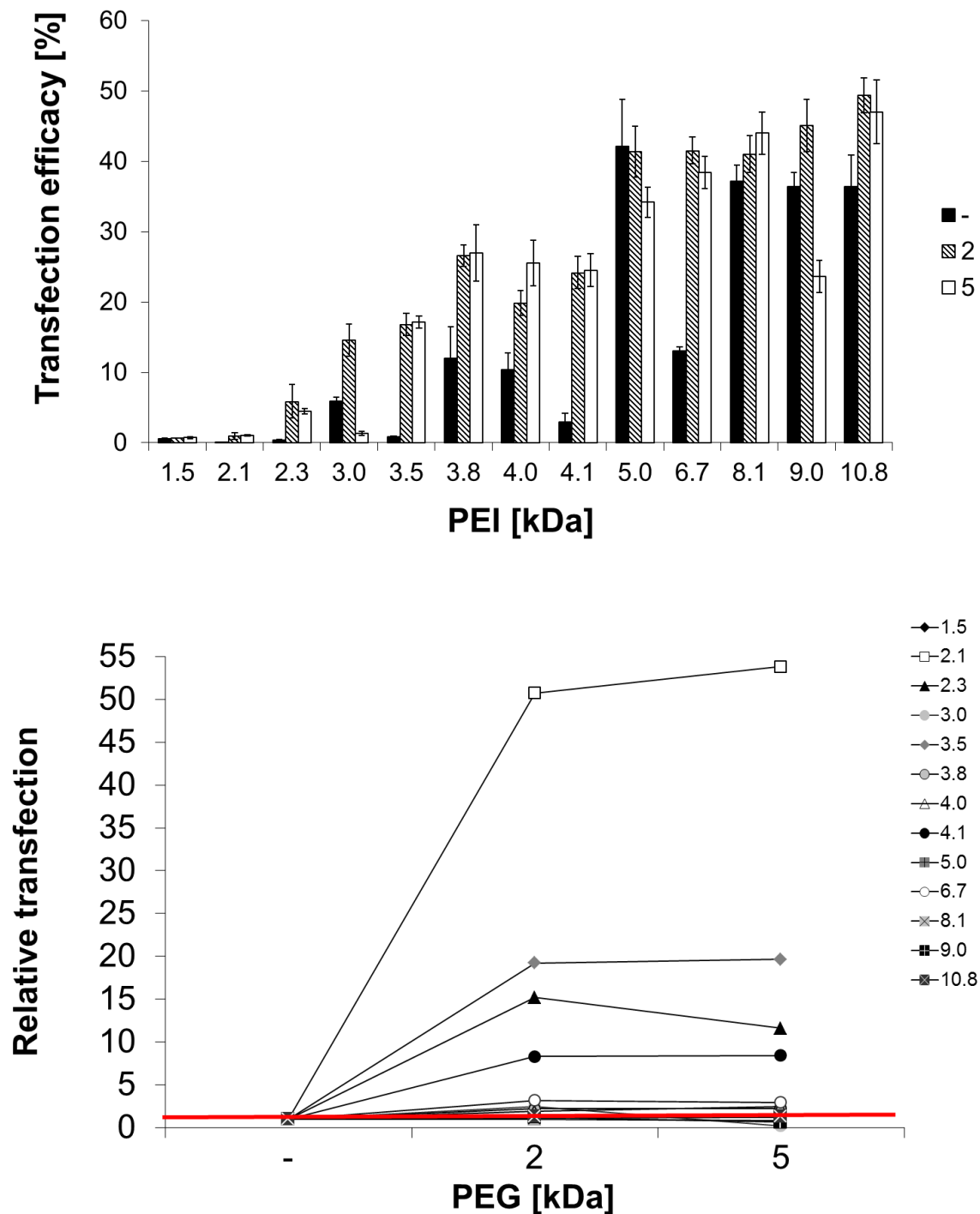
Figure 8. *(A) Transfection efficacy of polyplexes at a N/P ratio of 6 built with PEI (■) and the corresponding PEI-SS-PEG 2 (▨) and PEI-SS-PEG 5 (▢) copolymers in HeLa cells. The molecular weight of PEI [kDa] is indicated on the x-axis. Additionally, the values of the*

transfection efficacy of the PEI-SS-PEG-polyplexes were related to the corresponding PEI-polyplexes and expressed as relative transfection (B). Here, the molecular weight of PEG [kDa] is shown on the x-axis ("-" indicates the homopolymer), while the molecular weight of PEI [kDa] is given in the legend.

fection efficiency while 1% does not really matter in case of a transfection efficiency of about 40% or 50%. The efficiency of the carriers from high molecular weight PEI which did not gain size after incubation with DTT (e.g. PEI 8.1-SS-PEG) exhibited only slight increases in transfection efficiency compared to the homopolymers. Polyplexes made from copolymers which could be cleaved reductively (i.e. copolymers with PEIs of medium molecular weight such as PEI 3.5-SS-PEG) showed higher transfection efficiencies than the polyplexes from the corresponding homopolymers. So efficient transfection can be achieved by using intracellular cleavable PEI-SS-PEG copolymers which are stable in the extracellular space due to their PEG shielding.

Beside transfections analyzed by FACS, transfected cells were also observed in the confocal microscope. Both the pDNA and the polymers were stained. The polymers were labeled with fluorescein while the pDNA was reacted with a TO-PRO dye. So the pDNA was visible as red spots while the polymers gave green spots. If pDNA and polymers were colocalized yellow spots appeared. We chose PEI 4.0 as example because it exhibits medium molecular weight which makes it a well suited representative for our polymers. The polyplexes made from the homopolymer PEI were taken up by cells as well as the copolymers from PEI and PEG 3 kDa, PEG 5 kDa and PEG 10 kDa (Figure 9). The polyplexes made from PEI alone gave rather big spots within the cells. pDNA and PEI could be observed alone and colocalized (Figure 9 A). The cells treated with polyplexes from copolymers also showed green, red and yellow spots (Figure 9 A, B and C). But these spots were smaller and better distributed over the cells. Furthermore, there was a tendency towards smaller spots for polymeric carriers with longer PEG chains.
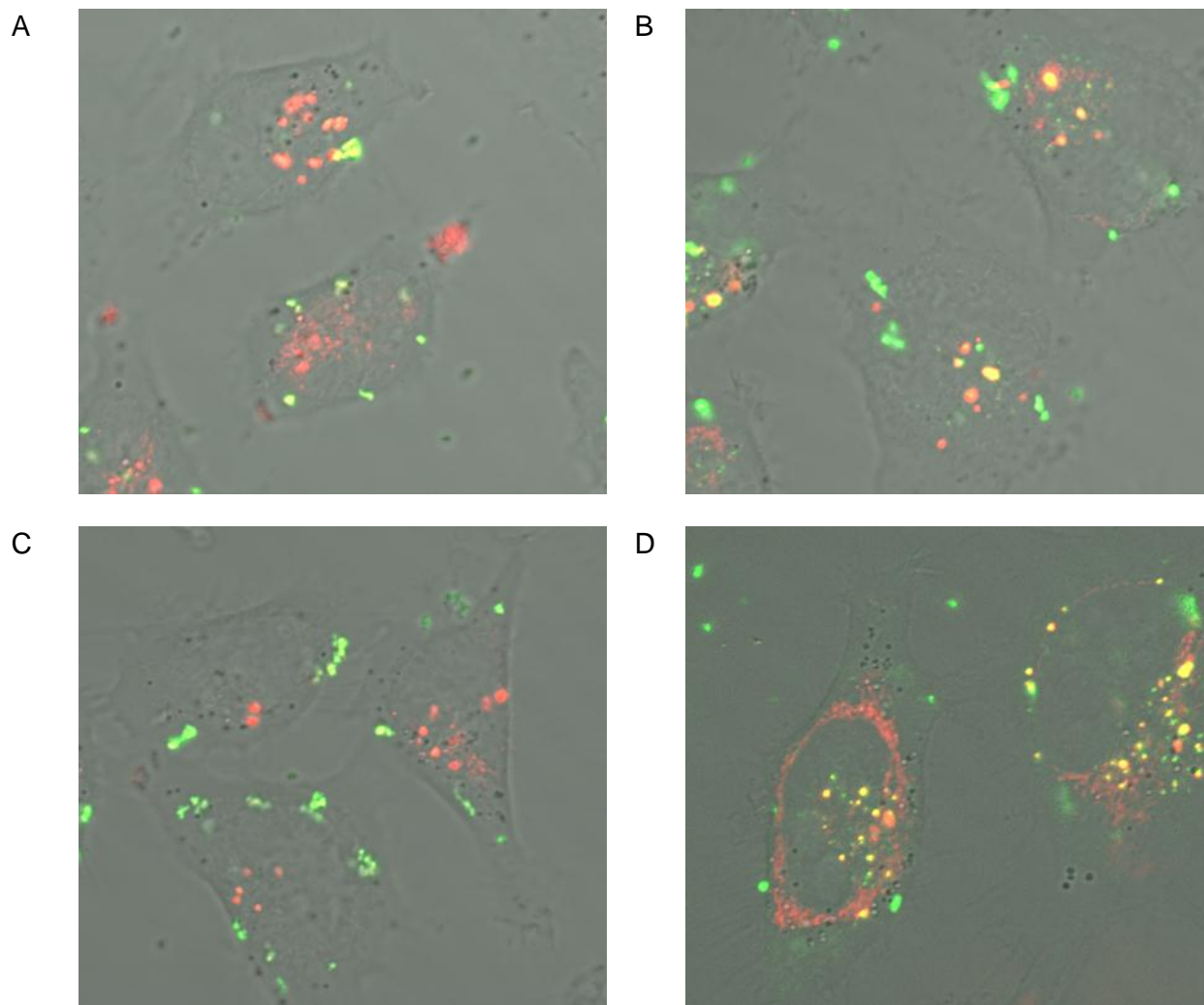
A

B

C

D

Figure 9. Confocal images of HeLa cells treated with polyplexes made from TO-PRO labeled pDNA and fluorescein labeled A) PEI 4.0, B) PEI 4.0-SS-PEG 3, C) PEI 4.0-SS-PEG 5 and D) PEI 4.0-SS-PEG 10 at N/P 6.

Discussion

Prerequisites for a good gene carrier are excellent diffusion through extracellular matrix, efficient uptake by cells, triggered disassembly inside cells combined with stability outside cells and finally high transfection efficiency [29, 30]. In order to guarantee for mobility in matrices, the carrier should be uncharged or bear only minor surface charge. This prevents slowing interactions or a sticking of the carrier to surrounding charged matrix components such as glycosamino glycans. Furthermore the carrier should be rather small, enabling its crawling through the network-like surrounding. It is known that reduced surface charge and small particles can be achieved by the attachment of a PEG shell [29, 30]. Thus, copolymers bearing PEG and PEI were synthesized. Their special feature was that they were strictly linear and that the synthesis allowed just for a single attachment of one PEG chain to one PEI molecule. Connected this way disturbing interactions of the PEG chain with the condensation of PEI and the nucleic acids are thought to be minimised due to the formation of a core-shell-structure. We expected these carriers to form smaller particles than those made from branched copolymers with multiple PEG-attachments. Such small carrier systems are also needed for cellular uptake because there is an upper uptake limit for particles. After internalization the carrier must detach its PEG shell and afterwards unload its cargo. This detachment should be triggered by a specific stimulus such as a change in the redox environment which is able to cleave disulfide bonds [29]. Having the change in redox potential in mind the strictly linear PEI-PEG-copolymers were connected via a disulfide bond which we expected to be cleaved more specifically inside cells than pH-responsive copolymers. In the step following the detachment of the PEG shell, the nucleic acid must traffic to the nucleus and achieve high transfection efficiency [29]. All these steps must be mastered in order to proof the usefulness of a carrier for nucleic acids. Thus, in order to mimic the single steps in gene delivery, the mobility of the polyplexes made from these new strictly linear and redox-cleavable copolymers was tested by FRAP experiments in the first step. Afterwards uptake studies were performed and the disulfide cleavage after addition of DTT was observed. In a last step the

217

transfection efficiency was estimated and polyplex treated cells were examined under the confocal microscope.

In order to determine if the polyplexes made from different fluorescently labelled polymers were able to diffuse through extracellular matrices, FRAP experiments were performed. For this purpose Matrigel™ was chosen as model matrix which consists of different extracellular matrix proteins such as laminin, collagen and heparin sulphate proteoglycan extracted from Englebreth-Holm-Swarm tumors [31]. Most tumors derived from endothelial cells produce significant amounts of this kind of basement matrix [31] and, thus, Matrigel™ is an ideal model for the investigation of diffusion processes in and around tumors. PEI 9.0 and its copolymers were chosen as an example because it has been shown that a PEG content of about 50% yields polyplexes with beneficial features [32]. PEI 9.0-SS-PEG 10 exactly corresponds to the ideal of 50% PEG content while the PEG content of the other copolymers was lower (23% and 33%). The finding that the mobility in this matrix became better, the longer the PEG chain was, can be explained with the structure of the polyplexes. If only PEI was applied for polyplex formation, the resulting particles had an overall positive surface charge which allowed for interactions with the charged components of Matrigel™. If the polyplexes were made from PEI-SS-PEG copolymers PEG shielded the charges of the polyplex core at least partially and, thus, less interactions with the surrounding matrix were possible. This effect was more pronounced for PEG chains of higher molecular weight which are thought to be better suited for shielding due to their longer size and their higher flexibility. Furthermore, polyplexes with better PEG shielding are generally smaller [32, 33] and are expected to diffuse easier than big carrier systems. Similar results were found by Lélu et al. who performed FRAP experiments with PEGylated chitosan particles in different collagen gels. They found that their chitosan polyplexes needed a PEG shell in order to diffuse through the gels [34]. Nevertheless, further experiments with other fluorescently labeled copolymers will be performed to back up our findings.

But good diffusion is not enough. In the course of the delivery cascade the polyplexes have also to be taken up by cells. The uptake studies revealed that there was nearly no difference in the uptake between the polyplexes made from PEI homopolymers and the corresponding copolymers. Only a slight improvement in uptake of most PEI homopolymers could be seen which is probably due to their high unshielded surface charge making interactions between the negatively charged cell surface and the polyplexes more probable. But although PEGylated copolymers generally exhibit a lower zeta potential than unshielded polymers [32] and interactions between cell surfaces and polyplexes are therefore weaker, these complexes were taken up as well. The absence of significant differences could have several reasons. One of them could be that the cleavage of the disulfide bonds partially starts when the carrier reaches the cell surface [35, 36]. A second reason may be the fact that the PEG shielded polyplexes are generally smaller than their counterparts built from PEI homopolymers. Since there is an upper uptake size limit of about 200 nm for clathrin-dependent endocytosis [37] -the most likely way of internalization- it is reasonable to assume that not all polyplexes from PEI homopolymers can be taken up due to their size. Thus, the reduced interactions with the cell surface due to a PEG shielding may be balanced out by the inability of cellular uptake due to PEI-polyplex sizes over 200 nm, leading to nearly no differences in the uptake levels between homo- and copolymers.

After cellular uptake the PEG shielding has to be removed in order to restore the endosomolytic activity of PEI and to destabilize the carrier system resulting in a release of the nucleic acid. This should be accomplished as a result to a specific stimulus such as a change in redox potential. There is a big difference in the redox potential inside and outside cells. While the glutathione concentration in the extracellular space is about 10 μM, it increases to 1-10 mM inside cells [18]. Our intention was to exploit this huge difference with disulfide linked carrier systems. Thus, we mimicked the reductive environment inside cells by incubating the polyplexes with DTT. The most interesting aspects concerning this treatment were the changes in zeta potential and size. The zeta potential decreased after incubation with DTT over time. This was a bit astounding

since the positively charged polyplex core should be exposed after PEG deshielding and, thus, we expected increasing zeta potentials. But since the zeta potential was measured over 24 h there was plenty time for rearrangements of the polyplexes after the cleavage of the PEG shield. The longer the incubation time, the more disulfide bonds were cleaved, removing the PEG shield step by step. As soon as the shielding moieties were removed, charge interactions were likely which could lead to severe aggregation and restructuring of the polyplexes. This could possibly result in reduced zeta potentials over time as observed. The removal of the PEG shield could also be traced by the measurement of the polyplex sizes after incubation with DTT. Most of the tested polyplexes grew a lot, especially those from medium chain PEIs. This strongly indicates that the disulfide bond between the PEI and the PEG moiety was cleaved by DTT. It can be assumed that as soon as the hydrophilic outer PEG layer was shed off, the charged cores of the polyplexes were exposed and ionic interactions led to the formation of aggregates. Thus, the increase in polyplex size indicated that the carrier lost its PEG shield and was probably able to restore its endosomolytic activity inside cells which is a prerequisite for efficient transfection. Such a detachment of PEG shields was also observed for a carrier system based on copolymers from PEG and poly-L-lysine. The components of this carrier system were connected by a disulfide bond and responded to a treatment with glutathione with a comparable increase in size [38]. Polyplexes made from low molecular weight PEI were generally instable over longer times, probably due to insufficient electrostatic interactions between the short PEI chains and the nucleic acids as seen from growing sizes and PdIs. In consequence the use of polyplexes made from PEIs with low molecular weight as long circulating gene carriers will be rather limited. In contrast, the polyplexes made from PEI of high molecular weight seemed to resist the complete cleavage of the disulfides. It is known that the electrostatic interaction between the positively charged PEIs and the negatively charged nucleic acids become stronger the longer the PEI part is [39-41]. Due to these increased interactions the formed polyplexes are generally stronger and in most cases also smaller which makes it harder for molecules in solution to get into the

polyplexes and cleave the bonds connecting PEI and PEG. We could observe this for our polyplexes made from PEI with higher molecular weight. Thus, there were upper and lower limits for the molecular weight of PEI in order to create extracellularly stable, but reductively cleavable carriers.

The last step in the delivery cascade is the transcription of the nucleic acid and the expression of a protein such as EGFP. In transfection experiments all polyplexes which were made from small PEIs performed rather poor. As in the case of the size measurements this can probably be ascribed to the instability of these polyplexes due to the short PEI chain. The attachment of a PEG chain enhanced their stability a bit and increased their transfection efficiency, but the overall gene expression was very low. In contrast, the polyplexes made from high molecular weight PEIs exhibited good transfection efficiency -no matter if they were PEGylated or not. The PEG chain seemed to have nearly no influence on the transfection efficiency. As the PEG chain cannot be cleaved in these cases it is not astounding that the differences between homo- and copolymers were not pronounced. The most interesting transfection results came from the polyplexes made from PEIs of intermediate chain length. They exhibited relevant differences in the transfection efficiency between the homo- and copolymers. All copolymers performed better than their corresponding homopolymers. An explanation for this behavior is that the extracellular stable polyplexes were small enough to be taken up by cells. Inside cells they were deshielded, restored the endosomolytic activity of PEI and released their payload efficiently resulting in enhanced transfection efficiency. So efficient transfection can be achieved by the use of intracellular cleavable PEI-SS-PEG copolymers which are stable in the extracellular space due to their PEG shielding, but can be deshielded in reducing environment.

Conclusion

A library of reductively degradable PEI-SS-PEG copolymers was successfully synthesized. In a second approach such linear copolymers were labeled with fluorescein and these copolymers were used for FRAP experiments. In these experiments it could be shown that the built polyplexes needed a PEG shell for beneficial diffusion in a model tumor matrix. Beside the diffusion behavior the cellular uptake of these polyplexes was investigated and it was found that all of them were picked up by HeLa cells. Furthermore the cleavability of the disulfide linked carriers was of great interest. Therefor these carriers were treated with DTT and their size and zeta potential was monitored. Especially from the size measurements it could be concluded that there were three types of polyplexes. The polyplexes made from low molecular weight PEIs were instable over time, while the polyplexes from high molecular weight were too stable to be completely degraded reductively. Only if the polyplexes were built from PEIs of intermediate molecular weight they could shed off their PEG shield triggered by the presence of the model reductant DTT. In transfection studies and with confocal microscopy it could be shown that polyplexes made from these cleavable polymers were able to disassemble intracellular and to transfect cells depending on their molecular weight. Thus, these copolymers guide the way towards safe, well-defined stimulus-responsive gene carriers which exhibit the possibility to further improve them by the attachment of targeting ligands or nuclear localization sequences instead of fluorescent labels.

References

[1] X. Zhang, S. R. Pan, H.-M. Hu, G.-F. Wu, M. Feng, W. Zhang, Poly(ethylene glycol)-block-polyethylenimine copolymers as carriers for gene delivery: Effects of PEG molecular weight and PEGylation degree. *Journal of Biomedical Materials Research Part A.* 84 (2008) 3, 795–804.

[2] S.-J. Sung, S. H. Min, K. Y. Cho, S. Lee, J.-Y. Min, Y. I. Yeom, J.-K. Park, Effect of Polyethyleneglycol on Gene Delivery of Polyethylenimine. *Biological and Pharmaceutcial Bulletin.* 26 (2003) 4, 492-500.

[3] H. K. Nguyen, P. Lemieux, S.V. Vinogradov, C. L. Gebhart, N. Guerin, G. Paradis, Evaluation of polyether-polyethyleneimine graft copolymers as gene transfer agents. *Gene Therapy.* 7 (2000) 2, 126-138.

[4] H. Petersen, P. M. Fechner, A. L. Martin, S. Stolnik, C J. Roberts, D. Fischer, M. C. Davies, T. Kissel, Polyethylenimine-graft-Poly(ethylene glycol) Copolymers: Influence of Copolymer Block Structure on DNA Complexation and Biological Activities as Gene Delivery System. *Bioconjugate Chemistry.* 13 (2002) 4, 845-854.

[5] S. Patnaik, S. K. Tripathi, R. Gyal, A. Arora, K. Mitra, A. Villaverde, Polyethylenimine-polyethyleneglycol-bis(aminoethylphosphate) nanoparticles mediated efficient DNA and siRNA transfection in mammalian cells. *Soft Matter.* 7 (2011) 13, 6103–6112.

[6] H. Petersen, K. Kunath, A. L. Martin, S. Stolnik, C. J. Roberts, M. C. Davies, T. Kissel, Star-Shaped Poly(ethylene glycol)-block-polyethylenimine Copolymers Enhance DNA Condensation of Low Molecular Weight Polyethylenimines. *Biomacromolecules.* 3 (2002) 5, 926-936.

[7] H. Petersen, A. L. Martin,.S. Stolnik, C. J. Roberts, M. C. Davies, T. Kissel, The Macrostopper Route: A New Synthesis Concept Leading Exclusively to Diblock Copolymers with Enhanced DNA Condensation Potential. *Macromolecules.* 35 (2002) 27, 9854–9856.

[8] M. Ogris, S. Brunner, S. Schueller, R. Kircheis, E. Wagner, PEGylated DNA/transferrin-PEI complexes: reduced interaction with blood components, extended circulation in blood and potential for systemic gene delivery. *Gene Therapy.* 6 (1999) 4, 595-605.

[9] D. Edinger, E. Wagner, Bioresponsive polymers for the delivery of therapeutic nucleic acids. *Wiley Interdisciplinary Reviews: Nanomedicine and Nanobiotechnology.* 3 (2011) 1, 33–46.

[10] V. Knorr, M. Ogris, E. Wagner, An Acid Sensitive Ketal-Based Polyethylene Glycol-Oligoethylenimine Copolymer Mediates Improved Transfection Efficiency at Reduced Toxicity. *Pharmaceutical Research.* 25 (2008) 12, 2937–2945.

[11] B. Romberg, W. Hennink, G. Storm,. Sheddable Coatings for Long-Circulating Nanoparticles. *Pharmaceutical Research.* 25 (2008) 1, 55–71.

[12] S. Lin, F. Du, Y. Wang, S. Ji, D. Liang, L. Yu, An Acid-Labile Block Copolymer of PDMAEMA and PEG as Potential Carrier for Intelligent Gene Delivery Systems. *Biomacromolecules.* 9 (2008) 1, 109–115.

[13] M. R. Park, K. O. Han, K. I. Han, M. H. Cho, J. W. Nah, Y. J. Choi, C.-S. Cho, Degradable polyethylenimine-alt-poly(ethylene glycol) copolymers as novel gene carriers. *Journal of Controlled Release.* 105 (2005) 3, 367–380.

[14] Y. Nie, M. Günther, Z. Gu, E. Wagner, Pyridylhydrazone-based PEGylation for pH-reversible lipopolyplex shielding. *Biomaterials.* 32 (2011) 3, 858–869.

[15] C. Fella, G. F. Walker, M. Ogris, E. Wagner, Amine-reactive pyridylhydrazone-based PEG reagents for pH-reversible PEI polyplex shielding. *European Journal of Pharmaceutical Sciences.* 34 (2008) 4-5, 309–320.

[16] G. F. Walker, C. Fella, J. Pelisek, J. Fahrmeir, S. Boeckle, M. Ogris, E.Wagner, Toward Synthetic Viruses: Endosomal pH-Triggered Deshielding of Targeted Polyplexes Greatly Enhances Gene Transfer in vitro and in vivo. *Molecular Therapy.* 11 (2005) 3, 418–425.

[17] M. Meyer, E. Wagner, pH-responsive shielding of non-viral gene vectors. *Expert Opinion on Drug Delivery.* 3 (2006) 5, 563–571.

[18] F. Schafer, B. Garry, Redox environment of the cell as viewed through the redox state of glutathione disulfide/ glutathione couple. *Free Radical Biology & Medicine,* 30 (2001) 11, 1191–1212.

[19] G. Cavallaro, M. Campisi, M. Licciardi, M. Ogris, G. Giammona, Reversibly stable thiopolyplexes for intracellular delivery of genes. *Journal of Controlled Release.* 115 (2006) 3, 322–334.

[20] M. Neu, J. Sitterberg, U. Bakowsky, T. Kissel, Stabilized Nanocarriers for Plasmids Based Upon Cross-linked Poly(ethylene imine). *Biomacromolecules.* 7 (2006) 12, 3428–3438.

[21] C. Chittimalla, L. Zammut-Italiano, G. Zuber, J.-P. Behr, Monomolecular DNA Nanoparticles for Intravenous Delivery of Genes. *Journal of the American Chemical Society.* 127 (2005) 32, 11436–11441.

[22] V. S. Trubetskoy, A. Loomis, P. M. Slattum, J. E. Hagstrom, V. K. Budker, J. A., Wolff, Caged DNA Does Not Aggregate in High Ionic Strength Solutions. *Bioconjugate Chemistry.* 10 (1999) 4, 624–628.

[23] D. L. McKenzie, E. Smiley, K. Y. Kwok, K. G. Rice, Low Molecular Weight Disulfide Cross-Linking Peptides as Nonviral Gene Delivery Carriers. *Bioconjugate Chemistry.* 11 (2000) 6, 901–909.

[24] M. Neu, O. Germershaus, S. Mao, K.-H. Voigt, M. Behe, T. Kissel, Crosslinked nanocarriers based upon poly(ethylene imine) for systemic plasmid delivery: In vitro characterization and in vivo studies in mice. *Journal of Controlled Release.* 118 (2007) 3, 370–380.

[25] U. Lungwitz, *Poly(ethylenimine) derived gene carriers and their complexes with plasmid DNA- Design, Synthesis ans Characterization.* Thesis, Regensburg, 2006.

[26] S. Takae, K. Miyata, M. Oba, T. Ishii, N. Nishiyama, K. Itaka, PEG-Detachable Polyplex Micelles Based on Disulfide-Linked Block Catiomers as Bioresponsive Nonviral Gene Vectors. *Journal of the American Chemical Society.* 130 (2008) 18, 6001–6009.

[27] C. Zhu, M. Zheng, F. Meng, F. M. Mickler, N. Ruthardt, X. Zhu, Reversibly Shielded DNA Polyplexes Based on Bioreducible PDMAEMA-SS-PEG-SS-PDMAEMA Triblock Copolymers Mediate Markedly Enhanced Nonviral Gene Transfection. *Biomacromolecules.* 13 (2012) 3, 769–778.

[28] Z.-H. Wang, Y. Zhu, M.-Y.Chai, W. T. Yang, F.-J. Xu, Biocleavable comb-shaped gene carriers from dextran backbones with bioreducible ATRP initiation sites. Biomaterials. 33 (2012) 6, 1873–1883.

[29] S. Bauhuber, C. Hozsa, M. Breunig, A. Goepferich, Delivery of Nucleic Acids via Disulfide-Based Carrier Systems. *Advanced Materials.* 21 (2009) 32-33, 3286–3306.

[30] U. Lungwitz, M. Breunig, T. Blunk, A. Goepferich, Polyethylenimine-based non-viral gene delivery systems. *European Journal of Pharmaceutics and Biopharmaceutics.* 60 (2005) 2, 247–266.

[31] G. Benton, H. K. Kleinman, J. George, I. Arnaoutova, Multiple uses of basement membrane-like matrix (BME/Matrigel) in vitro and in vivo with cancer cells. *International Journal of Cancer.* 128 (2011) 8, 1751–1757.

[32] S. Bauhuber, R. Liebl, L. Tomasetti, R. Rachel, A. Goepferich, M. Breunig, A library of strictly linear poly(ethylene glycol)–poly(ethylene imine) diblock copolymers to perform structure–function relationship of non-viral gene carriers. *Journal of Controlled Release.* 162 (2012) 2, 446–455.

[33] K. Kunath, A. Von Harpe, H. Petersen, D. Fischer, K. Voigt, T. Kissel, The Structure of PEG-Modified Poly(Ethylene Imines) Influences Biodistribution and Pharmacokinetics of Their Complexes with NF-κB Decoy in Mice. *Pharmaceutical Research.* 19 (2002) 6, 810–817.

[34] S. Lélu, S. P. Strand, J. Steine, C. L. Davies, Effect of PEGylation on the Diffusion and Stability of Chitosan–DNA Polyplexes in Collagen Gels. *Biomacromolecules.* 12 (2011) 10, 3656–3665.

[35] W. Sun, P. B. Davis, Reducible DNA nanoparticles enhance in vitro gene transfer via an extracellular mechanism. *Journal of Controlled Release.* 146 (2010) 1, 118–127.

[36] A.G. Torres, M. J. Gait, Exploiting cell surface thiols to enhance cellular uptake. *Trends in Biotechnology.* 30 (2012) 4, 185–190.

[37] J. Rejman, V. Oberle, I.S. Zuhorn, D.Hoeckstra, Size-dependent internalization of particles via the pathways of clathrin- and caveolae-mediated endocytosis. *Biochemical Journal.* 377 (2004) 1, 159–169.

[38] X. Cai, C. Dong, H. Dong, G. Wang, G. M. Pauletti, X. Pan, Effective Gene Delivery Using Stimulus-Responsive Catiomer Designed with Redox-Sensitive Disulfide and Acid-Labile Imine Linkers. *Biomacromolecules.* 13 (2012) 4, 1024–1034.

[39] D. V. Schaffer, N. A. Fidelman, N. Dan, D. A. Lauffenburger, Vector unpacking as a potential barrier for receptor-mediated polyplex gene delivery. *Biotechnology and Bioengineering.* 67 (2000) 5, 598-606.

[40] K. Kunath, A. von Harpe, D. Fischer, H. Petersen, U. Bickel, K.-H.Voigt, T. Kissel, Low-molecular-weight polyethylenimine as a non-viral vector for DNA delivery: comparison of physicochemical properties, transfection efficiency and in vivo distribution with high-molecular-weight polyethylenimine. *Journal of Controlled Release.* 89 (2003) 1, 113-125.

[41] U. Lungwitz, M. Breunig, R. Liebl, D. Pesl, T. Blunk, A.Goepferich, Degradable low molecular weight polyethyleneimines for non-viral gene transfer. in U. Lungwitz. *Poly(ethylenimine)-derived gene carriers and their complexes with plasmid DNA-Design, Synthesis and Characterization.* Thesis, Regensburg, 2006.

[42] X. Zhang, S.-R. Pan, H.-M. Hu, G.-F. Wu, M. Feng, W. Zhang, Poly(ethylene glycol)-block-polyethylenimine copolymers as carriers for gene delivery: Effects of PEG molecular weight and PEGylation degree. *Journal of Biomedical Materials Research Part A. (*2007) 795-804.

Chapter 7

Summary, conclusion and outlook

Summary

In the last years the delivery of nucleic acids has emerged as a promising strategy for the modulation of gene expression. It has been shown to be a useful tool for both, the insertion of therapeutic genes via DNA and the inhibition of harmful or non-functional proteins by the application of therapeutic RNA [1, 2]. These approaches proofed to be helpful for the therapy of severe acquired or inherited diseases as well as in the field of tissue engineering. While the first approaches mainly used viral vectors, more and more attention has been paid to non-viral delivery systems. Viral vectors especially bear the risks of infections and insertional oncogenesis, nevertheless they are very efficient vehicles which use sophisticated ways for the expression of their payload. But due to the high risks associated with viral vectors, non-viral carriers gained growing attention. Although up to now their transfection efficiency cannot compete with viral vectors, they exhibit lots of other advantages such as safety, ease of modification and production in large scale as well as chemical stability. The second big disadvantage beside their lower transfection efficiency is their cytotoxicity which correlates with the molecular weight of the carrier. This is especially true for the most used polymer poly(ethylene imine) (PEI) [3]. But it has been shown that also PEIs of low molecular weight can mediate efficient transfection while they exhibit no or nearly no toxicity [4]. Based on these findings, the scope of this thesis was to further modify these low molecular weight PEIs with a shielding moiety forming small, stable and over all non-toxic particles which do not interact with extracellular matrix components. The intention was to form strictly linear copolymers from PEI and poly(ethylene glycol) (PEG) which were either connected by a stable thioether bond or a cleavable disulfide bond. The rationale behind the disulfide bonds was to exploit the large extra/intracellular redox gradient every carrier has to face upon cell entry. As response to this trigger the disulfide bridge between the PEI and the PEG chain should be cleaved and, thus, the transfection efficiency of PEI which is reduced upon the addition of a shielding moiety [5] was expected to be restored. The importance of disulfides in carrier systems for the delivery of

nucleic acids was reviewed in **Chapter 1**. Here the biological rationale for the use of redox-active substances was explained and basic synthetic approaches for introducing disulfide bonds into molecules were described. Additionally, examples that provided the significance of disulfide bonds for the different aspects of delivery and tissue engineering were given.

The first practical objective of this thesis was the synthesis and analysis of thiol-modified, storage stable linear PEIs (lPEI) of low molecular weight (**Chapter 3**). Therefore, 13 lPEIs with a molecular weight ranging from 1.5 kDa to 10.8 kDa were synthesized. The standard synthesis route was modified in such a way that the resulting products of the first synthesis step had a thiol precursor-group at the chain end instead of the common hydroxyl group. In order to obtain high conversion rates different reaction conditions were tested and an excess of 7.5 equivalents modification reagent, room temperature and 4 h reaction times proofed to be best. The thiol precursor was cleaved in the second synthesis step yielding the desired thiol group. But since the resulting thiol group is known to be instable, a stable storage group had to be found. In order to obtain this group an optimized 2-step synthesis was introduced which comprised a reduction step with $NaBH_4$ followed by the addition of the activating disulfide reagent 2,2`-dithio dipyridine. Thus, polymers for the attachment of a second polymer were obtained. Moreover, it could also be shown by an ethidium bromide exclusion assay and the measurement of the polyplex sizes that all polymers were able to form particles with pDNA -an indispensable prerequisite for any efficient carrier.

The next step after the synthesis of thiol-modified lPEIs was the generation of copolymer libraries made from these polymers (**Chapter 4**). PEGs of different molecular weights (2, 5 and 10 kDa) were attached to these lPEIs -either via a stable thioether bond using methoxyPEG-maleimides or via a degradable disulfide bond made from a self-synthesized methoxyPEG-thioacetate. In contrast to other approaches, these copolymers demonstrated a clear separation between the hydrophilic PEG and the nucleic acid condensing PEI moieties due to the end-to-

end connection of the two polymers. This was thought to avoid sterical interference of the PEG chain with the interaction between the nucleic acid and PEI and in consequence the copolymers were expected to be perfectly suited to build small and stable polyplexes. The thioether-connected copolymers were used for a first test of the complexation abilities for pDNA and siRNA. The polyplexes made from pDNA revealed a distinct size division. While homopolymers and polymers with a short 2 kDa PEG chain built rather large polyplexes (up to 900 nm), the particles from copolymers with longer PEG chains (5 kDa and 10 kDa) gave much smaller sizes (commonly below 150 nm) and their size distribution was more uniform. In contrast, the polyplexes assembled from siRNA were all comparably small (about 100-350 nm). Furthermore, a quenching assay proved better complexation ability for siRNA as well as pDNA for nearly all copolymers compared to the homopolymers. These features make the PEG-PEI copolymers very promising carriers for such structurally diverse nucleic acids as siRNA and pDNA.

The library of thioether connected copolymers was further examined in detail in order to deduce structure-property-relationships (**Chapter 5**). A general guideline was that the PEG domain had a greater influence on the physicochemical properties of the polyplexes than PEI. A PEG content higher than 50% led to small (< 150 nm), nearly neutral polyplexes with favorable stability. Due to the PEG shielding the transfection efficiency of these polyplexes was significantly reduced compared to the PEI homopolymer. For the molecular weight of the PEI moiety, two findings catched the eyes: first, a molecular weight lower than 3 kDa was less suited to form compact and stable polyplexes. Second, it appeared that the transfection ability of the polyplexes increased with the chain length of PEI, but in the same order the toxicity also increased. Those toxic effects were at least partially reduced by the incorporation of a high molecular weight PEG domain into the copolymer. Thus, principles for the design of optimized gene carriers were found. Furthermore, it could be proven with selected copolymers that the transfection efficiency which was reduced due to the stable addition of PEG could be restored by the application of the corresponding degradable copolymer due to the redox trigger of the cells.

In a follow-up study the redox-active copolymers were further examined (**Chapter 6**). Therefore, also fluorescently labelled PEI-PEG copolymers were synthesized where fluorescein was selectively attached to the end of the PEG chain. The resulting polymers where used for fluorescence recovery after photobleaching (FRAP) experiments. The hypothesis was that the mobility of polyplexes in model matrices was the higher, the better the PEG shielding was due to reduced interactions with the surrounding matrix. With model copolymers it could be proven that polyplexes with longer PEG chain exhibited higher mobility in the model matrix than those without shielding and that the mobility corresponded to the molecular weight of the shielding moiety. The second aim was to test whether there were differences in the cleavability of the disulfide bonds and their transfection ability which depended on the molecular weight of PEI or PEG. It was found that there were three types of polyplexes. While polyplexes made from PEIs with short chains were generally rather instable and transfected poor, copolymers from PEIs of intermediate molecular weight were stable under nonreductive conditions, but degraded upon a redox trigger. Furthermore, their transfection performance was good. In contrast, copolymers with long chain PEIs could not be degraded under reductive conditions and differences in transfection efficiency between homo- and copolymers were not found. So it could be deduced that there is a small window of polymer molecular weight in which reductively degradable PEI-SS-PEG copolymers can be formed. If the PEI molecular weight is too low the resulting polyplexes are generally instable, while a PEI molecular weight which is too high results in nondegradable bonds.

Conclusion and outlook

In conclusion, this thesis successfully demonstrated the synthesis of strictly linear copolymer libraries and the usefulness of these libraries for the systematic investigation of structure-property-relationships. Due to the developed synthesis route it was possible to create strictly linear copolymers with an end-to-end connection of the PEG and PEI chains. This assembly seemed to prevent the interference of the shielding PEG moiety with the interaction between the PEI moiety and the nucleic acid. By the comprehensive evaluation of the influences of the molecular weights of both the PEI and the PEG moieties on polyplex properties, it was possible to deduce general guidelines for optimized carrier systems. Furthermore, it could be shown with the library of disulfide connected copolymers that not only the physicochemical properties of the polyplexes were determined by the molecular weights of the copolymer components but also the response to a redox trigger. Thus, a careful fine tuning of the polymeric carrier systems is indispensable for their efficiency. The presented redox-active copolymeric carriers are an excellent basis for the further development of non-viral carrier systems which are devoid of the risks of viral vectors, but are as efficient as their viral counterparts. In order to achieve efficient *in vivo* results further aspects of delivery have to be addressed by future non-viral vectors. They will need to be equipped with further targeting and endosomolytic sequences in order to specifically and efficiently transfect their target cells. Therefore, it will be necessary to keep to the approach of a selective attachment of these moieties onto the carrier in order to get detailed information of the obtained effect and to guarantee for uniform, reproducible carrier systems.

References

[1] S. Bauhuber, C. Hozsa, M. Breunig, A. Goepferich, Delivery of Nucleic Acids via Disulfide-Based Carrier Systems. *Advanced Materials.* 21 (2009) 32-33, 3286–3306.

[2] W. T. Godbey, K. Wu, A. G. Mikos, Poly(ethylenimine) and its role in gene delivery. *Journal of Controlled Release.* 16 (1999) 2-3, 149-160.

[3] W. T. Godbey, K. Wu, A. G. Mikos, Size matters: Molecular weight affects the efficiency of poly(ethylenimine) as a gene delivery vehicle. *Journal of Biomedical Materials Research.* 45 (1999) 3, 321–328.

[4] M. Breunig, U. Lungwitz, R. Liebl, C. Fontanari, J. Klar, A. Kurtz, T. Blunk, A.Goepferich, Gene delivery with low molecular weight linear polyethylenimines. *The Journal of Gene Medicine.* 7 (2005) 10, 1287–1298.

[5] S. Bauhuber, R. Liebl, L. Tomasetti, R. Rachel, A. Goepferich, M. Breunig, A library of strictly linear poly(ethylene glycol)–poly(ethylene imine) diblock copolymers to perform structure–function relationship of non-viral gene carriers. *Journal of Controlled Release.* 162 (2012) 2, 446–455

Appendix

List of abbreviations

AA	alkyl acrylates
ADPD	N-[4-(p-azidosalicylamido)butyl]-3`-(2`-pyridyldithio)propionamide
AEDP	bis(2-aminoethyl)-1,3-propandiamine
AMBH	2-acetamido-4-mercaptobutyric acid hydrazide
AMPT	ethyl S-acetyl propioniidate
APC	antigen presenting cell
asODN	antisense oligodesoxynucleotide
ASPG	asialoglycoprotein
BASED	bis-[β-(4-acidosalicylamido)ethyl]disulfide
Bcl2	B-cell lymphoma 2
BFA	brefeldin A
BMA	alkyl methacrylate
BMM	bone marrow-derived macrophage
bPEI	branched poly(ethylene imine)
C_{10}-C^{G+}	guanidinocysteine N-decylamide

CBA	cystamine bisacrylamide
CDPT	3-(4-carboxyamidophenyldithio)-propionthioimidate
CHDTAEA	cholesteryl hemidithioglycolyl tris(aminoethyl)amine
CHEMS	cholesteryl hemisuccinate
CLSM	confocal laser scanning microscopy
DAE	N-Boc-1,2-diaminoethane
DAH	N-Boc-diaminohexane
DBA	N-Boc-1,4-diaminobutane
DETA	diethylenetriamine
DMAEMA	dimethylaminoethyl methacrylate
DMAP	dimethylaminopyridine
DMF	dimethylformamide
DMSO	dimethylsulfoxide
DOGSDSO	1,2-dioleoyl-sn-glycero-3-succinyl-2-hydroxyethyl disulfide ornithine
DOPE	L-dioleoyl phosphatidyl ethanolamine
DOTAP	N-(1-(2,3-dioleoyloxy)propyl)-N,N,N-

	trimethylammonium chloride
DPDPB	1,4-di[3`-(2`-pyridyldithio) propionamido]butane
DPPC	dipalmitoylphosphatidylcholin
DSP	dithiobis(succinimidylpropionate)
DTBP	dimethyl 3,3-dithiopropionimidate
DTDP	2,2`-dithio dipyridine
DTNB	5,5`-dithio-bis(2-nitrobenzoic acid)
DTSSP	dithiobis(sulfosuccinimidyl propionate)
DTT	dithiothreitol
ECV	endosome carrier vehicle
EDA	ethylenediamine
EDTA	ethylene diamine tetra acetate
EGFP	enhanced green fluorescent protein
EGFP	enhanced green fluorescent protein
eq.	equivalent
ER	endoplasmatic reticulum
EtBr	ethidium bromide

FITC	fluorescein isothiocyanate
FR	folate receptor
FRAP	fluorescence recovery after photobleaching
FRET	fluorescence resonance energy transfer
GFP	green fluorescent protein
GILT	gamma-interferon-inducible lysosomal thiol reductase
GR	glutathione reductase
Grx	glutaredoxin
GSH	glutathione
GSSG	glutathione disulfide
h	hour
HER2	human epidermal growth factor receptor 2
HPMA	(N-(2-hydroxypropyl)methacrylamide)
LbL	layer-by-layer
LC-SPDP	long-chain N-succinimidyl 3-(2-pyridyldithio)propionate
LE	late endosome
Lipolex	lipid incorporating nucleic acids

LLO	listeriolysin O
LLO-SS-PN	listeriolysin O coupled to protamine via disulfide
lPEI	linear poly(ethylene imine)
l-PEIS	linear poly(ethylene imine disulfide)
M6P	mannose-6-phosphate
M6P-BSA	mannose-6-phosphate bovine serum albumine
MAAc	metharylic acid
MALS	muliple angle light scattering
MFI	mean fluorescence intensity
MHC	major histocompatibility complex
min	minute
mPEG-OH	methoxy poly(ethylene glycol)-OH
mPEG-SAc	methoxy poly(ethylene glycol)thioacetate
mPEG-S-S-DSPE	N-[2-ω-methoxypoly(ethylene glycol)-α-aminocarbonylethyl-dithiopropionate] covalently coupled to disteaorylphosphatidylethanolamine
MPP	membrane permeant peptide

mRNA	messenger ribonucleic acid
MTX	methotrexat
MW	molecular weight
N/P	ratio of nitrogen to phosphorous
NADPH	nicotinamide adenine dinucleotide phosphate
NLS	nuclear localization sequence
OD	optical density
ODN	oligodesoxynuleotide
P[Asp(DET)]	poly(aspartatamide)
p75NTR	p75 neurotrophin receptor
pAA	poly(α,β-aspartic acid)
PCBS-b-PEG	poly(L-cysteine bisamide-g -sulfadiazine)-b-poly(ethylene glycol)
PDI	protein disulfide isomerise
PdI	polydispersity index
pDNA	plasmid desoxyribonucleic acid
PDPH	3-(2-pyridyldithio)propionyl hydrazide
PDSA	pyridyldisulfide acrylate

PEG	poly(ethylene glycol)
PEG-PEI	poly(ethylene glycol)-poly(ethylene imine)
PEG-pLL	poly(ethylene glycol)-poly(L-lysine)
PEG-SS-P[Asp(DET]	poly(ethylene glycol) coupled to poly(aspartatamide) via disulfide bonds
PEG-thiopLL	thiolated Poly(ethylene glycol)-block-poly(L-lysine)
PEI	poly(ethylene imine)
PEI-SS-PEG	poly(ethylene imine)-poly(ethylene glycol) diblock copolymers connected via a disulfide bond
pEtOXZ	poly-2-ethyl-2-oxazoline
pEtOXZ-SAc	poly(2-ethyl-2-oxazoline)-thioacetate
PHEA	α,β-poly(N-2-hydroxyethyl)-D,L-aspartatamide
PHPMA	poly[N-(2-hydroxypropyl)methacrylamide]
PIC micelle	polyion micelle
pLL	poly(L-lysine)
PLLA-b-PEG	poly(L-lactic acid)-B-poly(ethylene glycol)
PN	protamine

poly(EDA/CBA)   poly(ethylene diamine/cystamine

bisacrylaminde)

poly(TETA/CBA)   poly(triethylenetetramine/cystamine

bisacrylamide)

polyplex   nucleic acid complexed with a polymer

PVP   poly(vinylpyrrolidon)

RNA   ribonucleic acid

roGFP1   reduction-oxidation-sensitive green

fluorescent protein

rpLL   reducible poly(L-lysine)

RR   rhodamine red

SADP   N-succinimidyl(4-azidophenyl)-1,3`-

dithiopropionate

SAED   sulfosuccinimidyl-2(7-azido-4-methyl

coumarin-3-acetamide)ethyl-1,3`-

dithiopropionate

SAMSA   S-acetylmercaptosuccinic anhydride

SAND   sulfosuccinimidyl-2-(m-azido-o-

nitrobenzamido)-ethyl-1,3´-dithiopropionate

SASD   sulfosuccinimidyl-2-(p-

acidosalicylamido)ethyl-1,3`-dithiopropionate

SATA	N-succinimidyl S-acetylthioacetate
SATP	N-succinimidyl acetylthiopropionate
SBT	S-4-succinimidyloxycarbonyl benzyl thiosulfate
SD	standard deviation
siRNA	small interfering ribonucleic acid
SMBT	S-4-succinimidyloxycarbonyl-α-methyl-benzyl thiosulfate
SMPT	4-succinimidyloxycarbonyl-α-methyl-α(2-pyridyldithio)toluene
sNHS-ATMBA	Sulfosuccinimidyl N-[3-(acetylthio)-3-methylbutyryl-β-alaninate
SPDP	N-succinimidyl 3-(2-pyridyldithio)propionate
SPP	N-succinimidyl 4-(2-pyridyldithio)pentanoate
SS-PAED	reducible disulfide poly(amido ethylenediamine)
SS-PAEI	reducible poly(amido ethylene imine)
ssPEI	disulfide cross-linked poly(ethylene imine)
Sulfo-LC-SMPT	Sulfosuccinimidyl-6-[α-methyl-α-(2-

pyridyldithio)toluamido]hexanoate

Sulfo-LC-SPDP	watersoluble longchain N-succinimidyl 3-(2-pyridyldithio)propionate
Sulfo-SADP	N-sulfo-succinimidyl(4-azidophenyl)-1,3`-dithiopropionate
TAT	HIV-1 transcriptional activator
TCEP	tris(2-carboxyethyl)phosphine
TE	tissue engineering
TEM	transmission electron microscopy
TETA	triethylenetetramine
TfR	transferrin receptor
TGN	trans-Golgi network
trastuzumab-SPP-RR	trastuzumab coupled to rhodamine red via N-succinimidyl 4-(2-pyridyldithio)pentanoate
TRIS	tris(hydroxymethyl)aminomethane
Trx	thioredoxin
VEGF	vascular endothelial growth factor

Curriculum vitae

Name:	Sonja Bauhuber
Date of birth:	09.11.1982
Place of birth:	Pfarrkirchen
Nationality:	German
Martial Status:	Single

Studies:

12/2007-11/2012	PhD thesis at University of Regensburg Department of Pharmaceutical Technology **Topic:** "Linear poly(ethylene imine)-poly(ethylene glycol) copolymers for nucleic acid delivery- Synthesis and characterization"
09/2007	Graduation: Diplom-Chemiker (Vertiefung Medizinische Chemie)
01/2007- 09/2007	Diploma thesis at University Regensburg Department of Pharmaceutical Technology **Topic:** "Gene Carriers based on Poly(ethylene imine)"
10/2002- 12/2006	Study of Chemistry (Diploma) at University Regensburg

School education:

6/2002	Graduation: Allgemeine Hochschulreife (Abitur)
09/1993- 06/2002	Grammar school: Gymnasium Pfarrkirchen
09/1989- 07/1993	Elementary school: Grundschule Bayerbach

List of publications

Conference abstracts
S. Bauhuber, M. Breunig, A. Göpferich,
Synthesis of reductively degradable Poly(ethylene glycol)-
Poly(ethylene imine)- Copolymers for the Delivery of Nucleic Acids,
DPhG-Jahrestagung, Jena, Germany, 2009

S. Bauhuber, A. Göpferich, M. Breunig,
Reductively Degradable Linear Poly(ethylene glycol)-Poly(ethylene
imine)- Copolymers for the Delivery of Nucleic Acids,
DPhG-Jahrestagung, Braunschweig, Germany, 2010

S. Bauhuber, A. Göpferich, M. Breunig,
Influence of the molecular weights of linear poly(ethylene glycol)-
poly(ethylene imine)–copolymers on the delivery of nucleic acids,
Joint Meeting ÖPhG-DPhG, Innsbruck, Austria, 2011

S. Bauhuber, R. Liebl, A. Göpferich, M. Breunig,
A library of strictly linear poly(ethylenenglycol)-poly(ethylene imine)
diblock copolymers for the delivery of nucleic acids,
World Meeting on Pharmaceutics, Biopharmaceutics and
Pharmaceutical Technology , Istanbul, Turkey, 2012

Publications
S. Bauhuber, C. Hozsa, M. Breunig, A. Göpferich,
Delivery of nucleic acids via disulfide-based carrier systems,
Advanced Materials, 21 (2009) 3286-3306

S. Bauhuber, R. Liebl, L. Tomasetti, R. Rachel, A. Göpferich,
M. Breunig,
A library of strictly linear poly(ethylene glycol9-poly(ethylene imine)
diblock copolymers to perform structure-function relationship of
non-viral gene carriers, Journal of Controlled release, 162 (2012)
446-455

Acknowledgements

Erklärung

Ich versichere hiermit, dass ich die vorliegende Arbeit selbst verfasst habe und keine anderen als die angegebenen Quellen und Hilfsmittel verwendet habe.

Regensburg, den……………..   ……………………………………

                                                                    (Sonja Bauhuber)